Elucidating agonist-induced signaling patterns of human G protein-coupled receptor GPR17 and uncovering pranlukast as a biased mixed agonist-antagonist at GPR17

Dissertation

zur

Erlangung des Doktorgrades (Dr. rer. nat.)

der Mathematisch-Naturwissenschaftlichen Fakultät

der Rheinischen Friedrich-Wilhelms-Universität Bonn

vorgelegt von

Stephanie Monika Hennen

aus Saarburg

Bonn 2011

Angefertigt mit Genehmigung der Mathematisch-Naturwissenschaftlichen Fakultät der Rheinischen Friedrich-Wilhelms Universität Bonn.

1. Gutachter: Prof. Dr. Evi Kostenis

2. Gutachter: Prof. Dr. Klaus Mohr

Tag der Promotion: 15.09.2011

Erscheinungsjahr: 2011

Die vorliegende Arbeit wurde in der Zeit von April 2008 bis März 2011 am Institut für Pharmazeutische Biologie der Rheinischen Friedrich-Wilhelms Universität Bonn unter der Leitung von Frau Prof. Dr. Evi Kostenis durchgeführt.

Meinen Eltern

Abstract

The progress of human genome sequencing has revealed the existence of several hundred orphan G protein-coupled receptors (GPCRs), whose endogenous ligands are not yet identified, thus their deorphanization and characterization is fundamental in order to clarify their physiological and pathological role as well as their relevance as new drug targets. Recently, the orphan GPCR GPR17 that is phylogenetically and structurally related to the known P2Y and CysLT receptors has been identified as a dual uracil nucleotide/cysteinyl-leukotriene receptor. In spite of this, these deorphanization efforts could not be verified yet by independent laboratories, thus this classification remains a controversial matter and GPR17 most likely still represents an orphan GPCR. Additionally, a subsequent study revealed a ligand-independent regulatory role for GPR17 suppressing CysLT1 receptor function via GPCR-GPCR interactions. By means of a high throughput pharmacogenomic approach our group has identified a small molecule agonist for GPR17 that is used as pharmacological tool for characterization of ligand-dependent behaviors triggered by this receptor. As a consequence, in the present thesis, evidence is provided that GPR17 does not lack the common features of GPCR signaling. Upon agonist challenge GPR17 induces signaling via promiscuous G protein-coupling (Gαi/o, Gαq and Gαs) in an agonist-concentration-dependent manner, as determined by means of traditional second messenger assays (cAMP and IP1) and by the label-free dynamic mass redistribution (DMR) technology in two different cellular backgrounds (CHO and HEK293 cells) engineered to stably express the short isoform of human GPR17. The use of ELISA and immunofluorescence techniques revealed that activation of GPR17 with the agonist is also linked with a time-dependent reduction of cell surface expression. Furthermore, GPR17 recruits β-arrestin2 upon ligand-stimulation in a G protein-dependent and –independent manner as monitored by use of bioluminescence resonance energy transfer (BRET2) analyses. The GPR17-mediated signaling can be efficiently abrogated by the CysLT1 antagonist pranlukast in a non-competitive mode of action, but not by montelukast, zafirlukast and MK571, as investigated by use of DMR analyses, traditional second messenger assays and BRET2 approach. Additionally, evidence is provided that pranlukast acts as a mixed agonist/antagonist at GPR17, differentially modulating individual signaling pathways. Furthermore, it is demonstrated that β-arrestin2, known as scaffolding protein involved in desensitization and trafficking processes of GPCRs, exhibits the capability to fine-tune G protein signaling specifity of GPR17 via shifting the preference to the most preferred G protein subunit (here Gαi/o), a phenomenon that has not been described before.

Keywords: G protein-coupled receptor (GPCR), GPR17, pranlukast, β-arrestin2, dynamic mass redistribution, multiplicity

Kurzbeschreibung

Die Sequenzierungsfortschritte des menschlichen Erbgutes offenbarten die Existenz von mehreren hundert *orphanen* G Protein-gekoppelten Rezeptoren (GPCRs), dessen endogene Liganden noch nicht identifiziert wurden. Ihre Deorphanisierung sowie Charakterisierung sind elementar um die physiologische und pathologische Rolle aufzuklären und sie können als neue potenzielle Arzneimittel Targets betrachtet werden. Kürzlich ist der *orphane* GPCR GPR17, der phylogenetisch und strukturell mit P2Y und CysLT Rezeptoren verwandt ist, als ein Uracil Nukleotid/Cysteinyl-Leukotrien Rezeptor identifiziert worden. Diese Deorphanisierung konnte jedoch noch nicht durch unabhängige Labore verifiziert werden, somit bleibt diese Klassifikation eine umstrittene Postulierung und GPR17 muss weiterhin als *orphaner* GPCR betrachtet werden. Weiterhin zeigte eine nachfolgende Studie eine Ligand-unabhängige Funktion für GPR17 über GPCR-GPCR Wechselwirkungen als negativer Regulator der CysLT1 Rezeptor-vermittelten Signalwegsaktivierung. Dennoch hat unsere Arbeitsgruppe einen synthetischen GPR17-Agonisten identifiziert, der als pharmakologisches Werkzeug für die Charakterisierung von Ligand-induzierten Rezeptor-nachgeschalteten Ereignissen verwendet wird. Entgegen der bisher postulierten Thesen wird in der gegenwärtigen Arbeit gezeigt, dass GPR17 allgemeine Eigenschaften der GPCR-Signaltransduktion aufweist. Agonist-Stimulierung des GPR17 induziert Signaltransduktion über Kopplung mit promiskuitiven G Proteinen (Gαi/o, Gαq und Gαs) in einer konzentrationsabhängigen Weise, wie mittels der klassischen funktionellen GPCR Analysen (cAMP und IP1) und durch die Technologie der dynamischen Massenumverteilung (DMR) gezeigt werden konnte, unter Verwendung von zwei verschiedenen rekombinanten Zelllinien (CHO und HEK293), welche die kurze Isoform des humanen GPR17 stabil exprimieren. Der Gebrauch von ELISA und Immunfluoreszenz Techniken offenbarte, dass die Aktivierung von GPR17 mit dem Agonisten auch mit einer zeitabhängigen Verminderung des Zelloberflächenexpression verbunden ist. Außerdem wird unter Verwendung der Biolumineszenz Resonanz Energietransfer (BRET2) Methode gezeigt, dass GPR17 β-Arrestin2 nach Ligand-Stimulierung rekrutiert, und zwar in einer G Protein-abhängigen als auch -unabhängigen Weise. Die GPR17-vermittelte Signaltransduktion kann vom CysLT1 Antagonisten Pranlukast in einer nicht-kompetitiven Weise gehemmt werden, aber nicht durch Montelukast, Zafirlukast und MK571. Weiterhin wird gezeigt, dass Pranlukast als ein gemischter Agonist/Antagonist am GPR17 wirkt, der partial und funktionell selektiv die Gαi/o-vermittelte Signalwegstransduktion aktiviert. Weiterhin wird dargelegt, dass β-Arrestin2, bekannt als Gerüst-Protein, das an der Desensibilisierung und Internalisierung von GPCRs beteiligt ist, die Fähigkeit besitzt die gemischte G Protein-Kopplung von GPR17 zu modulieren, und zwar über die Verschiebung der Kopplungspräferenzen zur bevorzugtesten G Protein-Untereinheit (hier Gαi/o). Dies stellt ein Phänomen dar, das zuvor nicht beschrieben worden ist.

Schlüsselwörter: G Protein-gekoppelte Rezeptoren (GPCR), GPR17, Pranlukast, β-Arrestin2, Dynamische Massenumverteilung (DMR), Multiplizität

Table of contents

List of figures

List of tables

1 Introduction

The word ‘receptor’ originates from the Latin word ‘recipere’, which means to receive or to accept. Hence, in biochemistry a receptor is known to be a protein that receives signals (endogenous ligands or synthetic drugs), which initiate a cellular response.

Guanine nucleotide-binding protein (G protein) coupled receptors (GPCRs) are integral membrane proteins, which convey extracellular signals into intracellular events. The “superfamily” of GPCRs, also known as seven-transmembrane receptors (7TMR), represents the largest group of cell surface receptors expressed by the human genome. Over 800 GPCR sequences can be found, making up approximately 2% of all human genes (Fredriksson et al. 2003, Vassilatis et al. 2003).

GPCRs respond to a wide variety of extracellular molecules, such as Ca^{2+} ions, small biogenic amines, nucleotides, eicosanoids, peptides, glycoproteins and sensory stimuli (Ji, Grossmann & Ji 1998, Wess 1998). They play a crucial role in cell-to-cell communication, as they control a broad range of cellular responses such as metabolism, contractility, secretion, motility, transcription and growth. Integration of these cellular responses at systemic levels leads to the regulation of many physiological functions such as embryonic development, gonadal development, learning and memory and organismal homeostasis (Neves, Ram & Iyengar 2002).

Due to their ubiquitous cell surface expression, and their involvement in a variety of physiological and pathophysiological processes, GPCRs represent an important class of very tractable drug targets. Approximately 30% of all pharmaceutical drugs on the market unfold their therapeutic effect on GPCRs, although only a small percentage of GPCRs are currently targeted (reviewed by Drews 2000, Drews 2006, Overington, Al-Lazikani & Hopkins 2006). These drugs typically function as agonists or antagonists to GPCRs for the treatment of various diseases including asthma, hypertension, peptic ulcers and schizophrenia (reviewed by Wise, Jupe & Rees 2004).

1.1 Structural architecture and classification of GPCRs

GPCRs are composed of a single peptide, usually 400-500 but also up to 1200 amino acids (Flower 1999). Conserved structural GPCR motifs include seven α-helical transmembrane domains of approximately 25-35 amino acids with connecting intracellular and extracellular loops, an extracellular amino terminus and an intracellular C-terminal domain (Lagerström & Schiöth 2008, Palczewski et al. 2000, Pierce, Premont & Lefkowitz 2002). The seven transmembrane helices (TM1-7) represent the conserved hydrophobic core of G protein-coupled receptors (Figure 1). In general the extracellular N-terminus and the exofacial portions of the transmembrane segments are involved in the interaction of the receptor with the ligand. Intracellular parts of the GPCR, including the C-terminal domain and the intracellular loops (in particular the endo2 and the endo3, see Figure 1), participate in the G protein activation and the interaction with other cellular proteins (Kobilka 1992; Wess 1997, Wess 1998). Furthermore, most GPCRs have two cysteines, which form an intramolecular

disulfide bridge between the first and second extracellular loops (Baldwin 1994). This covalent interaction enhances receptor stability and is involved in various functions including activation and binding, depending on the respective receptor.

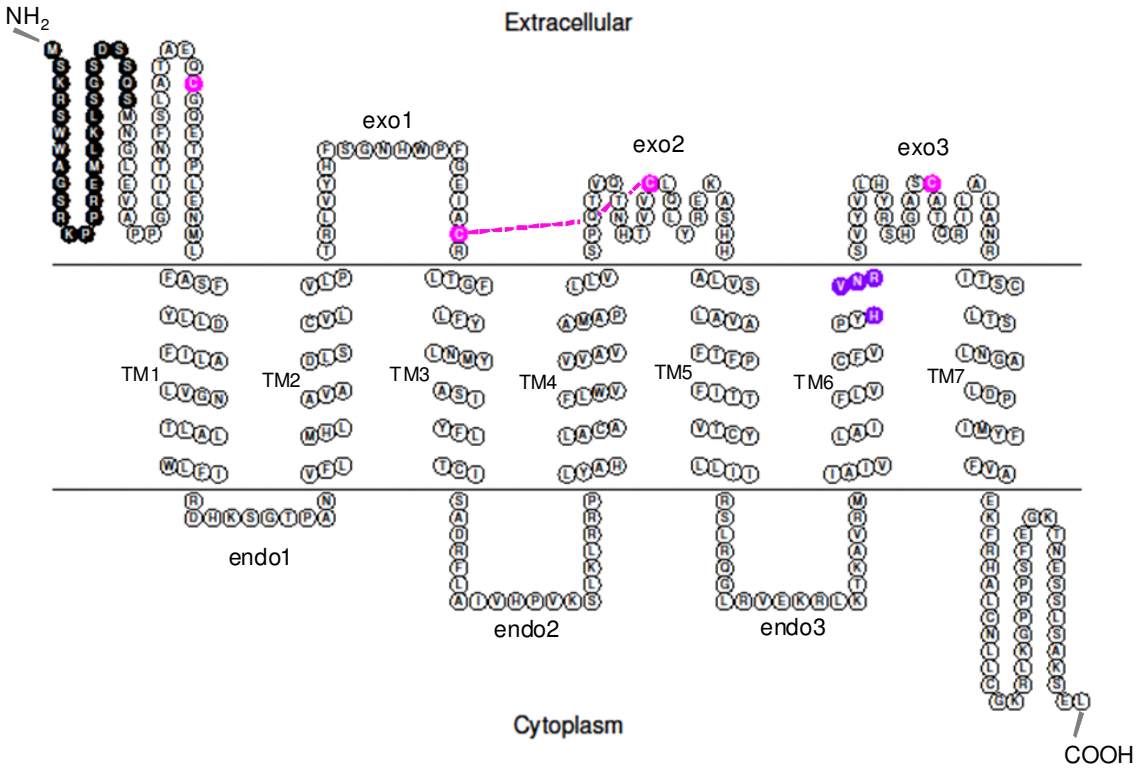

Figure 1 Snake plot of human seven transmembrane receptor GPR17

The schematic representation of hGPR17 (short (336 aa) and long (367 aa) splice variant) as a serpentine model demonstrates conserved structural features of family A of GPCRs, which are characterized by having a relatively small extracellular N-terminus (NH_2), 7 transmembrane (TM) domains linked by three intracellular and three extracellular loops and an intracellular C-terminus (COOH). Intracellular loops are marked as endo1 to endo3 and the extracellular loops as exo1 to exo3. The 28 amino acids comprising elongated N-terminus of the long GPR17splice variant are indicated as black circles with white letters. The conserved typical amino acid motif in TM6 (H-X-X-R), which is believed (at least for nucleotide receptors) to be essential for ligand binding, and that can be found in several GPCRs including all known P2Y and CysLT receptors (Ciana et al. 2006), is indicated with purple circles. Cysteine residues are highlighted in magenta circles and respective disulphide-bridge is denoted as a magenta staple line.

(Plot was designed with the help of an online available TM prediction server and a snake plot construction program from http://www.enzim.hu/hmmtop/html/submit.html (HMMTOP prediction of TM helices) and http://www.sacs.ucsf.edu/TOPO (TOPO2 Transmembrane Protein Display Page)).

Although the GPCRs do not show the overall sequence homology, a significant homology is found within the defined subfamilies (Gether 2000). GPCRs can be classified into three distinct families based on specific structural characteristics, and the degree of sequence identity in their TM domains. Family A is the rhodopsin-like receptor family with ligands such as neuropeptides, chemokines and prostanoids, family B are also referred to as secretin and glucagon receptor-like family, and family C receptors are related to metabotrophic neurotransmitter receptors. Compared to family A receptors, family B and C receptors have large extracellular N-terminal domains. Despite the fact that there is only little amino acid identity (less than 20%) between families, the overall helical arrangement of

the 7TM domain appears to be conserved across the entire superfamily (Pierce, Premont & Lefkowitz 2002).

1.2 Classical model of G protein-dependent signaling

As the name implies, GPCRs mediate signaling with the help of G proteins. These heterotrimeric guanine nucleotide binding proteins are composed of the α-subunit (Gα) and the dimer of the βγ-subunits (Gβγ). To date over 20 α-subunits, 6 β-subunits and 12 γ-subunits have been identified (Simon, Strathmann & Gautam 1991). The classical model of a G protein-coupled receptor signal transduction cascade requires the binding of an extracellular ligand to its respective receptor, causing a conformational change of the stimulated GPCR, which allows the receptor to activate an intracellular heterotrimeric G protein. The GPCR can be regarded as a guanine-nucleotide exchange factor (GEF) for the Gα subunit. Agonist-induced stimulation of the receptor results in the activation of its GEF activity toward the Gα subunit. This GEF activity triggers an increase in the dissociation of bound GDP from Gα, enabling a fast exchange with GTP. Following this replacement, the heterotrimer can dissociate into the separate Gα and Gβγ subunits (Downes & Gautam 1999, Hepler & Gilman 1992), even though some data imply that the G protein activation may also comprise the subunit rearrangement rather than the dissociation (Bünemann, Frank & Lohse 2003, Frank et al. 2005). However, the GTP-bound Gα subunits and Gβγ dimers can modulate a number of second messenger generating pathways including the activation of phospholipase C and the activation/inhibition of adenylate cyclase in addition to a variety of other downstream effectors, depending on the respective coupling preferences (Gilman 1987, Marinissen & Gutkind 2001). To date, there are four main classes of Gα proteins according to the amino acid sequence similarity (Gαs, Gαi/o, Gαq/11, Gα12/13), and furthermore based on functional similarities, regarding the effect that they elicit on downstream effectors (Pierce, Premont & Lefkowitz 2002, Simon, Strathmann & Gautam 1991). The heterotrimeric G proteins are conventionally named according to their α-subunits.

It has been demonstrated, that certain amino acid residues in the C-terminal regions of Gα protein can directly interact with the receptor and play a key role in regulating the specificity of coupling (Wess 1998). As this region is rather conserved for Gα proteins belonging to the same family, receptors are often capable of stimulating all the members of this family. Thus, based on their G protein-coupling preference, GPCRs can be broadly subclassified into Gαs-, Gαi/o-, Gαq/11- and Gα12/13-coupled receptors (Pierce, Premont & Lefkowitz 2002, Wess 1998).

1.2.1 Guanine nucleotide binding proteins and their major signaling characteristics

Activation of one G protein may give rise to a bifurcating signal, as not only the GTP-bound α-subunit does transmit a signal to effector molecules, but βγ-dimers can also generate part of the information (reviewed by Marinissen & Gutkind 2001). The major involved signal transduction pathways are roughly described in the following chapter and depicted in Figure 2, providing crucial information for the present thesis.

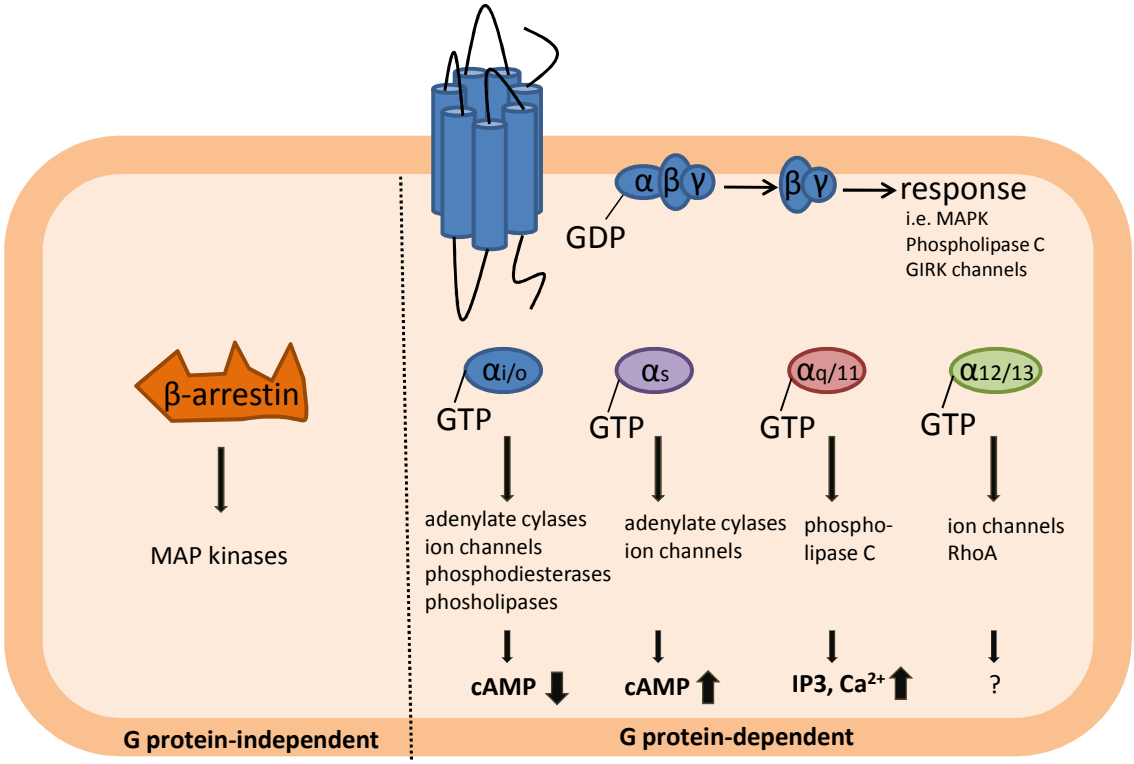

Figure 2 G protein-dependent and -independent signaling pathways of GPCRs

Ligand-induced activation of the seven-transmembrane receptor by an external stimulus initiates exchange of GDP to GTP, which promotes an activation of the G protein heterotrimer. The GTP-bound Gα subunit dissociates from the Gβγ complex, and both subunits activate their respective cytoplasmic effectors resulting in a modulation of intracellular second messenger levels. Besides the classical G protein-mediated signaling pathways, G protein-independent signaling upon agonist-induced stimulation occurs, mainly initiated by the scaffolding protein β-arrestin. (modified from Lefkowitz & Shenoy 2005 and Marinissen & Gutkind 2001)

1.2.1.1 Gαs-mediated signaling cascades

The Gαs-protein family, including Gαs and olfactory Gαolf, was the first to be identified. The regulatory component of adenylate cyclase was firstly described by Ross and Gilman in 1980 as “guanine nucleotide-binding regulator protein” (Ross & Gilman 1980). Furthermore, it has been found to be the least abundant of G proteins in the body (Gilman 1995). The “s” refers to the stimulatory effect, as the common property of Gαs is stimulation of the adenylate cyclase (AC) leading to an increase of intracellular cyclic adenosine monophosphate (cAMP) concentration.

1.2.1.2 Gαi/o-mediated signaling cascades

The class of Gαi/o-proteins represents the biggest family of the four Gα-subunits. It includes the almost ubiquitously expressed Gαi1, Gαi2, Gαi3 and Gαo proteins, as well as the brain- and the adrenal platelets-specific Gαz and the Gαt, and the Gαg expressed in the retina and the taste buds, respectively (reviewed by Woehler & Ponimaskin 2009). The protein was firstly isolated by Sternweis and Robishaw and characterized by Gilman’s group in 1984 (Sternweis & Robishaw 1984, Bokoch et al. 1984, Katada et al. 1984). The Gαi family was initially named for its ability to inhibit adenylate cyclase activity, thus promoting decreased intracellular cAMP synthesis in a pertussis toxin (PTX) sensitive manner (Katada & Ui 1982). This property of the bacterial toxin was widely exploited to check the involvement of Gαi and Gαo in cellular responses.

1.2.1.3 Gαq/11-mediated signaling cascades

The G proteins of this class, including Gαq, Gα11, Gα14 and Gα15/16 (mouse and human orthologues, respectively) activate the phospholipase C (PLC), an enzyme that catalyzes the hydrolysis of the phosphatidylinositol (4,5)-bisphosphate (PIP2), promoting the generation of diacylglycerol (DAG) and inositol 1,4,5-triphosphate (IP3). These second messengers serve to propagate and amplify the Gαq-mediated signal with intracellular calcium mobilization. DAG stimulates the protein kinase C (PKC), while IP3 triggers intracellular Ca^{2+} release by activation of receptors in the endoplasmic reticulum. The increase of intracellular Ca^{2+} has many effects, including activation of the phospholipase A2 (PLA) and PKC, respectively (reviewed by Marinissen & Gutkind 2001, Woehler & Ponimaskin 2009). Cockcroft and Gomperts were the first to demonstrate that PLC is activated by a G protein (Cockcroft & Gomperts).

1.2.1.4 Gα12/13-mediated signaling cascades

In 1991 Strathmann and Simon identified the Gα12 and the Gα13 subunits, which show relatively low sequence homology with the other Gα proteins (Strathmann & Simon 1991). These proteins are involved in the modulation of small GTPases activity (Rho family), thus in regulation of the cell morphology (Suzuki et al. 2003). The Gα12/13 proteins are also shown to activate an extracellular signal regulated activated kinase (ERK) (Voyno-Yasenetskaya et al. 1996) and the Na^+/H^+ exchange (Voyno-Yasenetskaya et al. 1994).

1.2.1.5 Gβγ-mediated signaling cascades

The β and γ subunits of the G proteins can be considered as one functional unit due to their continuous tight interaction. The five known mammalian β-subunits are characterized by a high degree of amino acid sequence identity, whereas γ-subunits are considerably more diverse (Simon, Strathmann & Gautam 1991). The βγ-dimers do not only act as an anchor for Gα subunits to form the functional heterotrimer, they also possess regulatory functions, such as the regulation of the GIRK channels, the activation of the phospholipases C and A2, the activation of the MAPK, and the modulation of some isoforms of adenylate cyclase (reviewed by Marinissen & Gutkind 2001, Woehler & Ponimaskin 2009).

1.2.2 Multiplicity in G protein-coupling and functional selectivity

It is becoming generally accepted that a single GPCR has the ability to simultaneously activate multiple pools of related and even unrelated G proteins, both when expressed endogenously and following transfection into heterologous systems. Multiplicity in G protein-coupling is more frequently observed in artificial expression systems where usually high densities of receptors are present. This raises the question whether such complex signaling reveals artefactual promiscuous coupling or whether it is a genuine property of GPCRs (reviewed by Gudermann, Schöneberg & Schultz 1997, Hermans 2003, Milligan 1993). The emerging knowledge of such promiscuous G protein-coupling adds more complexity and flexibility to this signaling system. In some cases, a

single receptor was found to simultaneously activate members of three or even four unrelated classes of G proteins (reviewed by Hermans 2003 and depicted in Table 1).

Table 1 Typical examples of GPCRs showing multiplicity in G protein-coupling (modified from Hermans 2003)

receptor	**Gαs**	**Gαi/o**	**Gαq/11**	**Gα12/13**
β-Adrenergic	x	x		
Corticotropin-releasing hormone	x	x	x	
Metabotrophic glutamate (1a)	x	x	x	
Gonadotropin releasing hormone	x	x	x	
Melatonin		x	x	
Muscarinic (M1 and M3)	x	x	x	
Prostacyclin	x	x	x	
Prostaglandin (EP3D)	x	x		
Thyrotropin	x	x	x	x
Thrombin		x	x	x

However, although many GPCRs can mediate their effects by coupling to multiple G proteins, the majority of GPCRs only interacts with a definite subset or even a specific G protein heterotrimer (Wess 1997; Gudermann, Schöneberg & Schultz 1997). The 20 Gα-subunits, 6 Gβ-subunits and 12 Gγ-subunits theoretically may assemble to 1.440 combinations of Gαβγ-heterotrimers, but it has been demonstrated by several groups, that not all potential combinations are possible (Iñiguez-Lluhi et al. 1992; Pronin & Gautam 1992; Yan, Kalyanaraman & Gautam 1996). Considering the high homology in the G protein sequences (Simon, Strathmann & Gautam 1991), it is a challenging task to understand how a specific receptor can distinguish among these highly homologous G proteins. As reviewed by Wess (Wess 1998), all four intracellular domains have been indicated to be involved in G protein-coupling with the most significant regions being the second intracellular loop, and the amino and carboxyl portions of the third intracellular loop (Wess 1997).

Besides the mentioned GPCR-dependent coupling-specifity and -multiplicity there is accumulating evidence that some ligands are able to bias the functional response in a selective manner. These compounds, promoting functional selectivity, are also referred to as biased ligands (reviewed by Evans et al. 2010, Kenakin 2007, Kenakin & Miller 2010). The antipsychotic drug aripiprazole, for example, reveals functional selectivity at the dopamine D2 receptor (Urban et al. 2007). These *in vitro* data were proposed to explain its therapeutic efficacy, as under treatment with aripiprazole, the useful antipsychotic effects prevail the undesired motor side effects. Likewise, the hallucinogenic

action of selected psychoactive substances interacting with 5-HT receptors is expected to be associated with the differential activation of a subset of signaling cascades (Nichols 2004). Along with other studies, these experimental data emphasize the importance of the emerging concept of functional selectivity, which should lead to the development of drugs showing enhanced clinical efficacy with less unwanted side effects (reviewed by Bosier & Hermans 2007).

In case a GPCR shows independent coupling with multiple distinct G proteins, a ligand might reveal diverse intrinsic efficacies as it can simultaneously act as a full or partial agonist and inverse agonist, respectively, or as an antagonist, at one single receptor when in view of the different involved signaling pathways (referred to as “pluridimensional efficacy”, Kenakin 2011). At the molecular level, this observation is widely explained by considering that several active conformations of the receptor exist, which differ in their coupling preferences with distinct G proteins (reviewed by Kenakin 2003, Kenakin 2007, Kenakin 2011, Perez & Karnik 2005).

1.3 Classical and new roles of β-arrestin

Herman Kühn was the first to discover the soluble 48-kDa protein arrestin during studies on the deactivation of the rhodopsin receptor (Kühn & Wilden 1987). Some years later while studying homologous desensitization of β-adrenergic receptor, two different isoforms named β-arrestin1 (Lohse et al. 1990) and β-arrestin2 (Attramadal et al. 1992) were purified and characterized. There are four main members of the arrestin family. Visual arrestin (arrestin1) and cone arrestin (arrestin4) are predominantly localized in the retina, whereas β-arrestins 1 and 2 (arrestin2 and arrestin3) are ubiquitously expressed in various tissue types (Ferguson 2001).

1.3.1 Desensitization

The agonist-induced activation of GPCRs leads to a number of processes that can attenuate GPCR signal transduction. The early events of signaling by GPCRs, such as generation of second messengers (e.g. cAMP and inositol 1,4,5-trisphosphate), are usually rapidly attenuated by regulatory processes collectively known as receptor desensitization (reviewed by Chuang et al. 1996, Freedman & Lefkowitz 1996). Two major patterns of rapid GPCR desensitization can be distinguished based on the underlying mechanisms. Homologous desensitization describes the process whereby stimulation of a particular GPCR leads to desensitization of the activated receptor, whereas heterologous desensitization occurs when GPCR stimulation leads to desensitization of other types of GPCRs (Chuang et al. 1996). Under conditions of continued agonist exposure, the receptor must respond in a rapid manner to dampen its own persistent activation. An important component of desensitization, which occurs within seconds to minutes of receptor activation, is uncoupling of the activated receptor from its cognate heterotrimeric G proteins by receptor phosphorylation, followed by a rapid recruitment of arrestins, which associate with activated and phosphorylated GPCRs. The binding of arrestins sterically interdicts further interactions with G proteins and effectively terminates the signaling. This ‘arrest’ interaction was originally eponymous for arrestins (Ferguson et al. 1996, Ferguson 2001, Goodman et al. 1996, Laporte et al. 1999). A number of protein kinases have been

discovered to phosphorylate serine and threonine residues within the intracellular domains of GPCRs following agonist exposure, including the second messenger-dependent kinases such as cAMP-dependent protein kinase (PKA) and protein kinase C (PKC), as well as specific G protein-coupled receptor kinases (GRKs) (Ferguson & Caron 1998; Ferguson et al. 1998, Lefkowitz 1993, Pierce, Premont & Lefkowitz 2002). The GRK family members have been demonstrated to selectively phosphorylate agonist-activated receptors and therefore initiate homologous desensitization, which depends on their functional co-factors, the arrestins. Conversely, the second messenger-dependent protein kinases do not only phosphorylate agonist-activated GPCRs, but also indiscriminately phosphorylate receptors that have not been exposed to agonists; hence these protein kinases are involved in the process of heterologous desensitization (Lefkowitz 1993). Although most of the activated GPCRs are supposed to be phosphorylated prior to β-arrestin recruitment, it has been demonstrated that there exist receptors whereby β-arrestin binding is independent of receptor phosphorylation, such as the protease-activated receptor (PAR)-1 and leukotriene B4 receptors, respectively (Chen, Paing & Trejo 2004, Jala, Shao & Haribabu 2005).

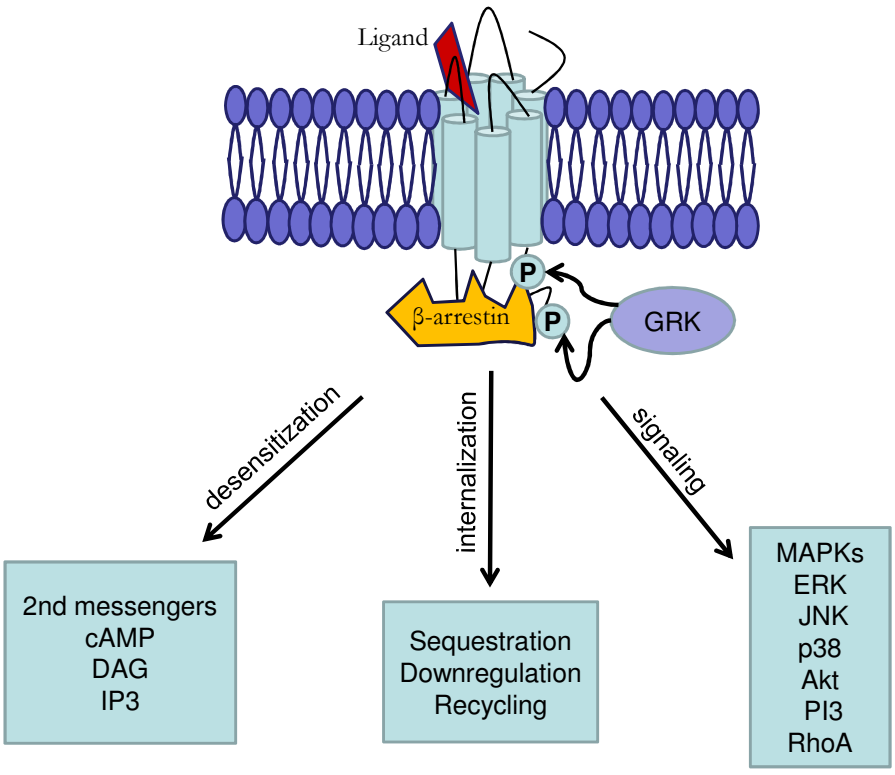

Figure 3 Classical and new roles of β-arrestin (modified from Lefkowitz & Shenoy 2005)
Following ligand-induced activation, GPCRs are phosphorylated (P) by kinases such as G protein-coupled receptor kinases (GRKs) resulting in binding of β-arrestins (1 and 2) to the phosphorylated third intracellular loops and carboxy-terminal tails. The presence of β-arrestins leads to a rapid desensitization due to steric hindrance of further G protein-coupling. In addition to their role as desensitizer, arrestins act as scaffolding proteins triggering the internalization of activated GPCRs to clathrin coated pits by interaction of the carboxy-terminal portions of arrestin with both the clathrin heavy chain and the β2-adaptin subunit of AP-2. These coated vesicles fuse with early endosomes where the receptors may be dephosphorylated by specific phosphatases and recycled back to the plasma membrane or targeted to lysosomes for degradation. Recent studies revealed furthermore that arrestins, acting as scaffold adaptors, are capable of initiating their own signaling cascade, such as extracellular signal-regulated kinase (ERK) and Src kinase.

1.3.2 Internalization

In addition to desensitization by steric hindrance, GPCRs are also sequestered into the cell by an agonist-dependent mechanism. The endocytosis of GPCRs to intracellular compartments is an important regulatory process for desensitization, recycling and down-regulation of GPCRs (Lefkowitz 1998). The prototypical and best-characterized agonist-induced internalization pathway of GPCRs is mediated through clathrin coated pits (reviewed by Ferguson 2001, Takei & Haucke 2001). This pathway requires the binding of arrestins; and due to their ability to bind simultaneously to agonist-occupied GPCRs and elements of the cellular endocytotic machinery, β-arrestins facilitate receptor endocytosis by clustering receptors within clathrin-coated pits. Following the association of β-arrestins with the phosphorylated receptor, GPCR-arrestin complexes migrate to clathrin-coated pits for subsequent endocytosis via the interaction of arrestin with both the heavy chain of clathrin (Goodman et al. 1996) and with the β2-adaptin subunit of the adaptor protein AP-2, which also interacts with clathrin (Laporte et al. 1999). After targeting to endosomal compartments, GPCRs can be rapidly de-phosphorylated and recycled back to the plasma membrane as fully functional receptors in a process known as resensitization and recycling, respectively, or are targeted to the lysosomal compartments for degradation, resulting in a down-regulation of cell surface expression.

Several studies from confocal microscopy have revealed that there are differences in the translocation kinetics of β-arrestin 1 and β-arrestin 2 to activated GPCRs, accordingly dividing them into two classes (A and B) based on their nature of internalization (Oakley et al. 1999, Oakley et al. 2000, Oakley et al. 2001). In the case of Class A receptors, β-arrestin 2 translocates to the receptor more readily than β-arrestin 1. This interaction is transient as β-arrestin rapidly dissociates from the receptor and does not co-internalize. The β2-adrenergic, mu opioid, endothelin type A and the D1 dopamine receptors are examples of GPCRs that belong to this class (Oakley et al. 2000). In contrast, Class B receptors including the AT1a angiotensin, vasopressin V2 and neurotensin receptor 1 have no preference for either β-arrestin isoform. Agonist activation of these receptors recruits β-arrestin into a stable association that is usually found in endosomes even after internalization. In addition to these different affinities for β-arrestin, the resensitization and recycling kinetics are much slower for Class B receptors than for Class A receptors (Oakley et al. 2000). The carboxyl tail appears to contain the molecular determinants that define these internalization properties as demonstrated by studies using chimeric GPCRs in which this region is exchanged between Class A and B receptors (Oakley et al. 2001).

1.3.3 Signaling

Initially, negative regulation of G protein signaling was the only known role for β-arrestins in GPCR regulation. Over the past decade, evidence has emerged that in addition to arrest ‘classical’ receptor-G protein signaling and to promote trafficking of activated receptors, β-arrestins are able to initiate their own signaling cascade, without the need of G proteins. The range of GPCR-coupled signaling systems that are engaged through the β-arrestins has grown rapidly. Receptor-stimulated activation of effectors such as the MAP kinases pathways, including extracellular signal-regulated kinase1/2

(ERK1/2), p38 kinase and c-Jun N-terminal kinase 3 (JNK3), as well as protein kinase B (AKT) and phosphatidylinositol 3-kinase (PI3K) pathways were reported (extensively reviewed by e.g. Pierce & Lefkowitz 2001, Luttrell & Lefkowitz 2002, Lefkowitz & Shenoy 2005, Reiter & Lefkowitz, DeWire et al. 2007, Defea 2008, Luttrell & Gesty-Palmer 2010).

The discovery that β-arrestins bind to a number of signaling proteins and are able to act as ligand-regulated scaffold proteins, further augmented the complexity of GPCR function. In general, these findings offer a multitude of new therapeutic opportunities. It opened access to develop ligands, which can uniquely activate or inhibit the β-arrestin-dependent pathway without affecting the G protein-dependent pathway. Such ligands are referred to as β-arrestin-biased ligands (in contrast to G protein-biased ligands), and dramatically change the current understanding of receptor agonism and antagonism, respectively. Such biased-ligands could more selectively target beneficial signaling and even block unwanted actions of receptor activation (e.g. side effects, tolerance or toxicity). A number of biased ligands for 7TMRs have been identified that selectively activate or counteract β-arrestins, and several of these seem to have distinct functional consequences when compared to traditional ligands (reviewed by Violin & Lefkowitz 2007, Rajagopal, Rajagopal & Lefkowitz 2010, Whalen, Rajagopal & Lefkowitz 2010).

The distinct nature of β-arrestin signaling was clearly demonstrated by the discovery of a perfectly biased ligand, Sar^{1}, Ile^{4}, Ile8- AngII (SII), an angiotensin AT1a receptor activator, that exclusively promotes β-arrestin recruitment and initiates signaling, such as mitogen-activated protein kinases extracellular signal-regulated kinase (ERK) 1/2, but fails to stimulate G protein-dependent signaling (Holloway et al. 2002, Wei et al. 2003, Violin et al. 2010). Further examples are the two β2-adrenergic receptor ligands propranolol and carvedilol, that act as partial inverse agonists with respect to Gαs activation, but as partial agonists for the ERK1/2 pathway through stimulation of β-arrestins (Azzi et al. 2003; Wisler et al. 2007; Drake et al. 2008). Recently, the selective histamine H4 receptor antagonist JNJ7777120 was shown to recruit β-arrestin to the H4 receptor, independent of G protein activation (Rosethorne & Charlton 2010). Besides biased activation of β-arrestin, there is also evidence about inhibition, such as the two CRTH2-antagonists that do not interfere with PGD2-initiated G protein-mediated signal transduction, but counteract the PGD2-promoted translocation of β-arrestin, and nevertheless were able to inhibit chemotactic activation of human eosinophilic granulocytes (Mathiesen et al. 2005). Another interesting observation regarding β-arrestin-mediated signaling, was the observation by Walters and coworkers, who demonstrated that the cutaneous flushing, a side effect of treatment with nicotinic acid, is promoted by activation of β-arrestin1, whereas the positive effects like elevation of high density lipoproteins (HDL) and decrease of triglycerides was mediated via Gαi/o-proteins (Walters et al. 2009). For a detailed summary of β-arrestin-biased ligands and their therapeutic potential see (Whalen, Rajagopal & Lefkowitz 2010).

Taken together, the change in the β-arrestin/GRK system over the last ten years revealed bifunctional properties, as there is on one side the desensitization mechanism, but on the other side simultaneously the G protein-independent signal transduction mechanism. This clearly highlights that

in order to fully characterize the molecular pharmacology of a GPCR it is necessary to consider the complete emerging spectrum of events induced upon ligand stimulation.

1.4 Orphan GPCRs

Recent genome sequencing projects and publicly available information on the human genome sequence revealed that approximately 720 sequences in the human genome belong to the GPCR family (Lander et al. 2001, Venter et al. 2001). It is assumed that half of the GPCRs are activated by sensory stimuli, whereas the other half can be regarded as potential drug targets (Fredriksson et al. 2003, Vassilatis et al. 2003). For about 145 out of these 360 GPCRs a defined endogenous relevant ligand is still lacking and nothing or only little is known about their physiological role (Wise, Jupe & Rees 2004). These uncharacterized heptahelical receptors are also referred to as “orphan GPCRs” and they provide a valuable and novel field of targets for the development of new drugs with unique therapeutic properties (Civelli 2005, Civelli et al. 2006). Strategies that were successfully employed and still applied as current methods to identify the endogenous ligand are reverse pharmacology (Civelli 2005, e.g. P2Y5, Pasternack et al. 2008), orphan receptor strategy (“tissue-extract based approach”) (Civelli et al. 2001, e.g. ORL-1 receptor, Reinscheid et al. 1995) and cross genome phylogenetic analyses (Metpally & Sowdhamini 2005, e.g. GPR55, Ryberg et al. 2007). Additional investigations as the determination of the expression pattern (e.g. GPR109B, Tunaru et al. 2003) and generation of knock-out mice (e.g. GPR85, Matsumoto et al. 2008) provide important information about physiological role and pathophysiological functions, respectively.

1.5 G protein-coupled receptor 17

In 1996, Raport et al. were the first to isolate the GPR17 gene (referred to as R12) by means of PCR using degenerated oligonucleotides based on regions conserved between interleukin-8 receptor (IL8RA) and the angiotensin II chemokine GPCR (Raport et al. 1996). Independently in 1998, Bläsius et al. identified novel P2Y nucleotide GPCRs by means of degenerated RT-PCR using primers of regions conserved between TM3 and TM7 of chicken P2Y1 and murine P2Y2 receptors (Bläsius et al. 1998). GPR17 cDNA was reported to undergo splicing events, yielding two different isoforms, which were designated as HIP4 and FB1, and which only differ by the length of the N-terminus. The short GPR17 isoform encodes a polypeptide with 339 amino acids with typical rhodopsin type 7TM motifs. The long isoform encodes a protein, where the N-terminus is 28 amino acids longer for a total length of 367 amino acids. The gene was localized to human chromosomal band 2q21 using fluorescence in situ hybridization (Bläsius et al. 1998).

1.5.1 Classification of GPR17 as dual nucleotide/lipid receptor is a controversial matter

Although GPR17 appears to be closely related to the P2Y family of GPCRs, Bläsius et al. (1998) stated that preliminary functional data, obtained by investigations of second messengers (IP1 and cAMP) in 1321N1 cells expressing GPR17, did not support the hypothesis that classical P2Y agonists serve as

ligands for this receptor (Bläsius et al. 1998). Controversially, 8 years later, Ciana et al. (2006) 'deorphanized' GPR17 as a dual uracil nucleotides/cysteinyl-leukotrienes receptor, which is consistent with its intermediate phylogenetic position between purinergic P2Y and cysteinyl-leukotriene (CysLT) receptors, as depicted in the phylogenetic tree (Figure 4). It was shown that stimulation with uracil nucleotides (UDP, UDP-glucose and UDP-galactose) and cysteinyl-leukotrienes (LTC4 and LTD4), resulted in specific and concentration-dependent responses. Confirmation for GPR17 functionality was established in different cellular backgrounds (1321N1, COS7, CHO and HEK293 cells), based on [^{35}S]GTPγS binding, cAMP inhibition assays as well as in single cell calcium imaging assays (Ciana et al. 2006).

Activation of GPR17 by uracil nucleotides and cysteinyl-leukotrienes was further reported by the same research group in several subsequent publications (Lecca et al. 2008, Temporini et al. 2009, Pugliese et al. 2009, Daniele et al. 2010, Calleri et al. 2010, Fumagalli et al. 2011).

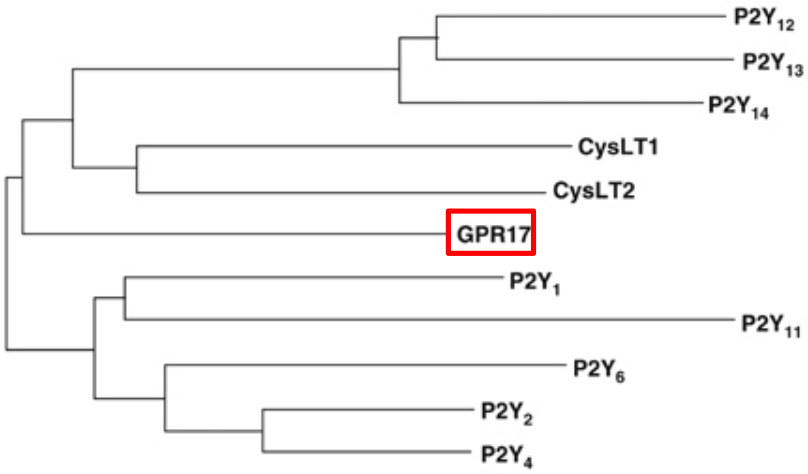

Figure 4 Phylogenetic tree (modified from Ciana et al. 2006)
Consistent to this phylogenetic tree, showing the relationship between GPR17 and P2Y and CysLT receptors, Ciana et al (2006) deorphanized GPR17 as a dualistic receptor responding to uracil nucleotides and cysteinyl-leukotrienes. However, this postulated characterization remains a contentious issue.

However, in our laboratory, these proposed endogenous ligands did not display any functional activity in different cell lines stably (1321N1, CHO and HEK293 cells) and transiently (HEK293), respectively, expressing the short isoform of GPR17 (PhD thesis of Andreas Spinrath, and informed personally by Lucas Peters, AK Kostenis). In agreement with our observations, the lack of activity of these ligands was further demonstrated by Maekawa et al., who postulated GPR17 to be a ligand-independent negative regulator of cysteinyl leukotriene receptor 1 (Maekawa et al. 2009). Additional, two independent laboratories were not able to reproduce GPR17 activation by LTD4 and LTC4, respectively, (Benned-Jensen & Rosenkilde 2010, Wunder et al. 2010), whereat Benned-Jensen et al. confirmed functional activity of uracil nucleotides (UDP, UDP-glucose and UDP-galactose) at GPR17. Furthermore, Benned-Jensen et al. observed that both GPR17 isoforms (short and long) were constitutively active through Gαi/o, based on CREB gene reporter assays as well as [^{35}S]GTPγS binding studies in transiently transfected HEK293 and 1321N1 cells, respectively. This ligand-independent activity of GPR17 has not been further proven by any other research group so far. Taken together,

deorphanization of GPR17 as a dual nucleotide/lipid receptor remains a controversial matter, and additional investigations are required to probe GPR17 pharmacology and function in more detail.

1.5.2 Expression patterns of GPR17

Bläsius and his working group were the first to report, that human GPR17 was expressed exclusively in brain, as 2.3- and 6.3-kb mRNAs, which was detected by northern blot analyses (Bläsius et al. 1998). In agreement with this publication, Ciana et al. published GPR17, human and rat, to be highly expressed in the brain as well as in other organs that may undergo ischemic damage, such as heart and kidney, with only little expression in the liver and lung, as determined by RT-PCR. In addition, human GPR17 was also found in HUVEC (human umbilical vein endothelial cells) and breast adenocarcinoma MCF7 cells (Ciana et al. 2006, Banfi et al. 2005). Benned-Jensen and Rosenkilde performed quantitative real time PCR analyses in eight different brain regions as well as whole brain, heart and kidney, in consideration of the two existing isoforms (short and long) (Benned-Jensen & Rosenkilde 2010). Examinations of both isoforms revealed lowest expression in thalamus, with progressively rising expression levels through the hypothalamus, cerebellum, amygdala cerebellar hemisphere, frontal cortex, hippocampus and striatum. The short isoform was predominantly expressed in the brain when compared to the long isoform (~10 fold higher), whereas heart and kidney revealed converse expression patterns, since the long splice variant was expressed at ~12-fold higher levels in the heart, while in the kidney the short isoform was completely absent (Benned-Jensen & Rosenkilde 2010). On the contrary, Pugliese et al. observed by RT-PCR that the long isoform was primarily detected in brain and not in the other tested human tissues (liver, kidney, lung, heart and skeletal muscle) or cell lines (HUVEC and the acute lymphocytic leukemia cells THP-1), which instead expressed the short isoform (Pugliese et al. 2009).

Upon physiological conditions, immunohistochemical analyses revealed that mouse and rat GPR17 was found to be expressed by pyramidal neurons, non-proliferating oligodendrocyte precursor cells (OPCs) and by ependymal cells lining the central canal, but never by astroglial cells in the adult CNS (Ciana et al. 2006, Lecca et al. 2008, Ceruti et al. 2009). Additionally human GPR17 was identified as one of the genes that are specifically expressed by hippocampal neuronal progenitor cells (NPCs) (Maisel et al. 2007). In contrast, Chen et al. described GPR17 to be restricted to the CNS (not heart, kidney, liver, lungs, smooth muscle, spleen, testes), and amongst neuronal cells limited to the oligodendrocyte lineage in the developing mouse CNS, with increasing expression levels until the beginning of the third postnatal week, followed by a decrease until adulthood (Chen et al. 2009). The restriction of GPR17 to very early differentiation stages of OPCs was further demonstrated by Fumagalli et al., where GPR17 was shown to be transiently upregulated at postnatal day 6, completely segregated from myelin markers such as the myelin basic protein (MBP). In primary rat postnatal OPCs, GPR17 was located on two subsets of slowly proliferating highly ramified $NG2^+$ pre-oligodendrocytes and its expression was turned down in morphologically mature myelinating cells (Fumagalli et al. 2011).

GPR17 was also reported to be expressed on $CD11c^+$ dendritic cells (Itagaki et al. 2009), mouse bone marrow-derived macrophages (Maekawa et al. 2009) and in nerve growth factor (NGF) induced rat pheocromocytoma cells (PC12) (Daniele et al. 2010).

Furthermore GPR17 was shown to be transiently upregulated on neurons (~24h) upon ischemic brain damages induced by middle cerebral artery occlusion (MCAo) model, in mouse and rat, followed (~48-72h) by an increase of GPR17 expressing microglia and macrophages recruited from distal parenchymal areas and moving towards the lesioned area. Starting from 72h after MCAo, OPCs expressing GPR17 were also significantly increased around the damaged zone (Ciana et al. 2006, Lecca et al. 2008). Additionally, GPR17 upregulation was observed in murine demyelinating lesions induced by experimental autoimmune encephalomyelitis (EAE) and in human multiple sclerosis plaques (Chen et al. 2009). Moreover, GPR17 was shown to be expressed on lymphocytic cells from patients with chronic lymphocytic leukemia (CLL) and its expression was reported to be associated with fast lymphocyte doubling time (Aalto et al. 2001).

Consequently, besides the mentioned tissue-specific expression pattern, GPR17 expression seems to be dependent on diverse physiological (development, maturation) as well as pathophysiological conditions (ischemic damage, demyelination, lymphocytic leukemia), which might be an explanation for the controversial GPR17 expression patterns published so far.

1.5.3 Current thoughts on the physiological role of GPR17

Although in the last years increasing information about GPR17 was reported, the clear physiological importance of the receptor remains rather elusive. The actual published knowledge about its potential role can be roughly divided into two main fields, specifically its impact on immune system and on neuronal dysfunctions, respectively, which will be further described in the following two chapters.

1.5.3.1 Role of GPR17 in allergic inflammations

The mouse receptor was reported to act as a ligand-independent negative regulator of the type 1 cysteinyl leukotriene receptor (CysLT1R) (Maekawa et al. 2009, Maekawa et al. 2010), which is known to exert a range of proinflammatory effects, possessing a clear role in pathophysiological conditions such as asthma and allergic rhinitis (reviewed by Capra et al. 2007, Rovati & Capra 2007). Cotransfection of GPR17 with CysLT1R in several cell lines (1321N1, CHO and HEK293T cells) completely suppressed CysLT1R-induced calcium flux and ERK phosphorylation upon activation with LTD4. Additionally, the binding of [^{3}H]LTD4 by cell membranes (CHO and 1321N1 cells) was suppressed by GPR17 cotransfection. Conversely, knock down of GPR17 in primary mouse bone marrow-derived macrophages by lentivirus infection with siRNA, clearly augmented CysLT1R expression, and likewise the calcium response to LTD4. The physiological evidence of this regulatory role was further demonstrated using GPR17-deficient mice, where CysLT1R-mediated vascular permeability in mast cell-mediated passive cutaneous anaphylaxis (PCA) was significantly increased (Maekawa et al. 2009). Additionally, GPR17 deficiency was shown to increase CysLT1R-initiated

pulmonary inflammation, inflammatory cell accumulation in the bronchoalveolar lavage (BAL) fluid, serum levels of total IgE and Th2/th17 cytokine expression in lungs upon challenge with house dust mites. These findings were shown to be completely abrogated in lungs from double knock-out mice, lacking GPR17 and CysLT1R, establishing a core role for both receptors (Maekawa et al. 2010).

1.5.3.1.1 Cysteinyl leukotriene receptor antagonists

The already marketed CysLT1R 'selective' antagonists ("lukasts") have been approved in various models of induced asthma as well as for the treatment of chronic asthma (reviewed by Brink et al. 2003, Capra et al. 2007). Zafirlukast (Accolate®, AstraZeneca) was the first CysLT1 receptor antagonist to be marketed in the USA (Krell et al. 1990); montelukast (Singulair, Merck &Co) has been introduced to market in 1998 for the treatment of asthma and allergic rhinitis (Jones et al. 1995); pranlukast is still waiting for a global extension of its commercialization and it is currently available only in Japan (Onon®, Ono Pharmaceutical) and Mexico (Azlaire®, Schering Plough corp). These antagonists are orally effective over a wide range of asthma severity, preventing the airway inflammatory response to cysteinyl-leukotrienes action as well as acting as bronchodilators to the leukotriene-induced bronchoconstriction. Preclinical and clinical studies have shown that montelukast, zafirlukast and pranlukast differ in terms of potency and pharmacokinetics, but possess comparable pharmacodynamic profiles (reviewed by Aharony 1998, Hay 1997). In Europe, leukotriene receptor antagonists (LTRA) are considered as third-line treatment and are intended as add-on therapy for patients already taking inhaled corticosteroids (reviewed by Capra et al. 2007).

Interestingly, the CysLT1 antagonists, montelukast and pranlukast were shown to functionally counteract LTD4-activated GPR17 signaling pathways. These observations were based on *in vitro* analyses of human (short and long isoform), rat and mouse GPR17 using [^{35}S]GTPγS binding and Gαi/o-cAMP assays as well as patch-clamp electrophysiological studies measuring receptor coupling to potassium channels (Ciana et al. 2006, Lecca et al. 2008, Pugliese et al. 2009, Fumagalli et al. 2011).

Furthermore, montelukast and pranlukast were reported to counteract calcium mobilization of nucleotide-activated P2Y receptors upon stimulation with UDP and UTP respectively (Mamedova et al. 2005).

1.5.3.2 Role of GPR17 for cerebral dysfunctions

Besides the reported role of GPR17 as a ligand-independent negative regulator of CysLT1R, GPR17 was shown to play key roles during brain damages. *In vivo* inhibition of GPR17 achieved either by pharmacological agents able to antagonize it's *in vitro* activation (e.g., montelukast or cangrelor) or by an anti-sense oligonucleotide specifically designed to knock-down the receptor, was examined in the middle cerebral artery occlusion (MCAo) model for ischemia, and resulted in an extensively reduced progression of cerebral ischemic damage (Ciana et al. 2006, Lecca et al. 2008). Likewise, the biotechnological knock-down of GPR17 by an antisense oligonucleotide strategy during spinal cord injury (SCI) clearly impaired tissue damages and ameliorated SCI-related motor deficits (Ceruti et al. 2009).

Furthermore, induction of brain damage and SCI was associated with spatiotemporal-dependent upregulation of GPR17 expression (Lecca et al. 2008, Ceruti et al. 2009). Initially, 24 h after MCAo, GPR17 was transiently upregulated by dying neurons within the ischemic core, colocalized with the cellular stress, injury and death marker heat shock protein 70 (HSP70). At later times after ischemia (48-72h after MCAo) GPR17 immuno-labeling appeared on microglia/macrophages infiltrating the lesioned area, whereas it should be noted that microglia were shown to play a neuroprotective role after ischemic stroke (reviewed by Jin, Yang & Li 2010). GPR17 was also found to be expressed on adult oligodendrocyte precursor cells that began to proliferate and express myelin specific genes, probably initiating remyelination in the peri-lesioned area (Lecca et al. 2008). Pharmacological manipulation of GPR17 with its proposed ligands (UDP-glucose, LTD4) promoted progression of preoligodendrocytes toward mature myelinating cells, suggesting a role of GPR17 in the transition between immature and myelinating oligodendrocytes (Lecca et al. 2008). Similar time-dependent regulations of GPR17 expression were reported after SCI (Ceruti et al. 2009). Additionally GPR17 was also found to be expressed on ependymal cells, which started proliferating and expressing multi-potential progenitor markers (GFAP and nestin), suggesting activation of repair mechanisms (Ceruti et al. 2009). Thus, GPR17 was claimed to play a dual and spatiotemporal-dependent role on the evolution of nervous system tissue damage and subsequent postinjury repair of damage in the brain and in spinal cord.

The role of GPR17 as a ‘sensor’ for pathological situations and a sensitizer for cell death was additionally confirmed by Ceruti et.al., as they demonstrated that only GPR17 expressing oligodendrocytes underwent massive cell death when exposed to high ATP concentrations (Ceruti et al. 2011).

Maisel et al. further have proven the potential role of GPR17 in long-term central nervous system (CNS) repair, since the receptor was identified as one out of three genes that are specifically expressed in adult hippocampal neuronal progenitor cells (NPCs), which are multipotent stem cells that can differentiate into all three types of the CNS (oligodendrocytes, neurons and astrocytes), thus possessing the potential to repair neurodegenerative disorders, such as stroke or multiple sclerosis (Maisel et al. 2007).

Additional evidence that GPR17 plays a role in CNS repair and development was provided by Daniele et al. It was presented that nerve growth factor (NGF) treated rat pheocromocytoma cells (PC12) express GPR17, and its stimulation with proposed GPR17 agonists (UDP-glucose, LTD4) promoted pro-survival neurotrophic effects and neurite outgrowth (Daniele et al. 2010).

Chen et al. also described GPR17 as an intrinsic regulator of oligodendrogliogenesis, but in contrast to the previously mentioned findings, they proposed that GPR17 might transmit extracellular signals to negatively regulate oligodendrocyte myelination (Chen et al. 2009). GPR17 was shown to be expressed in oligodendrocyte precursor cells (OPCs) in the developing mouse CNS with increasing expression levels until the beginning of the third postnatal week, but was down-regulated during the peak period of myelination and in adulthood. Over-expression of GPR17 either induced *in vitro* by transfection in primary wild type OPCs or *in vivo* by generation of transgenic mice with sustained

GPR17 over-expression, inhibited OPC differentiation into mature oligodendrocytes. Consequently, transgenic mice displayed typical features of CNS myelinating disorders such as generalized tremors, hind limb paralysis and seizures, and died early during the peak period of myelinogenesis at 3 weeks of age. Conversely, GPR17 knock-out mice revealed precocious onset of myelination and accelerated OPC differentiation (Chen et al. 2009). Furthermore, quantitative RT-PCR revealed that GPR17 was upregulated in demyelinating lesion induced by a mouse model of multiple sclerosis (experimental autoimmune encephalomyelitis (EAE)) and in human multiple sclerosis plaque tissue (Chen et al. 2009).

The role of GPR17 as a new timer for oligodendrogliogenesis was recently further proven by Fumagalli et.al., who explored the time-dependent changes of GPR17 during spontaneous *in vitro* OPC differentiation using purified OPCs isolated from rat cortex (Fumagalli et al. 2011). Immunocytochemistry as well as single cell real time PCR revealed that the presence of GPR17 was restricted to the first culture days, reaching a maximum around day 6 and was completely segregated from that of mature myelin. In contrast to postulations made by Chen et al., but in agreement with observations of Lecca et al., stimulation of OPCs with UDP-glucose promoted maturation of OPCs, whereas preincubation with cangrelor as well as biotechnological knock down of GPR17 with siRNAs delayed differentiation, thus establishing a mechanistic link between OPC differentiation and GPR17 (Chen et al. 2009, Fumagalli et al. 2011, Lecca et al. 2008).

Taken together, despite some controversial assertions, GPR17 can be regarded as a promising target for development of pharmacological inhibitors as anti-ischemic drugs able to counteract damage evolution in stroke and SCI, and as a new target for demyelinating diseases, such as multiple sclerosis.

1.6 Intention of this work

As mentioned above, deorphanization of GPR17 as a dual nucleotide/lipid receptor remains a controversial matter, and additional *in vitro* investigations are essential to probe GPR17 pharmacology and function in more detail. By means of a high throughput pharmacogenomic approach, our group has identified a synthetic small molecule agonist for GPR17 (here referred to as RA-II-150) that represents a precious pharmacological tool for further characterizations of ligand-dependent behaviors triggered by GPR17, especially as the postulated endogenous agonists remain disputable and likewise the previously uncovered signaling properties. Discovery of an activating ligand is a prerequisite to search for compounds that antagonize GPR17. Therefore, elucidation of the molecular mechanisms of signal transduction will not only help to better understand functionality of GPR17, but will additionally provide a basis for subsequent development of promising neuroprotective and regenerative drugs, which counteract GPR17-promoted signaling.

A first aim was to characterize signaling patterns of GPR17 upon activation with our small molecule agonist. Traditional second messenger assays based on HTRF® technology (cAMP, IP1) had to be established to analyze G protein-dependent signaling including Gαi/o, Gαs and Gαq pathways.

Additionally, GPR17-induced dynamic mass redistribution in living cells had to be examined by use of the Epic® system, a novel label-free technology to study GPCR functionality in real time and in a pathway unbiased but pathway-sensitive manner. Furthermore mechanistic insights into recruitment of β-arrestin to the activated GPR17 had to be investigated using a bioluminescence resonance energy transfer (BRET2)-based approach. Since cell surface expression as well as internalization upon agonist-stimulation constitute further common features of GPCRs, two approaches had to be established, namely indirect enzyme-linked immunosorbent assays (ELISA) and immunofluorescence analyses, respectively, both based on fixed whole cells.

Besides a CHO Flp-In™ T-REx™ cell line stably expressing the short isoform of GPR17, which was already available, additional GPR17 (short isoform) expressing cell lines had to be generated. Since no specific antibody for GPR17 was readily available, a sequence encoding a triple HA-epitope tag (haemagglutinin influenza virus epitope tag) had to be introduced in frame at the amino terminus of GPR17 to provide a useful tool for immunobiological analyses such as ELISA and immunofluorescence, respectively. Furthermore, to analyze β-arrestin recruitment, GPR17 had to be C-terminally tagged with Renilla luciferase (RLuc) using standard molecular biology techniques. Following the generation of distinct GPR17 expression plasmids (GPR17, 3xHA-GPR17, GPR17-RLuc, 3xHA-GPR17-RLuc), HEK293 cell lines were chosen as host cells to be stably transfected. For BRET2 analyses HEK293 cells stably expressing β-arrestin2 N-terminally tagged with GFP2, were generously provided by J. M. Mathiesen (Department of Medicinal Chemistry, University of Copenhagen).

After elucidating GPR17 signaling patterns in recombinant over-expressing cell lines, it was the intention to find a native cell line endogenously expressing GPR17 using Epic® technology, accordingly providing data more closely related to native GPR17 characteristics. Additionally, mouse embryonic stem cells had to be modified by heterologous recombination to knock-out the GPR17 gene, thus serving as a cellular tool for further differentiations into neuronal cells lacking GPR17.

Another intention was to examine the influence of increasing β-arrestin amounts on GPR17-mediated signaling patterns and internalization behavior upon agonist stimulation. Therefore, three HEK293 cell lines stably expressing varying amounts of β-arrestin2 (low, high and very high, generously provided by J. M. Mathiesen, Department of Medicinal Chemistry, University of Copenhagen) had to be stably cotransfected with GPR17, and subsequently investigated by means of all previously established functional assays (cAMP, IP1, Epic®, ELISA, immunofluorescence).

A final task was to analyze antagonistic properties of the postulated CysLT1R antagonists (montelukast, pranlukast, zafirlukast, MK571) on RA-II-150-induced GPR17 functional responses. As pranlukast was shown to possess the most promising potential to counteract GPR17-promoted signaling, the compound had to be further characterized regarding its pharmacological profile in all the functional settings described above (cAMP, IP1, Epic®, ELISA, immunofluorescence, BRET2.

2 Materials

2.1 Water purification

Solutions and media were prepared with purified water. A Milli-Q® Water System (Millipore, Eschborn) was employed for water purification (demineralization, dH_2O). For molecular and cell biological experiments, sterile UltraPure™ Distilled water (Gibco/Invitrogen™) was used.

2.2 Sterilization method

All heat stable materials, equipments, solutions and media were autoclaved in a Varioklav® (H+P Labortechnik AG, Oberschleißheim) at 121°C and 1.2 bar for 21 min. Temperature sensitive solutions and buffers were sterilized using sterile filter pore width 0.2 µl.

2.3 Chemicals

Table 2 Chemicals employed in the present work

abbreviation	substance	article number	company
C1	Agar	05040	Fluka
C2	Agarose UltraPure	15510027	Invitrogen™
C3	Albumin bovine essential fatty acid free	A6003	Sigma
C4	Ampicillin sodium salt	K029.1	Roth
C5	ATP	A6419	Sigma
C6	Atropine monohydrate sulfate salt	A0257	Sigma
C7	Bromophenol blue	18030	Fluka
C8	Calcium chloride, dihydrate	21097	Fluka
C9	Carbachol	212385	Merck
C10	Coelenterazine 400A	C-320-10	Gold Biotechnology
C11	DMSO	60153	Riedel-de Haen
C12	DMSO (cell culture)	A1584	AppliChem
C13	Dry milk blotting grade blocker, Non-fat dry milk	170-6404	Bio-Rad
C14	Ethylendiamine tetra acetic acid (EDTA)	CN06.3	Roth
C15	Ethanol absolute	08-205	KMF
C16	Ethidiumbromide 1%	2218.1	Roth
C17	Forskolin	1099	Tocris
C18	Gelatin	G2500	Sigma
C19	Glacial acetic acid 100%	00063.2511	Merck
C20	D-(+)-glucose	G7021	Sigma

abbreviation	substance	article number	company
C21	Glycerin 99%	11052	Grüssing GmbH
C22	Goat serum	S26-100ML	Millipore (Chemicon®)
C23	HEPES (*4-(2-hydroxyethyl)-1-piperazineethanesulfonic acid)*	54457	Fluka
C24	Hydrochloric acid min.37%	08-721	KMF
C25	3-Isobutyl-1-methylxanthine (IBMX)	2845	Tocris
C26	Magnesium chloride, hexahydrate	63072	Fluka
C27	Magnesium sulphate, hexahydrate	00627	Fluka
C28	Manganese(II) chloride tetrahydrate	T881.1	Roth
C29	MK571	10029	Cayman / Biozol
C30	Montelukast	10008318	Cayman / Biozol
C31	MOPS, 4-Morpholinepropanesulfonic acid	1254	Sigma
C32	Paraformaldehyde	0335.2	Roth
C33	Pertussis toxin (PTX)	2980	Sigma
C34	Poly-D-lysine hydrobromide	P6407	Sigma
C35	Potassium acetate	1.04820.1000	Merck
C36	Potassium chloride	12008	Grüssing GmbH
C37	Potassium dihydrogen phosphate	1.04873.5000	Merck
C38	Pranlukast	10008319	Cayman / Biozol
C39	Propan-2-ol	P-7507-15	Fisher Scientific
C40	Prostaglandin E1	13010	Cayman / Biozol
C41	Rubidium chloride	R-2252	Sigma
C42	Sodium acetate anhydrous	4555	Applichem
C43	Sodium chloride	12123	Grüssing GmbH
C44	Sodium dodecyl sulfate Pellets (SDS)	CN30.0	Roth
C45	Di-sodium hydrogen phosphate, anhydrous	71640	Fluka
C46	Sodium hydroxide	12156	Grüssing GmbH
C47	D(+) sucrose	84105	Fluka
C48	Sulfuric acid 95-97%	00731.2511	Merck
C49	3,3’,5,5’-Tetramethylbenzidine (TMB)	T8665	Sigma
C50	Tris	A2264	AppliChem
C51	Tris-HCl	90.90.3	Roth
C52	Triton X-100	93420	Fluka
C53	Tryptone	A1553	AppliChem
C54	Xylene cyanol	X4126	Sigma
C55	Yeast extract	2363.3	Roth
C56	Zafirlukast	10008282	Cayman / Biozol

2.4 Chemicals not acquired by purchase

Table 3 Chemicals not acquired by purchase

substance	function	source/reference
BIM-46187 (BIM)	reported as G protein pan-inhibitor	generous gift from Dr. Kaj Grandien, Sanofi Aventis (Ayoub et al. 2009)
RA-II-150	GPR17 agonist	synthesized by AK Müller, Pharmaceutical Chemistry, University of Bonn
YM 254890 (YM)	selective inhibitor of Gαq/11	provided by Prof. Dr. G Milligan, Faculty of Biomedical & Life Sciences, University of Glasgow, within a collaborative effort (Taniguchi et al. 2003)

2.5 Chemical structures of applied compounds

2.5.1 Small molecule GPR17 agonist

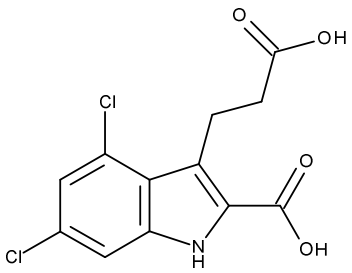

Figure 5 Chemical structure of RA-II-150
(provided by AK Müller, Pharmaceutical Chemistry, University of Bonn)

2.5.2 Potential GPR17 antagonists

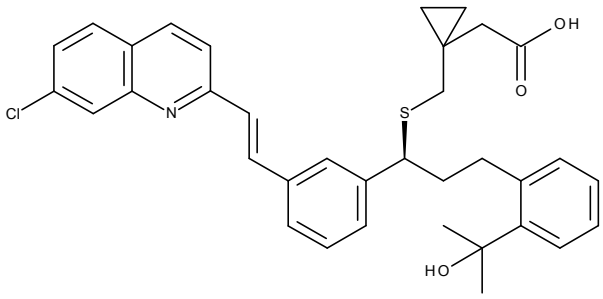

Figure 6 Chemical structure of montelukast (C30, Cayman / Biozol)

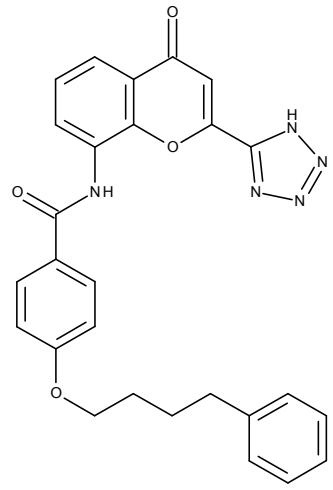

Figure 7 Chemical structure of pranlukast (C38, Cayman / Biozol)

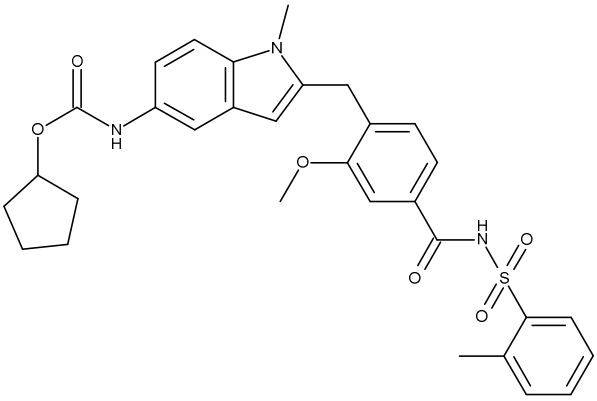

Figure 8 Chemical structure of zafirlukast (C56, Cayman / Biozol)

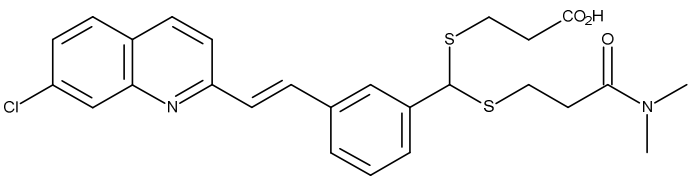

Figure 9 Chemical structure of MK571 (C29, Cayman / Biozol)

2.5.3 Pharmacological inhibitors

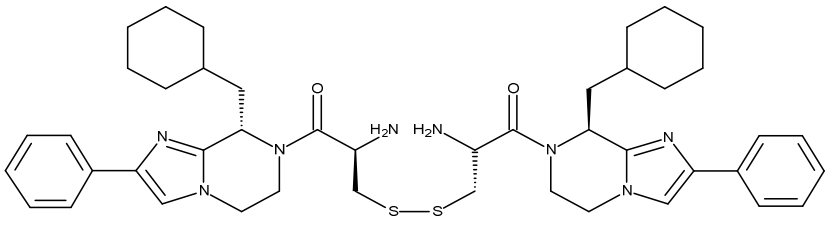

Figure 10 Chemical structure of BIM-46187 (Ayoub et al. 2009)

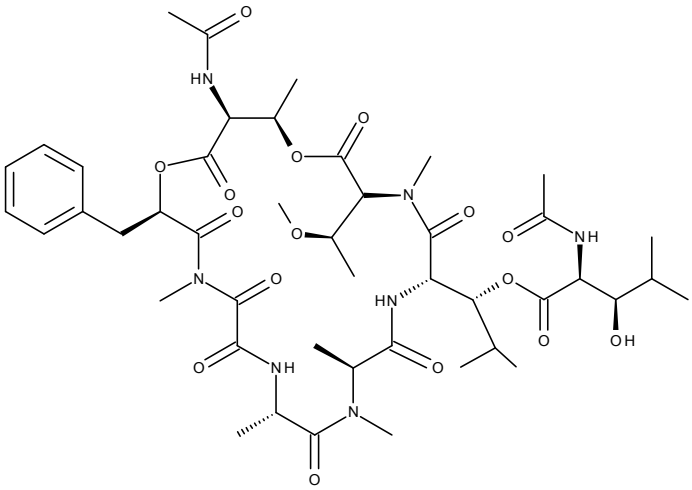

Figure 11 Chemical structure of YM 254890 (Taniguchi et al. 2003)

2.6 Buffer and solutions

S1 **Blotto** *(ELISA)*

	constituent	*amount*	*final concentration*
C13	Dry milk	1.5 g	3.0%
C52	Triton X-100	50 µl	0.1%
S22	Tris-HCl, 50 mM	ad 50 ml	-

Prepare Blotto always freshly before use. Dry milk is added to Tris-HCl and triton X-100 only if cell permeabilization is required.

S2 2 M Calcium Chloride *(calcium phosphate transfection)*

	constituent	*amount*	*final concentration*
C8	$CaCl_2$ x $2H_2O$	14.7 g	2 M
2.1	dH_2O	ad 50 ml	-

Sterilize via sterile filtration and store 10 ml aliquots at 2-8°C.

S3 DNA Loading dye buffer

	constituent	*amount*	*final concentration*
C7	Bromophenol blue	25 mg	0.25%
C54	Xylene cyanol	25 mg	0.25%
C47	Sucrose	4 g	4%
2.1	dH_2O	ad 10 ml	-

Dissolve constituents in dH_2O and store aliquots (1000 µl) at room temperature.

S4 Doxycycline (1 mg/ml)

	constituent	*amount*	*final concentration*
2.7.1	Doxycycline	1.0 mg	1 mg/ml
2.1	dH_2O	ad 1.0 ml	-

Dissolve 1 mg doxycycline in 1 ml dH_2O. Store at -20°C.

Note: Final receptor expression induction concentration: 1 µg/ml

S5 0.25 M / 0.5 M EDTA *(pH 8.0)*

	constituent	*amount*	*final concentration*
C14	EDTA	93.05 g / 186.1 g	0.25M / 0.5M
2.1	dH_2O	ad 1000 ml	-
C46	NaOH	q.s.	-

Adjust pH to 8.0 with NaOH (~20 g of NaOH pellets). EDTA will dissolve at pH 8.0. Correct volume to 1000 ml with dH_2O. Sterilize by autoclaving and store at room temperature.

S6 Ethanol (70%)

	constituent	*amount*	*final concentration*
C16	Ethanol absolute (96%)	730 ml	70%
2.1	dH_2O	ad 1000 ml	-

Store at RT.

S7 FIAU *(1-(2-Deoxy-2-fluoro-ß-D-arabinofuranosyl)-5-iodouracil, 0.2 mM)*

	constituent	*amount*	*final concentration*
2.7.1	FIAU	1.0 mg	0.2 mM
2.7.1	UltraPure™ Distilled water	ad 13.4 ml	-

Dissolve FIAU in cell culture grade water (UltraPure™ Distilled water) and sterilize via sterile filtration. Store aliquots (500 µl) at -20°C.

S8 Gelatin solution *(ES cell cultivation)*

	constituent	*amount*	*final concentration*
C18	Gelatin	2.0 g	1.0%
2.7.1	UltraPure™ Distilled water	ad 200 ml	-

Dissolve gelatin in cell culture grade water (UltraPure™ Distilled water). After autoclaved once, autoclave for a second time on the following day. Store stock solution at 4-8°C and freshly prepare working dilution (0.1% in UltraPure™ Distilled water).

S9 Goat serum blocking solution *(immunofluorescence)*

	constituent	*amount*	*final concentration*
C22	Goat serum	1.0 ml	.0
C3	BSA	100 mg	1%
C52	Triton X-100	50 µl	0.5%
S15	PBS	ad 10 ml	-

Prepare blocking solution always freshly before use. Goat serum and BSA are added to PBS and triton X-100 only if cell permeabilization is required.

S10 2X HBS *(calcium phosphate transfection)*

	constituent	*amount*	*final concentration*
C23	HEPES	5.95 g	50 mM
C43	NaCl	8.18 g	280 mM
C45	Na_2HPO_4	0.133 g	1.5 mM
2.1	dH_2O	ad 500 ml	-

Dissolve all constituents in 500 ml dH_2O. Sterilize via sterile filtration and store 50 ml aliquots at -20°C.

S11 10X HBS *(ES cell electroporation)*

	constituent	*amount*	*final concentration*
C20	D-Glucose	2.0 g	1.0%
C23	HEPES	10.0 g	20 mM
C36	KCl	0.74 g	50 mM
C43	NaCl	16.0 g	280 mM
C45	Na_2HPO_4	0.252 g	1.5 mM
2.7.1	UltraPure™ Distilled water	ad 200 ml	-

Dissolve all constituents in 180 ml UltraPure™ Distilled water and adjust pH to 7.2. Bring up to 200 ml and sterilize via sterile filtration. Store at -20°C. To prepare 1xHBS dilute with UltraPure™ Distilled water (1:10) to reach a pH of 7.05.

S12 1 M HEPES

	constituent	*amount*	*final concentration*
C23	HEPES	23.8 g	1 M
2.1	dH_2O	ad 10 ml	-
C46	NaOH	q.s.	-

Adjust pH to 7.2 with NaOH. Sterilize via sterile filtration and store 10 ml aliquots at -20°C.

S13 Lysis buffer *(DNA isolation from murine stem cells)*

	constituent	*amount*	*final concentration*
S22	1 M Tris-HCl	10 ml	0.1 M
S5	0.25 M EDTA	2 ml	0.025 M
S19	10% SDS	2 ml	1.0%
S18	1 M NaCl	20 ml	0.1 M
2.1	dH_2O	ad 100 ml	-

Dissolve all constituents in 80 ml dH_2O and adjust pH to 7.2 with NaOH (C46). Bring up to 100 ml and sterilize via sterile filtration and store 10 ml aliquots at -20°C.

S14 Paraformaldehyde solution *(fixation solution for ELISA and immunofluorescence)*

	constituent	*amount*	*final concentration*
C32	paraformaldehyde	8.0 g	4.0%
S15	PBS	ad 200 ml	-
C46	NaOH	q.s.	-

Add paraformaldehyde in 100 ml PBS (S15) and heat up to 60°C under a safety cabinet. Add NaOH to the white suspension and wait short period of time to dissolve the PFA. If solution does not clear add more NaOH and wait again. Repeat this procedure until solution is clear. Bring up to a total volume of 200 ml and store 10 ml aliquots at -20°C.

S15 Phosphate buffered saline *(1X PBS)*

	constituent	*amount*	*final concentration*
C36	KCl	0.2 g	2.7 mM
C37	KH_2PO_4	0.2 g	1.76 mM
C43	NaCl	8.0 g	137 mM
C45	Na_2HPO_4	1.44 g	10.0 mM
2.1	dH_2O	ad 1000 ml	-
C24	HCl	q.s.	-

Dissolve all constituents in 980 ml dH_2O and adjust pH to 7.4 with HCl. Correct volume with dH_2O up to 1000 ml. Sterilize by autoclaving. Store at RT.

S16 Poly-D-lysine solution *(fixation solution for cell culture)*

	constituent	*amount*	*final concentration*
C34	Poly-D-lysine	5.0 mg	0.1 mg / ml
2.1	dH_2O	ad 50 ml	-

Dissolve poly-D-lysine (PDL) in 50.0 ml dH_2O. Sterilize via sterile filtration and store at 2-8°C.

S17 3 M Sodium acetate *(precipitation of linearized plasmid DNA)*

	constituent	*amount*	*final concentration*
C42	Sodium acetate anhydrous	2.46 g	3 M
2.1	dH_2O	ad 10 ml	-

Dissolve sodium acetate in 8.0 ml dH_2O and adjust pH up to 5.1 with glacial acetic acid (C19). Sterilize via sterile filtration and store at RT.

S18 1 M Sodium chloride (NaCl)

	constituent	*amount*	*final concentration*
C43	NaCl	5.85 g	1 M
2.1	dH_2O	ad 100 ml	-

Dissolve NaCl in dH_2O. Store at RT.

S19 10% Sodium dodecyl sulphate (SDS)

	constituent	*amount*	*final concentration*
C44	SDS	10.00 g	10.0%
2.1	dH_2O	ad 100 ml	-

Dissolve SDS in dH_2O. Store at RT.

S20 TE buffer *(calcium phosphate transfection)*

	constituent	*amount*	*final concentration*
C51	Tris-HCl	0.61 g	10 mM
C14	EDTA	0.19 g	1 mM
2.1	dH_2O	ad 500 ml	-

Dissolve constituents in dH_2O and sterilize via sterile filtration. Store aliquots of 50 ml at -20°C.

S21 Tris-Acetate-EDTA *(50X TAE-buffer)*

	constituent	*amount*	*final concentration*
C50	Tris	242 g	2 M
C19	Glacial acetic acid	57.1 ml	5.71%
S5	0.5 M EDTA (pH 8.0)	100 ml	0.05 M
2.1	dH_2O	ad 1000 ml	-

Mix Tris base with stir bar to dissolve in about 600 ml of dH_2O. Add EDTA and glacial acetic acid and bring up to a final volume of 1000 ml with dH_2O. Store at RT.
Note: Final (1x) working concentration: 0.04 M Tris-acetate and 0.001 M EDTA

S22 50 mM / 1 M Tris-HCl

	constituent	*amount*	*final concentration*
C50	Tris	0.605 g / 12.11 g	50 mM / 1 M
2.1	dH_2O	ad 100 ml	-
C24	HCl (37%)	q.s.	-

Dissolve Tris in 80 ml dH_2O and adjust pH with HCl up to 7.4. Store at RT.

2.7 Media and solutions for cell culture

2.7.1 Buffer, media and supplements

Table 4 Cell culture buffer, media and supplements

name	article number	source
Blasticidin	ant-bl-1	InvivoGen
Dulbecco's Modified Eagle Medium (DMEM)	41965	Gibco/Invitrogen™
Dulbecco's Modified Eagle Medium: Nutrient Mixture F-12 (DMEM/F12)	21331	Gibco/Invitrogen™
Doxycycline hyclate	D9891	Sigma
ES cell qualified fetal bovine serum (Mexiko)	10439024	Gibco/Invitrogen™
ESGRO® (10^7 Units) *LIF= leukemia inhibitory factor*	ESG1107	Chemicon®
FIAU *1-(2-Deoxy-2-fluoro-ß-D-arabinofuranosyl)-5-iodouracil*	M251	Moravek Biochemicals
G418, liquid (Geneticin, 100mg/ml)	Ant-gn-5	InvivoGen
Hank's balanced salt solution (HBSS)	14025050	Gibco/Invitrogen™
Hygromycin B, liquid	10687010	Gibco/Invitrogen™

name	article number	source
L-Glutamine, 200 mM, liquid	25030	Gibco/Invitrogen™
2-Mercaptoethanol, 50 mM	31350010	Gibco/Invitrogen™
Minimum Essential Medium (MEM)	31095029	Gibco/Invitrogen™
MEM Non Essential Amino Acids Solution	11140035	Gibco/Invitrogen™
Nutrient Mixture Kaighn's Modification (F-12K)	21127022	Gibco/Invitrogen™
Penicillin-Streptomycin solution	15140130	Gibco/Invitrogen™
RPMI 1640	21875034	Gibco/Invitrogen™
Sera Plus special processed FBS	3702-P290616	PAN™ Biotech GmbH
Sodium pyruvate, 100 mM, liquid	11360	Gibco/Invitrogen™
Trypsin / EDTA (0.05%/0.02%)	P10-02318P	PAN™ Biotech GmbH
Trypsin, 0.25% (1x) with EDTA 4 Na, liquid	25200	Gibco/Invitrogen™
UltraPure™ Distilled water	10977	Gibco/Invitrogen™
Zeocin™	R25001	Invitrogen

2.7.2 Cell specific culture Media

Table 5 CHO-K1 cell culture medium

constituent	volume [ml]	final concentration
Dulbecco's Modified Eagle Medium: Nutrient Mixture F-12 (DMEM/F12)	500	
Fetal calf serum (FCS)	50	~10%
Penicillin-Streptomycin	5	~100 U/ml Penicillin, 0.1 mg/ml Streptomycin

Split ratio: 1:5 to 1:20 every 2-5 days

Table 6 CHO-FITR-GPR17 cell culture medium

constituent	volume [ml]	final concentration
Dulbecco's Modified Eagle Medium: Nutrient Mixture F-12 (DMEM/F12)	500	
Fetal calf serum (FCS)	50	~10%
Penicillin-Streptomycin	5	~100 U/ml Penicillin, 0.1 mg/ml Streptomycin
Blasticidin	1.7	30 µg/ml
Hygromycin	2.75	500 µg/ml

Split ratio: 1:5 to 1:20 every 2-5 days
The Flp-In T-Rex (FITR) system allows the generation of stable mammalian cell lines exhibiting tetracycline-inducible expression of a gene of interest from a specific genomic location. GPR17 expression is induced by addition of doxycycline (S4, final induction concentration: 1 µg/ml) into the culture medium for 14-20 h.

Table 7 COS-7 cell culture medium

constituent	volume [ml]	final concentration
Dulbecco's Modified Eagle Medium (DMEM)	500	
Fetal calf serum (FCS)	50	~10%
Penicillin-Streptomycin	5	~100 U/ml Penicillin, 0.1 mg/ml Streptomycin

Split ratio: 1:3 to 1:10 every 2-4 days

Table 8 HaCat cell culture medium

constituent	volume [ml]	final concentration
RPMI 1640	500	
Fetal calf serum (FCS)	50	~10%
Penicillin-Streptomycin	5	~100 U/ml Penicillin, 0.1 mg/ml Streptomycin

Split ratio: 1:2 to 1:10 every 2-5 days (0.25% trypsin needed)

Table 9 HEK293 cell culture medium

constituent	volume [ml]	final concentration
Dulbecco's Modified Eagle Medium (DMEM)	500	
Fetal calf serum (FCS)	50	~10%
Penicillin-Streptomycin	5	~100 U/ml Penicillin, 0.1 mg/ml Streptomycin

Split ratio: 1:3 to 1:20 every 2-4 days

Table 10 HEK-GFP2-β-arrestin2 cell culture medium *(HEK-BRET)*

constituent	volume [ml]	final concentration
Dulbecco's Modified Eagle Medium (DMEM)	500	
Fetal calf serum (FCS)	50	~10%
Penicillin-Streptomycin	5	~100 U/ml Penicillin, 0.1 mg/ml Streptomycin
G418	2.5	2.2 mg/ml

Split ratio: 1:2 to 1:20 every 2-4 days

Table 11 HEK-3xHA-GPR17 / HEK-3xHA-GPR17-RLuc cell culture medium

constituent	volume [ml]	final concentration
Dulbecco's Modified Eagle Medium (DMEM)	500	
Fetal calf serum (FCS)	50	~10%
Penicillin-Streptomycin	5	~100 U/ml Penicillin, 0.1 mg/ml Streptomycin
Zeomycin	0.31	56 µg/ml

Split ratio: 1:2 to 1:20 every 2-4 days

Table 12 HEK-GFP2-β-arrestin2-3xHA-GPR17-Rluc *(HEK-BRET-GPR17)*

constituent	volume [ml]	final concentration
Dulbecco's Modified Eagle Medium (DMEM)	500	
Fetal calf serum (FCS)	50	~10%
Penicillin-Streptomycin	5	~100 U/ml Penicillin, 0.1 mg/ml Streptomycin
G418	2.5	2.2 mg/ml
Zeomycin	0.31	56 µg/ml

Split ratio: 1:2 to 1:20 every 2-4 days

Table 13 Jurkat cell culture medium

constituent	volume [ml]	final concentration
RPMI 1640	500	
Fetal calf serum (FCS)	50	~10%
Penicillin-Streptomycin	5	~100 U/ml Penicillin, 0.1 mg/ml Streptomycin
Sodium pyruvate	5	2 mM

Split ratio: 1:2 to 1:3 every 2-3 days

Table 14 PC-3 cell culture medium

constituent	volume [ml]	final concentration
Nutrient Mixture Kaighn's Modification	500	
Fetal calf serum (FCS)	50	~10%
Penicillin-Streptomycin	5	~100 U/ml Penicillin, 0.1 mg/ml Streptomycin

Split ratio: 1:3 to 1:10 every 3-5 days

Table 15 SK-N-MC cell culture medium

constituent	volume [ml]	final concentration
Minimum Essential Medium (MEM)	500	
Fetal calf serum (FCS)	50	~10%
Penicillin-Streptomycin	5	~100 U/ml Penicillin, 0.1 mg/ml Streptomycin
Sodium pyruvate	5	2 mM

Split ratio: 1:3 to 1:6 every 3-5 days

Table 16 U2OS cell culture medium

constituent	volume [ml]	final concentration
Dulbecco's Modified Eagle Medium (DMEM)	500	
Fetal calf serum (FCS)	50	~10%
Penicillin-Streptomycin	5	~100 U/ml Penicillin, 0.1 mg/ml Streptomycin
Sodium pyruvate	5	2 mM
MEM non-essential amino acids solution	5	0.1 mM

Split ratio: 1:3 to 1:6 every 2-4 days

2.8 Characteristics of analyzed cell lines

Table 17 Cell lines used in the present work

name	characteristics	reference number
A431	Human epidermoid carcinoma Adherent epithelial cells	CRL-1555
ACHN	Human renal adenocarcinoma Adherent epithelial cells	CRL-1611
CHO-GPR17	Chinese hamster ovary Stable, inducible GPR17 expression cell line based on Flp-In™ T-Rex™ system	Generously provided by A. Spinrath (AK Kostenis)
CHO-K1	Chinese hamster ovary Adherent epithelial cells	CCL-61
COS-7	Green African Monkey kidney Adherent fibroblastoid cells	CRL-1651
DU-145	Human prostate carcinoma derived from brain metastasis Adherent epithelial cells	HTB-81

name	characteristics	reference number
Hacat	Human keratinocytes	CCL-228
	Adherent epithelial cells	
HEL-299	Human lung	CCL 137
	Adherent fibroblastoid cells	
HEK293	Human embryonic kidney	CRL-1573
	Adherent fibroblastoid cells	
HFF-1	Human skin / foreskin	SCRC-1041
	Adherent fibroblastoid cells	
HUVEC-2	Human umbilical cord	354151
	Adherent epithelial cells	
Jurkat	Human T cell leukemia	CRL-2063
	Suspension lymphoblastoid cells	
Keratinocytes	Human primary skin cells	kindly provided by Ralf Schröder (AK Kostenis)
Neutrophils	Human primary suspension cells	kindly provided by Stefanie Blättermann (AK Kostenis)
NHI 3T3L1	Murine embryonic cells	CL-173
	Adherent fibroblastoid cells	
PC-3	Human prostate adenocarcinoma	CRL-1435
	Adherent epithelial cells	
RMS13	Human muscle rhabdomyosarcoma	CRL-2061
	Adherent fibroblastoid cells	
SW-620	Human lymph node colorectal adenocarcinoma	CCL-227
	Adherent epithelial cells	
SW-872	Human liposarcoma	HTB-92
	Adherent fibroblastoid cells	
U2OS	Human bone osteosarcoma	HTB-96
	Adherent epithelial cells	
U-87MG	Human glioblastoma/astrocytoma	HTB-14
	Adherent epithelial cells	
UMR-106	Rat bone osteosarcoma	CRL-1661
	Adherent epithelial cells	

2.9 Media and solutions for bacteria culture

2.9.1 Generation of rubidium chloride competent bacteria

RB1 Rubidium chloride solution 1

	constituent	*amount*	*final concentration*
C35	KAc	0.088 g	30 mM
C28	$MnCl_2$ x 4 H_2O	0.297 g	50 mM
C41	RbCl	0.363 g	100 mM
C8	$CaCl_2$ x 2 H_2O	0.044 g	10 mM
C21	Glycerin	4.5 ml	15.0%
2.1	dH_2O	ad 30 ml	-

Adjust pH to 5.8 with HCl (C24). Sterilize via sterile filtration and store at RT.

RB2 Rubidium chloride solution 2

	constituent	*amount*	*final concentration*
C41	RbCl	0.012 g	10 mM
C8	$CaCl_2$ x 2 H_2O	0.110 g	75 mM
C31	MOPS	0.021 g	10 mM
C21	Glycerin	1.5 ml	15.0%
2.1	dH_2O	ad 10 ml	-

Adjust pH to 6.8 with HCl (C24). Sterilize via sterile filtration and store at RT.

RB3 1 M $MgCl_2$

	constituent	*amount*	*final concentration*
C26	$MgCl_2$ x 6 H_2O	2.033 g	1 M
2.1	dH_2O	ad 10 ml	-

Sterilize by autoclaving. Store at 2-8°C

RB4 1 M $MgSO_4$

	constituent	*amount*	*final concentration*
C27	$MgSO_4$ x 6 H_2O	2.285 g	1 M
2.1	dH_2O	ad 10 ml	-

Sterilize by autoclaving. Store at 2-8°C

RB5 Super optimal broth (SOB medium)

	constituent	*amount*	*final concentration*
C53	Tryptone	6.0 g	2.0%
C55	Yeast extract	1.5 g	0.5%
C43	NaCl	0.175 g	10 mM
C36	KCl	0.055 g	2.5 mM
RB3	1 M $MgCl_2$	3.0 ml	10 mM
RB4	1 M $MgSO_4$	3.0 ml	10 mM
2.1	dH_2O	ad 300 ml	-

Dissolve tryptone, yeast extract, NaCl and KCl in Milli-Q water and sterilize by autoclaving. Store at 2-8°C. Add $MgCl_2$ and $MgSO_4$ solutions directly before use.

2.9.2 Transformation and cultivation

T1 1000 x Ampicillin

	constituent	*amount*	*final concentration*
C4	Ampicillin	1.0 g	0.1 µg/µl
2.1	dH_2O	ad 10 ml	-

Sterilize via sterile filtration and store 1 ml aliquots at -20°C.

T2 LB agar (Luria Bertani agar)

	constituent	*amount*	*final concentration*
C53	Tryptone	10 g	1.0%
C55	Yeast extract	5 g	0.5%
C43	NaCl	10 g	1.0%
C1	Agar	15 g	1.5%
2.1	dH_2O	ad 1000 ml	-
C46	NaOH	q.s.	

Dissolve tryptone, yeast extract and NaCl in 800 ml in Milli-Q water and adjust pH to 7.5 with NaOH. Add agar into solution in a microwave and adjust volume to 1000 ml with Milli-Q water. Sterilize by autoclaving

T3 LB medium (Luria Bertani medium)

	constituent	*amount*	*final concentration*
C53	Tryptone	10 g	1.0%
C55	Yeast extract	5 g	0.5%
C43	NaCl	10 g	1.0%
2.1	dH_2O	ad 1000 ml	-
C46	NaOH	q.s.	

The LB-medium according to Luria Bertani is a complex or undefined medium. The exact composition is not known, as its constituents are for itself complex mixtures. Tryptone provides mainly amino acids and small peptides, whereas yeast extract contains nitrogen, sugar as well as organic and anorganic nutrients. Additionally sodium chloride is added.

Adjust the pH to 7.4 with NaOH and fill it up to 1000 ml with Milli-Q water. Sterilize by autoclaving.

T4 S.O.C. medium (Invitrogen™ #15544.034)

2% tryptone
0.5% yeast extract
10 mM sodium chloride
2.5 mM potassium chloride
10 mM magnesium chloride
10 mM magnesium sulfate
20 mM glucose

2.10 Bacterial strains

Table 18 Bacterial strains employed in the present work

name	function	company
NEB 10-beta Competent *E. coli*	Chemically competent *E. coli* cells suitable for high efficiency transformation (targeting vector)	New England BioLabs # C3019I
XL1-Blue Competent Cells	Host strain for routine cloning applications using plasmids	Agilent Technologies #200249

2.11 Consumables

Table 19 Consumables

consumable	article number	source
cAMP assay plate (low volume, 384 well)	784080	Greiner
Cell culture flasks 25 / 75 / 175 cm^2, TC	430168 / 430729 / 431079	Corning
Centrifuge tubes 15 ml / 50 ml	430791 / 430829	Corning
Combitips plus 2.5 / 5.0 / 10.0 / 25.0 ml	0030 069. 447/455/463/390	Eppendorf
Costar® 6 / 12 / 24 / 48 well clear TC-treated multiple well plates	3506 / 3512 / 3527 / 3548	Corning
Cryogenic vials (2.0ml)	5000-1020	Nalgene® *Thermo Fisher Scientific*
Culture dishes 21 / 55cm^2, TC	430166 / 430167	Corning
Disposable filter unit 0.2 µl	FB30/0.2 CA-s	Whatman®
ELISA microplate (96 well)	9017	Corning
Epic compound plate (384 well)	3657	Corning
Filter tips SSNC 10 / 20 / 200 / 1000 µl	B95012 / B95020 / B 90222 / B95210	Bioplastics BV
Gene Pulser® cuvette 0.4 cm electrode	165-2088	Bio-Rad
Immunofluorescence microplate (96well)	6005050	Perkin Elmer®
Incubation tube, PP	294718727	Labomedic
Microtubes snap-lock		
1.5 ml	115105	Labomedic
2.0 ml	115106	Labomedic
Parafilm™	1447011	Labomedic
Pasteur pipettes, glass	447016	Labomedic
Pasteur pipettes, PP, sterile	297804239	Labomedic
PCR tubes, 200 µl	0030 124.332	Eppendorf
Pipette tips		
Oxygen crystal tips 10 µl	110727	Labomedic
Yellow 200 µl tips	70.760.002	Sarstedt
Blue 1000 µl tips	686290	Greiner bio-one
Ritips professional 0.1 / 0.5 ml	40007 – 0000 / 0003	Ritter GmbH
Reagent reservoirs	4870	Corning
Stripette® serological pipettes, 2 / 5 / 10 / 25 / 50 ml	4486 – 4490	Corning

2.12 Enzymes and molecular weight markers

Table 20 Molecular biology enzymes and molecular weight markers

enzyme	product number	manufacturer
Antarctic Phosphatase	M0289S	NEB
BamHI	R0136S	NEB
EcoRI	R0101S	NEB
GoTaq Flexi DNA Polymerase	M8305	Promega
HindIII	R0104S	NEB
10xLong PCR buffer with $MgCl_2$	Out of K0201	Fermentas
NcoI	R0193S	NEB
NheI	R0131S	NEB
NotI	R0189S	NEB
1 kb DNA Ladder	N3232	NEB
100 bp DNA Ladder	N3231	NEB
Pfu DNA Polymerase	M7741	Promega
Proteinase K	82560	Fluka
PstI	R0140S	NEB
SacI	R0156S	NEB
SalI	R0138S	NEB
StuI	R0187S	NEB
T4 DNA Ligase	M0202S	NEB
XbaI	R0145S	NEB
XhoI	R0146S	NEB

2.13 Molecular and cellular biological Kits

Table 21 Kits applied in this work

abbreviation	Kit	article number	company
K1	QIAquick® Gel Extraction Kit	28706	QIAGEN GmbH
K2	QIAprep® Spin Miniprep Kit	27106	QIAGEN GmbH
K3	NucleoBond® Xtra Maxi	740414.50	Macherey-Nagel
K4	cAMP dynamic 2 HTRF® assay kit	62AM4PEC	Cisbio Bioassays
K5	IP-One HTRF® assay kit	62P1APEB	Cisbio Bioassays

2.14 Oligonucleotides

All applied oligonucleotide primers were synthesized by Invitrogen/Illumina collaboration. The deoxynucleotides were reconstituted in UltraPure™ Distilled water to obtain 100 µM stock solutions.

2.14.1 Cloning primers

abbreviation	sequence (5'-3')	function
PC1	GAAGGATCCCGGAGTGCCTGACTTGTGGT	short arm BamHI forward (TV)
PC2	CAAGAATTCGTTCTTACTTTTGAGAATTA	short arm EcoRI reverse (TV)
PC3	GAATTGCGGCCGCGAGCATGTGGGGTATCCG	long arm NotI forward (TV)
PC4	GAATTCTCGAGCACCGTTCAGTCTATGTG	long arm XhoI reverse (TV)
PC5	CTGAAGCTTATGAATGGCCTTGAA	hGPR17 HindIII forward
PC6	CTTCTCGAGTCACAGCTCTGACTT	hGPR17 XhoI reverse
PC7	GAAGCTAGCGACTCTAGAATGTAC	3xHA-tag NheI forward
PC8	CACTTCAAGGCCATTGTTTTGCTGACTCGA	3xHA-tag hGPR17 reverse

2.14.2 Sequencing primers *(targeting vector)*

abbreviation	sequence (5' to 3')	function
PS1	AACCCTCACTAAAGGGAACA	long arm forward 1
PS2	TCAGCCACCATCTGAAGCTT	long arm reverse 1
PS3	TACCGCCCAGACTTTGCTTA	long arm forward 2
PS4	ATTCGCCAACTTAAAACTCC	long arm reverse 2
PS5	CTTTGGGGGACAGAAGCTT	long arm forward 3
PS6	AGCATGTGGTGACCGCTCTA	long arm reverse 3
PS7	CCTTCATCTTAAGACTCAGT	long arm forward 4
PS8	GCCTTGGGAAAAGCGCCTCC	long arm reverse 4
PS9	CTTCATTCTCAGTATTGTTT	short arm forward 1
PS10	GCAAGCCAACACTAAAAGAC	short arm reverse 1
PS11	AAACGACTCCCCATAGGTC	short arm forward 2
PS12	AAGCGCATGCTCCAGACTGC	short arm reverse 2

2.14.3 Screening primers *(homologous recombination)*

abbreviation	sequence (5' to 3')	function
PScr1	CGGAACTTCTCAGCCACAA	long arm forward 1st
PScr2	ACCCTGTCAAGTCCCTCAAG	wild type reverse 1st
PScr3	TCCATCTTGTTCAATGGCCG	knock-out reverse 1st
PScr4	TCAAGAGACCGGGTGCAGGTG	outside of homologous regions forward
PScr5	CAGCTCATTCCTCCCACTCATGAT	neomycin resistance (knock-out) reverse

2.15 Antibodies

Table 22 Employed antibodies in the present work

abbreviation	antibody	article number	source
A1	Anti-HA (0.4 mg/ml) Mouse monoclonal antibody (clone 12CA5) to a peptide epitope derived from the haemagglutinin protein of human influenza virus	11583816001	Roche
A2	Anti-Mouse IgG (whole molecule) horse radish peroxidase antibody produced in goat (affinity isolated antibody)	A4416	Sigma
A3	Alexa Fluor 546 goat anti-mouse IgG (y2b), 2 mg/ml	A 21143	Invitrogen™

2.16 Recombinant plasmid maps of hGPR17

These plasmid maps represent hGPR17-expression plasmids, which were self-engineered during the present thesis.

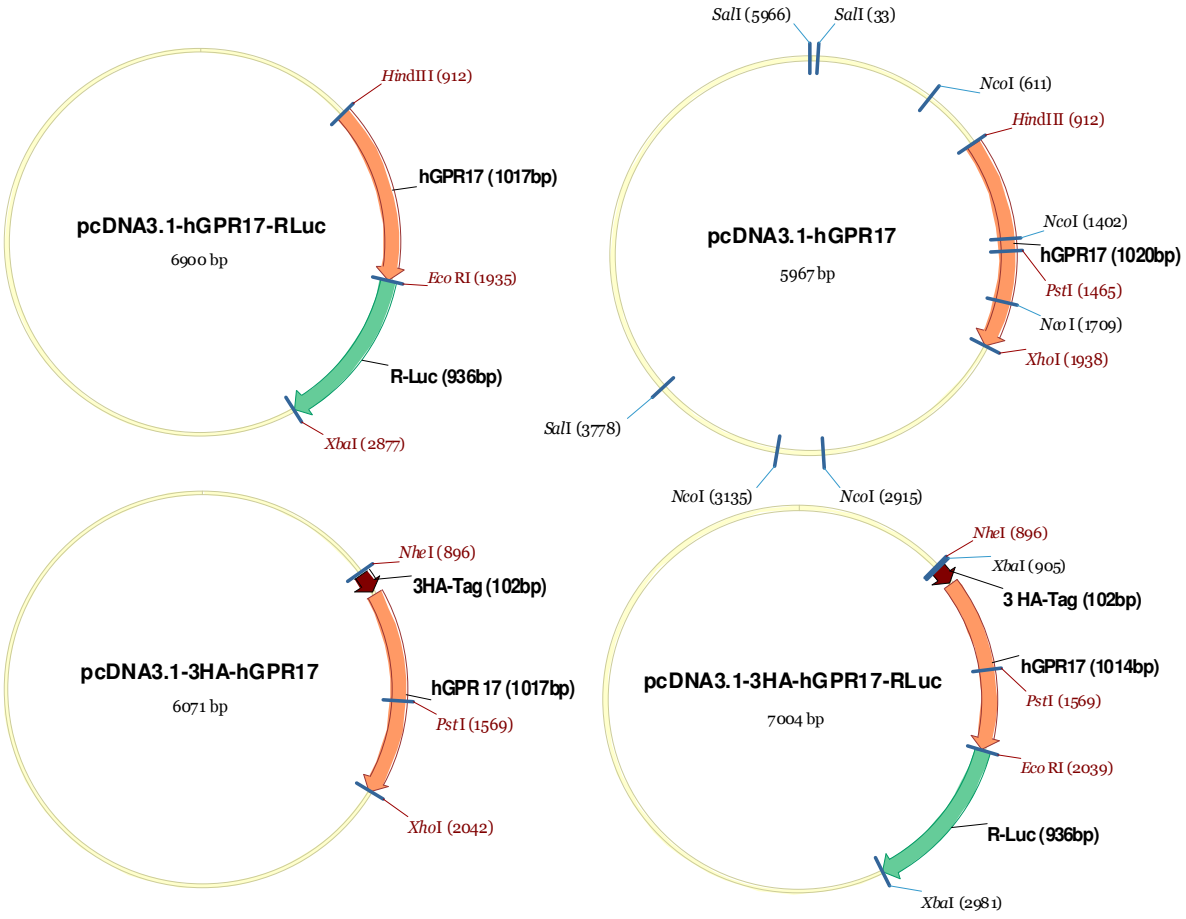

Figure 12 Self-constructed hGPR17 expression plasmid maps
Plasmid maps were designed with the use of bioinformatic software Vector NTI 8. For detailed information about molecular biology procedures used to generate the plasmids see 3.3.3.2 and 3.3.4.2.1.

2.17 Vector plasmids

Table 23 Vectors applied in the present work

vector	resistance/selection	size [bp]	promoter	reference
pcDNA3.1	ampicillin/zeomycin	5015	CMV	Invitrogen™
zeo (+)			*Phage T7*	
			SV40	
pPNT	ampicillin/neomycin/ thymidine kinase	7331	mPKG-1	(Thomas & Capecchi 1987)
			E. coli lac operon	
			Phage T3	(Tybulewicz et al. 1991)

2.18 Laboratory instruments and equipment

Table 24 Laboratory instruments and equipment

function	type	company
Autoclave	Varioklav®	H+P Labortechnik
Balances	TE64	Sartorius
	(precision balance)	
	TE6101	Sartorius
	BL310	Sartorius
Centrifuges	MiniSpin	Eppendorf
	Galaxy Mini	VWR
	Centrifuge 5810	Eppendorf
CO_2 incubator (cell culture)	Heraeus®HERAcell® 240	Thermo Fisher Scientific
Counting chamber	Fuchs-Rosenthal	Labomedic
Dry block heater	Thermomixer® comfort	Eppendorf
	QBT2	Grant Instruments
Electronic pipet filler	Easypet®	Eppendorf
Electrophoresis chambers	Mini-Sub® cell GT	BIO-RAD
	Wide Mini-Sub® cell GT	Bio-Rad
Fluorescence microscope	DM IL LED Fluo	Leica
camera	DFC 360 FX	Leica
objectives	HI PLAN I 10x/0.22 PH1	Leica
	HI PLAN I 20x/0.30 PH1	Leica
	HI PLAN I 40X/0.50 PH2	Leica
Freezer (-80°C)	Heraeus®Herafreeze®	Thermo Fisher Scientific
Freezer (liquid nitrogen)	MVE 815P-190	Chart BioMedical Ltd.
	System monitor MVETec 3000	Chart BioMedical Ltd.
Microplate readers	Mithras LB940 Multimode reader	Berthold Technologies

function	type	company
	Sunrise-Basic	Tecan Austria GmbH
Microscopes	CKX31SF	Olympus
	Leica DM IL LED Fluo	Leica
Microwave	Intello Wave	LG
Multichannel pipettes	Genex Alpha 12 channel	Genex Lab
	25-250 µl / 5-100 µl	
PCR cyclers	GeneAmp® PCR System 9700	Applied Biosystems
	2720 Thermal Cycler	
pH electrode	InLab Sciences pro, Academia	Mettler Toledo
pH-meter	SevenEasy™	Mettler Toledo
Photo documentation systems	De Vision DBOX	Decon Sience Tec
Pipettes	0.5-10 µl; 10-100 µl; 100-1000 µl	Eppendorf
	physiocare concept pipettes	
Power supplies (agarose gel electrophoresis)	PowerPac HC™	BIO-Rad
Safety cabinets	HeraSafe HS12	Thermo Electron
UV/VIS spectrophotometer	SmartSpec™ Plus	BIO-RAD
Vacuum pump system	AP 15 Membrane Vacuum Pump	HLC BioTech
Vortex	Reax Top	Heidolph

2.19 Software

name	company
Application Suite 3.3.1	Leica
DeVision G v1.0	Decon Science Tec GmbH
Microplate Analyzer v1.5 modified for Excel 2002	Corning® Incorporated
MikroWin2000	Berthold Technologies GmbH & Co. KG
Office Excel 2007	Microsoft® Corporation
Office Picture Manager	Microsoft® Corporation
Office PowerPoint®	Microsoft® Corporation
Office Word 2007	Microsoft® Corporation
Prism® 4.02	GraphPad Software
Vector NTI 8	Invitrogen™
XFluor4	Microsoft® Corporation/Tecan sunrise

2.20 Manufacturer

Agilent Technologies	D-76337 Waldbronn
Applichem	D-64291 Darmstadt
Applied Biosystems	CA 92008, USA

Berthold technologies	D-75323 Bad Wildbad
Bioplastics BV	6374 XW Landgraaf, NL
Bio Rad	CA 94547, USA
Biozol	D-85386 Eching
Cayman Chemical Company	MI 48108, USA
Chemicon® (Millipore)	MA 01821, USA
Cisbio Bioassays	BP 84175, France
Corning® Incorporated	NY 14831, USA
CyBio	D-07745 Jena
Decon Science Tec GmbH	D-37318 Hohengandern
Enzo Life Sciences	PA 19462-1202, USA
Eppendorf	D-22339 Hamburg
Fermentas	D-68789 St. Leon-Rot
Fisher Scientific	Leicestershire LE11 5R6, UK
Fluka	D-21147 Hamburg
Genex Lab	Torquay TQ2 8JG, UK
Gibco	Paisley PA4 9RF, UK
Gold Biotechnology	MO 63132, USA
GraphPad Software, Inc	CA 92037, USA
Greiner bio one	4550 Kremsmünster, Austria
Grüssing GmbH Analytika	D-26849 Filsum
Heraeus	D-63450 Hanau
HLC BioTech	D-37120 Bovenden
Invitrogen™	D-64293 Darmstadt
KMF Laborchemie Handels GmbH	D-53785 Lohmar
Labomedic GmbH	D-53115 Bonn
Leica	D-35578 Wetzlar
Merck	D-64293 Darmstadt
Mettler Toledo	D-35353 Giessen
Microsoft® Corporation	D-85716 Unterschleißheim
Moravek Biochemicals	CA 92821, USA
New England BioLabs® (NEB)	MA 01938-2723, USA
Olympus	D-20097 Hamburg
PerkinElmer Life Sciences	MA 02451, USA
Promega	WI 53711, USA
QIAGEN GmbH	D-40724 Hilden
Riedel-de Haen	D-30926 Seelze
Ritter GmbH	D- 86830 Schwabmünchen
Roth	D-76231 Karlsruhe
SAFC Supply Solutions	MO 63103, USA
Sarstedt	D-51582 Nümbrecht
Sartorius	D-37075 Göttingen
Sigma	D-21147 Hamburg
Thermo Fisher Scientific Germany Ltd. & Co. KG.	D-53113 Bonn
Tocris	Bristol BS11 0QL, UK

3 Methods

3.1 Methods in molecular biology

3.1.1 Transformation of chemically competent bacteria

The term transformation describes insertion of external DNA into host cells. Bacteria are transformed with plasmid DNA in order to increase its production along with the bacteria genome. Therefore host cells need to be prepared to enable permeation of DNA. This was done by chemical pretreatment with rubidium chloride and a subsequent heat shock. The transformation efficiency depends on plasmid size, since big plasmids are harder to transform than smaller ones.

3.1.1.1 Preparation of rubidium chloride competent E.coli

At first, a preparatory culture was arranged by inoculating 5 ml of SOB medium (RB5) with 5 µl of either XL-1 blue or NEB-10beta (Table 18). These suspensions were incubated over-night at 37°C and vigorously shaking (220 rpm). The following day 100 ml of SOB medium (RB5) were inoculated with 1 ml of preparatory culture and grown at 37°C with 220 rpm. When the OD_{550} reached 0.5 (takes ~2.5 hours), the cells were placed on ice for 10 min and then pelleted at 2800 g for 10 min in ice-cold 50 ml tubes at 4°C. The supernatant was removed and the bacteria resuspended gently in 25 ml of ice-cold rubidium chloride solution 1 (RB1) followed by incubation on ice for 10 min. The bacteria were centrifuged again at 2800 g (4°C), and gently resuspended in 8 ml rubidium chloride solution 2 (RB2). Finally, the bacteria were aliquoted (100 µl), immediately frozen in liquid nitrogen and stored at -80°C.

3.1.1.2 Transformation by heat shock

Aliquots (100 µl) of chemical competent bacteria, either XL-1 blue or NEB-10beta (Table 18), were thawed on ice (3-5 min). Approximately 50 ng of DNA were added and mixed gently by pipetting carefully up and down once. The bacteria were incubated for 30 min on ice, followed by a 30-60 seconds heat-shock (42°C) in the water bath. Afterwards the suspensions were transferred onto ice again and left there for 2 min before 300 µl of room temperature SOC medium (T4) were added. The tubes were then put into the incubator (37°C), shaking (220 rpm) for 60 min, so that encoded antibiotic resistance could develop. Thereafter, various amounts (mostly 100 and 200 µl) from each transformation were spread on a prewarmed LB agar plates (T2) containing an appropriate antibiotic (mostly ampicillin, T1) for selection and incubated overnight at 37°C.

3.1.2 Isolation of plasmid DNA

The isolation of plasmid DNA was performed with plasmid isolation kits (Table 21, K2, K3), which are based on the principle of basic lysis (Birnboim & Doly 1979). In a first step, bacteria are lysed by addition of NaOH and SDS, where DNA, RNA and proteins are precipitated by denaturation and the supplementation of RNAse-A degrades the RNA. The second step is neutralization with potassium acetate. The small renaturated plasmid DNA stays in solution, whereas the genomic bacterial DNA stays denaturated and remains, together with the proteins and other cellular components, precipitated and can be separated by centrifugation.

The subsequent purification of plasmid DNA by phenol extraction is substituted by chromatographic purification.

3.1.2.1 Analytical plasmid-isolation (mini-preparation)

To analyze the plasmids for inserts by restriction analysis, the plasmid DNA was isolated on a small scale using QIAprep® Spin Miniprep Kit (Table 21, K2). Typically, 10 colonies were picked and cultured overnight in 8 ml of LB medium (T3) containing 100 µg/ml ampicillin (T1) at 37°C.

The plasmid DNA isolation procedure: 2 ml of bacteria were pelleted, lysed and neutralized. The dispensable cell fragments were separated from the rest by centrifugation. The clarified supernatant contained plasmid DNA in an appropriate high-salt binding buffer and was centrifuged through a QIAprep® spin column where the DNA bound to the silica-gel membrane. Impurities were washed away, and pure DNA was eluted in a small volume of water.

The remaining bacteria suspension was used to generate a glycerol stock (see 3.1.3).

3.1.2.2 Preparative plasmid isolation (maxi-preparation)

To obtain high-purity and high-concentration plasmid DNA for transfection experiments, the DNA was isolated on a larger scale using NucleoBond® Xtra Maxi (Macherey-Nagel, Table 21, K3) according to the manufacturer's recommendations.

For that purpose, 300 ml of LB medium (T3) containing 100 µg/ml ampicillin (T1) were inoculated with the bacteria harboring the appropriate plasmid, either one colony from the LB agar plate (see 3.1.1.2) or bacteria culture left over from the mini preparation (see 3.1.2.1) or from a glycerol stock (see 3.1.3). The suspension was cultured overnight with vigorous shaking (220 rpm) at 37°C. The maxi preparation kit (Table 21, K3) works according to the same principle as the mini preparation kits, except that instead of silica-gel matrix the columns contain an anion exchanger matrix and the eluted DNA is precipitated with isopropanol (C39). Typical yield was ~0.3-1 mg.

3.1.3 Cryoconservation of bacterial strains

In order to have permanent stocks of bacterial strains that are harboring a desired plasmid, the respective bacteria were cryopreserved. 800 µl of bacterial suspension (see 3.1.2.1) were mixed with

200 µl of glycerin (C21) and stored at -80°C. For reactivation, a pipette tip was dipped into the glycerin culture and used to inoculate a LB-medium for preparative plasmid isolation (see 3.1.2.2).

3.1.4 Determination of nucleic acid concentration

Nucleic acid concentrations were determined photometrically by measurement of the optical density (OD) at a wavelength at 260 nm. Following equation was used for calculations:

$$\mathbf{c\ [\mu g/\ mL] = \ OD260\ x\ D\ x\ F}$$

c	concentration
OD_{260}	Optical density at 260 nm
D	Dilution factor
F	Multiplication factor (for DNA 50)

1 absorbance corresponds to 50 µg DNA per ml water

The quotient of OD_{260}/OD_{280} is a determinant of the purity and should be between 1.6 and 2.0 (in water), so that protein impurities can be disregarded.

3.1.5 Polymerase chain reaction (PCR)

The polymerase chain reaction (PCR) is a rapid procedure for *in vitro* enzymatic amplification of specific DNA sequences *(Mullis & Faloona 1987*). The discovery of a heat-stable bacterium Thermus aquaticus and its DNA polymerase (Taq polymerase) firstly enabled efficient polymerase chain reactions (Saiki et al. 1988). It is an enzyme with high efficiency through a fast DNA synthesis, but it causes a high error rate of approximately 1×10^{-5} errors per base (approximately one incorrectly integrated base per 10.000 nucleotides). Another utilized thermostable DNA polymerase is the Pfu polymerase, isolated from Thermococcus species. This polymerase shows lower rate of DNA synthesis in comparison to Taq polymerase, but offers 3’5’-exonuclease activity, which allows a correction of wrongly incorporated nucleotides (also referred to as proofreading).

For routine screening PCR, where simple detection of an amplification product was important, GoTaq Flexi® DNA polymerase was chosen. Whereas, if the amplified product was to be cloned or expressed in eukaryotic cell systems, the Pfu DNA polymerase was applied, as this enzyme exhibits a lower error rate. If long fragments with high accuracy were to be amplified, a mixture of Pfu and Taq polymerase was applied.

PCR reactions were performed in an automated thermal cycler (see 2.18).

PCR products were electrophoresed on an agarose gel appropriate for the PCR product size expected (see 3.1.7), isolated and purified via agarose gel electrophoresis using Gel Extraction-Kit from Qiagen (Table 21, K1, see 3.1.8).

3.1.5.1 Amplification of human GPR17

In order to amplify the sequence of human GPR17 (hGPR17, *GenBank accession no. U33447*), a plasmid vector (MSP70) containing the appropriate sequence was used, which was kindly provided by Andreas Spinrath (AK Kostenis, University of Bonn). The obtained PCR product was flanked by HindIII and XhoI restriction sites.

Table 25 PCR reaction conditions of hGPR17 amplification

PCR reaction mixture		Temperature program		
1.0 µl	template *(MSP70)*		Time	Temperature
1.0 µl	"sense" primer, PC5, 100 µM		[min]	[°C]
1.0 µl	"antisense" primer, PC6, 100 µM	initial denaturation	2:00	95
		35 cycles of		
5.0 µl	10x Pfu buffer (with $MgSO_4$)	denaturation	0:30	95
1.0 µl	dNTP-Mix, 2.5 mM each	hybridization	0:30	58
0.5 µl	Pfu DNA Polymerase (2-3 U/µl)	extension	2:30	72
2.0 µl	DMSO	final extension	5:00	72
38.5 µl	UltraPure™ Distilled water			

3.1.5.2 Amplification of 3xHA tagged hGPR17

For amplification of 3xHA epitope tag of hGPR17, two PCR reactions were consecutively performed. The first reaction was made to amplify an oligonucleotide primer, which was necessary for the second reaction. The applied template was pcDNA3.1/Neo (+) vector containing the sequence of a 3xHA-tagged GPCR (GPR55) that was already available in our group.

Table 26 PCR reaction conditions of 3xHA-hGPR17 primer amplification

PCR reaction mixture		Temperature program		
1.0 µl	template *(pcDNA3.1-3xHA-GPR55)*		Time	Temperature
1.0 µl	"sense" primer, PC7, 100 µM		[min]	[°C]
1.0 µl	"antisense" primer, PC8, 100 µM	initial denaturation	2:00	95
		35 cycles of		
5.0 µl	10x Pfu buffer (with $MgSO_4$)	denaturation	0:30	95
1.0 µl	dNTP-Mix, 2.5 mM each	hybridization	0:30	55
1.0 µl	Pfu DNA Polymerase	extension	1:00	72
	(2-3 U/µl)			
2.0 µl	DMSO	final extension	5:00	72
38.0 µl	UltraPure™ Distilled water			

The second amplification was performed to obtain the 3xHA epitope tagged hGPR17, flanked by NheI (5') and XhoI (3') restriction sites.

Table 27 PCR reaction conditions of 3xHA-hGPR17 amplification

PCR reaction mixture		Temperature program		
1.0 µl	template *(pcDNA3.1-hGPR17)*		Time	Temperature
1.0 µl	"sense" primer, PCR product		[min]	[°C]
1.0 µl	"antisense" primer, PC6, 100 µM	initial denaturation	2:00	95
		35 cycles of		
5.0 µl	10x Pfu buffer (with $MgSO_4$)	denaturation	1:00	95
1.0 µl	dNTP-Mix, 2.5 mM each	hybridization	0:30	60
0.5 µl	Pfu DNA Polymerase	extension	3:00	72
	(2-3 U/µl)			
2.0 µl	DMSO	final extension	5:00	72
38.5 µl	UltraPure™ Distilled water			

3.1.5.3 Targeting vector

The amplification of 5' and 3' homology regions of mouse GPR17 (mGPR17) gene (*GenBank accession no NM_001025381*) for generation of the targeting construct was performed in two PCR reactions with the use of genomic ES cell DNA derived from mouse strain Ola/SC129 as template, which was kindly provided by Daniel Schulz (AK Kostenis, University of Bonn).

The amplification of short homologous 3' region (*short arm*) was performed with the following conditions. Primers were designed to contain mGPR17 sequence flanked by artificial restriction enzyme sites (5' BamHI and 3' EcoRI).

Table 28 PCR reaction conditions of *short arm* amplification

PCR reaction mixture		Temperature program		
1.0 µl	template *(ES cell DNA)*		Time	Temperature
1.0 µl	"sense" primer, PC1, 100 µM		[min]	[°C]
1.0 µl	"antisense" primer, PC2, 100 µM	initial denaturation	2:00	94
		35 cycles of		
5.0 µl	10x Long PCR buffer	denaturation	0:30	94
1.0 µl	dNTP-Mix, 2.5 mM each	hybridization	0:30	55
0.5 µl	Pfu DNA Polymerase	extension	2:00	70
	(2-3 U/µl)			
0.5 µl	Taq DNA Polymerase (5 U /µl)	final extension	5:00	70
2.0 µl	DMSO			
38.0 µl	UltraPure™ Distilled water			

The amplification of long homologous 5' GPR17 sequence (*long arm*) was performed with slightly varied PCR conditions (see Table 29). Primers were designed to contain GPR17 sequence flanked by artificial restriction enzyme sites (5' NotI and 3' XhoI).

Table 29 PCR reaction conditions of *long arm* amplification

PCR reaction mixture		Temperature program		
1.0 µl	template *(ES cell DNA)*		Time	Temperature
1.0 µl	"sense" primer, PC3		[min]	[°C]
1.0 µl	"antisense" primer, PC4, 100 µM	initial denaturation	2:00	94
		35 cycles of		
5.0 µl	10x Long PCR buffer	denaturation	0:30	94
1.0 µl	dNTP-Mix, 2.5 mM each	hybridization	0:30	56
0.25 µl	Pfu DNA Polymerase	extension	6:00	70
	(2-3 U/µl)			
0.75 µl	Taq DNA Polymerase (5 U /µl)	final extension	10:0	70
2.0 µl	DMSO			
38.5 µl	UltraPure™ Distilled water			

3.1.5.4 Genotyping of genetically modified ES cells

For the screening of recombination events in targeted ES cells, a PCR-based genotyping was designed, which distinguished between wild type and heterozygous modified GPR17 gene.

Preliminary PCR screening was performed to check, whether targeting-construct was integrated, disregarding the fact, where recombination took place. The presence of wild type allele was proven

by an amplicon of 511bp, whereas the occurrence of heterozygous modification of GPR17 gene was shown by the appearance of a PCR product of 721bp.

Table 30 PCR reaction conditions of preliminary screening of ES cell clones

PCR reaction mixture		Temperature program		
1.0 µl	Isolated ES cell DNA		Time	Temperature
1.0 µl	"sense" primer, PScr1, 100 µM		[min]	[°C]
1.0 µl	"antisense" primer, PScr2-WT or PScr3-KO, 100 µM	initial denaturation	2:00	95
		28 cycles of		
5.0 µl	5x Taq buffer	denaturation	0:30	95
2.0 µl	$MgCl_2$	hybridization	0:30	62
1.0 µl	dNTP-Mix, 2.5 mM each	extension	0:30	72
0.3 µl	Taq DNA Polymerase (5 U /µl)			
1.0 µl	DMSO	final extension	6:00	72
12.7 µl	UltraPure™ Distilled water			

A second PCR genotyping was performed with the ES cell DNA, which was formerly proven in the preliminary analyses to possess heterozygous modified GPR17 allele. This more specified PCR reaction was carried out to check whether the recombination was homologous, and targeting construct was integrated in the accurate location. The presence of targeted GPR17 allele was proven by an amplicon of 1832bp.

Table 31 PCR reaction conditions of specified screening of ES cell clones

PCR reaction mixture		Temperature program		
1.0 µl	Isolated ES cell DNA		Time	Temperature
1.0 µl	"sense" primer, PScr4, 100 µM		[min]	[°C]
1.0 µl	"antisense" primer, PScr5, 100 µM	initial denaturation	2:00	94
		28 cycles of		
5.0 µl	10x Long PCR buffer	denaturation	0:30	94
1.0 µl	dNTP-Mix, 2.5 mM each	hybridization	0:30	61
0.2 µl	Taq DNA Polymerase (5 U /µl)			
0.2 µl	Pfu DNA Polymerase	extension	3:00	70
	(2-3 U/µl)			
1.0 µl	DMSO			
17.9 µl	UltraPure™ Distilled water	final extension	6:00	70

3.1.6 Sequencing of cloned PCR products

GATC Biotech AG, Konstanz, analyzed all PCR-derived products. Thus, the correct sequence and especially the absence of point mutations were ensured.

3.1.7 Agarose gel electrophoresis

Agarose gel electrophoresis is a simple and highly effective method for separating and purifying DNA fragments of different sizes (Vogelstein & Gillespie 1979). The molecules migrate through the agarose-matrix with varying speed, depending on their size and charge. The electrophoresis buffer (1xTAE, S21) enables the charge migration and due to its pH of 8, the DNA stays negatively charged. These anions migrate in the electric field to the positively charged anode. Smaller fragments travel faster than bigger ones through the network, because they do not interfere as much with the surrounding agarose gel matrix.

The gels were made of 0.6 – 1.0 % agarose in 1xTAE (S21) supplemented with 0.5 µg/ml ethidium bromide (C16). With this method, fragments of 0.5–15 kb can be sufficiently separated. Prior to loading, the samples were supplemented with DNA gel loading buffer (S3). Dependent on the size of the gel and the fragments, the electrophoresis was performed at 50-120 V. The addition of ethidium bromide allows a visualization of DNA fragments under UV-light. Ethidium bromide intercalates with the DNA helix, which induces an intensification of the fluorescence properties. The DNA fragments appear in a red color through UV illumination (302 nm), whereas other parts of the gel stay dark. Banding patterns were photographically documented. For determination of fragments size, a DNA marker was always separated in parallel.

3.1.8 DNA-elution from agarose gels

DNA fragments were purified using Gel Extraction-Kit from Qiagen (Table 21, K1) following manufacturer's instructions.

In brief: the gel slice containing the band of interest was removed from the gel and this agarose slice was solubilized at 55°C for 10 min by mixing it with the appropriate high-salt binding buffer and then applied to the spin column where DNA binds to the silica gel membrane. Impurities were washed away, and pure DNA was eluted in a small volume of water (30-100 µl).

3.1.9 Restriction endonuclease digestion

3.1.9.1 Analytical restriction enzyme cleavage

For analytical purposes, plasmids from mini preparations (see 3.1.2.1), were cut with restriction enzymes to identify positive clones with the correct insert. Approximately 500 ng of respective plasmid were digested in a mixture of 1 x appropriate restriction buffer, 1x BSA and 10 U of each restriction enzyme at 37°C for 1 h. The fragment pattern was visualized in a 1% agarose / ethidium bromide gel. Positive plasmids were sent to sequencing (see 3.1.6).

Restriction endonuclease cleavage was accomplished by incubating the enzyme(s) with the DNA in appropriate reaction conditions. The amounts of enzyme and DNA, the buffer and ionic concentrations, and the temperature and duration of the reaction were adjusted to the specific application according to the manufacturer´s recommendations.

3.1.9.2 Preparative restriction enzyme cleavage

For preparative purposes, respective vector DNA (pcDNA 3.1 / pPNT) and PCR products were cut with similar restriction enzymes to obtain compatible, sticky ends. PCRs were prepared (see 3.1.5) and PCR products were isolated from agarose gels (see 3.1.8). Afterwards, fragments and linearized vector were digested in a mixture of 1 x appropriate restriction buffer, 1x BSA and 10 U of each restriction enzyme at 37°C for 1h. Subsequently, fragments or vector were purified again with an agarose / ethidium bromide gel. These obtained digested products were used for further ligations (see 3.1.12).

3.1.9.3 Linearization of plasmids for stable transfection

In order to prepare plasmid DNA for stable transfection of eukaryotic cells (see 3.2.6.2), the DNA was linearized in advance. Approximately 50 µg of plasmid DNA were cleaved with 50 U of restriction enzyme (PvuI for pcDNA3.1 / NotI for pPNT) in a mixture of 1 x appropriate restriction buffer and 1 x BSA for 3 h at 37°C.

3.1.10 Precipitation of plasmid DNA

This method was applied to precipitate linearized plasmid DNA out of the reaction mixture (see 3.1.9.3). The digested DNA was mixed with 1/10 volume of sterile sodium acetate (S17, 3M, pH 5.1) and precipitated by addition of the double volume of absolute ethanol (C15). DNA was pelleted for 5 min at 13000 rpm and supernatant was discarded. The pellet was washed with 500 µl ethanol (S6, 70%) and centrifuged once more for 5 min at 13000 rpm. The supernatant was decanted and after the DNA pellet was dried under a safety cabinet, it was dissolved in 100 µl of UltraPure™ distilled water.

3.1.11 Dephosphorylation of cleaved vector DNA

In this work the Antarctic Phosphatase was applied to catalyze the removal of 5´ phosphate groups from restriction enzyme digested vector DNA prior to ligation reactions. Phosphatase-treated fragments lack the 5´ phosphoryl termini required by ligases, so that the effect self-ligation is diminished. The digested vector DNA (~2 µg) was incubated in a mixture of 1x Antarctic Phosphatase reaction buffer and 5 U of Antarctic Phosphatase at 37°C for 15 min. This reaction was heat-inactivated at 65°C for 5 min.

3.1.12 Ligation of DNA fragments

T4 DNA Ligase catalyzes the formation of a phosphodiester bond between juxtaposed 5'-phosphate and 3'-hydroxyl termini in duplex DNA. Digested (see 3.1.9.2) and dephosphorylated (see 3.1.11) vector DNA (50-400 ng) and respective insert DNA were mixed, where up to 5-fold molar excess of insert DNA over vector DNA was used. This reaction mixture was supplemented with 10 X ligation buffer and UltraPure™ distilled water to a total volume of 10 µl and 2 U of T4 DNA Ligase. The mixture was incubated over-night at 16°C and then either used directly for transformation or stored at –20°C.

3.2 Cell biological methods

All cells were grown under the same culture requirements in cell incubators, which were set to 37°C with an atmosphere of 5% CO_2 and 96% humidity. Applied cell culture solutions and media were prewarmed in a water bath (37°C). Every operation was carried out under aseptical conditions in safety cabinets with laminar air flow.

3.2.1 Passaging cell lines

Cells were splitted routinely at least twice a week (for detailed cell type specific information see 2.8). They were harvested either by trypsinization (adherent cell cultures) or by centrifugation at 800 g for 4 min (suspension cell cultures).

For trypsinization, the growth medium was removed from the flask and cells were washed carefully with prewarmed PBS (S15, 37°C) to remove remaining medium. Depending on the flask size, 0.5-3.0 ml of prewarmed trypsin (37°C) were added to the flask and incubated at 37°C until cells have detached (1-5 min). Trypsinization was stopped by addition of respective growth medium (see2.7.2). Cells were resuspended in an appropriate volume and transferred into a new culture flask, which was already filled with growth medium (5-25 ml, depending on flask size).

3.2.2 Cryopreservation of cell lines

In order to have permanent stocks of the utilized cell lines, cells were expanded until they nearly reached confluence (80-95%), using 1-5 cell culture flasks (175 cm^2). Cells were washed with PBS (S15, 37°C) to remove residual medium and then trypsinized with prewarmed trypsin (37°C) until they have detached (as brief exposure as possible). After resuspension in normal growth medium, cell suspensions were combined and centrifuged at 800 g (4 min). In the meantime freezing medium was freshly prepared by adding 20% FCS and 10% DMSO (C12) to the respective plain medium (see 2.7.2). Addition of DMSO serves as an antifreezing agent. Subsequent to centrifugation growth medium was removed. After resuspending the pellet with freezing medium (4-8°C), aliquots of 1 ml cell suspension (3-5 x 10^6 adherent cells or 5-10 x 10^6 suspension cells) were transferred into labeled freezing vials and placed into a -80°C freezer. This allowed freezing of the cells at an approximate

rate of 1°C/min. The following day freezing vials were transferred into a liquid nitrogen tank for long-term storage. One vial of frozen cell stocks was tested before discarding the cell line.

3.2.3 Revitalization of cell lines

For cell thawing after long-term storage, a vial of frozen cells was removed from the liquid nitrogen tank and rapidly unfrozen in a 37°C water bath. In order to remove the cell toxic DMSO from the freezing medium, the cell suspension was promptly transferred into a centrifuge tube containing 10 ml of prewarmed growth medium (without antibiotics) and pelleted at 800 g. After 4 min of centrifugation, the supernatant was discarded; cells were resuspended in fresh growth medium (without antibiotics) and transferred into a culture flask. Cells were incubated overnight under their usual culture conditions, and the next day the medium was replaced by complete growth medium, including antibiotics. Usually cells were cultured at least for one week before they were used for further analyses.

3.2.4 Counting cells with a hemocytometer

The hemocytometer is a device, as the name suggests, originally used to count blood cells, whereas in this work the Fuchs-Rosenthal chamber was used to determine the number of respective cells, which were needed for further analyses. The hemocytometer consists of 2 chambers, which are divided into 9 squares (1 x 1 mm). The cover glass is situated 0.1 mm over these squares so that the total volume over each square is 0.1 mm^3, which equals 1 ml. After cells were detached by trypsinization (see 3.2.1), a small amount of cell suspension was diluted (1:2 - 1:6) in PBS (S15) and placed onto the chamber. With the help of capillary forces, the chamber was completely filled with the sample. By use of a microscope, the number of cells was determined by manual counting. The cell concentration per ml is the average count per square times 10^4. Further dilutions were taken into account and usually cells were diluted, so that each square had between 20-60 cells.

3.2.5 Coating cell culture dishes with poly-D-lysine

In order to reduce cell detachment from shear stress in washing steps associated with cell labeling (see 3.3.4, 3.3.5) and to improve cell vitality, surfaces of cell culture dishes were pretreated with poly-D-lysine, which improves adhesive properties by altering the charge on the vessel surface from negative to positive and leads to a uniform net positive charge.

Culture plate surfaces were completely covered with PDL solution (S16, 50 µl per well in a 96 well plate) and incubated at 37°C for 30 min. After the redundant PDL was aspirated, surfaces were thoroughly rinsed three times with PBS (S15) and then dried in the safety cabinet. These prepared plates were directly used or sealed with parafilm and kept at 2-8°C until further usage.

3.2.6 Transfection of eukaryotic cells

The DNA transfer into eukaryotic cells can be divided into transient and stable transfections. While the transient method leads to a temporally limited DNA incorporation, stable transfection results in a permanently expression of the introduced gene, by integration of the plasmid DNA into the cell genome. The applied calcium phosphate transfection method according to Chen and Okayama (Chen & Okayama) was used for both kinds of transfection, stable and transient. This method is based on the formation of DNA/calcium phosphate coprecipitates, which first settle onto the cells and are then taken up by endocytosis. These precipitates should be formed freshly at the time of transfection. According to Orrantia and Chang (Orrantia & Chang 1990) it is thought that small DNA/calcium phosphate particles are taken up by endocytosis and transported to the nucleus, where some DNA escapes the precipitate and can be expressed.

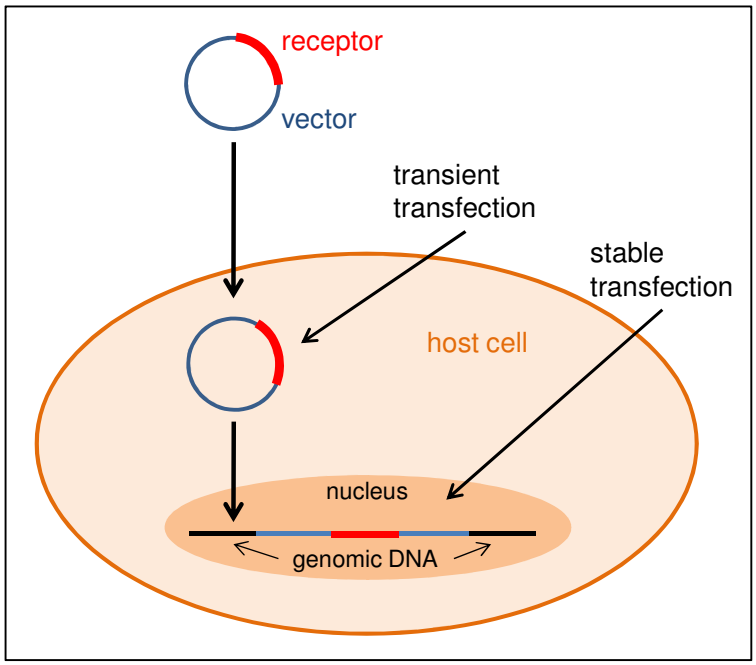

Figure 13 Diagram of transient and stable transfection of host cells with plasmid DNA
Expression of the gene of interest can be achieved by integration of a plasmid vector containing the respective sequence of interest (here receptor) into a host cell (e.g. HEK293 cells): Initially, for transient transfection, the gene of interest has to be introduced into the cell. Finally, for a stable transfection the gene has to be integrated into genomic DNA. The transiently transfected DNA is not passed from generation to generation during cell division and therefore the genetic alteration is not permanent, whereas in a very low number of cases, the exogenous DNA randomly integrates into chromosomal DNA of the recipient, which allows the transfected DNA to be carried stably from generation to generation. The incorporation of selectable markers, such as antibiotic resistances (e.g. neomycin, blasticidin or hygromycin), allows selection for cells that have integrated this exogenous DNA into their genomic DNA. While transient transfection is useful for fast analyses of genes, stable transfection enables long-term, reproducible, and defined gene expression.

3.2.6.1 Transient calcium phosphate–mediated transfection

Cells (3.8 – 4.4 x 10^6) were seeded onto 60 cm^2 tissue culture dishes one day prior to transfection, so that they were ~50-60% confluent at the time of transfection. Initially the plasmid DNA (20 µg) was carefully mixed with TE-buffer (S20, 500 µl) and $CaCl_2$ (S2, 60 µl). The DNA/calcium phosphate precipitates were formed via drop-by-drop addition of this DNA/$CaCl_2$ solution into round bottomed

falcon tubes prefilled with 2x HEPES-buffered saline (S10, 500 µl). Followed by incubation at room temperature for 20 min, the freshly formed precipitates were carefully pipetted drop-by-drop onto the dishes containing the adherent cultured cells and growth medium. The dishes were slewed carefully to achieve an even distribution. After the cells have been exposed to the precipitates for approximately 5 h in the incubator, the medium containing the transfection reagents was removed and fresh medium was added to prevent toxicity. Transiently transfected cell were usually analyzed 48 h after transfection.

3.2.6.2 Stable calcium phosphate–mediated transfection

Stable transfections were performed according to the transient protocol mentioned above (see 3.2.6.1) with some specific changes. First the plasmid DNA was linearized (see 3.1.9.3) prior to transfection to simplify its stable integration into the genome. 24 h after transfection cells were splitted (1:3 – 1:5) to avoid confluence and 48 h later medium was exchanged by medium containing selection antibiotics encoded on the transfected plasmids (see Table 23 for information about respective antibiotics). In this work only pooled clones were generated, meaning selective medium was exchanged every 2-3 days until every not stably transfected cell was dead and all surviving cells were combined to one pooled clone. These generated cells were always kept under selection pressure.

By use of this method, five different HEK293 cell lines stably expressing human GPR17 were generated:

- HEK-3xHA-hGPR17
- HEK-3xHA-hGPR17-RLuc
- HEK-β-ARR2-GFP2-3xHA-hGPR17-RLuc
  also referred to as HEK-BRET-GPR17
  (three distinct β-arrestin2 GFP2 expression levels: low, high and very high)

3.3 Cell-based experiments

In order to elucidate receptor function, selective and efficacious pharmacological tool ligands are required. As for the orphan GPR17 receptor neither endogenous ligands nor other pharmacological tools are available, our selective GPR17 agonist RA-II-150 was used for further functional investigations.

3.3.1 Dynamic mass redistribution assays

Conventional assay technologies applied for analyses of GPCR mediated signaling are mainly based on the use of dyes, antibodies or fusion gene constructs, which may influence the actual cellular physiology of the receptor. In addition they are usually focused on one specific cellular event, ranging from second messenger generation (e.g. cAMP, IP1) to the translocation of a particular target labeled

with a fluorescent tag (e.g. β-arrestin) or expression of a reporter gene. Furthermore, many of these traditional assays are end point assays, so that a sustained monitoring of cell signaling is not possible.

In order to circumvent these problems and provide greater biological insight, a label-free technique with a holistic and pathway-independent screening method was applied. For the detection of whole cell pleiotropic signaling events a beta version of the Corning®Epic® system was used. This biosensor consists of a temperature-control unit, an optical resonant waveguide grating (RWG) detection unit and an on-board robotic liquid handling device.

3.3.1.1 Principle of resonant waveguide sensing

Ligand induced activation of GPCRs leads to a series of spatial and temporal events that govern cell responses (Kholodenko 2006), which involve modulation of the cytoskeleton, and relocation of proteins, vesicles or organelles. This dynamic redistribution of cellular contents also referred to as dynamic mass redistribution (DMR), lead to a change of local optical density (Fang et al. 2005). The application of optical biosensors, which utilize waveguide grating surfaces embedded in the bottom of every well of special 384-well microtiter plates, enable detection of these redistributions.

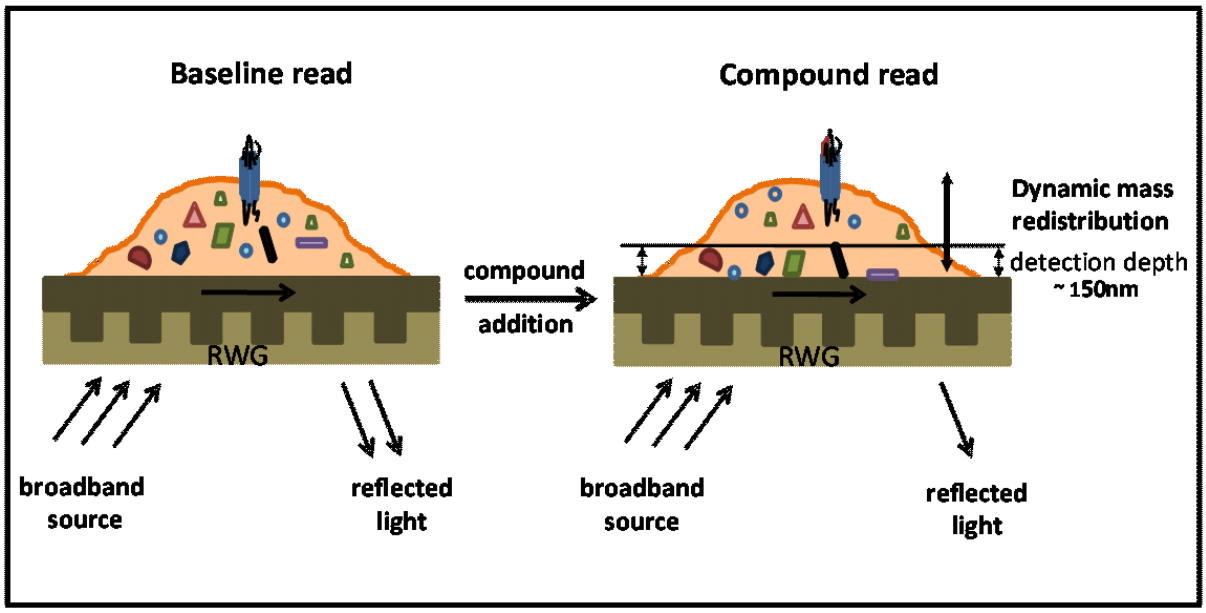

Figure 14 Principle of RWG sensing by means of the Epic® system (modified from Fang et al. 2005, Fang et al. 2006)
Cells are seeded onto microplates containing optical biosensors (resonant waveguide grating, RWG) at the bottom of each well. Stimulation-induced relocation of cellular constituents, also referred to as dynamic mass redistribution (DMR), influence the refractive index in an area up to 150 nm distance from the biosensor. This change leads to a relative shift of reflected wavelength. (for more details please refer to the text)

A broadband and polarized light is used to illuminate the waveguide and to pass polarized light through the bottom portion of cells. The grating surfaces reflect a very narrow band of light, which is characteristic of the refractive index near the sensor surface, which is sensitive to changes in the concentration of biomolecules. The relative shift of reflected resonant wavelength is proportional to changes in local mass density within the penetration depth of the biosensor, which is approximately 150 nm (Fang et al. 2005, Fang et al. 2006, Fang, Ferrie & Tran 2009, Lee et al. 2008). The resulting

optical trace can be recorded for minutes up to hours after ligand induced activation of GPCRs, which provides a real-time readout of pharmacologically mediated changes in cellular mass.

3.3.1.2 Experimental procedure of DMR analyses

Cells were seeded in a density of 12.500-20.000 cells per well in 384-well in fibronectin-coated microplates with 30 µl of growth medium and cultured at 37°C in an atmosphere of 5% CO_2 for about 16-24 hours to obtain confluent monolayers. If CHO-GPR17 were analyzed, the growth medium contained doxycycline (S4, 1 µg/ml) to induce receptor expression. If necessary, cells were treated over-night (16-20 h) with PTX (C33, 50 ng/ml) to elucidate particular GPCR coupling patterns.

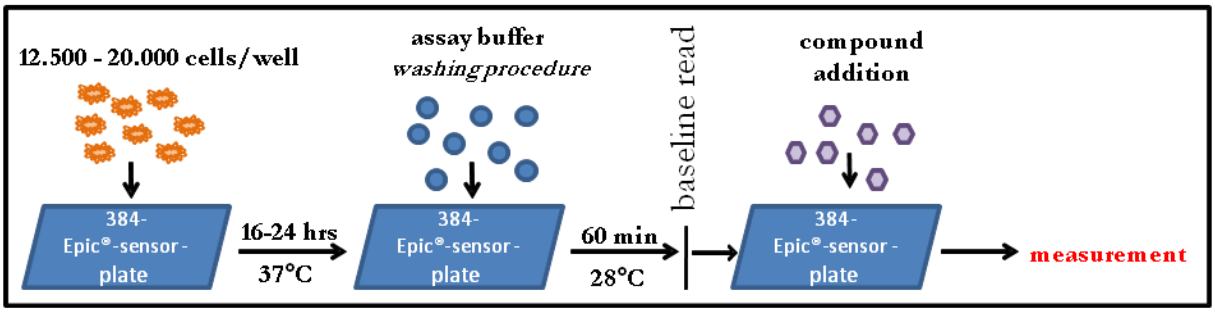

Figure 15 Experimental procedure of DMR assay (refer to the text for detailed information)

On the day of experiment cell culture medium was removed and cells were washed twice with assay buffer (HBSS + 20 mM HEPES (S12), pH 7.0). Supernatant was removed up to 10 µl by use of an eight channel manifold and cells were allowed to rest in 30 µl of assay buffer for at least 60 min in the Epic® reader at a constant temperature of 28°C. In prestimulation experiments with YM or BIM-46187, they were added in the appropriate concentration after the washing procedure and incubated for 2.5 h prior to addition of test compounds. After an initial baseline read of 300 s, 10 µl test compound diluted in assay buffer and dispensed in a microtiter source plate were added into the sensor plate by means of the liquid handling device. Induced DMR responses were monitored for at least 3600 s. As some compound stock solutions were prepared in DMSO (C11), assay buffer was always adjusted to obtain similar DMSO concentration during a measurement. In order to avoid unspecific responses due to DMSO, the concentration did never exceed 0.4%, which was proven to have no detectable effects on the cells.

3.3.1.3 Data evaluation of DMR analyses

For a computer-based evaluation of recorded wavelength shifts, data were opened in table form with the help of „Microplate Analyzer v2.0“ software and were transferred to GraphPad Prism4 software for further evaluation. Optical signatures were depicted as representative figures of one individual experiment performed in triplicates. Each experiment shown was repeated at least three times gaining comparable results (detailed information is given in respective legends of results). For generation of concentration-response curves (CRC) the maximum response (0-1800 s) and area under curve (AUC, 0-3600 s), respectively, were plotted against agonist concentrations, depending on the respective optical signature shape.

The illustrated optical recordings in the present thesis are all baseline corrected, meaning the ligand-induced wavelength shifts were corrected for signals obtained by addition of a compound-free assay buffer control. Buffer signal usually ranged between 0 and 40 pm.

Concentration-effect curves were fitted by least squares, non-linear sigmoidal regression based on Hill equation with the use of GraphPad Prism4 software. Curve fitting was checked by application of F-test, whether fitted curve was sufficiently described with a constant Hill-coefficient of $n_H = 1$ or if application of variable slope showed significantly better fitting. Pharmacological parameters of plotted sigmoidal CRC such as EC_{50} value (inflection point dedicating the agonist-concentration inducing half maximal effect) and E_{max} value (indicator of the intrinsic activity of a tested compound) were calculated by the GraphPad Prism4 software. Each data point of a depicted experiment represents a mean of at least three independent experiments performed in triplicates.

3.3.2 Homogeneous time resolved fluorescence (*HTRF®*) technology

Regulation (activation/inhibition) of cyclic AMP concentration and stimulation of inositol phospholipid hydrolysis constitute two major mechanisms by which GPCRs affect the cell metabolism. In order to analyze Gαs, Gαi/o and Gαq protein mediated signal transduction and their subsequent impact on effector proteins, such as adenylate cyclase (AC) and phospholipase C (PLC), cAMP and IP1 Kits (Table 21, K4, K5) from Cisbio were applied, which are based on the HTRF® technology. This non-radioactive dual labeling technique is based on the time-resolved fluorescence resonance energy transfer (reviewed by Degorce et al. 2009). TR-FRET combines standard FRET chemistry by application of lanthanoids as fluorescence donors, which are characterized by a very long emission half life (Selvin 2000). The HTRF® technology combines the advantages of FRETs homogeneity and the low background of TR-FRET.

3.3.2.1 Theoretical background of HTRF® technology

In the applied HTRF®-method the lanthanoid europium was used as fluorescence donor, which is complexed with three molecules bispyridin to a cryptate (Degorce et al. 2009, Trinquet & Mathis 2006). The bispyridin molecules form a three dimensional cage around the lanthanoid and serve as a light-collection device, thus transferring the absorbed excitation energy on the europium. The very long emission half life of the lanthanoids allows a delayed detection, which guarantees that only the persistent FRET based fluorescence signal will be measured and the non-specific short-lived background fluorescence can be neglected. The applied acceptor is the so-called d2, a modified allophycocyanin organic molecule with a relatively low molecular weight from about 1.000 DA (Trinquet et al. 2001).

When fluorescence donor (europium cryptate) and acceptor (d2) get into close proximity while simultaneously excited with 320 nm, fluorescence resonance energy transfer (FRET) occurs. The maximum of the d2 emission spectrum is measured at 665 nm and a part of the energy captured by the europium has its maximum at 620 nm. A ratiometric measurement of these two emission wavelength enables corrections of well variability, signal quenching from assay components and

medium variability. Emissions at 665 nm (acceptor fluor) indicate the investigated biological reaction, whereas emissions at 620 nm (donor fluor) are used as an internal reference. In addition, the ratiometric readout can minimize the system errors caused by liquid handling instruments and detectors. To ensure a simultaneous detection of the cryptate donor emission at 620 nm and the d2 acceptor transmission at 665 nm, the multimode reader Mithras LB940 (Berthold) was utilized.

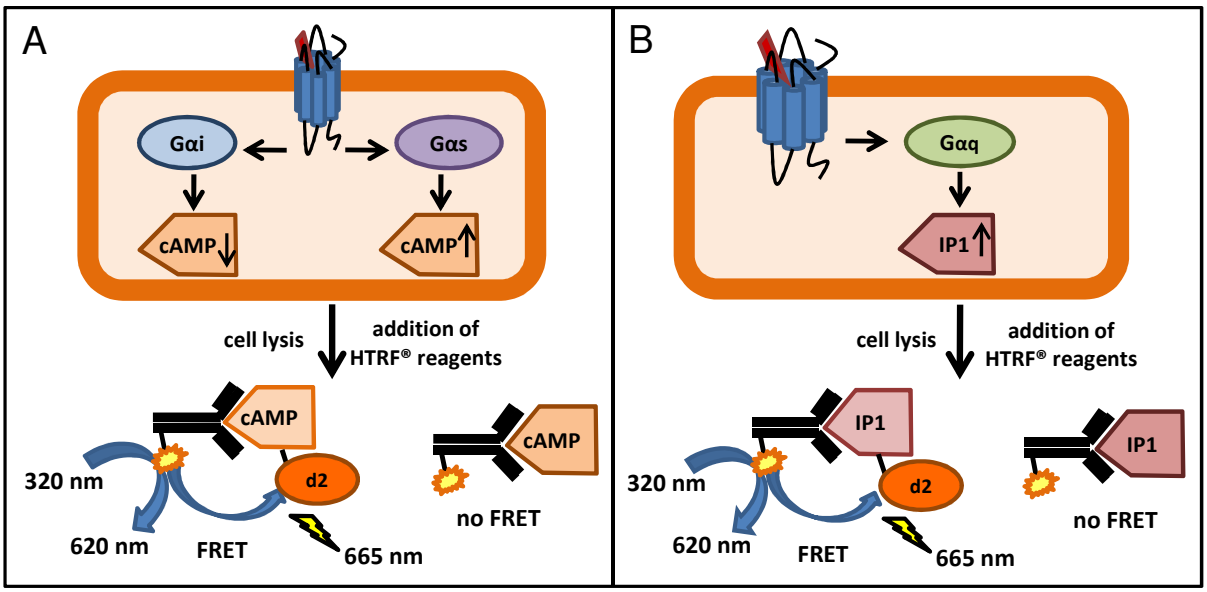

Figure 16 HTRF® cAMP / IP1 assay principle (modified from Degorce et al. 2009)
The underlying method is a competitive immunoassay between endogenously accumulated second messengers and added d2-labeled second messengers. Specific monoclonal antibodies (Mab) labeled with europium cryptate (depicted as yellow cloud), which are targeted against either cAMP (A) or IP1 (B), serve as fluorescence donor. The respective second messengers are labeled with the dye d2 and serve as acceptor. The binding of the labeled Mab to its appropriate labeled second messenger (cAMP / IP1) results in a fluorescence resonance energy transfer (FRET) from the europium cryptate to the d2. This induces light emissions at 620 and 665 nm. The endogenously produced cAMP / IP1 binds as well to the specific labeled Mab, which leads to compensation of FRET and a decrease of the emission signal. Thus the resulting specific signal is inversely proportional to the endogenously available cAMP / IP1.

3.3.2.2 Generation of cyclic AMP

The observation of intracellular cAMP accumulation enables investigations of two distinct G protein mediated signal transductions, Gαs and Gαi/o (reviewed by Williams 2004, Gabriel et al. 2003).

Generation of cAMP is controlled through the adenylate cyclase (AC) family of enzymes, which convert adenosine triphosphate (ATP) into cyclic adenosine monophosphate (cAMP) and inorganic pyrophosphate (PP). Two distinct heterotrimeric GTP binding proteins, Gαs and Gαi/o, have an impact on AC activity. Gαs primarily induces activation of AC, whereas Gαi/o shows inhibitory influences. Since the basal cyclic AMP production is usually low in a living cell, it is not possible to observe the inhibitory effect of receptors on the AC activity without prior stimulation of the enzyme. This was avoided by simultaneous addition of a constant forskolin concentration to the compound dilutions to activate the AC in a G protein-independent manner (Seamon, Padgett & Daly 1981). Furthermore the phosphodiesterase inhibitor IBMX (C25) was added to the assay buffer in order to inhibit degradation of accumulated cAMP.

3.3.2.3 Generation of IP1

Signal transduction via Gαq subunit induces, amongst others, activation of PLC, which hydrolyzes phosphatidylinositol 4,5-phosphate into diacylglycerol and D-myo-inositol 1,4,5-triphosphate (IP3). IP3 will be further degraded into D-myo-inositoldiphosphate (IP2) and D-myo-inositolmonophosphate (IP1) and finally D-myo-inositol. Since the half life of IP3 is extremely short, but degradation of IP1 can be prevented by the presence of LiCl, the intracellular IP3 concentrations can be measured indirectly via detection of accumulated IP1 (Trinquet et al. 2006, Zhang et al. 2010), thus giving information about Gαq mediated signaling.

3.3.2.4 cAMP HTRF® assay experimental procedure

Agonist induced changes in cAMP accumulation were measured according to manufacturer's instructions unless otherwise specified (summarized in Figure 17).

The required amount of cells was harvested and washed once in HBSS (20 mM HEPES (S12)), involving one centrifugation step for 15 s at 2700 rpm. Pelleted cells were resuspended in appropriate volume of assay buffer (HBSS, 20 mM HEPES (S12), 1 mM of IBMX (C25)) and dispensed at 50.000 cells/5 µl/well in 384-well microtiter plates on the day of experiment. After 30 min of preincubation at 37°C, cells were stimulated by addition of 2-fold concentrated agonist (5 µl) in the presence or absence of forskolin (C17), diluted in assay buffer. If the effects of antagonists were analyzed, they were added 30 min prior to agonist addition and incubated at 37°C. Following a 30 min incubation at 37°C, the reaction was stopped by the addition of 5 µl of IP-d2 followed by 5 µl of europium(Eu)-cryptate-labeled cAMP Mab diluted (1:20) in lysis buffer (50 mM phosphate buffer (pH 7.0), 1 M KF and 1.25% triton X-100).

The plates were allowed to incubate for 60 min at RT and were then read after excitation at 320 nm using the multimode reader Mithras LB940 (Berthold) with 100 µs delay and 200 µs window time.

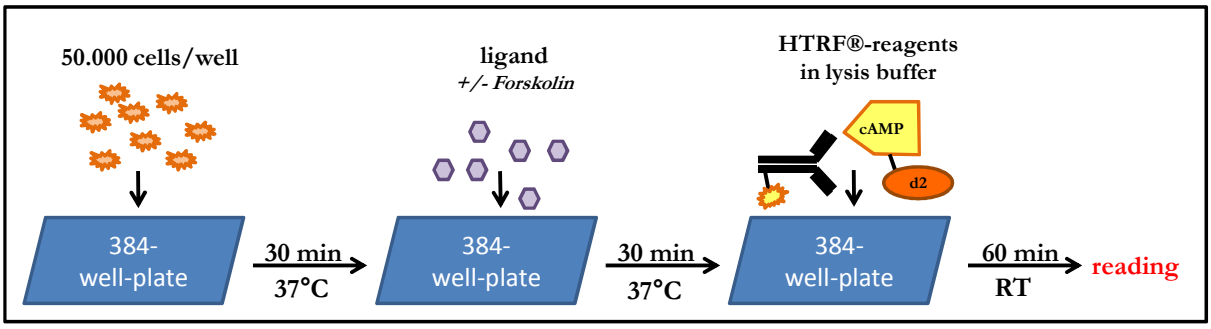

Figure 17 Schematic HTRF® cAMP assay protocol diagram (please refer to the text above for detailed information)

3.3.2.5 IP1 HTRF® assay experimental procedure

Agonist induced IP1 accumulation was determined similar as described for cAMP (see 3.3.2.4) according to manufacturer's instructions (summarized in Figure 18).

On the day of experiment the required amount of cells was harvested and washed twice in HBSS (20 mM HEPES (S12)), including two centrifugation step for 15 s at 2700 rpm. Pelleted cells were resuspended in appropriate volume of stimulation buffer (containing LiCl) and dispensed at 100.000 cells/7 µl/well in 384-well microtiter plates. Following incubation at 37°C for 30 min, cells were stimulated by addition of 7 µl 2-fold concentrated agonists diluted in stimulation buffer. If the impact of antagonists was investigated, they were added 30 min prior to agonist addition and incubated at 37°C. After another 30 min incubation at 37°C, the reaction was terminated by addition of 3 µl of IP-d2 followed by 3 µl of europium(Eu)-cryptate-labeled IP1 Mab diluted (1:20) in lysis buffer. The plates were allowed to incubate for 60 min at room temperature and were then read by Mithras LB940 (Berthold) with 100 µs delay and 200 µs window time.

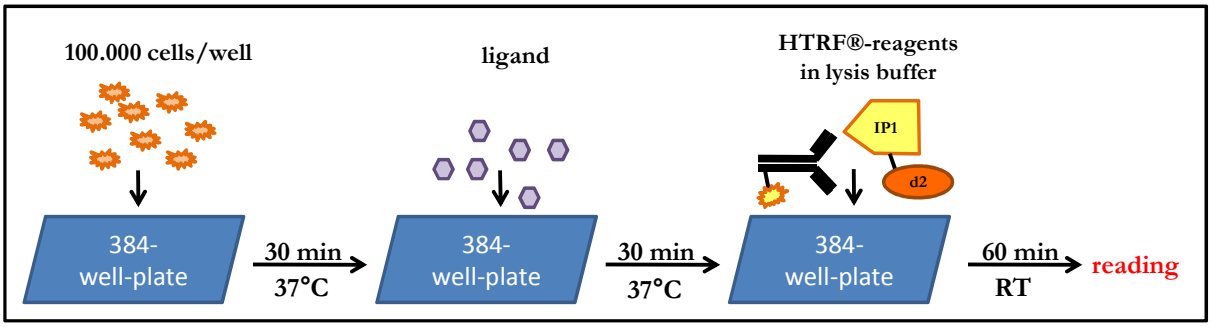

Figure 18 Schematic HTRF® IP1 assay protocol diagram (please refer to the text above for detailed information)

3.3.2.6 Data evaluation of second messenger HTRF® assay

The evaluation of HTRF® data was performed according to manufacturer's instructions. Data analyses were made based on the HTRF® ratio given as 10,000 × [emission (665 nm)/emission (615 nm)], meaning light emitted by labeled IP1/cAMP over the light emitted by the europium cryptate-labeled anti-IP1 / anti-cAMP. Levels of cAMP were normalized to the amount of cAMP elevated by forskolin and levels of IP1 were normalized to the maximum amount of IP1 generated by ligand-induced GPCR activation. In some analyses, data were presented as arbitrary units, meaning amount of cAMP or IP1 related to the examined basal levels ((buffer HTRF® ratio subtracted by agonist-induced HTRF® ratio) +buffer HTRF® ratio).

In order to generate concentration-response curves (CRCs), accumulated cAMP / IP1 or representative values were plotted against agonist concentrations. Each data point of a single experiment represents a mean of at least three independent experiments performed in duplicates or triplicates. CRCs were fitted as described in 3.3.1.3.

3.3.3 Bioluminescence Resonance Energy Transfer (BRET)

Bioluminescence resonance energy transfer (BRET) was discovered in marine organisms and is a naturally occurring physical phenomenon with non-radiative energy transfer from a donor enzyme to a suitable acceptor molecule after substrate oxidation. Renilla luciferase (RLuc), isolated from the sea pansy *Renilla reniformis,* is traditionally used as a bioluminescence donor (Ward & Cormier 1979).

The enzyme generates bioluminescence through oxidation of its substrate coelenterazine h and thus excites the fluorescence acceptor YFP (Yellow Fluorescent Protein). A further development of this classical BRET technique is the here applied BRET2 method, which is based on the application of coelenterazine 400A (DeepBlue C) as the substrate, while the Green Fluorescent Protein 2 (GFP2) is used as the acceptor protein (Bertrand et al., Hamdan et al. 2005, Ramsay et al. 2002, Vrecl et al. 2004, Vrecl et al. 2009, reviewed by Pfleger & Eidne 2006). Coelenterazine are small, hydrophobic molecules that can easily cross cell membranes. This chemical property enables analyses of intact living cells (Xu, Piston & Johnson 1999).

By use of the BRET technique a few practical problems occurring with FRET can be circumvented. Unlike FRET, BRET avoids the need for excitation, thus avoiding problems associated with auto fluorescence, photo bleaching and cell damage (Tsien, Bacskai & Adams 1993, Tsien 1998, reviewed by Milligan 2004). One main disadvantage of BRET method is the need of heterologous expression of fusion proteins, either C-terminally with RLuc or N-terminally with GFP2, which may alter the physiological and mechanistic function of proteins of interest.

3.3.3.1 Theoretical background of BRET2 technique

In principle many intracellular protein-protein-interactions can be examined by means of BRET technology. In the field of GPCR research the method was mainly applied to analyze homo- and heterodimerization of receptors, but the analyses of β-arrestin recruitment induced by an activated GPCR gets more and more into the focus of interest (Angers et al. 2000, Bertrand et al., Hamdan et al. 2005, Vrecl et al. 2004, Vrecl et al. 2009, reviewed by Milligan 2004, Pfleger & Eidne 2005, Pfleger & Eidne 2006, Pfleger et al. 2007). In the year of 2000 Angers et al. were the first to report about the application of BRET to observe and quantify agonist-induced β-arrestin2 recruitment to the β2-adrenergic receptor in living cells (Angers et al. 2000). This opened up new possibilities of analyzing GPCR activation, independent of its preferred G protein-coupling, as agonist-mediated arrestin translocation by GPCRs is an almost universal event. Furthermore, Hamdan et al. showed that use of BRET for analyses of GPCR-β-arrestin interactions is applicable for High Throughput Screening (HTS) of GPCR-specific ligands (Hamdan et al. 2005).

In order to elucidate GPR17 mediated β-arrestin2 recruitment by means of BRET2, the receptor was C-terminally fused to Renilla Luciferase (RLuc) and β-arrestin2 was N-terminally tagged with the Green Fluorescent Protein (GFP2). These two fusion proteins were stable coexpressed in HEK293 cells. In the presence of oxygen, RLuc catalyzes the oxidation of its substrate coelenterazine 400A into coelenteramide while emitting blue light at 400 nm. If ligand-mediated activation of GPR17 induces recruitment of β-arrestin2 to the activated receptor, an energy transfer will occur between RLuc and GFP2 as the two molecules are brought into close proximity (within 100 Å, Xu, Piston & Johnson 1999). The GFP2 molecule will then emit green light at 515 nm. The effectiveness of energy transfer between RLuc/Coelenterazine 400A and GFP2 is demonstrated in the ratio of acceptor energy emission (515 nm) relative to the donor emission (400 nm). This quotient is also referred to as BRET ratio and is a degree for proximity of GFP2 to RLuc (Pfleger & Eidne 2006).

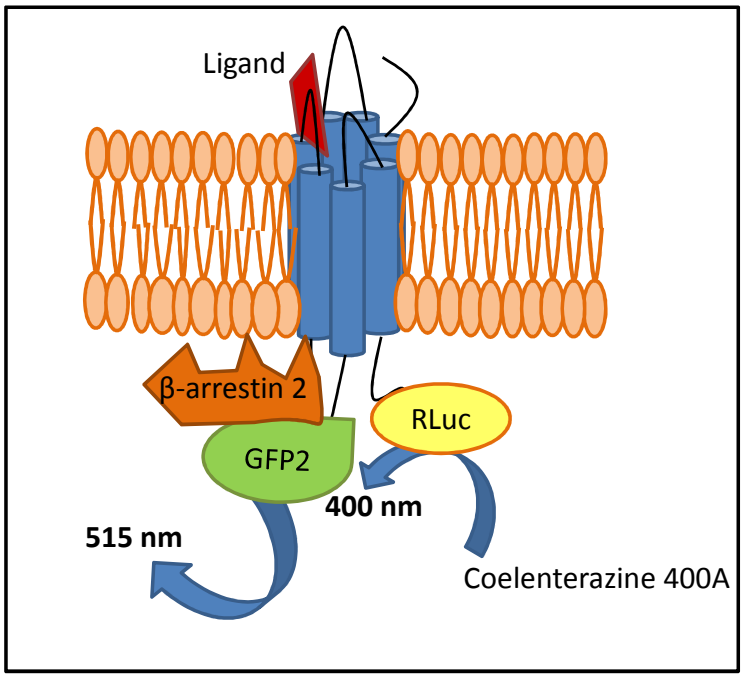

Figure 19 Analysis of β-arrestin2 recruitment by means of BRET2
In unstimulated cells, the receptor resides in the plasma membrane, whereas β-arrestin2 is located in the cytosol. During ligand-induced stimulation β-arrestin2, N-terminally fused to green fluorescent protein 2 (GFP2), translocates to the plasma membrane and forms a complex with the activated receptor, which is C-terminally fused to Renilla luciferase (RLuc) The spatial proximity of the two proteins brings RLuc and GFP2 close together, which, upon addition of coelenterazine 400A (C10), leads to bioluminescence resonance energy transfer (BRET).

3.3.3.2 Generation of BRET2 fusion constructs

HEK293 cells stably expressing various amounts of β-arrestin2, N-terminally tagged with GFP2, were kindly provided by Jesper Mosolff Mathiesen (Department of Medicinal Chemistry, University of Copenhagen). The C-terminally tagged RLuc-GPR17 construct was made using standard molecular biology techniques employing fragment replacement strategies. A plasmid (pcDNA3.1 (+), neomycin) containing the human GPR17 (GenBank accession no. U33447) fused in-frame to the coding sequence of RLuc already existed in our group. Nevertheless, it was necessary to subclone the sequence into a zeomycin resistant expression vector, as the provided stable β-arrestin2-GFP2 HEK293 cells possessed neomycin resistance. Therefore a pcDNA3.1(+) Zeo expression vector comprising the Protease Activated Receptor 1 (PAR1) fused in-frame to the coding sequence of RLuc was cut with the restriction enzymes HindIII and EcoRI (see 3.1.9.2) and replaced by hGPR17 (see 3.1.12), which previously has been cut with the same restriction enzymes (HindIII and EcoRI) out of its pcDNA3.1(+) Neo-RLuc expression vector.

For functional validations of the fusion protein (hGPR17-RLuc), the wild type GPR17 was additionally subcloned into pcDNA3.1 (+) Zeo. The coding sequence of GPR17 was PCR amplified from a plasmid template (MSP70, kindly provided by Andreas Spinrath, AK Kostenis, University of Bonn), containing the required sequence of human GPR17 (GenBank accession no. U33447). By use of specific oligonucleotide PCR primers (see 2.14.1) external to the GPR17 cDNA, a product of 1020bp was

amplified (see 3.1.5.1) and inserted (see 3.1.12) into the pcDNA3.1 (+) Zeo expression vector via 5‘ HindIII and 3’XhoI (see 3.1.9.2).

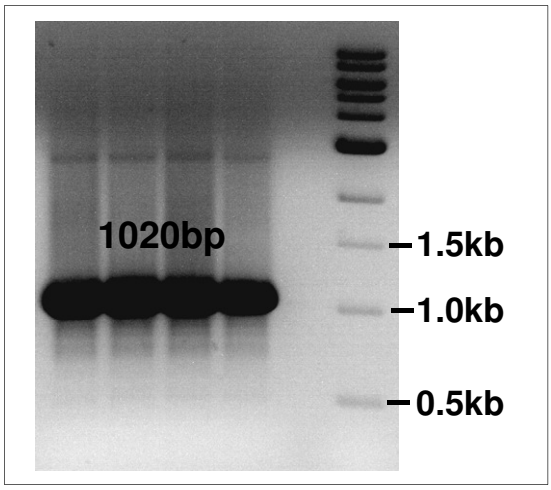

Figure 20 Agarose gel electrophoresis of hGPR17 PCR product detected with ethidium bromide under UV light.
The PCR reaction revealed a product of a size slightly bigger than 1.0 kb, thus certainly representing the expected size of hGPR17 cDNA (1020bp). For detailed information about PCR conditions see 3.1.5.1.

The completed vectors were transformed into XL1-blue (see 3.1.1.2) and, following a primary analytical screening by restriction endonuclease digest (see 3.1.2.1 and 3.1.9.1), sufficient amounts of vector DNA were obtained by preparative plasmid isolation (see 3.1.2.2). Restriction cleavage of GPR17-RLuc construct with HindIII and EcoRI resulted in linearized pcDNA3.1 vector (4947bp) including the RLuc sequence (936bp) and the smaller fragment verified the correct insertion of GPR17 sequence without its stop codon (1017bp) due to in frame fusion with RLuc sequence. The wild type GPR17 plasmid was cut with HindIII and XhoI (B), resulting in one fragment of 4.9kb, illustrating the linearized pcDNA3.1 vector, and one fragment of 1020bp, verifying the correct insertion of GPR17 sequence. Due to very low rate of successful transformation, the wild type GPR17 plasmid was additionally proven by cleavage with SalI and NcoI, respectively (C). Restriction analysis resulted in expected fragments, as depicted in Figure 21.

The sequence identity of both constructs was further verified by sequencing in both directions with the use of standard oligonucleotide primers T7 and BGH reverse (see 3.1.6).

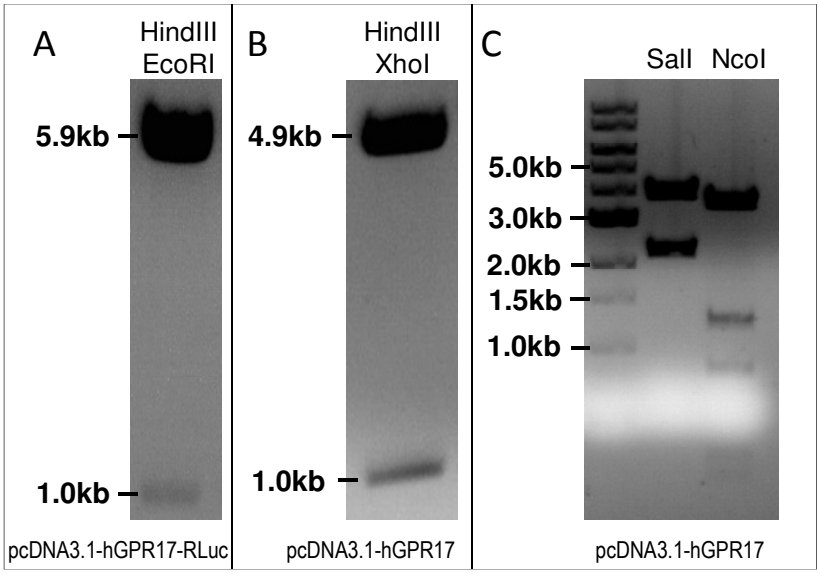

Figure 21 Analytical cleavage of pcDNA3.1-hGPR17-RLuc and pcDNA3.1-hGPR17
A, Restriction endonuclease digest with HindIII and EcoRI of pcDNA3.1/Zeo(+)-hGPR17-RLuc resulted in two fragments: 5883 bp of vector DNA (4947 bp) including the RLuc sequence (936 bp) and 1017 bp of hGPR17 sequence exclusive of its stop codon B, Restriction endonuclease digest with HindIII and XhoI of pcDNA3.1/Zeo(+)-hGPR17 resulted in two fragments: 4947 bp of vector DNA and 1020 bp of hGPR17 sequence C, restriction endonuclease digest of pcDNA3.1/Zeo(+)-hGPR17 with SalI lead to two main fragments (3.7 kb and 2.2 kb) and one not visual band of 30 bp. The restriction enzyme NcoI cut the plasmid into 5 fragments (3.4 kb, 1.2 kb, 0.8 kb, 0.3 kb and 0.2 kb). For detailed information about plasmid maps see 2.16.

3.3.3.3 Experimental procedure of BRET2

Functional BRET2 (here also referred to as BRET) assays were performed on HEK293 cells stably expressing human GPR17-Rluc and GFP2-β-arrestin2.

Cells were detached by trypsinization, counted and washed once in assay buffer (HBSS, 20 mM HEPES (S12), pH 7.0). After centrifugation at 800 rpm for 4 min, the pelleted cells were resuspended in an appropriate volume of assay buffer to a density of 1 x 10^6 cells per ml. In order to stabilize readings, cells were allowed to incubate at 28°C for 30 min while slowly shaking (180 rpm), prior to experiments.

The coelenterazine 400A stock solution (C10, 1 mM in ethanol) was freshly diluted (3:100) in PBS (S15) containing 20% of ethanol (C15) to obtain a 30 µM solution, which was always kept in the dark, due to its light-sensitivity.

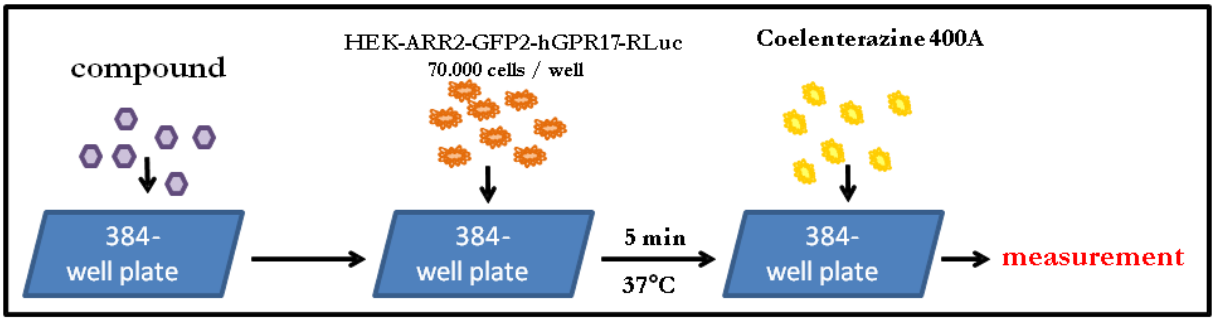

Figure 22 Experimental procedure of agonist BRET2 (please refer to the text for detailed information)

3.3.3.3.1 Agonist assay

As a first step, the agonist solutions were prepared and 10 µl of each 8-fold dilution was dispensed in the 384-well assay plate. DMSO (C11) concentrations were adjusted and did not exceed 0.1% in final concentrations.

Harvested and stabilized cells were manually distributed (70 µl, 70.000 c/well) to the assay plate containing the agonist dilutions. Cells were stimulated at 28°C at 450 rpm for 5 min or a respective time period for *long* adhesion kinetic measurements(1, 5, 10, 15, 30 or 60 min). Following cell stimulation, Coelenterazine 400A (C10, 10 µl) was injected by the Mithras injector 3 at a final concentration of 3.3 µM (10 µl of 30 µM solution). Two seconds after the injections, the light output from the well was measured at 400 and 515 nm by use of Mithras LB 940 plate reader, which allows the sequential integration of light signals detected with two filter settings. The BRET signal, milliBRET ratio, was calculated by the quotient of the fluorescence emitted by GFP2-β-arrestin2 (515 nm) over the light emitted by the GPR17-Rluc (400 nm).

For BRET2 experiments in the presence of Pertussis toxin, cells were preincubated over-night in the presence of the toxin at a final concentration of 50 ng/ml.

3.3.3.3.2 Measurement of recruitment kinetics

For recruitment kinetic analyses (0-140 s) of GPR17-RLuc and GFP2-βarrestin2 interactions, cells were seeded in empty 384-well assay plate. Coelenterazine 400A (C10) was added (Mithras injector 3, final concentration 3.3 µM) 20 s before injection of the agonist (10 µl, 9-fold) with the Mithras injector 1. Readings were performed immediately at 1.0 s intervals and during 140 s using the Mithras LB 940 plate reader.

3.3.3.3.3 Antagonist assay

Antagonists (5 µl, 15-fold) were preincubated with the cells for 30 min (28°C, 450 rpm) before agonist dilutions (5 µl, 16-fold) were manually added. Following 5 min of agonist-stimulation at 28°C and 450 rpm, Coelenterazine 400A (C10, 10 µl) was injected by the Mithras injector 3 at a final concentration of 3.3 µM (10 µl). Two seconds after the injection, the light emission was measured at 400 and 515 nm by use of Mithras LB 940 plate reader.

3.3.3.4 Data evaluation of BRET2

Data were collected using the MikroWin200 software. For concentration-response data, curves were fitted with nonlinear regression equation using Prism software. Results were calculated as the ratio of GFP2 emitted light over RLuc catalyzed light emission. Agonist-promoted net BRET was calculated by subtracting the BRET ratio obtained in the absence of agonist from the one obtained in the presence of an agonist.

3.3.4 Enzyme-linked immunosorbent assay (ELISA)

ELISA, enzyme-linked immunosorbent assay, is a technique based on the reaction of antigens and antibodies. In this work the indirect ELISA method was applied to quantitate cell surface expression of the N-terminally 3xHA-tagged GPR17 receptor as well as investigate its internalization behavior.

3.3.4.1 Theoretical background of indirect ELISA

The method involves an unlabeled primary antibody (Table 22, A1) targeted against the desired antigen (N-terminally 3xHA-tag labeled GPR17) in conjunction with an enzyme-labeled (horseradish peroxidase, HRP) secondary antibody (Table 22, A2), which is directed against all antibodies of a given species (here e.g. anti-goat).

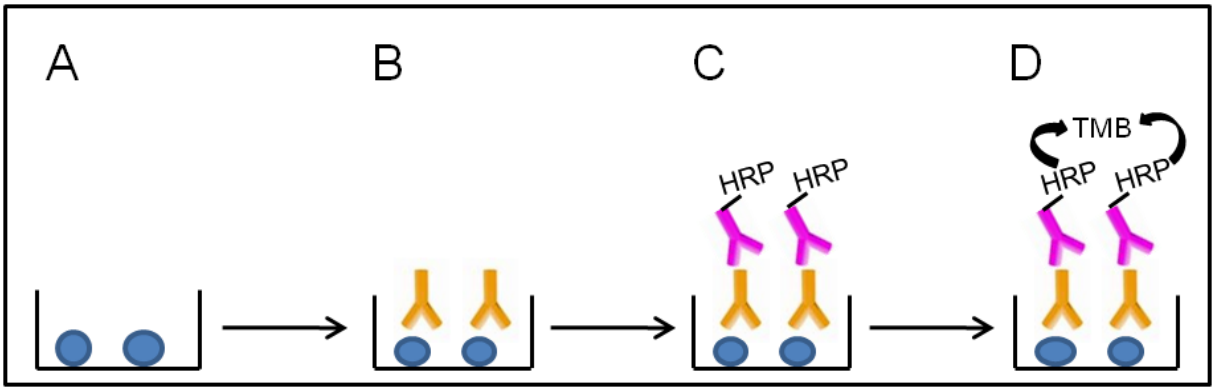

Figure 23 Indirect ELISA principle (for detailed information please refer to the text)
A, Blue circles represent fixed cells expressing 3xHA-tagged GPR17. B, Specific antibody (yellow) binds to antigen (3xHA) C Enzyme-linked antibody (pink) binds to specific antibody (yellow). D, Substrate (tetramethyl benzidine, TMB) is added and converted by the enzyme (horseradish peroxidase, HRP) into a color product (blue). Rate of color formation is proportional to the amount of 3xHA-tagged GPR17.

3.3.4.2 Experimental procedure of indirect ELISA

3.3.4.2.1 Generation of 3xHA tagged hGPR17

Since no specific antibody for GPR17 was readily available, a sequence (102 bp) encoding a 3xHA-epitope tag (haemagglutinin influenza virus epitope tag) was introduced in frame by PCR at the amino terminus of the GPR17. As there are commercially available antibodies directed against this tag, the genetically engineered GPR17 provided a useful tool for immunobiological analyses (ELISA and immunofluorescence). The uniqueness of the epitope in the genome and the use of monoclonal antibodies assure a high-affinity, specific and abundant antibody binding (Kolodziej & Young 1991).

In order to generate these constructs, two PCR reactions were consecutively performed. At first an oligonucleotide primer consisting of a 3xHA tag sequence and additionally in-frame the 5’ start sequence of human GPR17 was amplified by PCR. Therefore a plasmid containing the sequence of a 3xHA tagged GPCR (GPR55) was used as the template (for further information about PCR conditions see 3.1.5.2). The PCR product was separated by agarose gel electrophoresis (Figure 24) and purified with gel extraction kit (see 3.1.8).

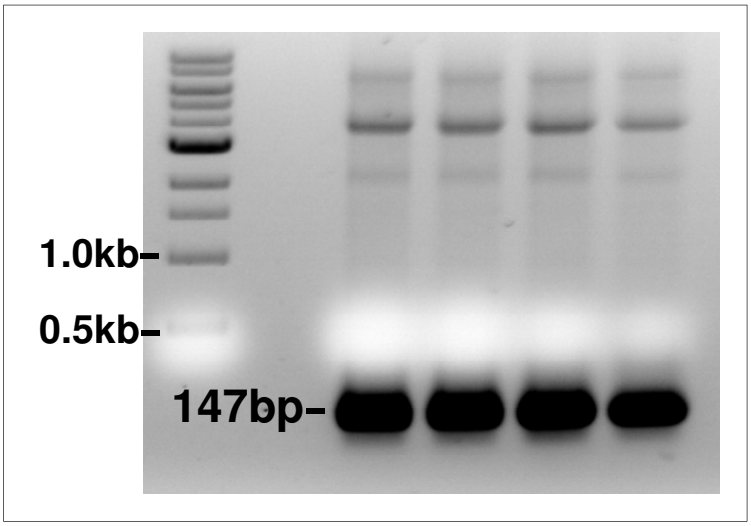

Figure 24 Agarose gel electrophoresis of 3xHA tag primer PCR product detected with ethidium bromide under UV-light.
PCR primers were designed to obtain a PCR product (147bp) consisting of 3xHA tag sequence in frame with the 5' start sequence of hGPR17 and flanked by an artificial NheI restriction site (5'). Please refer to Table 26 for details of the PCR conditions.

With a second PCR reaction the 3xHA-tagged GPR17 sequence was amplified. Therefore, the preliminarily amplified PCR product was used as forward primer and pcDNA3.1/zeo-GPR17 plasmid as the template (see 3.1.5.2 for further information about PCR conditions). The resulting construct was inserted in-frame via 5'NheI and 3'XhoI into pcDNA3.1/zeo. In order to obtain a 3xHA-epitope tagged GPR17 C-terminally fused to Renilla Luciferase (RLuc), the resulting fragment was inserted in-frame via 5'NheI and 3'PstI into pcDNA3.1/zeo-GPR17-RLuc.

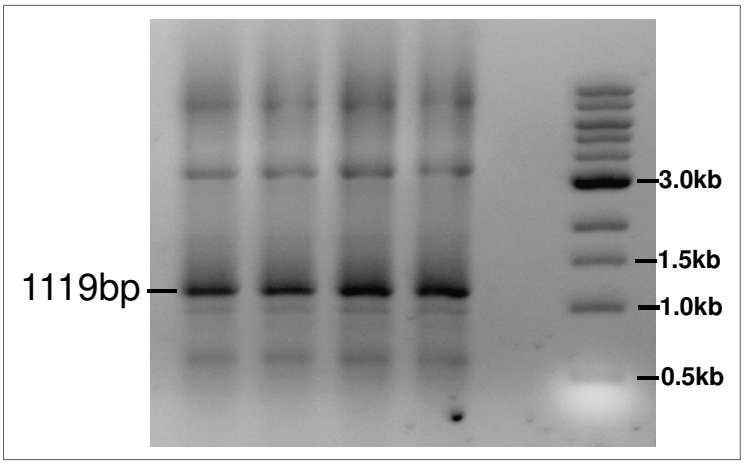

Figure 25 PCR amplicon of 3xHA tagged hGPR17 envisaged by agarose gel electrophoresis
PCR primers were designed to obtain a PCR product consisting of 3xHA tag sequence (102bp) in frame with the 5' hGPR17 sequence (1017bp) without its start codon, and flanked by artificial restriction sites (5' NheI, 3' XhoI). Please refer to Table 27 for details of the PCR conditions.

The sequence identity of the constructs was verified by restriction endonuclease cleavage and the expected fragments were detected by agarose gel electrophoresis, as depicted in Figure 26. The sequence identity of both constructs was further verified by sequencing in both directions with the use of standard oligonucleotide primers T7 and BGH reverse (see 3.1.6).

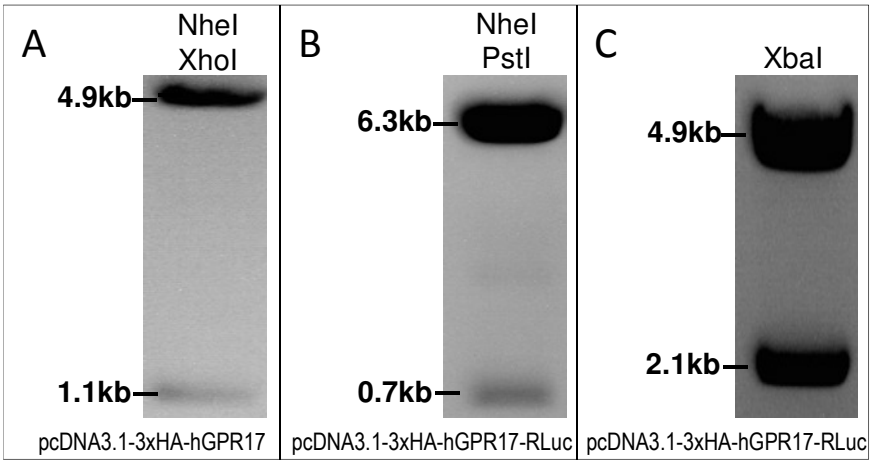

Figure 26 Restriction endonuclease cleavage of 3xHA tagged GPR17 constructs
A, Restriction endonuclease cleavage of pcDNA3.1-3xHA-GPR17 with XhoI and NheI resulted in two fragments, pcDNA3.1 vector consisting of 4954bp and 3xHA-GPR17 sequence (1119bp), respectively. B, Restriction endonuclease cleavage with NheI and PstI of pcDNA3.1-3xHA-GPR17-RLuc showed two main fragments, whereat 6331bp represented pcDNA3.1 vector (4954bp) including sequence of RLuc (936bp) and a part of GPR17 sequence (441bp), and a fragment of 673bp belonging the other part of 3xHA-GPR17. C, Restriction endonuclease digest with XbaI of pcDNA3.1-3xHA-GPR17-RLuc resulted in two bands, one of 4952bp (pcDNA3.1) and one of 2052bp (3xHA-GPR17-RLuc). For more information about constructed plasmids and respective restriction sites, see Figure 12.

3.3.4.2.2 Quantification of receptor expression levels

Whether for quantification of receptor expression levels or for examination of internalization behavior, cells stably expressing 3xHA-tagged GPR17 (50.000 cells/well) were seeded onto PDL coated 96 well plates and grown in the incubator (37°C, 5%CO_2) 24 h prior to analyses. On the day of experiment medium was carefully aspirated and cells were fixed with 4% paraformaldehyde (S14, 100 µl/well) for 25 min at RT. After washing three times with PBS (S15, 200 µl/well), cells were blocked with non-fat dried milk (blotto, S1, 100 µl/well) for 60 min at 37°C. If permeabilization was required for quantification of total receptor expression, triton X-100 (0.5%, C52) was added to blocking solution. After aspirating the blocking solution, cells were incubated with goat anti-HA antibody (Table 22, A1, diluted 1:400 in blotto, S1) for 45 min at RT. Following three washes with PBS (S15), the cells were incubated for 45 min at RT. The cells were washed again and incubated with tetramethyl benzidine liquid substrate (TMB, C49, 100 µl/well) for up to 5 min. The reaction was stopped by addition of sulfuric acid (C48, 0.5 M H_2SO_4, 50 µl/well) to a final concentration of approximately 0.17 M and the optical density (OD) of the supernatant was measured at 450 nm with the Tecan Sunrise-Basic. Cells without transfection were similarly treated and used as negative control.

3.3.4.2.3 Quantification of internalization

In addition to the protocol of expression analyses, the cells were initially stimulated for various time periods (15, 30, 60 and 120 min) at 37°C to induce receptor internalization. After washing once carefully with PBS (S15), cells were fixed with PFA (4%). It was then preceded as described for

receptor expression analyses (see 3.3.4.2.2). The degree of internalization was expressed as percent (%) relative to cells without ligand stimulation.

3.3.4.3 Data evaluation of ELISA

The respective OD_{450} values were collected using the XFluor2 software and evaluated with the help of Prism software. The OD_{450} value for the negative control was subtracted from all other samples.

3.3.5 Immunofluorescence microscopy

The generated 3xHA-epitope tagged GPR17 (see 3.3.4.2.1) allowed studying its subcellular localization by immunofluorescence microscopy. HEK293 cell lines stable expressing the epitope tagged GPR17 were used for analyses.

3.3.5.1 Theoretical background of immunofluorescence

The immunofluorescence analyses were based on an indirect fluorescent technique, similar to the applied ELISA method (see 3.3.4.1). An unlabeled primary antibody (Table 22, A1) targeted against the desired antigen (N-terminally 3xHA-tag labeled GPR17) is utilized in conjunction with an fluorescence-labeled (Alexa Fluor 546) secondary antibody (Table 22, A3), which is directed against antibodies of a given species (here e.g. anti-goat).

3.3.5.2 Experimental procedure immunofluorescence

For immunocytochemical studies of subcellular localization of unstimulated 3xHA-GPR17, stable transfected HEK293 cells (30.000 cells/well/100 µl) were plated onto poly-D-lysine coated 96well plates (black with clear bottom) 20-24 h prior to analyses. On the day of experiment, cells were washed once with PBS (S15, 200 µl) and then fixed with 4% paraformaldehyde in PBS (S14, 100 µl) for 30 min at RT. The fixed cells were washed three times with PBS (S15, each 200 µl, 10-15 min at RT), and then incubated with goat serum blocking solution (S9, containing goat serum, BSA, and triton X-100 for permeabilization) for 60 min at RT. Subsequent to the blocking procedure, cells were incubated with the primary anti-HA antibody (Table 22, A1, diluted 1:500 in blocking solution) (100 µl) for 60 min at 37°C. Following three washes with PBS (S15, 200 µl, 10 min each, 37°C), cells were incubated with the secondary antibody Alexa Fluor 546 goat anti-mouse (Table 22, A3, diluted 1:2000 in blocking solution) for 60 min at 37°C. After three last washing steps with PBS (S15, 200 µl, 10 min each, 37°C), wells were completely filled with PBS (S15), and sealed with self-sticky foil. Plates were kept at 2-8°C for further analyses.

3.3.5.2.1 Internalization

For immunocytochemical studies of subcellular localization of agonist-stimulated and -internalized 3xHA-GPR17, stable transfected HEK293 cells (30.000 cells/well/100 µl) were plated onto black poly-D-lysine coated 96well plates (with clear bottom) 20-24 h prior to analyses. On the day of experiment, the 3xHA-epitope tagged GPR17 on the plasma membrane was labeled by incubation

with anti-HA antibody (Table 22, A1, diluted 1:200 in cell medium without FCS) for 60 min for at 37°C. Afterwards cells were treated with ligands (diluted in cell medium without FCS to avoid unspecific blocking reactions) for the indicated time periods. The stimulated cells were then washed once in PBS (S15, 200 µl), and then fixed in 4% paraformaldehyde (S14) for 30 min at RT. After three 10 min washes with PBS (S15) the cells were permeabilized, and nonspecific binding was blocked with goat serum blocking solution (S9, containing 0.5% triton X-100) for 60 min at RT. Following three washing steps (each 10 min) with PBS (S15), cells were stained with goat anti-mouse Alexa Fluor 546-conjugated secondary antibody (Table 22, A3, 1:2000 in blocking solution) for 1 h at 37°C. After three last washing steps with PBS (S15, 200 µl, 10 min, 37°C), wells were completely filled with PBS (S15), and sealed with self-sticky foil. Plates were kept at 2-8°C for further analyses.

3.3.5.3 Data evaluation

Cells were examined by immunofluorescence microscopy on a Leica DM IL LED Fluo fluorescence microscope using a 20 or 40X objective and the received pictures with a resolution of 1.4 megapixels were pseudo-colored using the Leica DFC 360 FX. Images were collected using Leica Application Suite 3.3.1 imaging software and were processed with Microsoft Office Picture Manager. All experiments were confirmed at least three times, and a representative image is shown.

3.3.6 Schild regression analysis

In order to evaluate antagonistic potencies as well as to determine antagonistic behaviors, Schild regression analyses were performed, which represent the major pharmacological tool used to quantify affinities of antagonists. Antagonist Ki values could be calculated from their IC_{50} values from competition binding experiments; provided that the radioligand's Kd value was known. As for GPR17 no radioligand is readily available, the method developed by Schild and coworkers (ARUNLAKSHANA & SCHILD 1959) was utilized to obtain antagonist K_B values with functional studies. Utilizing this method, a system-independent estimate of the affinity of an antagonist can be made in a functional system. Furthermore, the method can also compare the pattern of antagonism, thereby allowing definition of the mechanism of action of the antagonist.

The method is based on the fact that competitive antagonists produce a parallel rightward shift of the agonist concentration-response curve, which is measured in the presence of increasing, constant concentrations of the antagonist. Dose ratios (DR), which are usually defined as the ratio of EC_{50} values in presence and absence of the antagonist, were calculated. Accordingly, for every concentration of antagonist there will be a corresponding DR value. The next step is to plot the common logarithm of the DR subtracted by 1 (log DR-1) against the common logarithm of the applied antagonist concentration (log M). This plot is referred to as Schild plot, and it reflects that, when log DR subtracted by 1 equals 0, the plot intercepts with the abscissa and, in this situation, log K_B is equal to log M.

$$\mathbf{Log(DR-1) = Log(M) - Log(KB)}$$

Thus, the concentration of antagonist that produces a log (DR-1) = 0 value will be equal to the log K_B, the equilibrium dissociation constant of the antagonist-receptor complex. The antagonist's log K_B can be easily calculated by linear regression of Schild Plot according to Arunlakshana and Schild (ARUNLAKSHANA & SCHILD 1959). Since K_B values are obtained from a logarithmic plot, they are log normally distributed and are therefore conventionally reported as pK_B values. The negative logarithm to base 10 of the molar concentration of an antagonist that makes it necessary to double the concentration of the agonist needed to elicit the original submaximal response obtained in the absence of antagonist (SCHILD 1997). The negative logarithm of this concentration is often referred to as the pA_2. Hence, the pA_2 value is formally the pK_B for simple competitive antagonists, but furthermore also approximates the pK_B for insurmountable antagonists if a parallel rightward shift of the curve occurs concomitant with depression of maximal response. Instead of utilizing EC_{50} values for calculation of dose ratios (DR), the DR values are calculated from values of response below where depression of response occurs, for example at 20% maximal response level, whereas curves should be fitted to a common slope (Kenakin, Jenkinson & Watson 2006). As the model of simple competitive antagonism predicts that the slope of the Schild regression should be unity, statistical estimation of the 95% confidence limit of the slope were used to determine whether the sample data revealed a unit slope, thus describing simple competitive antagonism.

3.4 Homologous recombination in embryonic stem cells

In 1981, Evans and Kaufman (Evans & Kaufman 1981) and Martin (Martin 1981) were the first to isolate and cultivate murine pluripotent embryonic stem cells. This was a prerequisite for the generation of gene-modified animals or pluripotent cells with the ability for further differentiations. The switch-off of a specific gene enables the analysis of its coded protein and investigations of its physiological role. Therefore, foreign DNA molecules (targeting vector) are transfected into embryonic stem cells, where they can integrate into the host genome, which is also referred to as crossing over.

3.4.1 Targeting vector

A first step for a successful gene targeting is the generation of an appropriate targeting construct.

The murine GPR17 (mGPR17, *GenBank accession no. NM_001025381*) consists of two exons (exon1: 0.18 kb, exon2: 5.0 kb) and is located on chromosome 18. The protein coding region is situated in the first segment of exon 2. The transcript length is 1020 bp, and the translated protein consists of 339 amino acids.

In principle a targeting construct consists of four segments: two homologous regions (one 5' of the respective gene and one 3'), which are inserted in a plasmid vector (here pPNT) and separated by the neomycin resistance cassette. The homologous regions are also referred to as 'arms' (short and long arm). Following linearization and electroporation, they attach to their respective homologous regions in the genomic DNA (heteroduplex formation), and replace the particular DNA segments, due to the

crossing-over (Thomas, Folger & Capecchi 1986). The possibility of a homologous recombination increases with the size of these homologous regions (Hasty, Rivera-Pérez & Bradley 1991). Optimal sizes were found to be in between 5 and 10 kb, as the application of even bigger sequences increases efficiency of recombination, but especially the cloning strategies were no longer feasible.

For generation of the targeting vector, a homologous genomic sequence (6.2 kb), including a part of intron 1 and exon 2, was chosen. In order to knock-out the functionality of the 7TM receptor GPR17, the sequence of its transmembrane domains 2-6 (TM2-6, 564 bp) was replaced by neomycin-resistance-cassette (1.8 kb). Since the transmembrane domains 3 and 6 are essential for a correct transition of GPCRs to its full active state (Hulme et al. 1999), their knock-out leads to a loss of complete function.

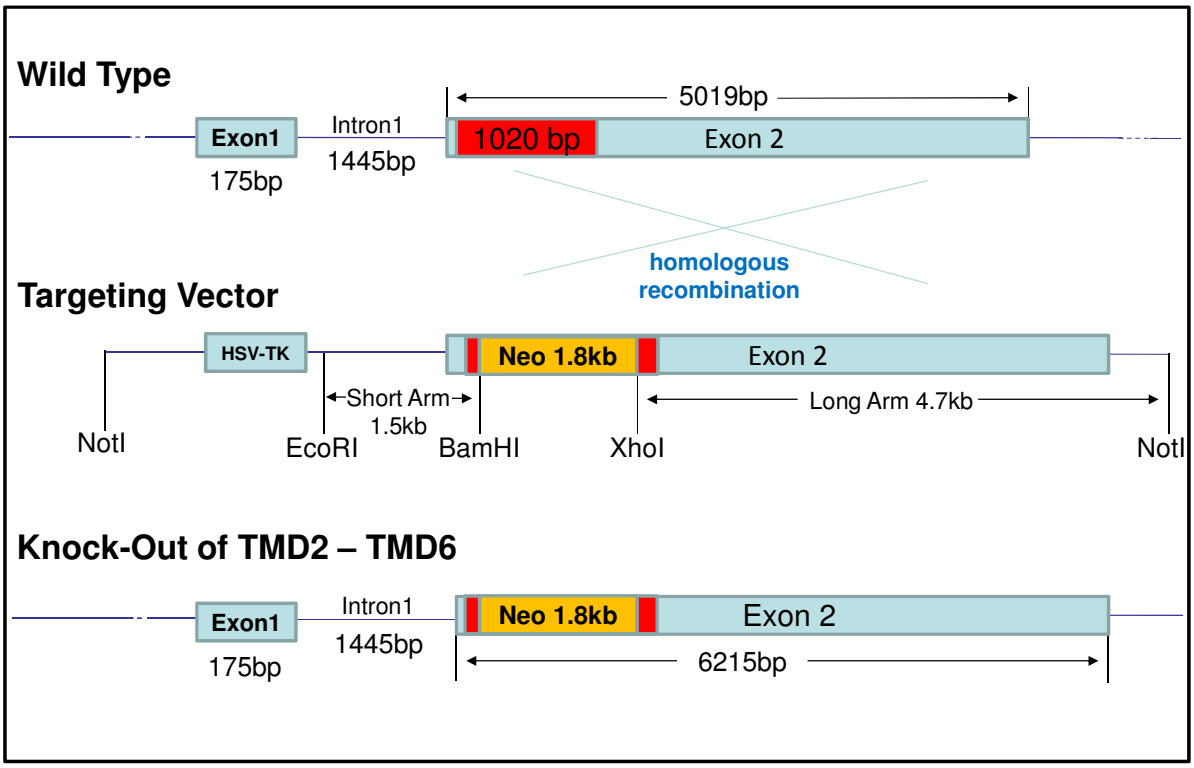

Figure 27 Knock-out strategy
Murine GPR17 (wild type) locus encompassing two exons (light blue bars), whereat the coding region (1020bp, red bar) is situated on Exon2. Experimental construct design of the targeted mouse GPR17 allele, based on homologous recombination with a targeting vector comprising the bacterial neomycin-resistance cassette (neo, yellow bar), which disrupts the coding sequence of the mouse GPR17 gene (transmembrane domains 2 until 6 / TMD2-TMD6) (please refer to the text for more information).

3.4.1.1 Cloning procedure

For amplification of homologous regions (short and long arm), PCR reactions were performed with the use of genomic ES cell DNA (HM-1, kindly provided by Daniel Schulz, AK Kostenis, University of Bonn) as template, as well as appropriate oligonucleotide primers and a mixture of Taq and Pfu polymerases (for further information about PCR conditions see 3.1.5.3). As shown in Figure 28, PCR products were purified by agarose gel electrophoresis (see 3.1.7) and isolated by subsequent gel extraction (see 3.1.8).

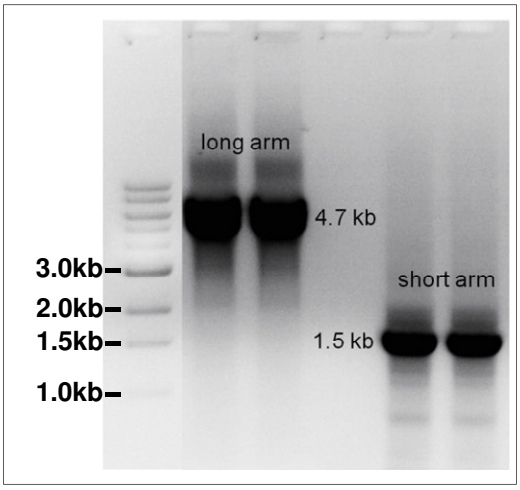

Figure 28 Agarose gel electrophoresis of homologous sequence PCR products detected with ethidium bromide under UV-light

PCR primers were designed to obtain a PCR product consisting of homologous sequence 5'and 3' of mGPR17. Both amplicons were flanked by artificial restriction sites (*long arm* 5' NotI, 3' XhoI; *short arm* 5' BamHI, 3' EcoRI). 1kb DNA ladder was applied for size estimations. Please refer to Table 28 and Table 29 for detailed information about respective PCR conditions.

The short arm sequence was firstly introduced into the pPNT vector via 5' BamHI and 3' EcoRI. Prior to insertion of the remaining long region, the sequence identity of the hitherto existing construct (pPNT vector – short arm) was verified by restriction endonuclease digests (see 3.1.9.1), as presented in Figure 29.

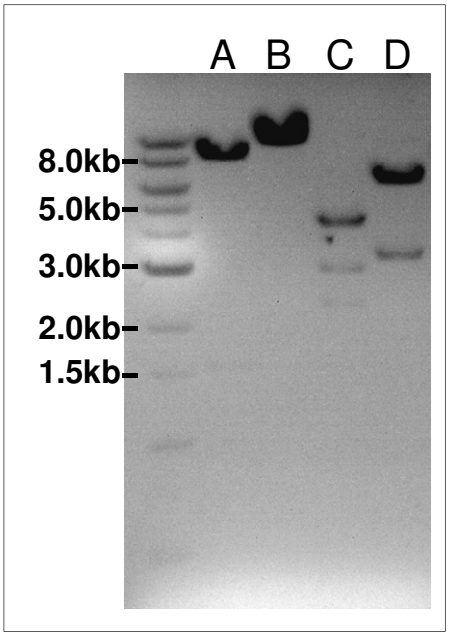

Figure 29 Verification of the introduction of the short homologous sequence in pPNT vector by restriction endonuclease cleavage and envisaged by agarose gel electrophoresis.

A, Endonuclease restriction cleavage with BamHI and EcoRI revealed fragments of the accurate inserted short arm (1529bp) and pPNT vector (8211bp). B, Linearization with BamHI resulted in one DNA fragment (9760bp). C, Endonuclease restriction cleavage with SacI showed the expected 3 visible bands (4424bp, 2347bp and 2068bp). D, Restriction enzyme StuI cut plasmid into two fragments with the expected size (5515bp and 3342bp). 1kb DNA ladder was applied for size estimations. For further information about endonuclease restriction sites see Annex Figure 1.

The long arm PCR product was subcloned into the pPNT vector-short arm construct with the use of 5'NotI and 3'XhoI. The correct insertion of the long homologous region was verified by restriction endonuclease digestion (XhoI and NotI, see Figure 30). Sequencing by GATC Biotech (see3.1.6) revealed no mutations.

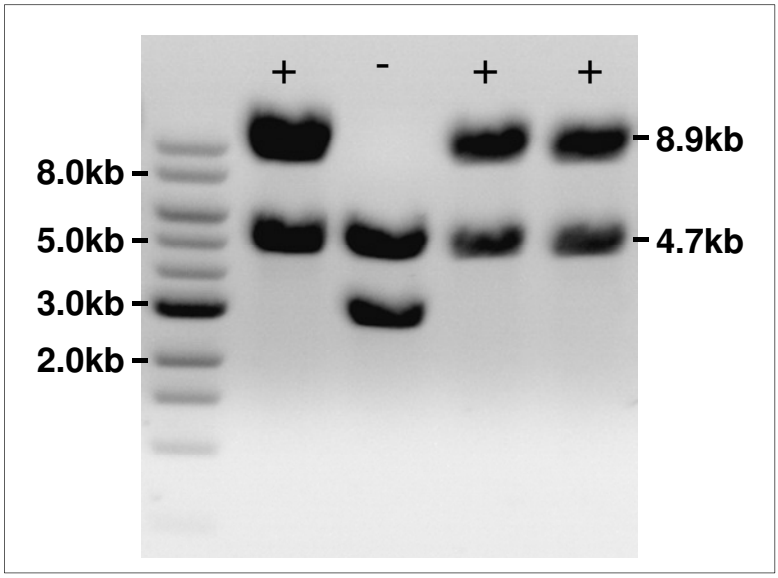

Figure 30 Analytical cleavage of the inserted long homologous sequence in pPNT-short-arm vector by endonuclease restriction cleavage and envisaged by agarose gel electrophoresis
Three out of four isolated plasmids revealed correct DNA band pattern (+) after restriction with XhoI and NotI (8.9kb of pPNT-short-arm, 4.7kb of inserted long arm), whereas one revealed unknown fragments (-). 1kb DNA ladder was applied for size estimations. For further information about endonuclease restriction sites see Annex Figure 1.

3.4.2 Cultivation of murine embryonic stem cells

In general stem cells are cells that are not yet differentiated, meaning they are not yet specialized regarding their cellular functions. Since they derive from the inner cell mass of embryo blastocytes (3.5 days post coitum), they are also referred to as embryonic stem cells (ES cells). These ES cells are able to differentiate into virtually all kinds of cell types, tissue or organs, due to their pluripotent capability. As they are isolated from inner cell mass, they are not able to differentiate into external cell mass as e.g. umbilical cord or placenta, thus they are not totipotent. In order to maintain their pluripotency and to prevent untimely differentiation, it is necessary to cultivate them under special conditions.

The applied embryonic stem cells, which derive from mice with Ola/SV129 strain, were kindly provided by Dr. Jesús Gomeza (AK Kostenis, University of Bonn).

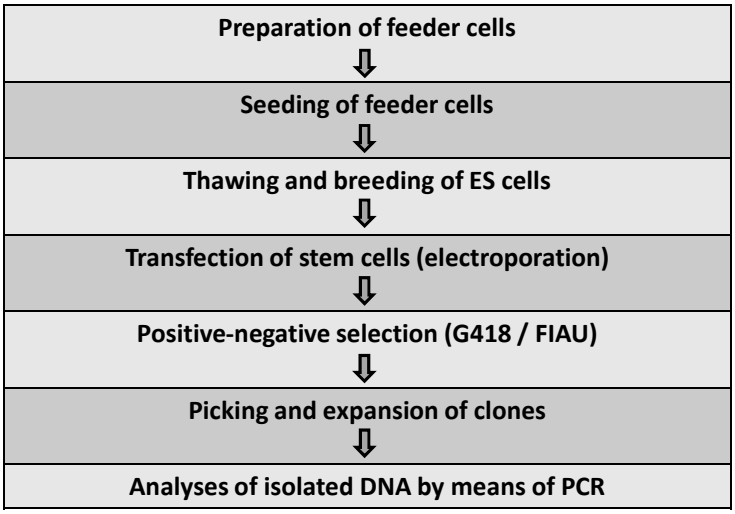

Figure 31 Flow chart for the experimental procedures of gene targeting in ES cells
This figure represents a schematic overview of the performed methods to generate gene modified ES cells, as described in detail in text.

3.4.2.1 ES cell culture media and solutions

ES cell culture medium

One main supplement of the stem cell culture medium is the myeloid leukemia inhibitory factor (LIF). LIF is a polypeptide-cytokine and was discovered as an essential factor to prevent differentiation und thus helps to maintain the pluripotent state of the stem cells (Smith et al. 1988, Williams et al. 1988). LIF acts as a ligand at LIF-receptor-complex (Davis et al. 1993, Gearing et al. 1991). The ES cell culture medium additionally contains sodium pyruvate, non-essential amino acids, L-glutamine, heat-inactivated fetal bovine serum (30 min, 56°C) and 2-mercaptoethanol. The latter prevents oxidation and subsequent inactivation of LIF and represents a sulfur source for the ES cells. In order to obtain ideal culture conditions, a daily change of culture medium is inevitable.

Table 32 ES cell culture medium

constituent	volume [ml]	final concentration
Dulbecco's Modified Eagle Medium (DMEM)	500	
Fetal bovine Serum ES Cell-qualified	56	10%
l-Glutamine, 200 mM	5.6	2 mM
Sodium pyruvate	5.6	2 mM
Non-Essential Amino Acids	5.6	0.1 mM
2-Mercaptoethanol, 50 mM	1.1	0.1 mM
ESGRO® (10^7 units/ml)	0.05	1000 units/ml

LIF= leukocyte inhibitory factor

Medium was always freshly prepared once a week and unnecessary warm-up cycles in water bath were avoided.

ES cell freezing medium (2x)

ES cell freezing medium was freshly prepared by addition of fetal bovine serum (40%) and DMSO (C12, 20%) to complete ES cell culture medium. The respective final concentrations after 1:1 dilution with cell suspension were 20% fetal bovine serum and 10% DMSO (C12).

ES cell positive-negative selection medium

The medium for positive-negative selection was prepared by addition of 2000 µl of G418 (f. c. 360 µg/ml) and 500 µl of FIAU (S7, f. c. 0.2 µM).

Feeder cell medium

Feeder cells were cultured in Dulbecco's Modified Eagle Medium (DMEM) supplemented with fetal bovine serum (10%), L-glutamine (f. c. 2 mM) and sodium pyruvate (f. c. 2 mM).

3.4.2.2 Preparation of feeder cells

Mouse Embryonic Fibroblast (MEF) cells are required to provide nutrients, including cytokines such as LIF, to ES cells and to support the growth of undifferentiated ES cells, thus they are also referred to as feeder cells. MEF cells are isolated from mouse embryos and are used at their early passages. In order to prevent cell death due to treatment with selection antibiotics (G418, positive-negative selection), cells were isolated from mouse embryos containing transgene bacterial neomycin-resistance-gen. These cells were kindly provided by Dr. Jesús Gomeza (AK Kostenis, University of Bonn).

3.4.2.2.1 Thawing and cultivation of MEFs

Frozen MEFs were quickly thawed in a water bath (37°C), then transferred to 10 ml of warm MEF medium, and pelleted by centrifugation (4 min, 800 rpm) in order to remove the DMSO contained in the freezing medium. The supernatant was soaked off; cells were resuspended in warm MEF medium and plated out. The time required until cells were grown to confluence depended on the splitting ratio (1:1 to 1:5).

Before generating feeder layers from the MEFs, cells were expanded several times, letting the cells grow to confluence (see 3.2.1).

3.4.2.2.2 Gamma ray treatment of feeder cells

Feeder layer fibroblasts need to be mitotically inactivated prior to addition of ES cells. Applied cells were treated by irradiation to stop them from growing, while maintaining the abilities to secrete growth factors. The gamma ray treatment of 96 Gray for 5.53 min has been performed by Dr. Stefan Garbe (Radiology, University Medical Center of Bonn).

These radiated cells were directly frozen after the radiation (see 3.2.2).

3.4.2.2.3 Seeding of feeder cells

Embryonic stem cells are usually grown on a layer of mitotically inactivated primary mouse embryonic fibroblasts to promote growth and prevent differentiation.

In general, one day before ES cells were plated, cell culture dishes were gelatinized with 3-10 ml of gelatin working solution (S8, 0.1%), so that surface was completely covered with gelatin. After 10 min incubation at RT, gelatin solution was aspirated and an appropriate amount of thawed feeder cells was seeded (see 3.2.3) on gelatin-coated dishes. The feeder layers were used for one week after plating.

3.4.2.3 Thawing and plating ES cells

Frozen ES cells were revitalized (see 3.2.3) and plated on cell culture dishes, which were coated with gelatin (S8) and feeder cells (see 3.4.2.2.3). In order to expand cells for electroporation, ES cells were passaged twice a week, splitting them 1:3 to 1:10, depending on their growth rate, when they reached approximately 70% confluence (see 3.2.1). Cells were incubated with ES cell trypsin at 37°C for up to 5 min, and large cell clumps were avoided by pipetting cell suspension up and down against dish wall about 10-20 times with varying distances. After each round of trypsinization, fresh feeder cells were added in advance, so that ES cells were grown on confluent feeder layers. Medium exchange was performed daily and cultures were never allowed to become over-confluent, as this triggers cell differentiation. Typical doubling time was about 24 h.

3.4.3 Electroporation of murine embryonic stem cells

Electroporation constitutes an efficient technique to transfect eukaryotic cells (Neumann et al. 1982). Short impetuses of high voltage induce a disturbance of cell membrane potential. This leads to formation of pores in the membrane und foreign DNA can be incorporated into the cell (Sukharev et al. 1992).

For electroporation a densely grown 10 cm (55 cm^2) cell culture dish, with approximately 10-20 x 10^6 ES cells, was used. ES medium was aspirated, cells were washed with PBS (S15), and detached with 2 ml of Trypsin/EDTA. Trypsinization was stopped by addition of ES medium, and cell number was determined in a counting chamber (see 3.2.4). Cells were centrifuged (4 min, 800 rpm) and resuspended in 10 ml of fresh ES medium. In order to get rid of the feeders, cells were dissolved by gently shaking and centrifuged once more (4 min, 800 rpm). Pelleted cells were resuspended in 980 µl of electroporation buffer (S11, 1xHBS) and 20 µl (25 µg) of linearized targeting construct (NotI, see 3.1.9.3) were added. Suspension was mixed carefully by pipetting up and down, and after 5 min incubation at RT, transferred into an electroporation cuvette (0.4 cm). Electroporation was carried out with one pulse by 500 µF and 230 V, and the time constant was 117.2 ms. After the suspension was allowed to stand for 10 min at RT, cells were resuspended in appropriate amount of ES medium (1-2x10^6 cells per 10 ml per 55 cm^2) on dishes covered with feeder cells.

3.4.4 Positive-negative selection

The targeting construct contains the bacterial neomycin-resistance gene, which disrupts the coding sequence of the mouse GPR17 gene (TM2-TM6). When the linearized plasmid is introduced into the ES cells via electroporation, a few cells gain resistance against the aminoglykoside antibiotic Geneticin (G418), independent on the fact, where exactly the construct was integrated. Since during this type of selection only cells survive that stably integrated the resistance gene, it is also referred to as positive-selection. Besides the desired homologous recombination it happens more frequently, that the plasmid is randomly integrated.

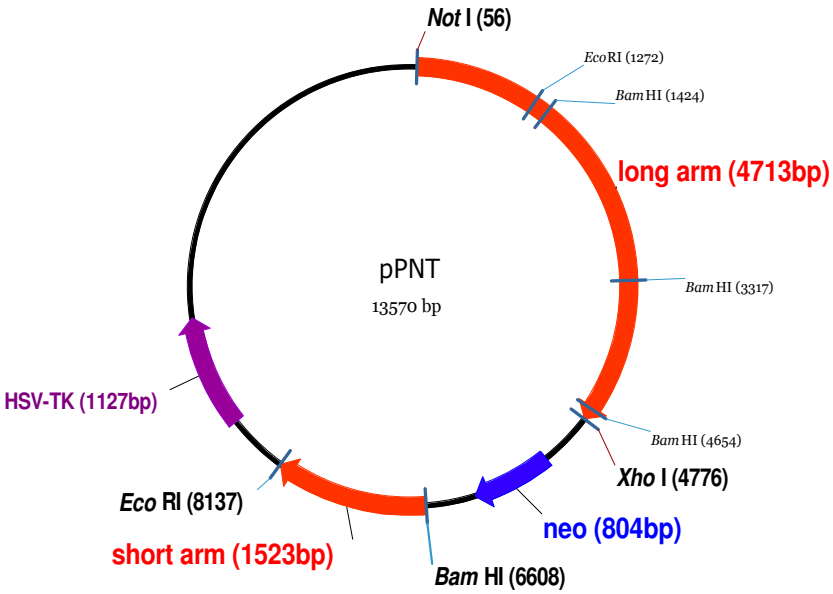

Figure 32 Plasmid map of constructed targeting vector
(designed by use of bioinformatic software Vector NTI 8)

In order to exclude these randomly integrated clones, a second selection marker (herpes-simplex-virus thymidine-kinase-gen, HSV-TK), besides the positive selection (neomycin resistance gene), is applied. The thymidine-kinase is a viral enzyme, which converts prodrug analogs such as aciclovir, ganciclovir or fialuridine (FIAU) into nucleoside monophosphates. Subsequently, the monophosphate form is further phosphorylated into the active triphosphate form by cellular kinases. Thereby the analogs serve as wrong substrates for the polymerase; they are integrated into the DNA and inhibit its synthesis by induction of chain termination. If the selection medium is supplemented with ganciclovir or FIAU, it can only be activated when thymidine-kinase is present in the cell. When recombination takes place at the correct location, the HSV-TK sequence that is located 3' outside the homologous regions falls away. Accordingly, only cells expressing this marker, due to non-homologous recombination, do not survive the negative-selection (Mansour, Thomas & Capecchi 1988).

3.4.4.1 Picking of G418 and FIAU resistant clones

One day after electroporation of ES cells, ES medium was exchanged by ES cell selection medium, containing G418 (360 µg/ml). On day number two after electroporation, selection with FIAU (S7, 0.2 µM f.c.) was started. After 3 days of selection, medium was exchanged once more and following another 3 days (in total 6 days) the FIAU selection was stopped by addition of ES medium containing G418 but not FIAU.

First colonies appeared 8 days subsequent to electroporation and after 9 days, sharply-bounded clones, resistant to G418 and FIAU, were isolated. Prior to clone isolation, the ES medium was replaced by prewarmed PBS (S15). Cell clones were picked under a microscope with the use of a 200 µl pipette, which was prefilled with 100 µl ES cell trypsin. Each colony was soaked up with the pipette and transferred together with the 100 µl ES trypsin into an empty 24 well-plate cell culture dish. Following trypsinization at RT for 5-10 min, cells were singularized by pipetting up and down 3-5 times and were transferred into 24-well plate cell culture dishes, previously coated with feeder cells, and filled with 1 ml of selective ES cell medium.

As a whole, 120 colonies, resistant to G418 and FIAU, were picked and further cultivated.

3.4.4.2 Cryopreservation of G418 and FIAU resistant clones

When the isolated cell clones reached a confluence of approximately 80-90%, two-thirds of the cells were frozen, whereas the rest was kept in culture for further DNA isolation purposes (see 3.4.5). For cryopreservation, cells were washed with PBS (S15) and detached with 100 µl of ES trypsin (3-5 min, 37°C). Trypsinization was stopped with 500 µl of ES medium and cells were singularized by pipetting 10-20 times up and down against the dish wall. Two-thirds of the resuspended cells (400 µl) were transferred into labeled cryovials, which were prefilled with 400 µl of 2xfreezing medium (see 3.4.2.1). After a short mixing, cells were briefly cooled at -20°C (1 h) and then frozen over-night at -80°C. The following day cryovials were transferred into a liquid nitrogen tank for long-term storage at -210°C.

3.4.5 Isolation of genomic ES cell DNA

Isolation of genomic DNA from eukaryotic cell material is a far more delicate issue than preparation of plasmid DNA (see 3.1.2), due to its vast molecular size. Big DNA molecules easily disrupt into small fragments due to shear forces like pipetting, shaking or centrifugation. Therefore isolation has to be performed with adequate care.

The lysis buffer (S13) contains SDS as a detergent to solubilize cell membranes and the supplemented proteinase K denaturates and degrades proteins. EDTA, as a chelating agent, is added in order to sequester divalent cations, such as Mg^{2+} or Ca^{2+}, thus diminishing activity of present DNAses. Afterwards, DNA is purified via ethanol and NaCl precipitation. Monovalent cations (Na^{+}) replace the hydration shell that is keeping DNA dissolved by ionic (salt bonds) and the DNA molecule is knocked out of solution (precipitates). Ethanol has a lower dielectric constant than water, so when mixed with

pure water, it effectively lowers the dielectric constant of the solution. Electrical attraction between negatively charged phosphate groups of DNA backbone and supplemented Na^+ becomes strong enough to form stable ionic bonds and the DNA precipitates.

Prior to addition of lysis buffer (S13, 300 µl), medium of confluent grown ES cells was aspirated. Cells were scratched from 24-well-plate and transferred into microliter tubes (1.5 ml) for incubation at 55°C for 2 h. Following a supplement of saturated NaCl solution (150 µl), DNA was precipitated by addition of 900 µl of absolute ethanol (C15). The thin precipitated DNA threads were transferred into reaction tubes (1.5 ml), which already contained 500 µl of ethanol (S6, 70%). After centrifugation at 12000 rpm for 5 min, the pelleted DNA was dissolved in 100 µl of cell culture grade water. Isolated genomic DNA was stored at 4-8°C.

3.4.6 PCR genotyping of targeted ES cell clones

The occurrence of recombination at the correct location is relatively rare, only in approximately 0.1-1% of transfected cells an accurate insertion can be found (Thomas, Folger & Capecchi 1986). In the rest of the transfected cells, the construct can be randomly integrated or it happens not at all. Therefore, besides the positive-negative selection, an appropriate screening method is necessary to identify the clones, who integrated the targeting construct into the genome and furthermore to spot the ones, who integrated the linearized plasmids the correct location by homologous recombination. For this reason two PCR screenings were performed.

The PCR screening strategy used to analyze the genotype of isolated DNA from targeted and positively-selected ES cell clones is presented in Figure 33. The sequences of the respective screening primers are listed in 2.14.3.

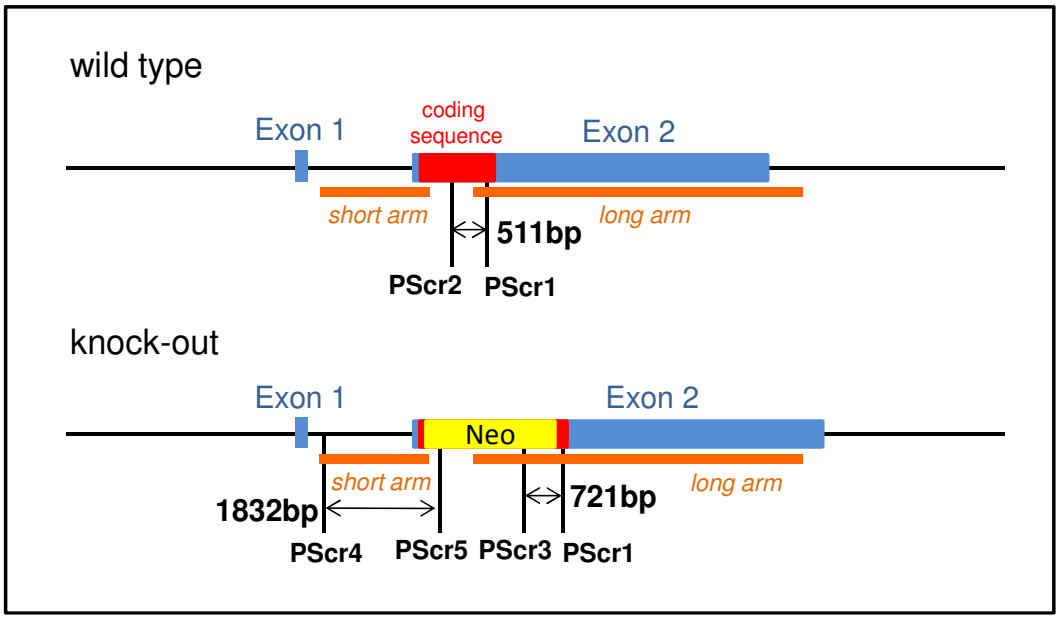

Figure 33 PCR genotyping strategy

Primers were designed to anneal a part of 3'homology region (PScr1, long arm, Exon2), desired knock-out coding sequence (PScr2, Exon2), Neomycin resistance cassette (Neo, PScr3, PScr5) and 5'homolgy region (PScr4, short arm, Intron1). In the preliminary PCR analyses in the case of wild type allele, primer pairs PScr1 and PScr2 give rise to a band of 511bp, whereas primer pairs PScr1 and PScr3 amplify amplicons of 721bp. In the case of the more specified PCR analyses, the primer pair PScr4 and PScr5 gives rise to a band of 1832bp, indicating the correct homologous recombination. See Figure 34 and Figure 35 for the utility of the designed genotyping. Please refer to Annex Figure 1 for detailed information about respective primer binding sites in the targeting vector.

A first preliminary screening was made to identify clones, which integrated the construct. Both oligonucleotide primers were designed to bind inside the sequence of the targeting construct, so that independent from the fact where the construct was integrated, targeted clones were identified.

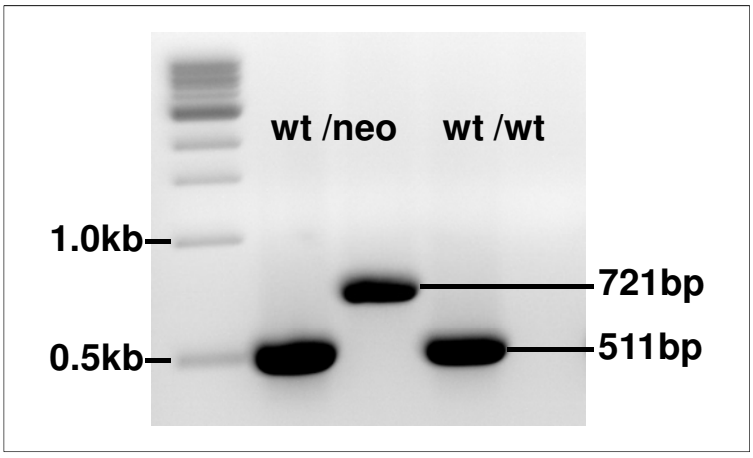

Figure 34 Preliminary PCR analyses of genomic DNA from targeted ES cells

PCR screening revealed amplicons of 551bp for wild type (wt) and 721bp for the targeted allele (neo). 1 kb DNA ladder was applied for size estimations. For detailed information about PCR conditions see Table 30 and for further information about PCR strategy see Figure 33.

The second performed PCR was more specified regarding the correct homologous recombination. The choice of PCR oligonucleotide primers were made based on a forward primer that binds outside of the homologous sequence (5') of the targeting construct and a reverse primer that binds to the

neomycin resistance gene. Consequently, PCR products amplified by this reaction indicate an accurate homologous recombination.

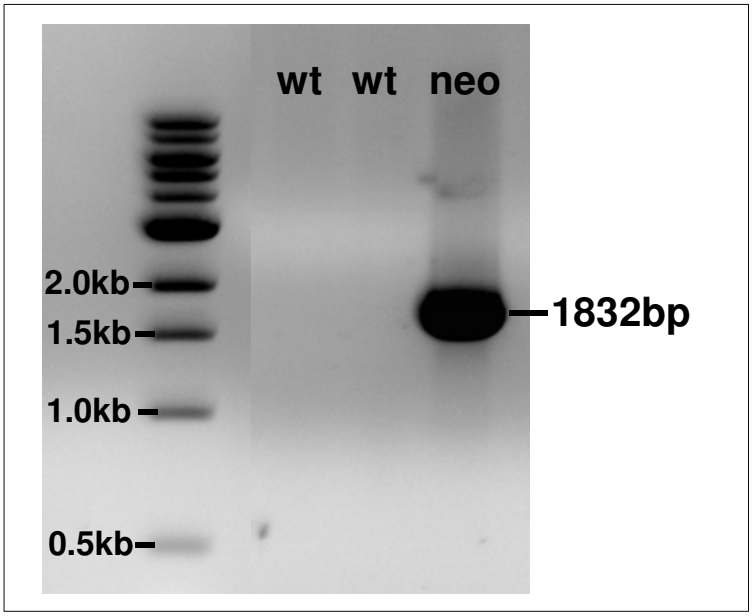

Figure 35 PCR analyses of genomic DNA from correctly targeted ES cells
PCR screening revealed a fragment of 1832bp for the targeted allele (neo), whereas wild type allele did not result in any amplification, which has already been checked in preliminary PCR screening (see Figure 34). 1 kb DNA ladder was applied for size estimations. Please refer to Table 31 for detailed information about PCR conditions and see Figure 33 for further information about PCR strategy.

Following incorporation of the linearized targeting construct into Ola/SV129 ES cells by electroporation, 120 G418- and FIAU-resistant colonies were picked. Due to slow and bad cell expansion, only 93 of these clones were screened for homologous recombination by PCR. The first preliminary screening revealed 28 wild type clones (~30%) and 65 clones (~70%) who integrated the targeting construct. Since this PCR only proved stable incorporation of the vector, but no homologous recombination, the second PCR was performed with these 65 clones. The more specified PCR uncovered three clones (~3%), in which the targeting construct was inserted by homologous recombination, thus leading to heterozygous modification of GPR17.

4 Results

By means of a high throughput pharmacogenomic approach, our group has identified a synthetic small molecule agonist for GPR17, here referred to as RA-II-150, which has not been published yet. As the reported endogenous ligands (Ciana et al. 2006) did not display functional activity in our laboratory (data not shown, Ph.D. thesis of Andreas Spinrath, AK Kostenis), as well as in other independent laboratories (Benned-Jensen & Rosenkilde 2010, Maekawa et al. 2009, Wunder et al. 2010), the identification of an activating ligand was the prerequisite to analyze signaling patterns of GPR17, and to further evaluate inhibiting properties of potential antagonists.

4.1 Uncovering signaling patterns of GPR17

Regarding the fact that recent studies revealed a ligand-independent regulatory role for GPR17, suppressing CysLT1 receptor function (Maekawa et al. 2009, Maekawa et al. 2010), it was a goal of this work to elucidate that GPR17 does not lack the common features of GPCR signaling upon stimulation with a small molecule agonist (RA-II-150). Analyses were performed in two different cellular backgrounds (CHO and HEK293 cells) generated to stably express GPR17. Untransfected wild type cells were used as negative controls.

4.1.1 GPR17 mediates promiscuous G protein-coupling

Traditional second messenger assays were performed to evaluate the GPR17 mediated cellular events upon agonist stimulation, and the focus was set on quantification of cAMP and IP1 generation, respectively.

4.1.1.1 GPR17 inhibits cAMP accumulation via Gαi/o-coupling

In the original deorphaning publication, GPR17 was shown to act via coupling with Gαi/o protein, based on ^{35}[S]GTPγS binding and cAMP inhibition assays (Ciana et al. 2006). Thus, a functional assay was established to analyze the ability of our GPR17 agonist RA-II-150 to inhibit adenylate cyclase in intact cells. As presented in Figure 36, RA-II-150 revealed inhibition of forskolin-stimulated cAMP accumulation in a concentration-dependent manner, in both analyzed cellular backgrounds (CHO-GPR17, HEK-GPR17). The determined pharmacological parameters are summarized in Table 33. As the inhibition effect mediated by the agonist-stimulated GPR17 was hardly detectable in HEK-GPR17 cells, data from challenged untransfected HEK293 cells were plotted in parallel to illustrate the significant differences. The concentration-response curve of RA-II-150 using CHO-GPR17 cells was shifted to the right with an EC_{50} value more than six times higher in comparison with the one obtained with HEK-GPR17 cells (CHO-GPR17: 15.5 nM; HEK-GPR17: 2.4 nM). It should be noted, that the CRC in CHO-GPR17 cells was determined in the presence of 10 µM forskolin, whereas in HEK-GPR17 only 0.3 µM forskolin were employed. Thus, the different forskolin concentrations might have

an impact on the respective agonist pharmacology in both cell lines. Nevertheless, for the purpose of this work, it is sufficient to conclude, that agonist-mediated stimulation of GPR17 leads to concentration-dependent inhibition of cAMP accumulation, in both examined cellular backgrounds.

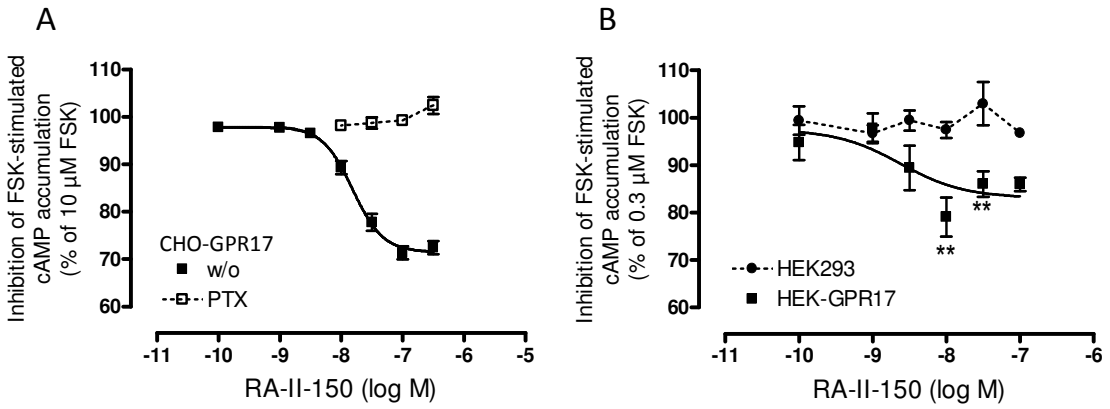

Figure 36 Concentration-dependent effect of GPR17 agonist RA-II-150 on forskolin-stimulated cAMP production in CHO-GPR17 and HEK-GPR17 cells, respectively.

Cells stably expressing GPR17 (A: CHO, B: HEK293) were stimulated with increasing concentrations of RA-II-150 in the presence of 10 and 0.3 µM forskolin, respectively. GPR17-mediated decrease of intracellular cAMP was calculated as percent inhibition of adenylate cyclase stimulated with forskolin (10 and 0.3 µM, respectively). A, Pretreatment with Gαi/o inhibitor PTX (50 ng/ml, 18 h) completely abolished inhibition of FSK induced cAMP accumulation B, HEK293 cells were taken as control. All data are means (+/- s.e.m.) of at least three experiments. B, For statistical analyses, individual concentrations were compared by two-way ANOVA with Bonferroni's correction for multiple comparisons (**p < 0.01).

Table 33 Parameters of averaged RA-II-150 concentration-effect curves determined by Gαi/o-cAMP assays, as depicted in Figure 36 (± s.e.m.)

cell line	pEC_{50}	bottom value (%)	top value (%)	n_H	n
CHO-GPR17	7.81 ± 0.05	71.5 ± 1.0	97.9 ± 0.9	-1,8 ± 0.3	4-5
HEK-GPR17	8.62 ± 0.54	83.1 ± 3.0	97.6 ± 4.1	1.0 *(fixed)*	5

Pertussis toxin (PTX) that inhibits the Gαi/o subunit by catalyzing its irreversible ADP-ribosylation (Katada & Ui 1982) was utilized to uncover Gαi/o-dependence of the GPR17-mediated inhibiting effect in CHO-GPR17 cells (Figure 36, A). Pertussis toxin pretreatment (50 ng/ml, 18 h) completely diminished the concentration-dependent response, thus demonstrating that Gαi/o subunit was essential for the observed response. Due to the barely detectable Gαi/o activity in HEK-GPR17 cells by means of traditional cAMP inhibition assays, PTX sensitivity and thereby Gαi/o-mediated signaling of HEK-GPR17 cells was further elucidated with the use of Epic® system (Figure 37). The monitored optical traces induced by challenge of GPR17 with RA-II-150 (0.3 and 0.1 µM) in the presence and absence of PTX pretreatment (50 ng/ml, 18 h), revealed Gαi/o-dependence of the dynamic redistribution, since the optical signatures were almost completely abrogated in the presence of PTX. Consequently these analyses verified the results obtained by cAMP inhibition assays, namely that agonist-stimulated GPR17 inhibits cAMP synthesis via Gαi/o-coupling, in both analyzed cellular backgrounds.

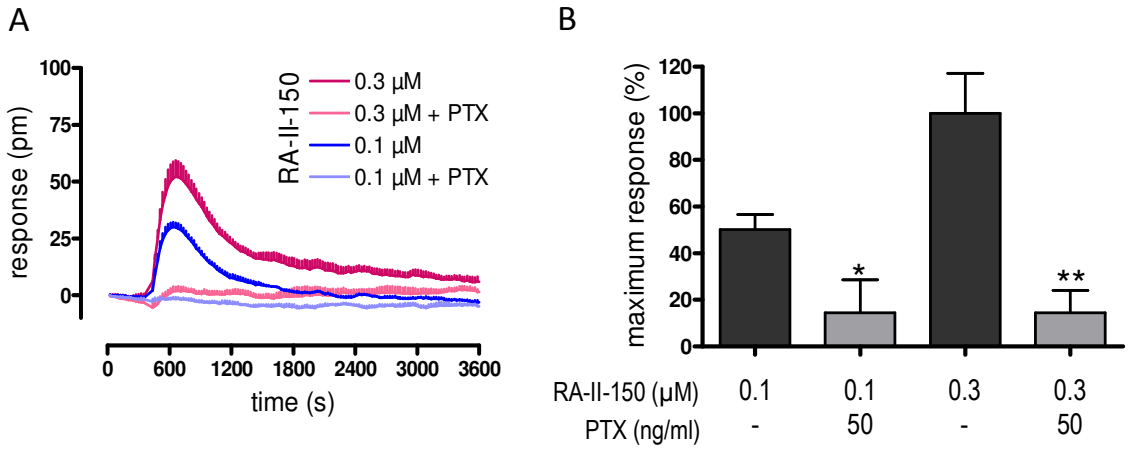

Figure 37 Verification of Gαi/o-coupling in HEK-hGPR17 cells via DMR analyses
A, HEK293 cells stably expressing hGPR17 were stimulated with the indicated concentrations of RA-II-150 and the effect of the Gαi/o inhibitor PTX (50 ng/ml, 18 h) on the optical signatures elicited by RA-II-150 was analyzed. Wavelength shift (pm) was monitored as a measure of receptor activation. Representative data (mean + s.e.m.) of at least three independent experiments performed in triplicates. B, Bar chart resulting from DMR traces of validation by PTX pretreatment (50 ng/ml, 18 h) of RA-II-150 (1 and 3 µM) induced Gαi/o activation. Data are represented as means +/- s.e.m. normalized to the maximum response elicited by 0.3 µM RA-II-150 of four independent experiments, performed in triplicates. For statistical analyses, paired t-tests with two-tailed p values and 95% confidence interval were applied and revealed significant differences of RA-II-150 induced responses in PTX pretreated cells compared to untreated ones (*$p < 0.05$; **$p < 0.01$).

4.1.1.2 GPR17 activates adenylate cyclase

While analyzing inhibition of forskolin-stimulated cAMP accumulation by agonist-activated GPR17, an additional stimulatory effect on adenylate cyclase was observed. Reverse bell-shaped concentration-response curves in both cellular backgrounds (A: CHO-GPR17, B: HEK-GPR17) uncovered, that by application of higher RA-II-150 concentrations the induced stimulatory signaling cascade prevailed the inhibiting effect (Figure 38). The reverse bell-shaped concentration–response curves induced by RA-II-150 were analyzed by dividing them into one inhibitory and one stimulatory curve (bell-shaped concentration-response curve equation by GraphPad Prism4). In both cellular backgrounds maximum inhibition of cAMP synthesis (CHO-GPR17: ~30%; HEK-GPR17: ~11%) was reached with 0.3 µM RA-II-150, while further increases of the agonist concentration reversed the inhibitory effect and increased cAMP production. Whereas in CHO-GPR17 cells maximum of cAMP level was similar to the one obtained with 10 µM forskolin (E_{max} ~102%), the maximum in HEK-GPR17 cells outranged the cAMP concentration induced by 1 µM of forskolin (E_{max} ~124%). The differences in the maximum effect can be explained by the varying concentration of forskolin (10 µM versus 1 µM), and it should be regarded that RA-II-150 showed higher opposing efficacy via Gαi/o protein in CHO-GPR17 cells, observable in higher percentage inhibition (E_{max} 30% ↔ 11%). The stimulatory response was about 50-fold less potent (EC_{50} values: 17.0 nM ↔ 851.1 nM) than the inhibitory response in CHO-GPR17 cells, whereas in HEK-GPR17 cells the Gαs mediated pathway was approximately 75-fold less sensitive (EC_{50} values: 17.7 nM ↔1 259.9 nM). The pharmacological parameters are summarized in Table 34.

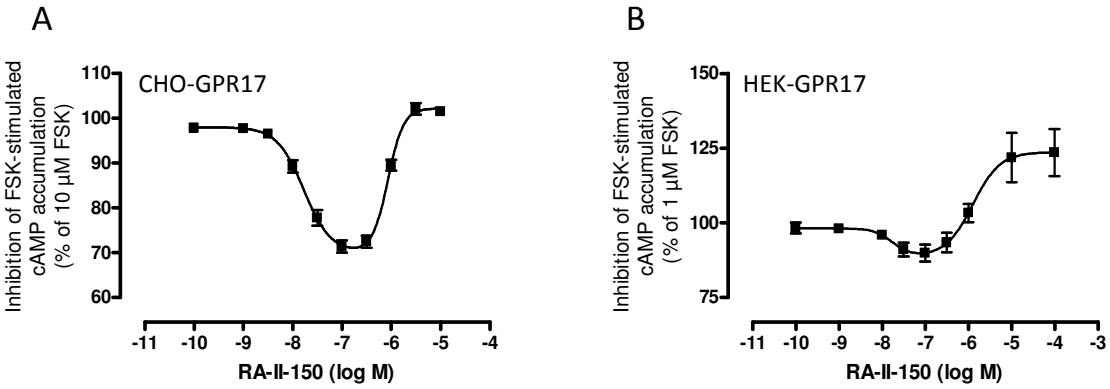

Figure 38 Reverse bell-shaped CRCs reveal concentration-dependent modulation of intracellular cAMP levels

Cells stably expressing GPR17 (A: CHO, B: HEK293) were stimulated with varying concentrations of RA-II-150 in the presence of 10 (A) and 1 µM (B) forskolin, respectively. GPR17-mediated change of intracellular cAMP was calculated as percent inhibition of adenylate cyclase stimulated with forskolin (10 and 1 µM, respectively). All data are means (+/- s.e.m.) of three to five experiments performed in duplicates.

Table 34 Parameters of averaged reverse bell-shaped RA-II-150 concentration-effect curves determined by Gαi/o-cAMP assays, as depicted in Figure 38 (± s.e.m.)

cell line	pEC_{50}	bottom value (%)	top value (%)	n_H	n
CHO-GPR17 *inhibitory*	7.77 ± 0.07	70.0 ± 2.2	98.0 ± 0.9	-1.6 ± 0.3	4-5
CHO-GPR17 *stimulatory*	6.07 ± 0.04	70.0 ± 2.2	102.2 ± 1.2	2.8 ± 0.9	4-5
HEK-GPR17 *inhibitory*	7.77 ± 0.67	88.7 ± 8.6	98.1 ± 3.1	-2.0 ± 4.4	5
HEK-GPR17 *stimulatory*	5.90 ± 0.23	88.7 ± 8.6	123.7 ± 4.5	1.4 ± 1.4	5

As the reverse bell-shaped concentration-response curves were obtained in the presence of forskolin, further analyses were performed to evaluate the unbiased GPR17-mediated increase of cAMP, avoiding simultaneous stimulation of adenylate cyclase by forskolin. Furthermore, the inhibitory component was eliminated by pretreatment of cells with PTX (50 ng/ml, 18 h), for a more accurate assessment of the stimulatory effect. Stimulation of GPR17 with increasing RA-II-150 concentrations resulted in an elevated synthesis of cyclic AMP. As presented in Figure 39, effects were concentration-dependent, and CRC obtained in CHO-GPR17 cells was shifted to the right in comparison to the one determined in HEK-GPR17 cells (see Table 35 for pharmacological parameters). The stimulatory response was about 110-fold less potent (15.5 nM ↔ 1.7 µM) than the inhibitory response in CHO-GPR17, whereas in HEK-GPR17 the Gαs mediated pathway was approximately 350-fold less sensitive (2.4 nM ↔ 0.8 µM), when comparing the inhibition in untreated cells (Figure 36) with the stimulation in PTX-pretreated cells.

Since the stimulatory effects on adenylate cyclase were not eliminated by preincubation with Gαi/o inhibitor PTX, whereas the inhibitory effects were completely blunted (see 4.1.1.1), a bifurcation

between both G proteins in the transduction can be neglected. Thus, the observed reverse bell-shaped behavior was mediated by a promiscuous interaction by agonist-activated GPR17 with both proteins, Gαi/o and Gαs, in an independent manner.

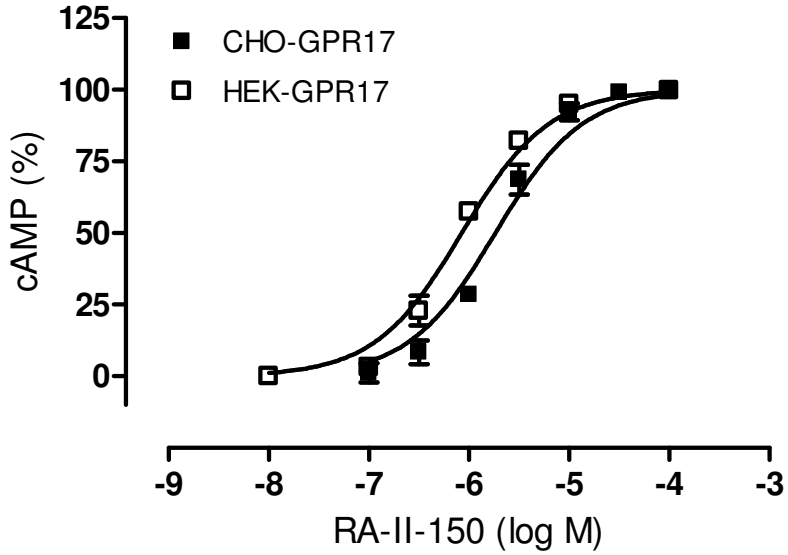

Figure 39 Concentration-response-curves of cAMP accumulation in CHO-GPR17 and HEK-GPR17 cells determined in the presence of Gαi/o inhibitor PTX

Cells stably expressing GPR17 (CHO and HEK293) were pretreated with Gαi/o inhibitor PTX (50 ng/ml, 18 h), and stimulated with increasing concentrations of RA-II-150. GPR17-mediated increase of intracellular cAMP was normalized and expressed as percent of maximum activation induced by a saturating concentration of RA-II-150 (100 µM). All data are means (+/- s.e.m.) of three to four experiments performed in duplicates.

Table 35 Parameters of averaged RA-II-150 concentration-effect curves determined by Gαs-cAMP assays, as depicted in Figure 39 (± s.e.m.)

cell line	pEC_{50}	bottom value (%)	top value (%)	n_H	n
CHO-GPR17	5.74 ± 0.04	0.0 *fixed*	100.0 *fixed*	1.0 *fixed*	4
HEK-GPR17	6.07 ± 0.03	0.0 *fixed*	100.0 *fixed*	1.0 *fixed*	3

4.1.1.3 GPR17 raises intracellular IP-One concentrations

Following elucidation of dual G protein-coupling via Gαi/o and Gαs, and regarding the fact that nucleotide-activated GPR17 was reported to elevate intracellular calcium levels, based on single cell calcium imaging (Ciana et al. 2006), a functional assay to analyze potential Gαq protein coupling was established. Therefore, the ability of our GPR17 agonist RA-II-150 to raise intracellular IP1 concentrations in intact cells was evaluated.

As depicted in Figure 40 stimulation of stably transfected cells (CHO-GPR17, HEK-GPR17) yielded concentration-dependent increases of intracellular IP1 levels. The CRC of RA-II-150 obtained in CHO-GPR17 cells was shifted to the left in comparison to the one determined in HEK-GPR17 cells. The GPR17-mediated increase of IP1 synthesis in HEK-GPR17 cells was about 3-fold less potent than the response in CHO-GPR17 (EC_{50} values: 288.4 nM ↔ 85.3nM), a phenomenon which was observed

inversely in cAMP accumulation assays, where CRC obtained in CHO-GPR17 cells were shifted to the right for both inhibitory and stimulatory effects (see 4.1.1.1, 4.1.1.2).

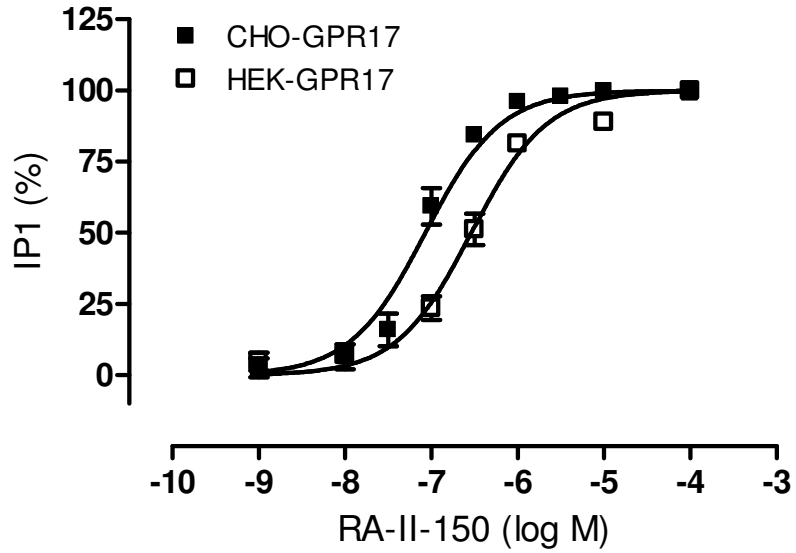

Figure 40 Concentration-dependent raise of intracellular IP1 by agonist-activated GPR17 in CHO-GPR17 and HEK-GPR17 cells

Cells stably expressing GPR17 (CHO-GPR17, HEK-GPR17) were stimulated with varying concentrations of RA-II-150. GPR17-mediated increase of intracellular IP1 was normalized and expressed as percent of maximum activation induced by a saturating concentration of RA-II-150 (100 µM). All data are means (+/- s.e.m.) of three to four experiments performed in duplicates.

Table 36 Parameters of averaged RA-II-150 concentration-effect curves determined by IP1 assays, as depicted in Figure 40 (± s.e.m.)

cell line	pEC_{50}	basal value (%)	E_{max} (%)	n_H	n
CHO-GPR17	7.07 ± 0.05	0.0 *(fixed)*	100.0 *(fixed)*	1.0 *(fixed)*	3-4
HEK-GPR17	6.54 ± 0.04	0.0 *(fixed)*	100.0 *(fixed)*	1.0 *(fixed)*	3

4.1.2 Agonist-activated GPR17 triggers dynamic mass redistribution in a PTX-sensitive manner

After uncovering promiscuous G protein-coupling of agonist-activated GPR17 via Gαi/o, Gαs and Gαq proteins, the cell lines stably expressing GPR17 were analyzed by the label-free dynamic mass redistribution technology, which has been proven to be a powerful means for interrogating GPCR function in non-disturbed cellular settings without the need of labels (Fang, Frutos & Verklereen 2008, Fang, Ferrie & Tran 2009, Schröder et al. 2010). The term ‘signature’ is used to describe the dynamic response profile displayed over time following ligand stimulation.

Our GPR17-agonist RA-II-150 was analyzed according to its ability to trigger dynamic mass redistribution in cells stably transfected with GPR17 (CHO-GPR17, HEK-GPR17), thus signaling capability of agonist-activated GPR17 was monitored in real time. Representative experiments are depicted in Figure 41. Following stimulation with varying RA-II-150 concentrations, CHO-GPR17 cells

responded with a rapid positive DMR event, followed by a short negative DMR phase with a decay in signal and finally, especially with higher concentrations (1-100 µM), a slow positive DMR event was monitored that lead to another elevated plateau (Figure 41, A). HEK-GPR17 cells responded as well with specific optical signatures when exposed to increasing concentrations of RA-II-150 (Figure 41, C). Higher concentrations (10 and 100 µM) induced a rapid positive DMR followed by an elevated plateau, whereas lower concentrations did trigger a rapid positive DMR, followed by a short DMR decline and ending in another elevated plateau.

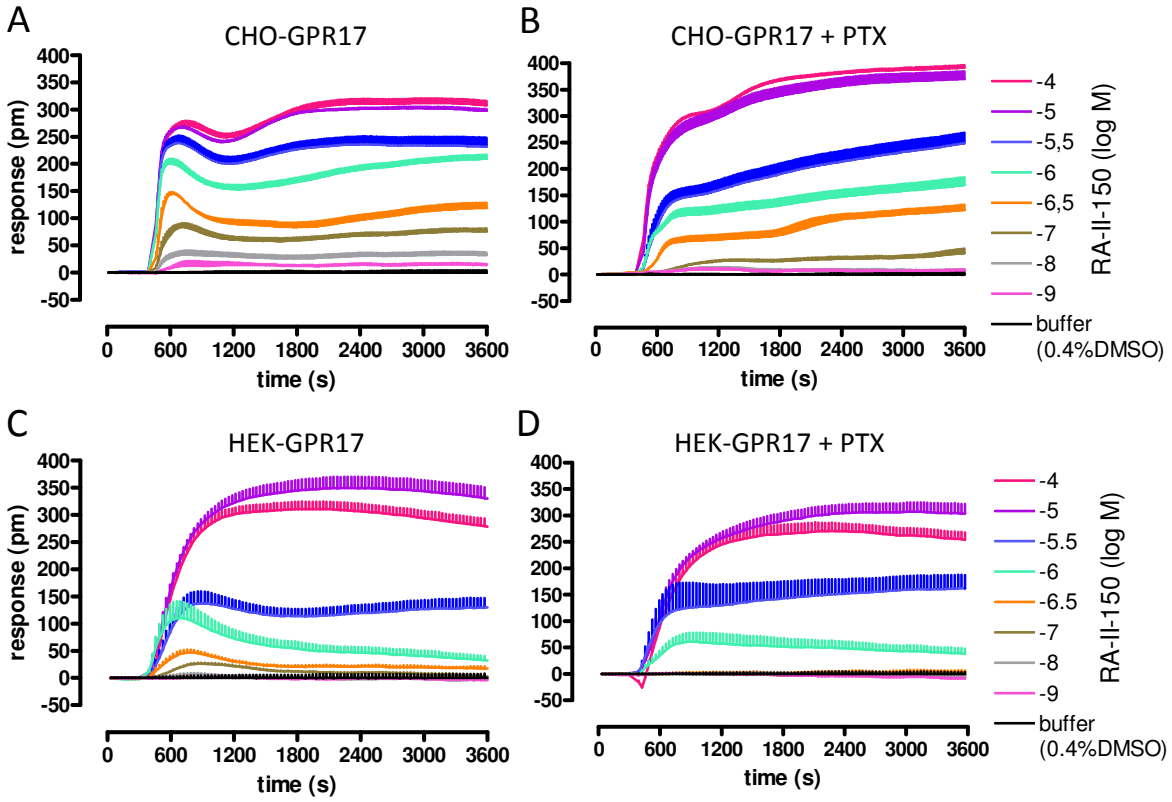

Figure 41 Dynamic mass redistribution analyses reveal PTX-sensitive functional activity of GPR17 by activation with RA-II-150

A-D, The cell lines stably expressing GPR17 were stimulated with the indicated concentrations of RA-II-150 and wavelength shift [pm] over time [s] was monitored as a measure of functional activity. Signatures were baseline-corrected by subtraction of buffer traces from the DMR response after receptor activation. Representative optical trace experiment (mean + s.e.m.) of at least three independent experiments performed in triplicates. A,B, CHO cells stably expressing GPR17 (CHO-GPR17). C, D, HEK293 cells stably transfected with GPR17 (HEK-GPR17). B,D, The effect of the Gαi/o inhibitor PTX (50 ng/ml, 18 h) on the optical signatures elicited by RA-II-150 in CHO-GPR17 cells (B) and HEK-GPR17 cells (D).

Since the integrated response monitored in real time by use of the Epic® system is a complex phenomenon, which reflects multiple overlapping cellular events downstream of the agonist-activated receptor, the data interpretation remains challenging especially regarding the promiscuous G protein-coupling of GPR17. To further determine whether heterotrimeric G proteins are responsible for initiating the monitored temporal response profiles, pertussis toxin was applied to pharmacologically silence Gαi/o signaling. As suspected from previously performed second messenger assays, PTX pretreatment did result in a shape change of the optical signatures, verifying promiscuous G protein-coupling including Gαi/o mediated signal transduction (Figure 41, B and D).

Regarding the data obtained by second messenger assays, the remaining optical signatures should be induced at least by Gαs and Gαq/11 mediated signaling pathways.

The optical signatures induced by agonist-stimulated GPR17, in the presence and absence of PTX pretreatment, were transformed into concentration-response curves for RA-II-150 using area under curve (AUC) for CHO-GPR17 and maximum response for HEK-GPR17 (Figure 42), and normalized to respective response obtained in the absence of PTX.

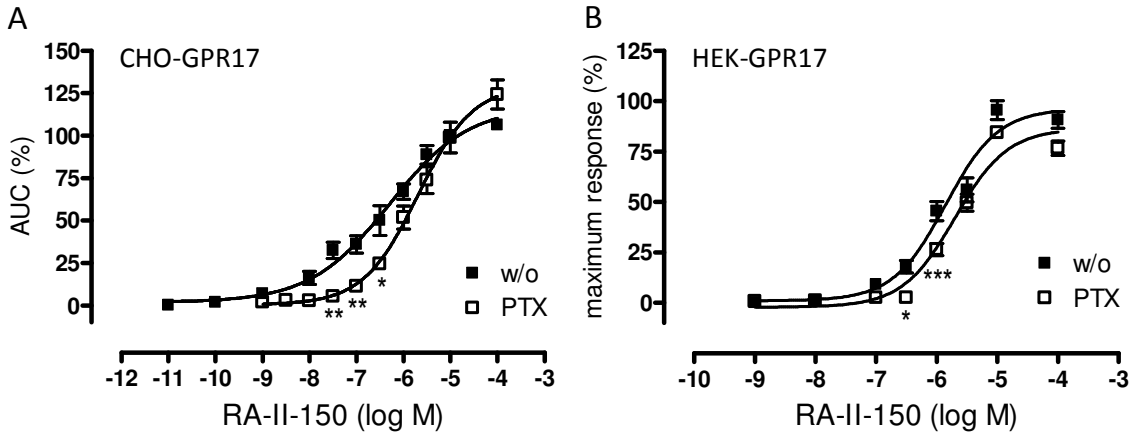

Figure 42 Concentration-dependency and PTX-sensitivity of RA-II-150 induced DMR
Transformation of optical signatures into concentration-response curves for the GPR17 agonist RA-II-50 using the AUC values between 0 and 3600 s time points for CHO cells stably expressing GPR17 (A, CHO-GPR17), and maximum response (B) for HEK293 cells stably transfected with GPR17 (HEK-GPR17), respectively. All data are normalized to the AUC (A) or the maximum response (B) obtained in the absence of PTX. All data are means (+/- s.e.m.) of three to nine experiments performed in triplicates. For statistical analyses, individual concentrations were compared by two-way ANOVA with Bonferroni's correction for multiple comparisons (*p < 0.05; **p < 0.01; ***p < 0.001).

Table 37 Parameters of averaged RA-II-150 concentration-effect curves determined by DMR assays, as depicted in Figure 42 (± s.e.m.)

cell line	pEC_{50}	basal value (%)	E_{max} (%)	n_H	n
CHO-GPR17	6.30 ± 0.14	1.8 ± 3.5	117.3 ± 7.6	0.51 ± 0.08	3-9
CHO-GPR17 *+ PTX*	5.69 ± 0.13	0.4 ± 4.0	130.0 ± 10.5	0.74 ± 0.13	3-8
HEK-GPR17	5.85 ± 0.09	1.0 ± 2.8	96.3 ± 4.0	1.0 *(fixed)*	4
HEK-GPR17 *+ PTX*	5.70 ± 0.08	2.1 ± 2.4	86.5 ± 3.7	1.0 *(fixed)*	4

The concentration-response curve of RA-II-150 obtained in CHO-GPR17 cells without PTX pretreatment was slightly shifted to the left in comparison to the one determined in HEK-GPR17 cells (EC_{50} values: 0.5 µM ↔ 1.4 µM). The PTX preincubation triggered a slight, but not significant ($p > 0.05$) rightward shift of concentration-response curves, in both analyzed cellular backgrounds. Especially with lower agonist concentration a significant inhibition effect of PTX preincubation was monitored, which is in agreement with data obtained in second messenger assays, where stimulatory effect on cAMP synthesis prevailed with application of higher RA-II-150 concentrations (see 4.1.1.2). A sigmoidal curve fitted for RA-II-150 response in CHO-GPR17 cells exhibited a shallow Hill slope (n_H= 0.51 +/- 0.08), whereas pretreatment with PTX was accompanied by a small increase (n_H= 0.74

+/- 0.13). The observed shallow Hill slope probably was due to crosstalk between signaling pathways, as EC_{50} values obtained by means of second messenger assays differed amongst each other, and depending on RA-II-150 concentration signaling preferences of GPR17 changed. Since holistic measurement of the Epic® system reflects multiple overlapping cellular events downstream of the agonist-activated receptor, these heterogeneous signaling events might cause such shallow Hill coefficients. Another proof for this hypothesis was the fact, that exclusion of one signaling pathway (Gαi/o) with PTX rather steepened curve slope closer to unity. Concentration-response curves explored in HEK-GPR17 cells were fitted with a constant Hill slope (n_H= 1), thus in this cellular system crosstalk between involved signaling pathways did not result in dampened curve slopes.

4.1.3 GPR17 internalizes upon ligand activation

In order to evaluate whether GPR17 internalizes upon agonist activation, HEK293 cells stably expressing triple HA-tagged GPR17 (HEK-3xHA-GPR17) were examined by fluorescence microscopy and ELISA assays. Fusion of GPR17 with the haemagglutinin (HA) epitope tag did not impair its functionality as monitored by use of the Epic® technology (Figure 43). The GPR17 agonist RA-II-150 concentration-dependently elicited dynamic mass redistribution (DMR), and the monitored optical signatures did slightly differ in magnitude but not in shape, indicating comparable signaling properties of the analyzed fusion receptor.

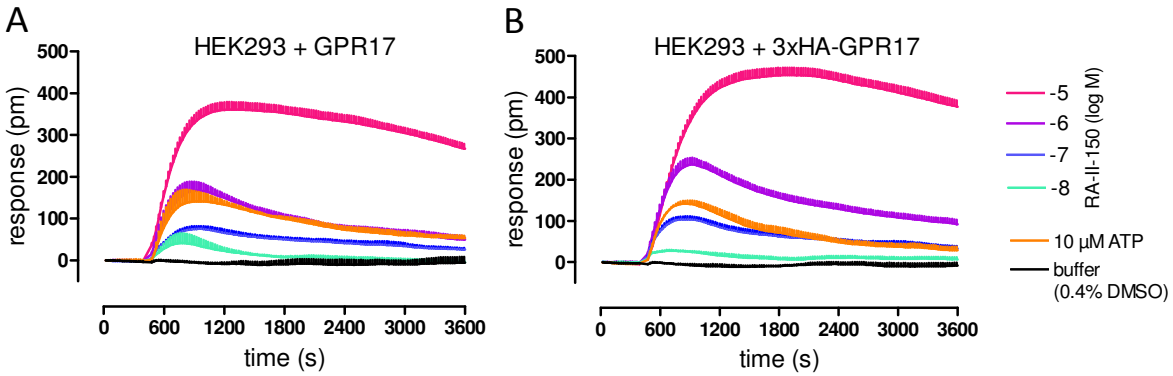

Figure 43 GPR17 fused to epitope tag haemagglutinin retains functionality

HEK293 cells transiently transfected (calcium phosphate precipitation) with distinct GPR17 constructs (GPR17: wild type and 3xHA-GPR17: N-terminally fused with haemagglutinin) were challenged with the indicated concentrations of the GPR17 agonist RA-II-150 and 10 µM ATP. The resulting picometer-shifts of reflected light wavelength over time [s] were monitored as a measure of functional activity. Presented data are means + s.e.m. from a representative optical trace experiment of two independent experiments performed in triplicates.

The examination of HA-immunoreactivity gives information about the subcellular localization, whereas cell surface ELISA measurements allow monitoring of the quantitative changes in surface-expressed GPR17. As seen in Figure 44, immunofluorescence analyses revealed that under control conditions GPR17 was predominantly located on the cell surface (A), but upon activation with 10 µM RA-II-150 for 1 h, GPR17 internalized from the cell surface into the cytoplasm with a punctate distribution into intracellular vesicles (B). To verify these observed data and further characterize the agonist-induced internalization of GPR17, HEK-3xHA-GPR17 cells were treated with 10 µM RA-II-50

for various time periods, and cell surface GPR17 was quantitatively detected by ELISA. The agonist treatment induced endocytosis within 15 min, and the GPR17 continued to internalize, leading to ~26.2% (+/- 2.3%) loss of cell surface expression (Figure 44, C). Thus, the data obtained from immunofluorescence microscopy and surface ELISA exhibit equivalent patterns, namely that GPR17 internalizes from the cell membrane into the intracellular membrane compartments of the cell in a time-dependent manner upon agonist challenge.

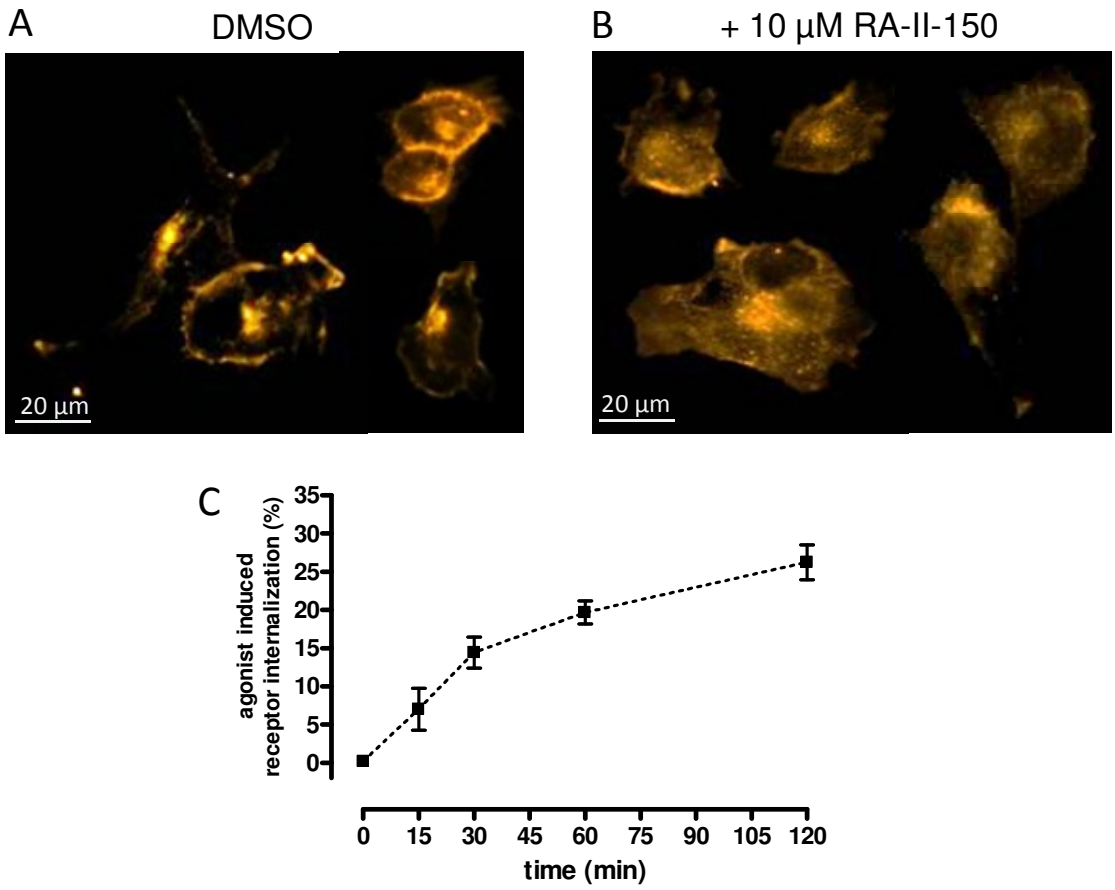

Figure 44 Agonist-induced internalization of GPR17

A-C, Receptor expression was imaged by immunofluorescence microscopy (A-B), and quantitated by indirect cellular ELISA. HEK293 cells stably expressing GPR17 fused to an N-terminal 3xHA tag were pre-labeled with anti-HA antibody (Table 22, A1), and after agonist-induced stimulation, all cells were permeabilized and immunostained. A-B, Fluorescence images of cell surface and intracellular 3xHA-GPR17 immunoreactivity. Cells were treated for 1 h at 37°C with 0.1% DMSO (A, C11) or 10 µM RA-II-150 (B). A, Control cells showed primarily plasma membrane localization of GPR17 and less internalized receptor. B, RA-II-150 induced distinguishable endocytosis. The following settings were used for Alexa Fluor 546 recordings: 400 fold magnification, 100 ms exposure time, 0.99 γ and 2-22 histogram. Representative cells from at least three independent experiments are shown. After indirect immunofluorescence staining, no specific fluorescence was observed in untransfected HEK293 cells. Scale bars = 20 µM. C, Colorimetric ELISA measurements of RA-II-150 (10 µM) induced GPR17 sequestration for the indicated time period. The amount of internalized receptor was calculated from the decrease in the level of surface-expressed receptor after agonist treatment compared with untreated, control cells (HEK293). Each data point represents mean (+/- s.e.m.) of four to five independent experiments performed in triplicates.

4.1.4 GPR17 agonist RA-II-150 shows no activity on untransfected CHO-K1 and HEK293 cells

In order to ensure that the results obtained with the stably transfected cells (CHO-GPR17, HEK-GPR17) were specifically due to an activation of GPR17, the corresponding untransfected cells (CHO-K1, HEK293) were analyzed by means of DMR, cAMP and IP1 assays, after challenging with GPR17 agonist RA-II-150. As presented in Figure 45, RA-II-150 did not induce any visible dynamic mass redistribution, neither in CHO-K1 (A) nor in HEK293 (B) cells. The functional capability of assay conditions and viability of examined cell lines was controlled by stimulation with ATP (A) and carbachol (B), respectively, whereby ATP stimulates endogenous purinergic receptors in CHO-K1 cells (P2Y1 and P2Y2, Iredale & Hill 1993, Marcet et al. 2004) and carbachol activates muscarinic receptors endogenously expressed in HEK293 cells (M1 M3, Estacion et al. 2004, Mundell & Benovic 2000).

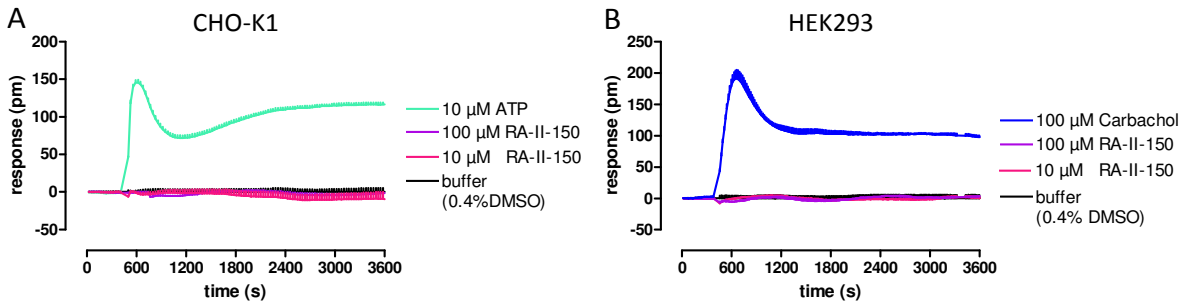

Figure 45 GPR17 agonist RA-II-150 does not trigger dynamic mass redistribution in untransfected CHO-K1 and HEK293 cells, respectively.
A-B, The untransfected cell lines (A:CHO-K1, B:HEK293) were challenged with 10 and 100 µM of RA-II-150, and ATP (A) or carbachol (B) were used as controls of assay conditions by activation of endogenously expressed purinergic (P2Y) and muscarinic receptors (M3). Wavelength shift [pm] over time [s] was monitored as a measure of functional activity by use of the Epic® system. Representative optical trace experiment (mean + s.e.m.) of at least three independent experiments performed in triplicates are shown.

The results from DMR analyses were further corroborated in cAMP and IP1 assays, where GPR17 agonist RA-II-150 did not reveal any activity, both conducted with CHO-K1 and HEK293 cells, respectively (Figure 46). Neither cAMP levels were elevated after stimulation with RA-II-150 nor forskolin-stimulated cAMP accumulation was inhibited (A). The increase of cAMP by addition of forskolin revealed good assay conditions as well as appropriate cell viability. In addition, activation of untransfected cells did not result in an increase of intracellular IP1 levels, but rather a little non-significant decrease, whereas ATP and carbachol, used as positive controls, did reveal significant elevations. Purinergic (P2Y1 and P2Y2) as well as muscarinic (M1 and M3) receptors are known to couple via Gαq protein leading to an increase in intracellular IP1 concentrations.

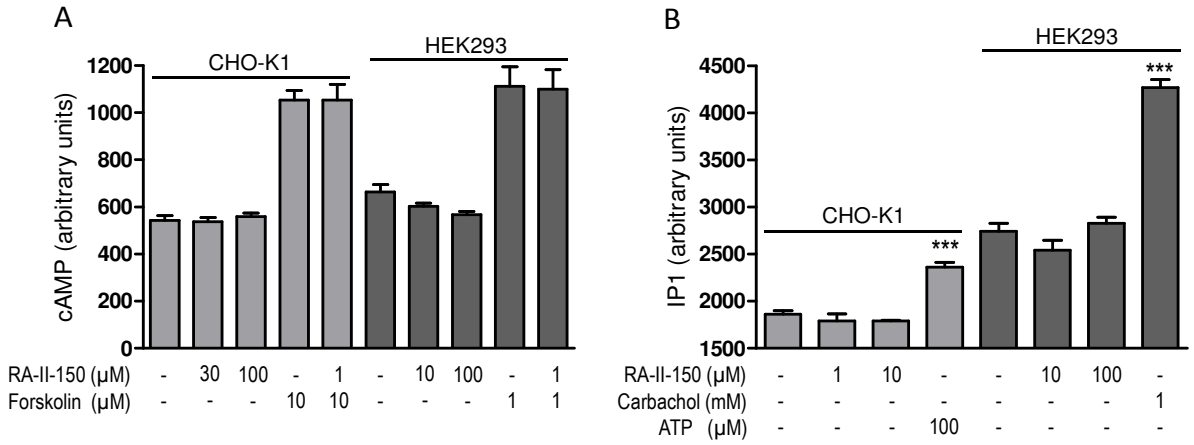

Figure 46 GPR17 agonist RA-II-150 shows no activity in untransfected CHO-K1 and HEK293 cells, respectively, analyzed by cAMP and IP1 assays.

A-B, Untransfected cell lines (CHO-K1, HEK293) were challenged with indicated RA-II-150 concentrations and analyzed by cAMP (A) and IP1 (B) assays, respectively. Forskolin (A), carbachol (B) and ATP (B) were used as positive controls. All data are means (+/- s.e.m.) of three to six experiments performed in duplicates. For statistical analyses, unpaired t-tests with two-tailed p values and 95% confidence interval were applied and revealed no significant differences of RA-II-150 induced values compared to unstimulated ones, whereas positive controls were significant (**$p < 0.01$, ***$p < 0.001$).

4.1.5 GPR17 is not a constitutively active receptor

Beyond these classical features, a number of additional functional paradigms of GPCRs are of importance, including constitutive activity (Costa & Cotecchia 2005, Milligan, Bond & Lee 1995). By raising the number of receptors present in a system, the number of spontaneously active receptors can be augmented until a threshold is reached where the resulting functional response from a spontaneously active receptor can be observed. This explains why in recombinant systems, over-expressed receptors are capable of showing constitutive activity, resulting in a receptor-mediated increase in basal activity without any agonist intervention (Bond et al. 1995, Milligan, Bond & Lee 1995, Newman-Tancredi et al. 1997). Regarding the fact that GPR17 was demonstrated to be constitutively active through Gαi/o (Benned-Jensen & Rosenkilde 2010), the cell lines applied in this work, engineered to stably express GPR17, were analyzed with respect to constitutive activity by means of cAMP and IP1 assays.

In order to evaluate the intrinsic activity via Gαi/o or Gαs, the G protein-independent stimulation of adenylate cyclase with increasing concentrations of forskolin (Seamon, Padgett & Daly 1981) was examined in untransfected cells (CHO-K1, HEK293) and compared to the data obtained in stably transfected cell lines (CHO-GPR17, HEK-GPR17). Thus, a rightward shift of the forskolin concentration-response curve obtained in cells engineered to stably express GPR17 would indicate a constitutive Gαi/o activity. As presented in Figure 47 (A and B), neither in CHO nor in HEK cells, ligand-independent activity of GPR17 was observed, concentration-response curves did not significantly differ from each other. Furthermore the determined basal IP1 levels, again untransfected cells (CHO-K1, HEK293) were compared with stably transfected cells (CHO-GPR17, HEK-GPR17), did not significantly vary, but recombinant GPR17 cells showed rather slightly lowered

basal IP1 levels (Figure 47, C). Thus, indicating that GPR17 is not constitutively active through Gαq protein.

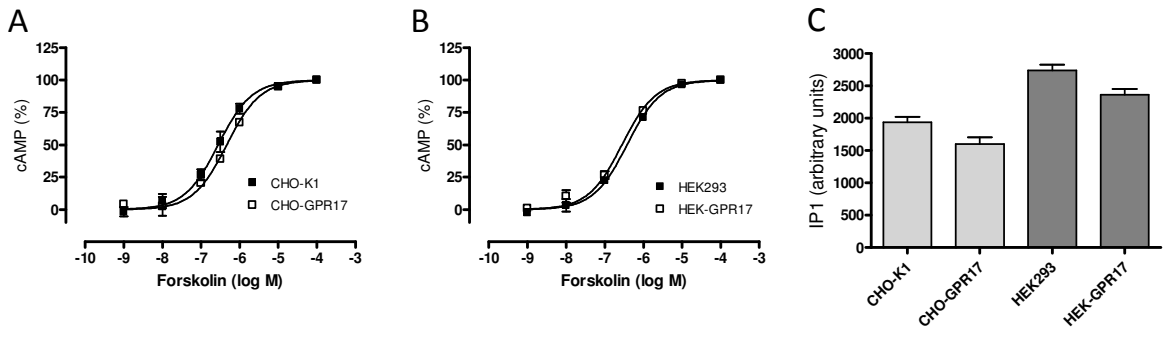

Figure 47 GPR17 does not show constitutive activity

A-B, Comparison of G protein-independent activation of adenylate cyclase with increasing forskolin concentration in untransfected (A: CHO-K1, B: HEK293) and stably transfected cell lines (A: CHO-GPR17, B: HEK-GPR17). Data were normalized to cAMP accumulation induced in untransfected cells by 100 µM forskolin. All data are means (+/- s.e.m.) of two to four experiments performed in duplicates. Calculated pEC_{50} values are: CHO-K1: -6.55 +/- 0.05, CHO-GPR17: -6.33 +/- 0.04, HEK293: -6.42 +/- 0.04, HEK-GPR17: -6.55 +/- 0.05. C, Comparison of basal IP1 concentrations in untransfected cells (CHO-K1, HEK293) and stably transfected cells (CHO-GPR17, HEK-GPR17). Data were expressed as arbitrary units and are all means (+/- s.e.m.) of three to five experiments performed in duplicates. A-C, For statistical analyses, paired t-tests with two-tailed p values and 95% confidence interval were applied and revealed no significance (cAMP: p= 0.1146 for CHOs and p= 0.0666 for HEKs; IP1: p= 0.1325 for CHOs and p= 0.1581 for HEKs).

4.1.6 GPR17 recruits β-arrestin2 upon ligand activation

After elucidating the G protein-dependent signaling properties of GPR17 and its internalization behavior, the agonist-induced translocation of β-arrestin2 to the activated receptor was analyzed, which has been shown to occur for the vast majority of GPCRs independent of their G protein signaling pathways (Claing et al. 2002, Perry & Lefkowitz 2002). Therefore the BRET2 methodology was employed with the use of a double stable cell line that constitutively expressed β-arrestin2 N-terminally fused to GFP2 and GPR17 C-terminally tagged with Renilla luciferase (RLuc). This cell line will be further referred to as HEK-BRET-GPR17.

4.1.6.1 GPR17-RLuc-fusion construct retains functional activity

Functional validation of fusion proteins is essential for subsequent BRET2 data to be interpreted as precisely reflecting cellular function (Pfleger & Eidne 2006). Therefore, in a first series of experiments the pharmacological properties of GPR17 C-terminally fused to Renilla luciferase (RLuc) were investigated, with the focus on the cellular localization (ELISA, immunofluorescence), the internalization behavior (ELISA), as well as the functional characteristics (DMR, cAMP, IP1). To facilitate analyses of the fusion protein GPR17-RLuc behavior in subsequent experiments, a HEK293 cell line stably expressing 3xHA tagged GPR17 C-terminally fused to RLuc (HEK-GPR17-RLuc) was generated and compared to wild type 3xHA labeled GPR17 expressing HEK293 cells.

4.1.6.1.1 Cell surface expression of GPR17-RLuc is diminished

As presented in Figure 48 (A), ELISA analyses of cell surface expression revealed a significant decrease of GPR17-RLuc in comparison with the wild type GPR17. The relative surface expression of wild type GPR17 (mean +/- s.e.m.: 99.91 +/- 0.11%) expressed on the cell surface exceeded more than three times the surface expression level of the fusion protein GPR17-RLuc (mean +/- s.e.m.: 29.55 +/- 2.36%). Importantly, decrease in cell surface expression of GPR17-RLuc in comparison to wild type GPR17 was not due to deficient cellular expression, as similar total cellular levels of WT and fusion protein were detected by ELISA. In agreement with the obtained ELISA data, immunofluorescence studies using the same cell lines showed that GPR17-RLuc was expressed at the cell surface (C), but at reduced levels as compared with wild type GPR17 (B), and with discrete accumulation in the cytosol of the cells.

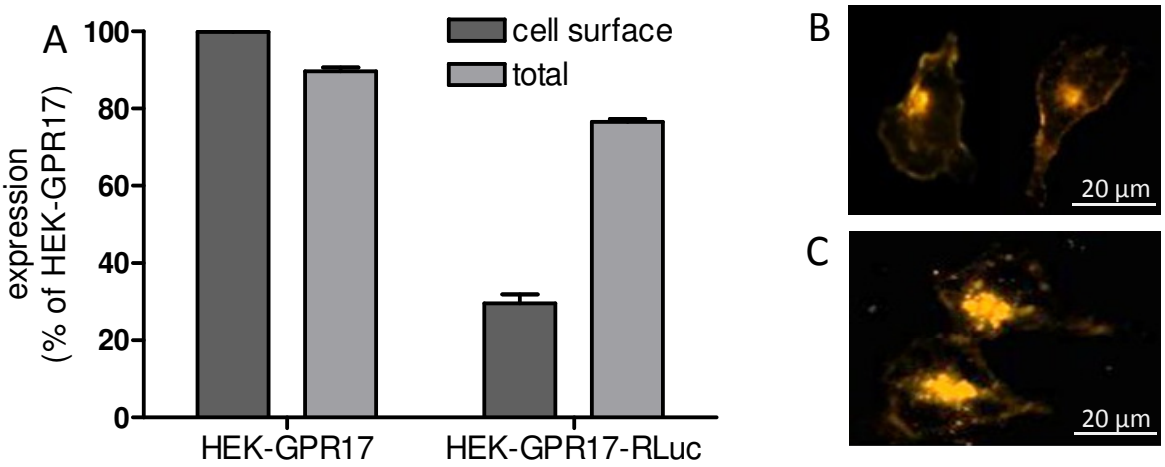

Figure 48 Cell-surface expression of 3xHA-GPR17 C-terminally fused to Renilla luciferase (RLuc) is diminished

A, The levels of surface and total GPR17 expression were determined by indirect ELISA. Immunological detection of an N-terminal 3xHA-epitope allowed a quantification of receptor proteins at the plasma membrane (dark grey bars). Permeabilization with triton X-100 (C52) enabled a determination of total receptor expression (light grey bars). The non-specific OD surface value was A450 nm: 0.051 +/- 0.009 and the OD surface value of the wild type HA-tagged GPR17 was A450 nm: 0.217 +/- 0.011. ELISA data are given as mean +/- s.e.m. of four to five independent experiments, each carried out in triplicate. Specific optical density (OD) readings were normalized to OD value of wild type 3xHA-tagged GPR17 cell surface expression. B, Fluorescence microscopy images on HEK293 cells stably expressing 3xHA tagged hGPR17 (wt), and 3xHA tagged hGPR17 C-terminally fused to Renilla luciferase (RLuc) are shown. The following settings were used for Alexa Fluor 546 recordings: 400 fold magnification, 100 ms exposure time, 0.99 γ and 2-22 histogram. Representative cells from at least three independent experiments are shown. After indirect immunofluorescence staining, no specific fluorescence was observed in untransfected HEK293 cells. Scale bars = 20 µM.

4.1.6.1.1.1 GPR17-RLuc fusion protein internalizes upon agonist activation

Internalization assay was used as an additional means to measure expression of fusion receptor GPR17-RLuc at the cell surface as well as receptor function compared to the wild type. In order to evaluate endocytosis of agonist-activated GPR17-RLuc, HEK293 cells stably expressing 3xHA-tagged GPR17-RLuc (HEK-GPR17-RLuc) were examined by indirect cellular ELISA, which enabled evaluation of

the quantitative changes of surface expressed GPR17-RLuc upon agonist activation (10 µM RA-II-150) for indicated time periods. The agonist treatment induced receptor endocytosis within 15 min, and GPR17-RLuc continued to internalize, leading to ~32.2 +/- 4.7% (mean +/- s.e.m.) loss of cell surface expression (Figure 49). The extent of GPR17-RLuc internalization was slightly increased in comparison to wild type GPR17 (~26.2 +/- 2.3%). This relative enhancement does not regard the fact, that the fusion receptor GPR17-RLuc showed lower cell surface expression (Figure 48), which might lead to a mistakable, relatively higher internalization extent, although the total amount of internalized receptor might be similar. If precise information about respective internalization extent was needed, cell lines expressing equal amounts of receptors, wild type and RLuc fusion protein, would be necessary. For the present thesis, this information was negligible, as it was only important to see, that the fusion construct remains competent to internalize upon agonist stimulation, and this conclusion was undoubtedly possible. However, in addition this assay revealed, that the fusion receptor showed a more rapid endocytosis, as after 15 min already 18.2 +/- 6.1% of surface receptors were internalized, which relates to over 30% of the receptor internalized after 120 min. In comparison, the wild type showed lower rate of endocytosis (7.0 +/- 2.8%, 15 min), which represents only 26.7% of the internalized receptor at 120 min. Nevertheless, this information is likewise not crucial for subsequent BRET2 experiments.

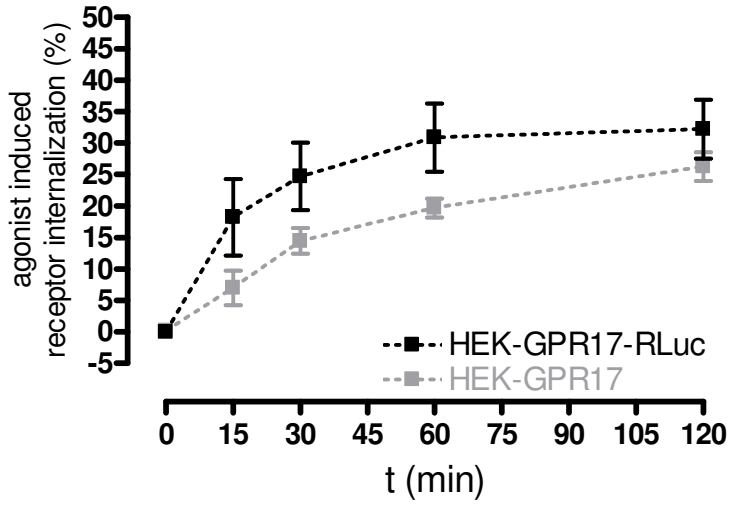

Figure 49 Time-dependent internalization behavior of agonist-activated GPR17-RLuc
Colorimetric ELISA measurements of RA-II-150 (10 µM) induced GPR17 sequestration for the indicated time period. The amount of internalized receptor was calculated from the decrease in the level of surface-expressed receptor after agonist treatment compared with untreated, control cells. Each data point represents mean (+/- s.e.m.) of three to five independent experiments performed in triplicates. Data from HEK-GPR17 are shown in light grey color, as these data have already been presented before in Figure 44.

4.1.6.1.2 GPR17-RLuc fusion protein maintains coupling via Gαq and Gαi/o

After GPR17 C-terminally fused to Renilla luciferase (RLuc) has been proven to be expressed at the cell surface, even though in a reduced extent compared to wild type, and internalization analyses revealed no significant differences to the wild type receptor, the functional characteristics of agonist-activated receptor were determined based on cAMP and IP1 assays.

As presented in Figure 50, the BRET2 fusion receptor retains its capability to couple via Gαq/11 and Gαi/o proteins. Challenging of GPR17-RLuc with increasing RA-II-150 concentrations revealed concentration-dependent IP1 accumulation (A) as well as inhibition of forskolin-stimulated cyclic AMP synthesis (B). As the latter effect was completely blunted by preincubation with PTX, the involvement of Gαi/o protein was proven. Both concentration-response curves were shifted to the right in comparison to curves obtained with analyses of wild type HEK-GPR17 cells. Whereas the potency to induce IP1 synthesis was only ~7-fold less (EC_{50} values 2.1 µM ↔ 0.3 µM), the potency to inhibit cAMP accumulation was ~500-fold decreased (EC_{50} values 1.0 µM ↔ 0.002 µM). Even more impressive was the fact, that the BRET2 fusion protein completely lost its ability to couple via Gαs proteins, since neither reverse bell-shaped CRCs were monitored, nor any increase of cAMP synthesis by stimulation with RA-II-150 concentrations, as high as possible, was detected. The loss of the stimulatory signaling pathway (Gαs) might be the reason for the stronger efficacy of the inhibitory (Gαi/o) effect on cAMP synthesis (E_{max} RLuc: 37.6 +/- 3.0% ↔ WT: 16.9 +/- 3.0%).

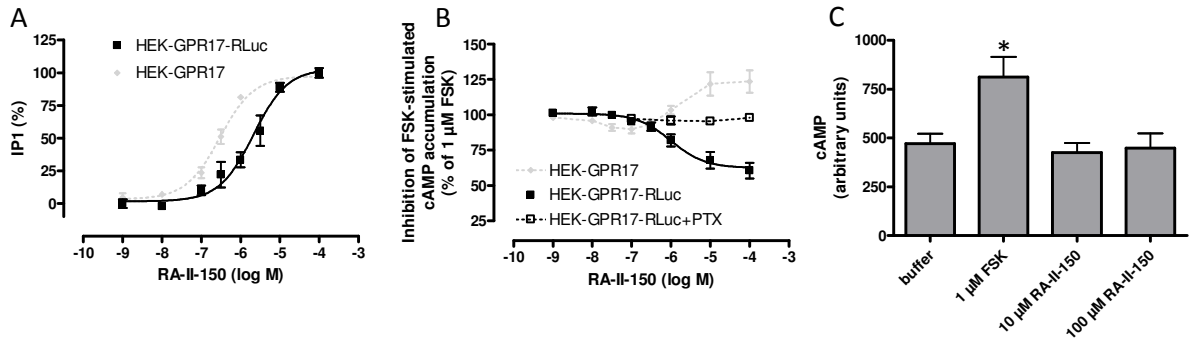

Figure 50 GPR17-RLuc remains signaling competent via Gαq and Gαi/o proteins

A-C, HEK293 cells stably expressing GPR17 C-terminally fused to Renilla luciferase were challenged with varying RA-II-150 concentrations. A-B, Data of wild type HEK-GPR17 were included for comparison. A, GPR17-mediated increase of intracellular IP1 was normalized and expressed as percent activation induced by 10 µM RA-II-150. B, Stimulation of GPR17 with increasing concentrations of RA-II-150 in the presence of 1 µM forskolin. GPR17-mediated decrease of intracellular cAMP was calculated as percent inhibition of adenylate cyclase stimulated with forskolin (1 µM). Pretreatment with Gαi/o inhibitor PTX (50 ng/ml, 18 h) completely abolished inhibition of FSK induced cAMP accumulation C, Stimulation of GPR17 did not increase intracellular cAMP synthesis, whereas 1 µM forskolin elevated basal cAMP levels. Data were expressed as arbitrary units. For statistical analyses, paired t-tests with two-tailed p values and 95% confidence interval were applied and revealed no significant differences of RA-II-150 induced values compared to basal levels, whereas forskolin induced elevation was significant (*$p < 0.05$). A-C, All data are means (+/- s.e.m.) of three to four experiments performed in duplicates.

Table 38 Parameters of averaged RA-II-150 concentration-effect curves determined by IP1 and cAMP assays with the BRET2 fusion receptor GPR17-RLuc, as depicted in Figure 50 (± s.e.m.)

assay	pEC_{50}	bottom value (%)	top value (%)	n_H	n
IP1	5.68 ± 0.09	-1.8 ± 2.9	103.2 ± 4.2	1.0 *(fixed)*	3-6
cAMP	6.00 ± 0.16	62.4 ± 3.0	100.9 ± 1.8	1.0 *(fixed)*	3-4

4.1.6.1.3 BRET2 fusion receptor GPR17-RLuc induces dynamic mass redistribution upon agonist activation

The resonant waveguide grating biosensor technology was employed to resolve signaling capability of the BRET2 fusion receptor GPR17 C-terminally fused to RLuc in real time. The stable HEK-GPR17-RLuc cells responded with specific optical signatures when exposed to increasing concentrations of GPR17 agonist RA-II-150 (Figure 51). The obtained signature profile resembled the one observed for Gαi-coupled CRTH2 receptor in HEK293 cells (Schröder et al. 2009, Schröder et al. 2010). As it is known, that the major G protein signaling pathways engaged by receptors from different coupling classes yield pathway-specific optical traces dependent on the cellular background (Fang, Frutos & Verklereen 2008, Lee et al. 2008, Schröder et al. 2010), one could conclude that GPR17-RLuc couples via Gαi protein. This assumption was further proven, as the pretreatment with the Gαi/o inhibitor PTX resulted in a partial inhibition of the optical traces (B).

The optical signatures of GPR17-RLuc virtually overtopped those of the wild type receptor (see Figure 41 for comparison), despite the fact that the fusion receptor showed significantly lower cell surface expression (Figure 48). Thus the fusion receptor GPR17-RLuc turned out to be superior in real time DMR assays, regarding the maximum response. As Gαs-induced DMR signals might begin with a negative DMR event (Fang, Li & Ferrie, Kebig et al. 2009, Schröder et al. 2010), the loss of this pathway, which has been reported in 4.1.6.1.2, could be the reason for the observed amplification of DMR response.

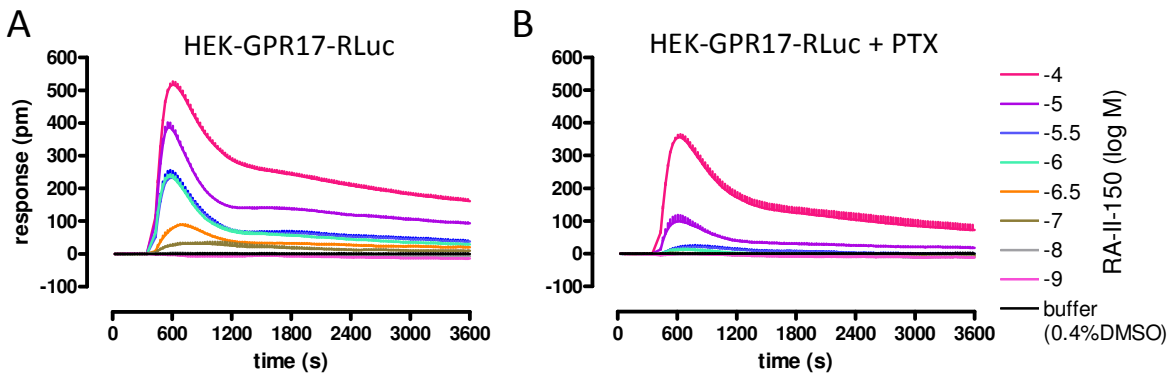

Figure 51 Agonist-induced activation of GPR17-RLuc triggers DMR in a PTX-sensitive manner
A-B, HEK293 cells stably expressing GPR17-RLuc were challenged with the indicated concentrations of the GPR17 agonist RA-II-150 in the absence (A) or presence (B) of the Gαi/o inhibitor PTX (50 ng/ml, 18 h). The resulting picometer-shifts of reflected light wavelength over time [s] were monitored as a measure of functional activity. Presented data are means + s.e.m. from a representative optical trace experiment of five to six independent experiments performed in triplicates.

The transformation of the GPR17-RLuc optical signatures into concentration-response curves for RA-II-150 using maximum response (pm) revealed an EC_{50} value of 1.5 µM (Figure 52), which is very similar to the one obtained from wild type GPR17 DMR assays (1.4 µM, see Figure 42 for comparison). Thus, despite the apparent higher efficacy of GPR17-RLuc in DMR assays in comparison to the wild type receptor, the potency of RA-II-150 is virtually identical at both receptors, demonstrating that the BRET2 fusion receptor retains its proper functional characteristics. Furthermore it could be concluded that the EC_{50} value determined by use of DMR assays (1.5 µM)

represents a mean value of both EC_{50} values obtained with the second messenger assays (Gαi/o ~1.0 µM; Gαq ~2.1 µM), thus both pathways seem to contribute with the same impact on DMR responses. PTX pretreatment caused a significant (student t-test, p= 0.0006) rightward shift of concentration-response curve, and individual data points revealed higher PTX-sensitivity than data points determined with wild type HEK-GPR17 cells (Figure 42). The increase of PTX-sensitivity is most likely caused due to the loss of Gαs-mediated signal transduction. Based on performed second messenger analyses, the remaining DMR is most likely caused by Gαq-mediated transduction. However, the EC_{50} value of PTX pretreated cells does not resemble the EC_{50} value determined in IP1 assays.

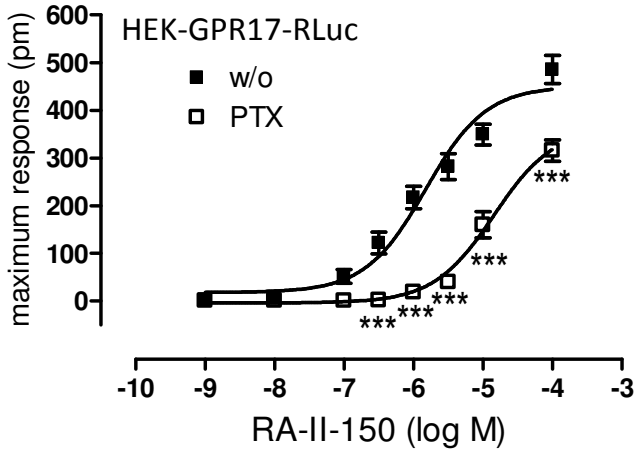

Figure 52 Concentration-dependence and partial PTX-sensitivity of RA-II-150 induced DMR
Comparison of concentration-effect curves resulting from DMR assays of HEK-GPR17-RLuc cells challenged with indicated concentrations of GPR17 agonist RA-II-150 in the presence or absence of the Gαi/o inhibitor PTX (50 ng/ml, 18 h). Data are presented as maximum response of wavelength shift and all data points represent mean (+/- s.e.m.) of five to six independent experiments performed in triplicates. For statistical analyses, individual concentrations were compared by two-way ANOVA with Bonferroni's correction for multiple comparisons (***p < 0.001).

Table 39 Parameters of averaged RA-II-150 concentration-effect curves determined by DMR assays, as depicted in Figure 52 (± s.e.m.)

cell line	pEC_{50}	bottom value (pm)	top value (pm)	n_H	n
HEK-GPR17-RLuc	5.82 ± 0.10	18.2 ± 13.4	450.3 ± 19.6	1.0 *(fixed)*	5-6
HEK-GPR17-RLuc *+ PTX*	4.84 ± 0.09	-3.7 ± 6.5	363.6 ± 20.6	1.0 *(fixed)*	5-6

4.1.6.2 Rapid recruitment of β-arrestin2 to the agonist-activated GPR17 and sustained protein-protein interaction

Since fusion of GPR17 to Renilla luciferase (RLuc) did not impair its ability to promote agonist-stimulated inositol phosphate accumulation and cyclic AMP inhibition, respectively, as well as the rate of internalization, a BRET2 assay was established for further analyses of the generated construct.

The kinetic analyses of the ligand induced BRET signal between GPR17-RLuc and β-arrestin2-GFP2 was performed on two time windows. The recruitment kinetic was determined on a time window of 120 s after RA-II-150 injection, whereas the sustained receptor-arrestin interaction was evaluated on a time window from 1 to 60 min after RA-II-150 injection. As depicted in Figure 53, RA-II-150-induced BRET increase occurred rapidly without any lag time and half maximum BRET ratio was already reached after 20.9 +/- 2.0 s (A). This rapid translocation of β-arrestin2-GFP2 to the agonist-activated GPR17-RLuc, followed by a constant rise, was further substantiated with endpoint kinetic assays (B), as already after one minute the maximum BRET ratio was reached and persisted for the next 5 min. The β-arrestin2-GFP2 and GPR17-RLuc association declined only slowly, with a 18% decrease after 10 min and 66% decrease after 60 min (*p < 0.05).

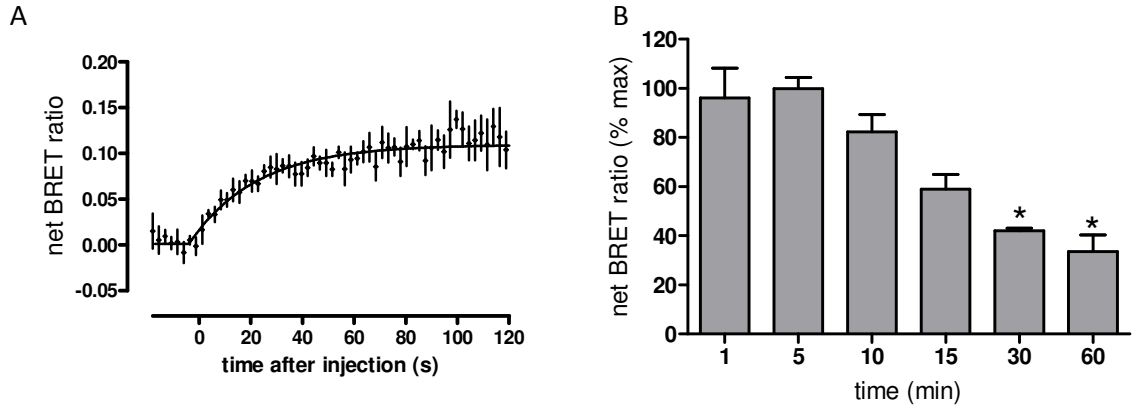

Figure 53 Kinetic analyses of RA-II-150-induced BRET increase between GPR17 and β-arrestin2
A-B, HEK293 cells stably coexpressing GPR17-RLuc and β-arrestin2-GFP2 were used for BRET2 experiments, and repetitive signals were recorded before and after the injection of RA-II-150 (1 µM) during 140 s (A) and 60 min (B), respectively. A, BRET measured every 2.4 s. BRET signal was fitted with GraphPad Prism4 (*plateau than increase to top* equation). B, Data were normalized and expressed as percent of maximum recruitment induced by RA-II-150 (5 min). A-B, Each data point represents mean (+/- s.e.m.) of three to five independent experiments performed in triplicates. For statistical analyses, paired t-tests with two-tailed p values and 95% confidence interval were applied (*p < 0.05).

4.1.6.3 Recruitment of β-arrestin2 to agonist-activated GPR17 in a concentration-dependent and partially PTX-sensitive manner

After determination of translocation and adhesion kinetics of β-arrestin2 recruitment to the RA-II-150-activated GPR17, a time window of 5 min was chosen for agonist stimulation to analyze concentration-dependence. The BRET2 signal was measured in the absence and presence of increasing concentrations of the GPR17 agonist RA-II-150. As presented in Figure 54, RA-II-150 promoted a concentration-dependent increase in BRET2, indicative of an association between GPR17-RLuc and β-arrestin2-GFP2. The absolute EC_{50} value calculated for this agonist-induced interaction was ~0.4 µM, thus the potency determined by BRET2 assays was 2.5- up to 5.5-fold higher in comparison with the data obtained in second messenger and DMR assays. Preincubation with Gαi/o inhibitor PTX induced a slight rightward shift of the concentration-response curve. Even though this effect was not statistically significant (p < 0.05), this phenomenon was in good

agreement with previous data obtained with PTX preincubation (DMR analyses, Figure 52), and indicated participation of Gαi/o-mediated signaling in β-arrestin2 recruitment.

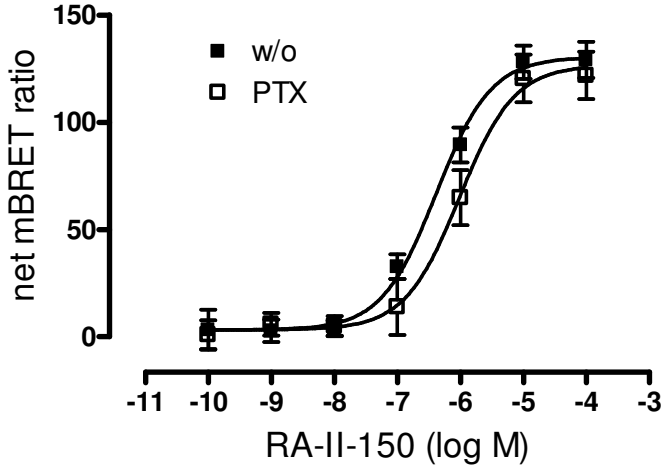

Figure 54 Concentration-dependent β-arrestin2 recruitment to agonist-activated GPR17
HEK293 cells stably transfected with β-arrestin2-GFP2 and GPR17-RLuc (HEK-BRET-GPR17) were exposed to indicated concentrations of RA-II-150, and agonist-induced increases in BRET ratio were monitored. Pretreatment with Gαi/o inhibitor PTX (50 ng/ml, 18 h) did not have a significant influence ($p < 0.05$). Each data point represents mean (+/- s.e.m.) of three to six independent experiments performed in triplicates. For statistical analyses, paired t-tests with two-tailed p values and 95% confidence interval were applied.

Table 40 Parameters of averaged RA-II-150 concentration-effect curves determined by DMR assays, as depicted in Figure 54 (± s.e.m.)

cell line	pEC_{50}	bottom value (net BRET ratio)	top value (net BRET ratio)	n_H	n
HEK-BRET-GPR17	6.38 ± 0.12	3.0 ± 4.0	130.3 ± 5.2	1.0 *(fixed)*	6
HEK-BRET-GPR17 *+ PTX*	6.01 ± 0.14	3.1 ± 4.8	126.6 ± 7.3	1.0 *(fixed)*	3

4.1.6.4 Mechanistic insights into the β-arrestin2 recruitment to GPR17 upon stimulation with RA-II-150

Now that β-arrestin2 recruitment to activated GPR17 upon RA-II-150 stimulation has been proven by BRET2 assays, it was the aim to further investigate the underlying mechanism of this translocation. Especially the impact of the heterotrimeric G proteins was of interest, as at least for some receptors, β-arrestin-mediated functions, such as internalization or signaling, have been demonstrated to occur independent of prior G protein-coupling (reviewed by Defea 2008, DeWire et al. 2007, Violin & Lefkowitz 2007).

4.1.6.4.1 BIM-46187: a suitable tool to analyze G protein independent recruitment of β-arrestin?

The analyses of GPR17 C-terminally fused to Renilla luciferase (RLuc) revealed its capability to couple via Gαi/o and Gαq proteins (see 4.1.6.1). Thus, a small molecule modulating both pathways in parallel was needed to further analyze whether the observed β-arrestin-recruitment occurs in a

G protein independent manner. As no such compound exists, the small molecule BIM-46187 was chosen for further analyses. BIM-46187 was published as a small molecule pan-inhibitor of G protein signaling, that prevents the accurate interaction of receptors with the G protein heterotrimer through a direct binding to the Gα subunit, consequently promoting inhibition of the agonist-induced GDP/GTP exchange (Ayoub et al. 2009).

4.1.6.4.1.1 Label-free dynamic mass redistribution technology unsuitable to characterize pan G protein inhibition by BIM-46187

As a first attempt, the impact of BIM-46187 was analyzed using dynamic mass redistribution (DMR) technology, since this method is able to analyze both G protein pathways of interest simultaneously.

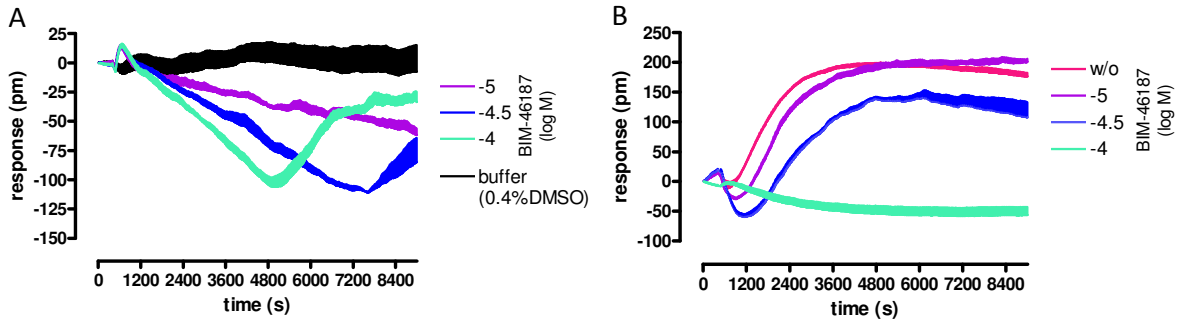

Figure 55 BIM-46187 induces prominent negative dynamic mass redistribution
A-B, HEK293 cells stably coexpressing β-arrestin2-GFP2 and GPR17-RLuc were challenged with the indicated concentrations of BIM-46187 in the absence (A) or presence (B) of forskolin (10 µM). Wavelength shift [pm] over time [s] was monitored by use of the Epic® system. Representative optical trace experiment (mean + s.e.m.) of at least three independent experiments performed in triplicates are shown.

HEK293 cells stably co-expressing β-arrestin2-GFP2 and GPR17-RLuc (HEK-BRET-GPR17) were challenged with three different BIM-46187 concentrations (10, 30 and 100 µM), and cells responded with a strong negative DMR, in a concentration-dependent manner (Figure 55, A). Furthermore, the influence of BIM-46187 on forskolin induced DMR was investigated for control purposes. Therefore HEK-BRET-GPR17 cells were preincubated (2.5h) with the indicated BIM-46187 concentrations, followed by stimulation with forskolin (Figure 55, B). As this diterpene is known to act directly via stimulation of the adenylate cyclase, independent of G proteins, BIM-46187 should not have any impact on forskolin-triggered DMR. However, preincubation with BIM-46187 resulted in concentration-dependent inhibition of forskolin-mediated wavelength shifts. The negative DMR induced by BIM-46187 probably compensated the forskolin-triggered positive DMR, thus resulting in a neutralized optical signature, even though the actual signaling event might not be influenced. Regarding these results, it was concluded that DMR technology does not represent an appropriate method to analyze the impact of BIM-46187 on GPR17-mediated signaling.

4.1.6.4.1.2 Cell type dependent properties of BIM-46187

Subsequent to the analyses of BIM-46187 in Epic® assays, traditional second messenger assays were performed to further elucidate suitability of this small molecule. Therefore, first of all, the influence on forskolin-stimulated cAMP accumulation was examined. As presented in Figure 56 (A),

preincubation with increasing BIM-46187 concentrations did not result in reduction of forskolin-induced synthesis of cAMP. Thus, these data support the conclusion that inhibition of forskolin-induced DMR, monitored with the Epic® system (see 4.1.6.4.1.1), was due to compensation effects of negative and positive DMR events and not mediated by direct inhibition of adenylate cyclase.

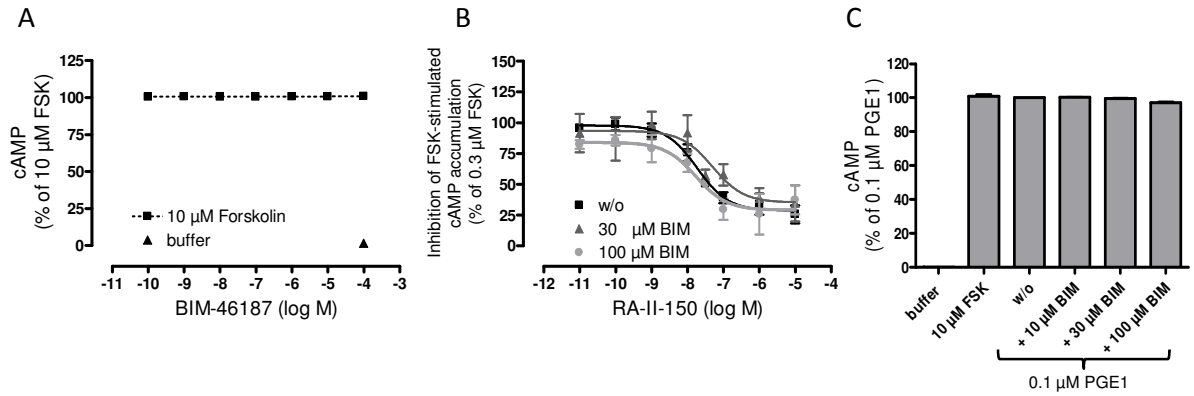

Figure 56 Influence of BIM-46187 on cAMP accumulation analyzed in HEK293 cells stably coexpressing GPR17-RLuc and β-arrestin2-GFP2

A-C, HEK293 cells stably coexpressing β-arrestin2-GFP2 and GPR17-RLuc were analyzed by cAMP assays. A, Stimulation of adenylate cyclase with constant forskolin concentration (10 µM), preincubated (2.5h, 37°C) with increasing BIM-46187 concentrations. Forskolin induced increase of intracellular cAMP was calculated as percent of cAMP determined by stimulation with forskolin (10 µM) in the absence of BIM-46187. B, Cells were stimulated with increasing concentrations of RA-II-150 in the presence of 0.3 µM forskolin. GPR17-mediated decrease of intracellular cAMP was calculated as percent inhibition of adenylate cyclase stimulated with forskolin (0.3 µM). Pretreatment with BIM-46187 (30 and 100 µM) did not significantly influence GPR17-mediated inhibition. C, Cells, endogenously expressing prostanoid receptors (EP2 and EP4) were challenged with 10 µM forskolin (FSK) as a control, as well as with 0.1 µM prostaglandin E1 (PGE1, C40) without (w/o) or with preincubation of increasing BIM-46187 concentrations. Elevation of intracellular cAMP was normalized and expressed as percent of maximum activation induced by 0.1 µM PGE1. B-C, For statistical analyses, paired t-tests with two-tailed p values and 95% confidence interval were performed. A-C, All data are means (+/- s.e.m.) of three to five experiments performed in duplicates.

Based on SRE-Luc gene reporter assays applied to COS-7 cells transiently expressing PAR1 (protease-activated receptor 1), which is known to activate many different G proteins including Gαi/o, Gαq and Gα12/13, BIM-46187 has been reported to diminish Gαi/o-mediated effects (Ayoub et al. 2009). Based on this information, the influence of BIM-46187 on GPR17-induced inhibition of cAMP accumulation was investigated. However, preincubation with two BIM-46187 concentrations (30 and 100 µM) did not significantly influence RA-II-150-induced concentration-response curves, thus contrary to expectations; BIM-46187 did not inhibit GPR17-mediated Gαi/o-induced effect on adenylate cyclase (Figure 56, B).

Ayoub et al. further observed the effects of BIM-46187 in whole cells, monitored by cAMP production. COS-7 cells, transiently expressing GPCRs known to couple via Gαs (V2, β2-AR and 5-HT4a), were preincubated with BIM-46187, that dramatically inhibited Gαs-mediated cAMP production in a concentration-dependent manner. Despite their observation, preincubation of HEK293 cells, endogenously expressing Gαs-linked prostanoid receptors (EP2R and EP4R, Willoughby et al. 2007), with BIM-46187, did not significantly alter prostaglandin E1 (PGE1) mediated increase of intracellular cAMP (Figure 56, C).

Furthermore, Ayoub et al. reported inhibition effects of BIM-46187 in COS-7 cells, transiently expressing GPCRs known to couple via Gαq (PAR1, LPAR1 and 5-HT2ca), monitored by means of IP1 assays. Similar to cAMP analyses, preincubation with BIM-46187 dramatically inhibited Gαq-mediated IP1 production in a concentration-dependent manner. Regarding this information, HEK293 cells stably expressing GPR17-RLuc were analyzed according to inhibition effects of BIM-46187 on RA-II-150-induced intracellular IP1 accumulation. Interestingly, preincubation with the small molecule (30 and 100 µM) did significantly and almost completely diminish the GPR17-mediated IP1 production in a concentration-dependent manner (Figure 57, A). This apparent pathway-specific inhibition was further proven, as carbachol-induced IP1 production through activation of endogenously expressed muscarinic receptors (M1 and M3, Estacion et al. 2004, Mundell & Benovic 2000) was likewise inhibited by preincubation with BIM 46187. To control that observed inhibition effects on Gαq-mediated IP1 increase were not due to any peculiar effects of BIM-46187, the influence on basal IP1 levels was examined and did not reveal any significant unspecific impact (Figure 57, B).

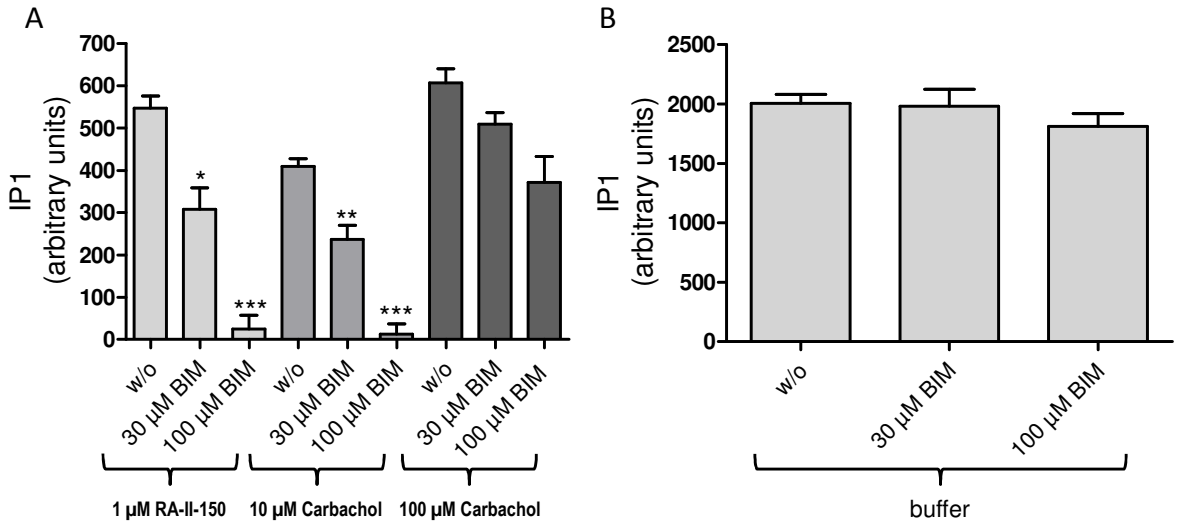

Figure 57 Influence of BIM-46187 on IP1 accumulation analyzed in HEK293 cells stably coexpressing GPR17-RLuc and β-arrestin2-GFP2

A-B, HEK293 cells stably coexpressing β-arrestin2-GFP2 and GPR17-RLuc were analyzed by IP1 assays. Intracellular IP1 levels were expressed as arbitrary units. For statistical analyses, paired t-tests with two-tailed p values and 95% confidence interval were applied (*$p < 0.05$, **$p < 0.01$, ***$p < 0.001$). All data are means (+/- s.e.m.) of three to four experiments performed in duplicates.

Based on the results with BIM-46187 preincubation, one could conclude that, despite the reported information about this small molecule as a pan-inhibitor of G protein-dependent signaling (Ayoub et al. 2009) it only acts as a pathway specific inhibitor by diminishing Gαq-mediated signaling events. Since all so far observed results presented in this thesis were obtained in HEK293 cells stably coexpressing β-arrestin2-GFP2 and GPR17-RLuc, and regarding the fact that Ayoub et al. mainly investigated BIM-46187 in COS-7 cells transiently transfected with appropriate GPCRs, it was a next aim to further evaluate the small molecule and its inhibition effects in COS-7 cells.

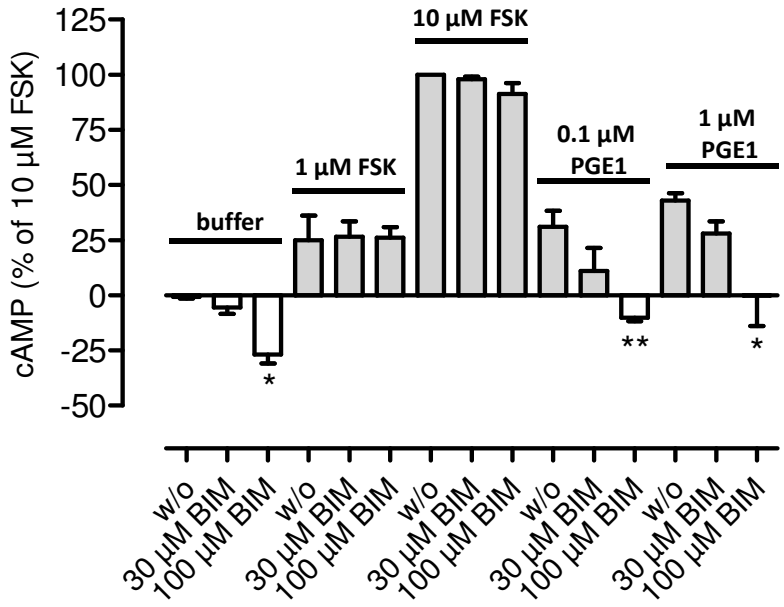

Figure 58 Influence of BIM-46187 on cAMP accumulation in COS-7 cells
Untransfected COS-7 cells, endogenously expressing prostanoid receptors were challenged with forskolin (1 and 10 µM FSK) as a control, as well as with prostaglandin E1 (0.1 and 1 µM PGE1, C40), both without (w/o) or with preincubation of increasing BIM-46187 (BIM) concentrations (30 and 100 µM). Elevation of intracellular cAMP was normalized and expressed as percent of maximum activation induced by 10 µM forskolin. For statistical analyses, unpaired t-tests with two-tailed p values and 95% confidence interval were performed (*p < 0.05, **p < 0.01). All data are means (+/- s.e.m.) of three experiments performed in triplicates.

Therefore PGE1 was chosen to stimulate cAMP accumulation via endogenously expressed prostanoid receptors. Similar to the results obtained in HEK293 cells, elevation of forskolin-induced cAMP levels were not inhibited by preincubation with BIM-46187, confirming its absence of nonspecific AC inhibition. However interestingly, in COS-7 cells preincubation with BIM-46187 resulted in a significant inhibition of PGE1-induced Gαs-mediated cAMP accumulation. Both applied PGE1 concentrations, 0.1 and 1 µM, did increase intracellular cAMP concentrations in a concentration-dependent manner (without preincubation, w/o), and both utilized BIM-46187 concentrations (30 and 100 µM, respectively) did inhibit this effect (Figure 58). Regarding the fact that BIM-46187 did also significantly decrease the basal intracellular cAMP level (buffer values in Figure 58), one could conclude that these examined inhibition effects were some unspecific artifacts, but as preincubation with BIM-46187 did not have any impact on forskolin-induced cAMP elevation, it should be reliable, that inhibition effects of the small molecule were due to its ability of inhibiting Gαs-initiated intracellular effects on adenylate cyclase. The decrease of the basal cAMP level could be explained by the presence of constitutively active GPCRs endogenously expressed in COS-7 cells, thus inhibiting these receptors would result in a lowered basal cAMP level. Similar effects are known for YM-254890, as preincubation with the specific Gαq/11 inhibitor might result in a lowered IP1 concentration (Figure 59, and Schröder et al. 2010).

4.1.6.4.2 GPR17 acts as a balanced receptor

After uncovering Gαi/o and Gαq as the G protein-dependent signaling pathways of the BRET2 fusion construct GPR17-RLuc upon stimulation with RA-II-150 (see 4.1.6.1.2), and evaluation of the small molecule BIM-46187 to not represent a suitable tool to diminish both pathways simultaneously in HEK293 cells (see 4.1.6.4.1), it was the next goal to assess, whether combination of the Gαi/o inhibitor pertussis toxin (PTX) and the Gαq inhibitor YM-254890 would be a feasible method to analyze whether G protein-independent β-arrestin2-recruitment upon GPR17 activation occurs.

Initially, as depicted in Figure 59 (A-C), the pharmacological inhibitors were examined by means of second messenger assays (cAMP and IP1) and dynamic mass redistribution technology (DMR, Epic® system) by use of HEK293 cells stably expressing GPR17 C-terminally fused to RLuc and β-arrestin2 N-terminally labeled with GFP2 (HEK-BRET-GPR17). Pretreatment with Gαi/o inhibitor PTX (50 ng/ml, 18 h) completely abolished the concentration-dependent inhibition of forskolin-induced cAMP accumulation initiated by RA-II-150-activated GPR17 (Figure 59, A). Likewise, the Gαq inhibitor YM-254890 (300 nM, 2.5h) completely diminished the RA-II-150 induced IP1 accumulation (B). These results were further confirmed in Epic® assays (C), as the optical DMR signatures triggered with RA-II-150 (1 µM) were partly sensitive to pretreatment with PTX (50 ng/ml, 18 h) and YM-254890 (300 nM, 2.5 h), respectively, but completely abrogated in the presence of a combination of both pharmacological modulators (PTX and YM). Thus, simultaneous incubation with PTX and YM-254890 of HEK-BRET-GPR17 cells prior to β-arrestin-translocation assays (BRET2) enables analyses of G protein-independent recruitment to the activated receptor. In addition, the influence of BIM-46187 that has been shown to inhibit GPR17-mediated IP1 accumulation (Figure 57) on β-arrestin2-recruitment has been analyzed.

The obtained results, as depicted in Figure 59 (D), revealed that GPR17 acts as a balanced receptor, meaning that even though the G protein-mediated signaling pathways were completely abrogated, β-arrestin2 was still partly recruited to the agonist-activated GPR17, thus in a G protein-independent manner. The Gαi/o inhibitor revealed a superior inhibition on GPR17-mediated β-arrestin2 translocation in comparison to the Gαq inhibitor YM-254890 (PTX: 34.2 +/- 6.2 % ↔ YM: 17.4 +/- 8.4 %), comparable to the results obtained by means of DMR analyses. Whereas the additive effect of both inhibitors resulted in a complete abrogation of GPR17-induced optical signatures, the β-arrestin2-recruitment was only decreased slightly above the half (55 +/- 7 %), which is consistent with the calculated theoretical sum of each inhibitor (~51.6 %), thus confirming that it was an additive effect. Preincubation with BIM-46187 resulted in comparable results as obtained with YM-254890, whereas 30 µM revealed slightly lower (13.9 +/- 9.9 %) and 100 µM a slightly bigger (23.3 +/- 5.8 %) inhibition effect. Likewise, additive effects were monitored by simultaneous preincubation with PTX, causing strongest inhibition (63.7 +/- 5.7 %) with PTX and 100 µM BIM-46187. These findings further prove the previously postulated Gαq-selective inhibition of BIM-46187 in HEK293 cells.

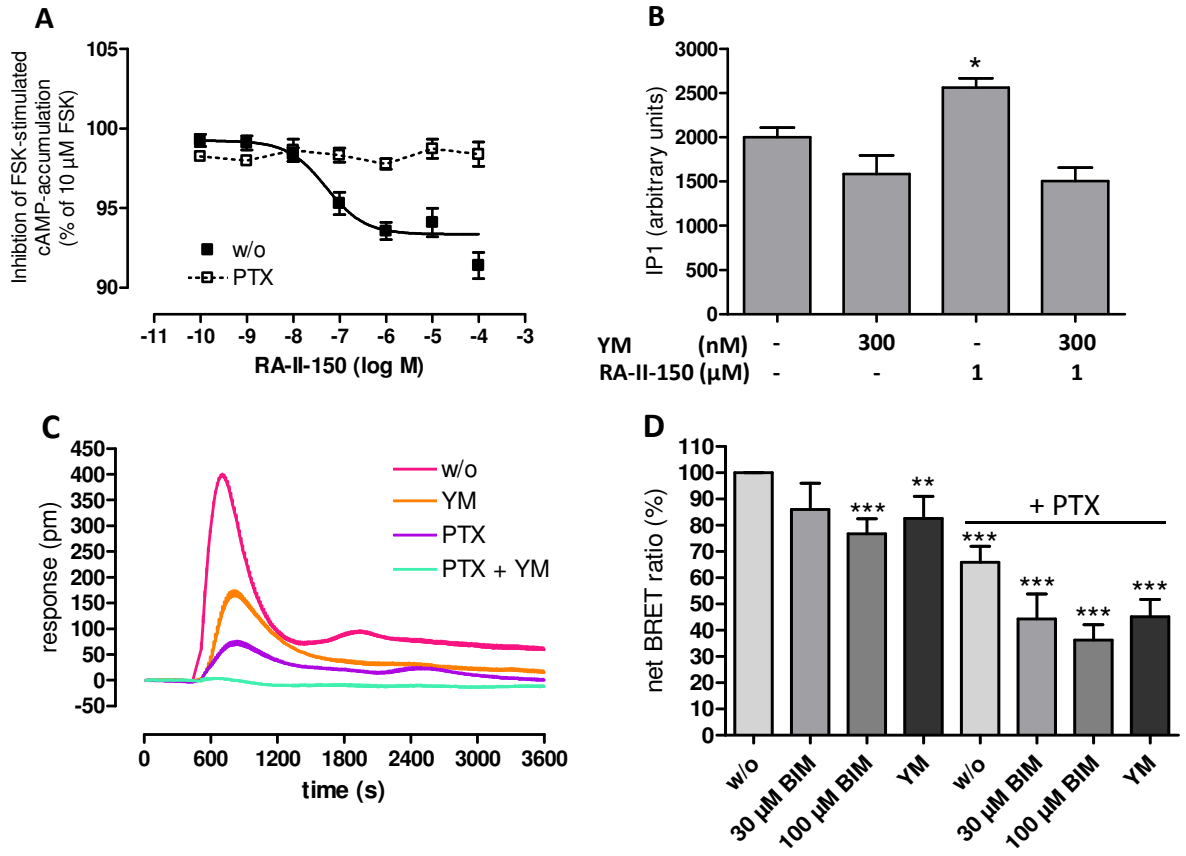

Figure 59 GPR17-mediated β-arrestin2 recruitment is only partly G protein-dependent

A-D, HEK293 cells stably coexpressing GPR17 C-terminally fused to Renilla luciferase (RLuc) and β-arrestin2 N-terminally fused to GFP2 (HEK-BRET-GPR17 low) were challenged with indicated concentrations of GPR17-agonist RA-II-150. A, Cells were stimulated with increasing RA-II-150 concentrations in the presence of 10 µM forskolin (FSK). GPR17-mediated decrease of intracellular cAMP was calculated as percent inhibition of adenylate cyclase stimulated with forskolin (10 µM). Pretreatment with Gαi/o inhibitor PTX (50 ng/ml, 18 h) completely abolished inhibition of FSK induced cAMP accumulation. B, RA-II-150 (1 µM) induced IP1 production was completely abrogated in the presence of Gαq inhibitor YM-254890 (YM, 300 nM, 2.5h). Intracellular IP1 levels were expressed as arbitrary units. C, The optical DMR signature obtained with RA-II-150 (1 µM) was partly sensitive to pretreatment with PTX (50 ng/ml, 18 h) and YM-254890 (300 nM, 2.5 h), respectively, but completely abolished in the presence of a combination of both modulators (PTX + YM). D, Influences of Gαi/o inhibitor PTX (50 ng/ml, 18 h), Gαq inhibitor YM-254890 (300 nM, 2.5h) and BIM-46187 (30 and 100 µM, 2.5h) on agonist-induced increases in BRET2 ratio were monitored. Data were normalized and expressed as percent of maximum activation induced by RA-II-150 (1 µM) without (w/o) pretreatment. A-D, Each data point represents mean (+/- s.e.m.) of three to six independent experiments performed in triplicates. For statistical analyses, unpaired t-tests with two-tailed p values and 95% confidence interval were applied. A-D, All data are means (+/- s.e.m.) of three to nine experiments performed in triplicates.

4.1.7 Receptor panning of multiple cell systems with GPR17 agonist

The strategies applied so far to elucidate signaling patterns of GPR17, such as over expression into host cells (here CHO and HEK) and / or receptor labeling, offer benefit in sensitivity of detection, but do not inevitably exhibit biological relevance or predictability of physiological importance. GPCRs are able to activate different signaling pathways depending on their cellular surroundings, thus the ability of a ligand to trigger functional responses is dependent on cellular background, receptor expression levels and coupling efficiencies (Eglen 2005, Kenakin 2002, Kenakin 2005, Milligan 1993). The previous results, as determined before, verified that the potency and efficacy of RA-II-150 showed differences between the two analyzed cellular backgrounds as well as between different signaling pathways. In order to obtain more insight into the physiological importance of the described signaling pathways, it was the aim to identify a cellular system endogenously expressing GPR17. Therefore various cell systems, including mostly immortalized but also primary cell lines, were analyzed by use of the Epic® system, which enables whole-cell and label-free detection of endogenously expressed GPCRs with high sensitivity (Fang, Li & Ferrie, Fang & Ferrie 2007, Schröder et al. 2010). Thus, a panning of the GPR17 agonist RA-II-150 against cell systems by means of DMR analyses was used to map endogenously expressed GPR17. Part of the panning was generously provided by Dr. Ye Fang (Corning® Company, NY, USA).

Unfortunately, as depicted in Figure 60, none of the analyzed cell lines responded to the stimulation with the GPR17-agonist RA-II-150, whereas the applied positive controls always revealed that assay conditions were properly chosen as well as cell viability was highly sufficient. Even HUVEC cells (human umbilical vein endothelial cells), which have been reported to express GPR17 (Ciana et al. 2006), did not reveal any detectable DMR after challenge with RA-II-150.

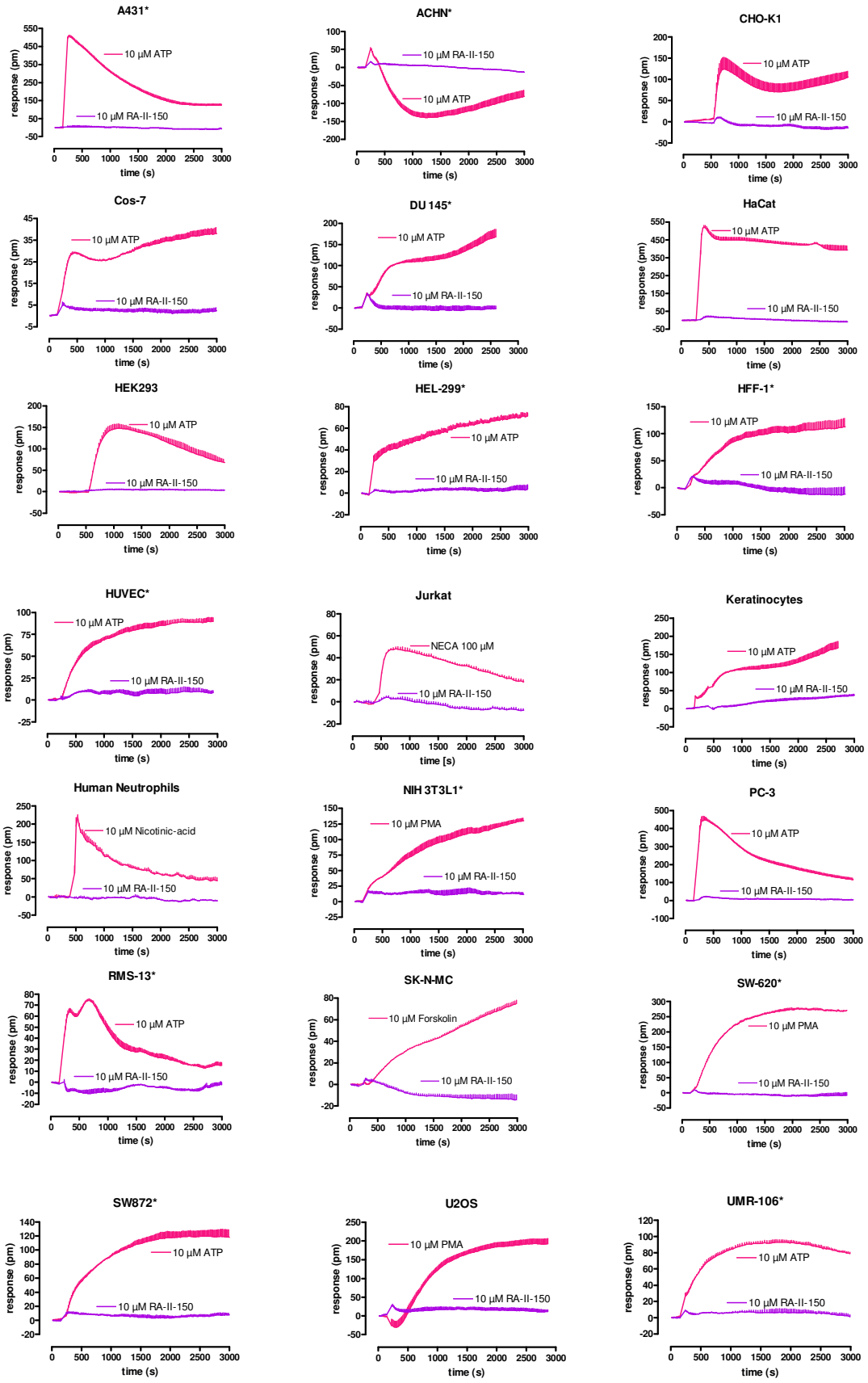

Figure 60 Receptor panning with GPR17-agonist RA-II-150 by DMR assays

Figure 60 Native cell lines were challenged with the GPR17-agonist RA-II-150 (10 µM) and the indicated positive controls (10 µM adenosine triphosphate / ATP, 10 µM adenosine-5-N-ethylcarboxamide / NECA, 10 µM nicotinic acid, 10 µM phorbol myristate acetate / PMA and 10 µM forskolin). Wavelength shift [pm] over time [s] was monitored as a measure of functional activity. Signatures were baseline-corrected by subtraction of buffer traces from the DMR responses after receptor activation. Data kindly provided by Dr. Ye Fang are indicated with *. Representative optical trace experiment (mean + s.e.m.) of one to five independent experiments performed in triplicates.

4.1.7.1 Generation of a GPR17-deficient cellular tool for further cell differentiations derived from murine embryonic stem cells

Since all the efforts finding an appropriate cell system, which endogenously expresses GPR17 by means of DMR analyses failed, it was the aim to generate a cellular tool, which offers the capability to be differentiated into a desired cell system, especially of neural cell type such as cortical neurons (Gaspard et al. 2009) or spinal cord motor neurons (Wichterle et al. 2002). Therefore murine embryonic stem cells were modified by gene targeting to obtain pluripotent cells with heterozygous knocked-out GPR17 (see 3.4). The homologous recombination was verified by PCR screening and revealed three clones where TM2-TM6 of GPR17 were heterozygously knocked-out (Figure 35), discerned by the presence of an integrated neomycin-resistance cassette. The proceeding modifications of the heterozygous modified embryonic stem cells, such as homologous knock-out and differentiation into the desired neural cell type, were beyond the scope of the present thesis, and will be conducted in the future.

4.2 The influence of β-arrestin2 coexpression on GPR17-mediated signaling patterns upon agonist-induced activation

Following the elucidation of GPR17-mediated signaling patterns, the focus was set on β-arrestin coexpression and its impact on the receptor's signaling outcome. As described in chapter 1.3 and reviewed by many authors (e.g. Lefkowitz & Shenoy 2005, Luttrell & Lefkowitz 2002), β-arrestins possess multiple functions regarding regulation of agonist-activated GPCR signaling, particularly desensitization of subsequent G protein-coupling, promotion of receptor trafficking, and stimulation of signaling cascades in a G protein-independent manner. To analyze whether increasing β-arrestin expression levels exhibit an influence on GPR17-induced signaling, HEK293 cells stably expressing distinct β-arrestin2 amounts (kindly provided by J. M. Mathiesen, Department of Medicinal Chemistry, University of Copenhagen) were stably transfected with GPR17-RLuc fusion protein labeled with 3xHA tag to enable further expression analyses. Thus, one single and three double stable cell lines, initially generated for β-arrestin-recruitment studies (BRET2 assay), were analyzed:

- HEK293 cells + 3xHA-hGPR17-RLuc

  → ***endogenous***

- HEK293 cells + 3xHA-hGPR17-RLuc + low amounts of β-arrestin2-GFP2

  → ***low***

- HEK293 cells + 3xHA-hGPR17-RLuc + high amounts of β-arrestin2-GFP2

  → ***high***

- HEK293 cells + 3xHA-hGPR17-RLuc + very high amounts of β-arrestin2-GFP2

  → ***very high***

The HEK293 cells stably transfected with fusion protein β-arrestin2-GFP2 were sorted based on respective fluorescence intensity caused by the autofluorescent tag GFP2 by use of FACS analyses (fluorescence activated cell sorting, kindly conducted by J. M. Mathiesen, Department of Medicinal Chemistry, University of Copenhagen), and photos of respective cell lines obtained by fluorescence microscopy are depicted in the appendix of this thesis (Annex Figure 2). Cell lines will be further referred to as *endogenous, low, high and very high*, based on their β-arrestin2 expression levels.

The impact of β-arrestin2 coexpression on GPR17-mediated signaling outcome was analyzed regarding the previously determined G protein-dependent signaling events.

4.2.1 No linear correlation between coexpression of β-arrestin2 and GPR17 cell surface expression

Initially, self-engineered stable HEK293 cell lines were analyzed concerning their GPR17 expression levels, to determine whether these pooled clones were suitable for further comparative analyses.

As already presented in Figure 48, the fusion of the receptor C-terminally to the Renilla luciferase (RLuc) did result in a significantly lowered cell surface expression in comparison to the total receptor expression, determined by permeabilization with triton X-100 (Figure 61).

In contrast to a suspected lowered cell surface expression due to enhanced β-arrestin2-mediated internalization, data obtained with indirect ELISA analyses revealed a slight, but significant increase of relative cell surface expression with low (115.7 +/- 4.0%) and high (136.7 +/- 4.9%) amounts of β-arrestin2 coexpression in comparison to the endogenous levels present in HEK293 cells, which was set as 100 percent (100.4 +/- 0.2%) (Figure 61). Only the GPR17 surface expression in HEK293 cells comprising very high amounts of β-arrestin2 was significantly lowered by 83.4 +/- 5.3%.

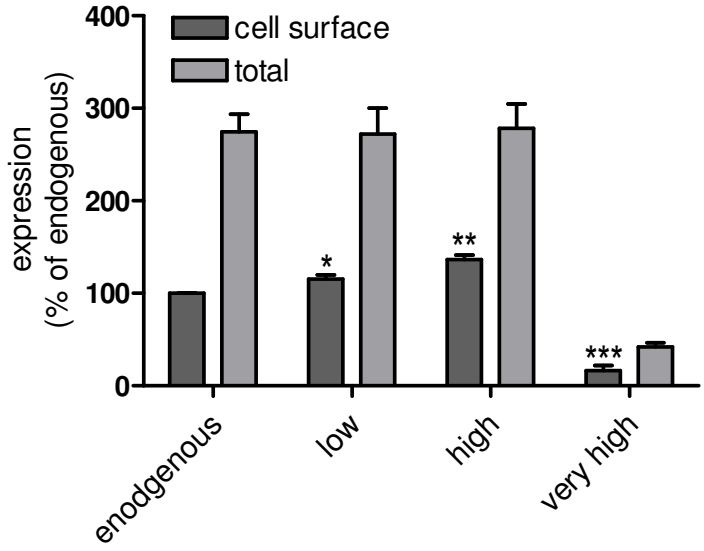

Figure 61 Cell-surface expression of 3xHA-GPR17 C-terminally fused to Renilla luciferase (RLuc) coexpressed with increasing β-arrestin2 amounts

The levels of surface and total GPR17 expression were determined by indirect ELISA. Immunological detection of an N-terminal 3xHA-epitope allowed quantification of receptor proteins at the plasma membrane (dark grey bars). Permeabilization with triton X-100 (C52) enabled determination of total receptor expression (light grey bars). The non-specific OD surface value was A450 nm: 0.057 +/- 0.007 and the OD surface value of the 3xHA-tagged GPR17-RLuc expressed in native HEK293 cells (endogenous) was A450 nm: 0.105 +/- 0.008. ELISA data are given as mean +/- s.e.m. of three to seven independent experiments, each carried out in triplicate. Specific optical density (OD) readings were normalized to OD value of 3xHA-tagged GPR17-RLuc cell surface expression in native HEK293 cells (endogenous). For statistical analyses, paired (low and high) and unpaired (very high), respectively, t-tests with two-tailed p values and 95% confidence interval were applied (*$p < 0.05$, **$p < 0.01$, ***$p < 0.001$).

This might be caused by the assumed higher internalization rate, but as well simply due to the total very high amount of proteins necessarily synthesized by the cell, which could be seen as well in the lowered total amount of GPR17 protein in the *very high* cells, whereas the three remaining cells (*endogenous, low and high*) did not differ significantly in their total GPR17 expression levels, indicating an insufficient protein synthesis in the *very high* cells.

Thus, it was concluded, that three (*endogenous, low and high*) of the four generated cell lines represented appropriate tools to analyze the impact of increasing β-arrestin2 concentrations on GPR17 signaling patterns, whereas the *very high* cells turned out to be not as suitable, due to a

strongly decreased GPR17 expression level, but nevertheless might be a useful device to give some hints about β-arrestin2 influences.

4.2.2 Effect of β-arrestin2 over-expression on RA-II-150-promoted GPR17 endocytosis

Since β-arrestin2 is known for its role in mediating agonist-promoted G protein-coupled receptor trafficking (reviewed by Claing et al. 2002, Ferguson et al. 1996, Luttrell & Lefkowitz 2002), it was the aim to study whether increasing amounts of β-arrestin2 reveal some influence on RA-II-150-induced endocytosis of GPR17. The observation that β-arrestin2 was recruited to the RA-II-150 activated GPR17, revealing a strong and long lasting association (see 4.1.6.2), further highlighted potential influence on GPR17 trafficking.

For that reason colorimetric cell surface ELISA analyses were performed utilizing three of the four generated cell lines stably expressing GPR17-RLuc and differing amounts of β arrestin2 (*endogenous, low and high*), whereas *very high* cells were disregarded due their very low GPR17 expression levels. In agreement with previous results (Figure 49) GPR17-RLuc was internalized from the cell surface following agonist application in all three cell lines. Equilibrium between surface and internalized receptors was reached after 60 min of permanent agonist exposure with the estimated intracellular pool of receptors being around 30%. GPR17 revealed a slightly enhanced endocytosis in *high* cells compared to receptor behavior in *endogenous* cells (32.2 +/- 4.7% ↔ 37.3 +/- 0.8% after 120 min), but this increase, probably caused by coexpression of β-arrestin2, was not significant as computed by two-way ANOVA with Bonferroni's correction for multiple comparisons. Internalization rate determined in *low* cells appeared to be unchanged (31.4 +/- 3.0% after 120 min) in comparison to *endogenous* cells. Nevertheless, it should be regarded that *high* and *low* cells revealed a higher cell surface GPR17 expression than *endogenous*, thus, although the calculated relative internalization rate was not significantly increased, the total amount of internalized receptor, which was not examined, could be potentially even higher, as receptor number needed to obtain similar relative endocytosis needs to be higher when surface expression is higher.

In agreement with expression analyses using colorimetric ELISA analyses (Figure 61), visualization of 3xHA-GPR17 by immunofluorescence microscopy revealed predominant distribution in cytosolic vesicles devoid of agonist application (Figure 62, B). As a consequence, attempts to visualize GPR17 internalization upon agonist-stimulation from cell membrane into the cytosol following receptor stimulation by immunofluorescence microscopy proved unsuccessful, as no clear visible change was detectable (data not shown).

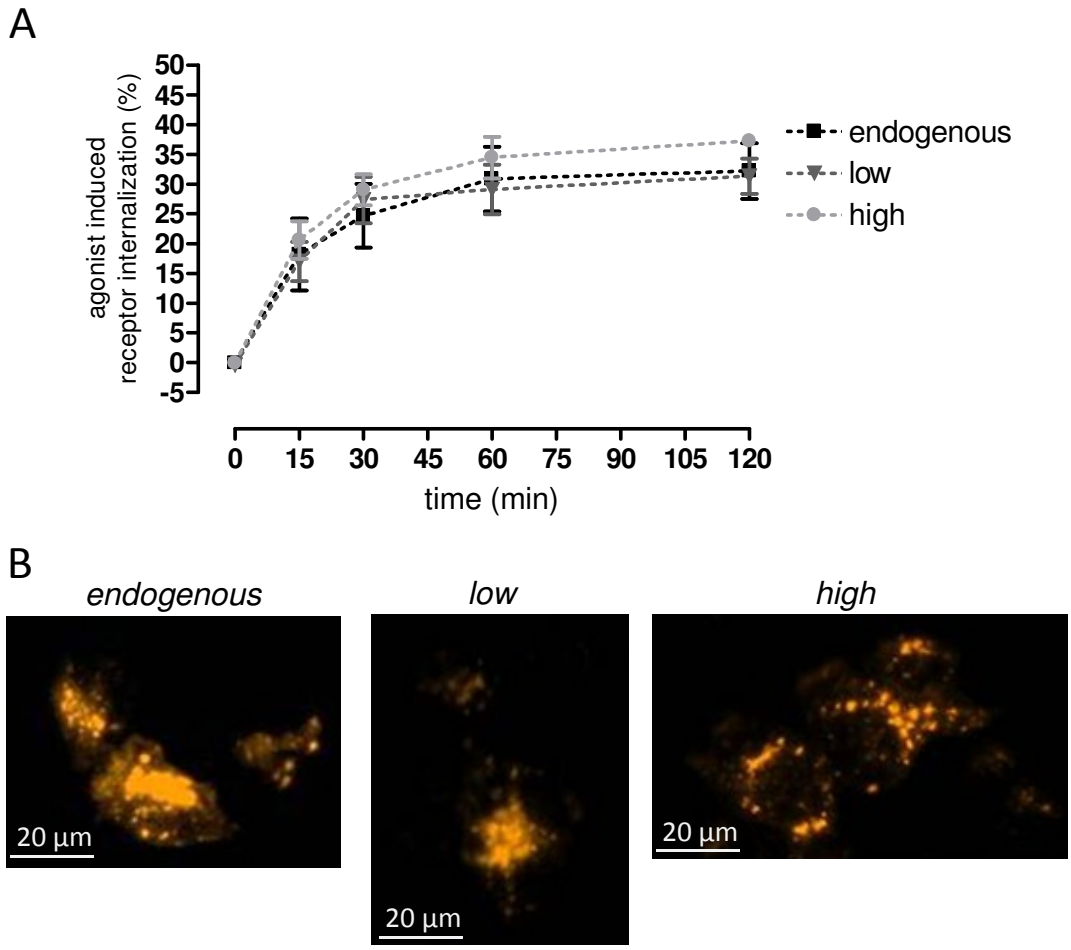

Figure 62 Influence of β-arrestin2 coexpression on agonist-induced GPR17 internalization behavior
A, Colorimetric ELISA measurements of RA-II-150 (10 µM) induced GPR17 sequestration for the indicated time period. The amount of internalized receptor was calculated from the decrease in the level of surface-expressed receptor after agonist treatment compared with untreated, control cells (HEK293). Each data point represents mean (+/- s.e.m.) of three to five independent experiments performed in triplicates. B, Receptor localization was imaged by immunofluorescence microscopy. HEK293 cells stably expressing GPR17-RLuc fused to an N-terminal 3xHA tag were pre-labeled with anti-HA antibody (Table 22, A1), permeabilized with triton X-100 (C52) and immunostained with fluorescence antibody (Alexa Fluor 546 goat anti-mouse IgG, Table 22, A3). The following settings were used for Alexa Fluor 546 recordings: 400 fold magnification, 100 ms exposure time, 0.99 γ and 2-22 histogram. Representative cells from at least three independent experiments are shown. After indirect immunofluorescence staining, no specific fluorescence was observed in untransfected HEK293 cells. Scale bars = 20 µm.

4.2.3 Impact of β-arrestin2 coexpression on GPR17 initiated dynamic mass redistribution upon agonist stimulation

As a first attempt to examine whether the increasing β-arrestin2 levels exhibit some influence on GPR17-mediated signaling, the dynamic mass redistribution (DMR) assay was chosen, since this method enables real time monitoring of the overall agonist-activated receptor signaling outcome.

4.2.3.1 Overall DMR induced by GPR17 is decreased in the presence of elevated β-arrestin2 amounts while potencies are increased

All analyzed cell lines (*endogenous (A), low (B), high (C) and very high (D), see 4.2*) responded with specific optical signatures when exposed to increasing concentrations of GPR17 agonist RA-II-150 (Figure 63). The obtained signature profiles showed a rapid positive DMR event followed by an almost equally fast negative DMR episode, resulting in a spiky elevation, which might be also referred to as a 'Gαi-nose', as they resemble signatures observed for Gαi-coupled receptors in HEK293 cells, such as CRTH2 (Schröder et al. 2009, Schröder et al. 2010). Whereas the *endogenous* cells yielded a slower decreasing plateau after the sharp rise, and at least the highest concentrations (10 and 100 µM) did remain positive after 3600 s, the β-arrestin2 coexpressing cells (*low, high and very high*) showed less of this constant elevated plateau and all signatures were nearly at the basal level after the monitored time (3600 s).

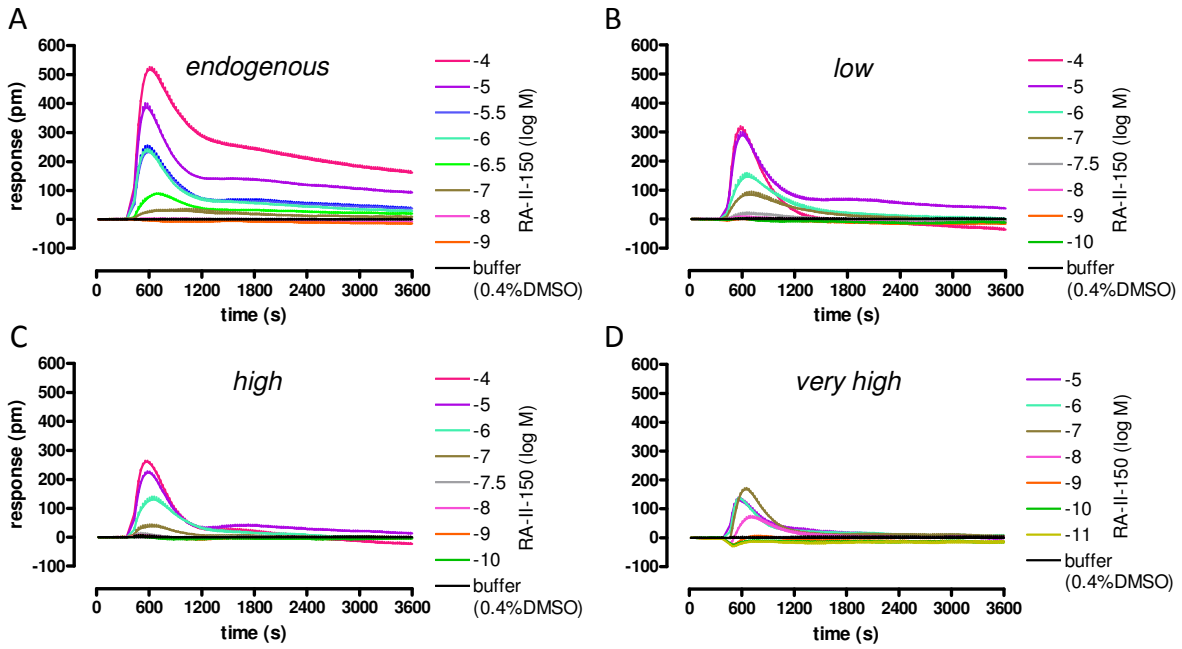

Figure 63 Influence of β-arrestin2 expression levels on GPR17-mediated dynamic mass redistribution optical signatures

HEK293 cells stably expressing GPR17-RLuc (A) and HEK293 cells stably cotransfected with increasing amounts of β-arrestin2-GFP2 (B: low, C: high, D: very high) were challenged with the indicated concentrations of the GPR17 agonist RA-II-150. The resulting picometer-shifts of reflected light wavelength over time [s] were monitored by use of the Epic® system as a measure of functional activity. Presented data are means + s.e.m. from a representative optical trace experiment of three to nine independent experiments performed in triplicates.

Thus, out of these optical signatures it was concluded, that GPR17 retains at least its capability to couple preferentially via Gαi/o-protein in the presence of increasing β-arrestin2 amounts, but additionally some change in signaling was suspected due to the changes of the signature shape.

Even more interesting was the fact, that the optical signatures induced by GPR17-RLuc in HEK293 cells without cotransfection of β-arrestin2 (*endogenous, A*) virtually overtopped all three double stable cell lines (*low (B), high (C) and very high (D)*), despite the fact that the *endogenous* cell line

showed significantly lower cell surface expression than *low* and *high*, respectively (Figure 61). Hence, increasing β-arrestin2 concentrations exhibited a repressive effect on the overall DMR response initiated by RA-II-150-activated GPR17. Only the decreased optical signatures monitored with *very high* cells might be as well diminished due to very low receptor expression levels (Figure 61).

In order to draw further conclusions out of this assay, the optical traces were transformed into concentration-response curves, where maximum response (pm) was plotted against increasing RA-II-150 concentrations (Figure 64, A). In addition, the determined pharmacological parameters (relative efficacy (B) and pEC_{50} (C)) were represented as bar charts for a clear illustration of obtained differences (Figure 64).

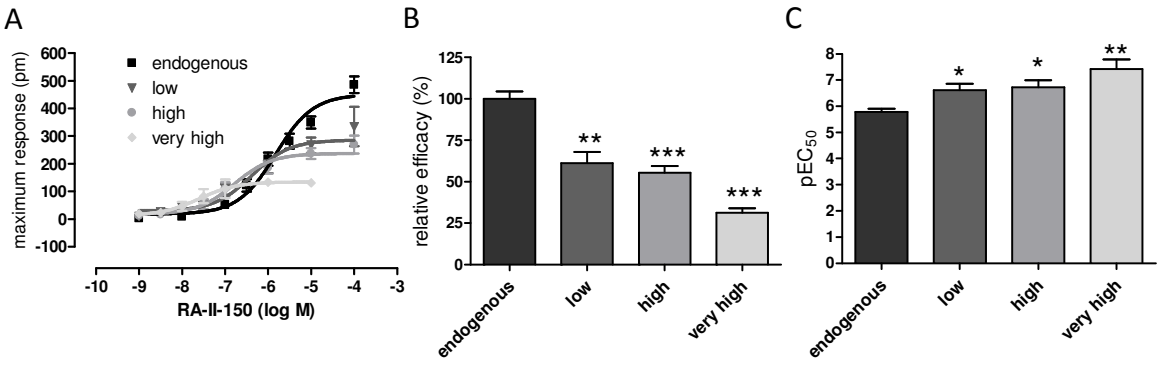

Figure 64 Influence of β-arrestin2 coexpression on RA-II-150-induced concentration-dependent dynamic mass redistribution

A, Comparison of concentration-effect curves resulting from DMR assays of HEK293 cells stably expressing GPR17-RLuc (endogenous) and HEK293 cells stably cotransfected with GPR17-RLuc and increasing β-arrestin2-GFP2 amounts (low, high and very high) challenged with indicated concentrations of GPR17 agonist RA-II-150. Data are presented as maximum response of wavelength shift [pm]. B-C, Bar diagrams derived from concentration-response curves (A) presenting E_{max} (B) and pEC_{50} values (C), respectively. E_{max} values were normalized and expressed as percent of E_{max} determined with *endogenous* cells. For statistical analyses unpaired t-tests with two-tailed p values and 95% confidence interval were applied (*$p < 0.05$, **$p < 0.01$, ***$p < 0.001$). A-C, All data points represent mean (+/- s.e.m.) of three to nine independent experiments performed in triplicates.

Table 41 Parameters of averaged RA-II-150 concentration-effect curves determined by DMR assays, as depicted in Figure 64 (± s.e.m.)

β-arrestin2 level	pEC_{50}	basal value (pm)	E_{max} (pm)	n_H	n
endogenous	5.82 ± 0.09	18.2 ± 13.4	450.3 ± 19.6	1.0 *(fixed)*	5-6
low	6.38 ± 0.18	29.8 ± 12.0	285.5 ± 19.2	1.0 *(fixed)*	3-9
high	6.78 ± 0.16	17.6 ± 11.9	237.3 ± 13.6	1.0 *(fixed)*	3-9
very high	7.61 ± 0.27	12.8 ± 16.2	134.1 ± 12.1	1.0 *(fixed)*	3-4

These data agree very well with the conclusions that were drawn from the optical signatures, especially insofar as the E_{max} value (maximum response) decreases with increasing β-arrestin2 amounts. The relative efficacy obtained with *low* cells was reduced by 38.9% (+/- 6.9%) and *high* cells revealed an even stronger reduction of the maximum overall DMR effect with 44.6% (+/- 4.0). Regarding the fact, that both cell lines (*low* and *high*) were shown to express higher amounts of

GPR17 on the cell surface (Figure 61), one could conclude that similar expression levels would result in even higher reduction of the maximum effect, due to lower receptor densities. Even though *very high* cells revealed the highest repression of the overall response, data need to be taken into account with care, due to the already mentioned low cell surface expression of GPR17 (Figure 61).

In addition to the decreased relative efficacy by coexpression of increasing β-arrestin2 concentrations, another interesting phenomenon was observed, as the concentration-response curves were significantly shifted to the left in the presence of rising β-arrestin2 amounts (Figure 64, A). These mounting pEC_{50} values indicate a rise of the overall RA-II-150 potency mediated by GPR17. The absolute EC_{50} values determined with *low* cells were 3.6 times lower (0.42 µM), and with *high* cells even 8.8 times decreased (0.17 µM) in comparison to the *endogenous* (1.5 µM). The highest potency increase by the factor 75 was determined with *very high* cells (0.02 µM).

In conclusion, these findings indicated that increasing amounts of coexpressed β-arrestin2 caused a diminishment of efficacy but elevation of potency elicited by GPR17-agonist RA-II-150, highlighted by decreased maximum effects and leftward shifts of concentration-response curves.

4.2.3.2 Increased β-arrestin2 expression levels enhance pertussis toxin sensitivity of GPR17 initiated DMR

Besides the unmodified real time monitoring of GPR17-induced dynamic mass redistribution upon agonist stimulation, the influence of PTX-pretreatment was examined to uncover whether β-arrestin2 coexpression shows additional effects on GPR17-induced signaling, independent of the Gαi/o-mediated cascades.

Therefore, HEK293 cells stably expressing GPR17-RLuc and differing β-arrestin2 concentrations (*low, high* and *very high*) were preincubated with the Gαi/o inhibitor pertussis toxin (PTX, 50 ng/ml, 18 h) prior to DMR analyses. As shown in Figure 65, stimulation of the cells with increasing RA-II-150 concentrations revealed optical signatures, which were similar in shape, but partly obliterated in comparison to the untreated investigations (Figure 63), thus establishing an essential role for Gαi/o-proteins in GPR17 response, which is in agreement with the previously determined signaling patterns of GPR17. Nevertheless, a difference between the four analyzed cell lines was detectable, as PTX-sensitivity increased with increasing amounts of β-arrestin2 concentrations, mounting in an almost complete abrogation of DMR response in *very high* cells. Hence, coexpression of increasing β-arrestin2 concentrations seemed to shift G protein-coupling preferences from dual coupling (Gαi/o and Gαq) to interaction with a single G protein (Gαi/o).

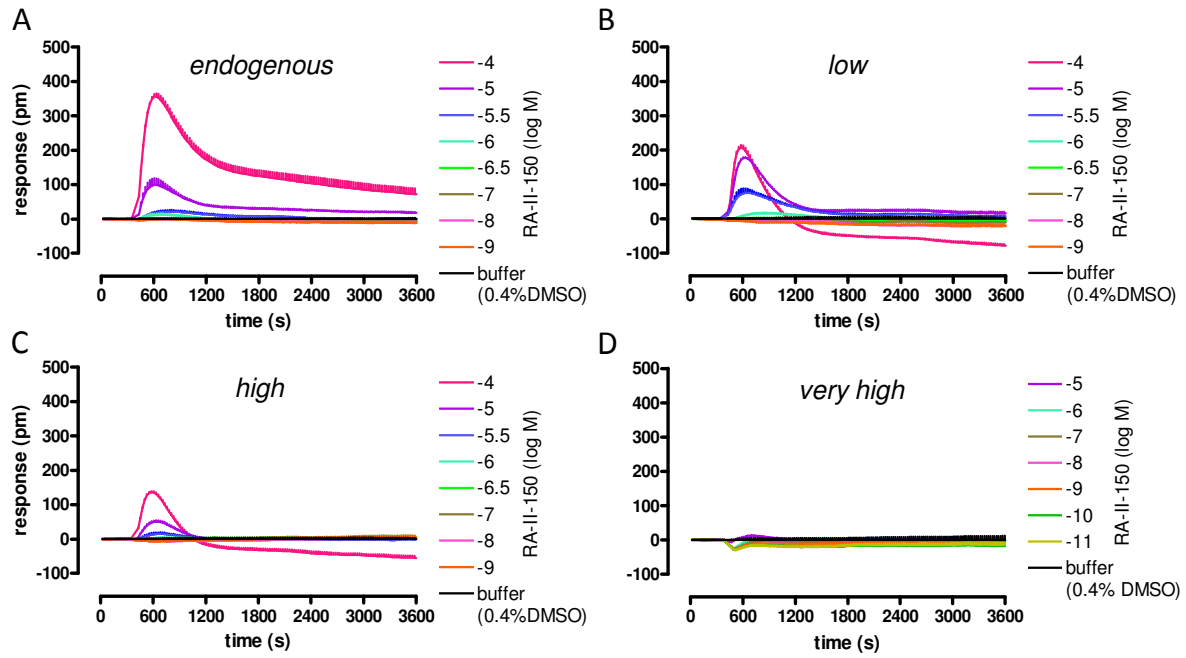

Figure 65 Influence of β-arrestin2 expression levels on GPR17-mediated dynamic mass redistribution optical signatures in the presence of Gαi/o inhibitor PTX

HEK293 cells stably expressing GPR17-RLuc (A) and HEK293 cells stably cotransfected with increasing amounts of β-arrestin2-GFP2 (B: low, C: high, D: very high) were challenged with the indicated concentrations of the GPR17 agonist RA-II-150 in presence of the Gαi/o inhibitor PTX (50 ng/ml, 18 h). The resulting picometer-shifts of reflected light wavelength over time [s] were monitored by use of the Epic® system as a measure of functional activity. Presented data are means + s.e.m. from a representative optical trace experiment of three to six independent experiments performed in triplicates.

When data were transformed into concentration-response curves (Figure 66, A), the potencies of all four cell lines did not differ significantly, in contrast to the previously monitored values without PTX pretreatment (Figure 64, A). This observable fact was further demonstrated by the bar charts, in which calculated pEC_{50} values were plotted against the respective cell line, clearly highlighting that the significant differences between pEC_{50} values were not present anymore. The pharmacological parameters are summarized in Table 42.

The already mentioned capability of elevated β-arrestin2 levels to decrease the maximum effect of overall DMR response, despite the fact that *endogenous* cells revealed lower receptor surface expression levels (Figure 61), was still present when cells were preincubated with PTX (Figure 66, B). The coexpression of *low* amounts of β-arrestin2 yielded in a 2 times lower relative efficacy (46.3 +/- 9.1%), whereas *high* amounts resulted even in a 3 fold decrease (31.1 +/- 4.8%). The 10 times lower E_{max} value (10.5 +/- 1.8%) monitored with *very high* cells should be again regarded with care, due to the previously mentioned low receptor surface expression (Figure 61).

To summarize these DMR investigations using Gαi/o inhibitor PTX, maximum responses were decreased due to increasing β-arrestin2 concentrations, whereas potencies of RA-II-150 remained comparable and did not differ significantly between all four analyzed cell lines.

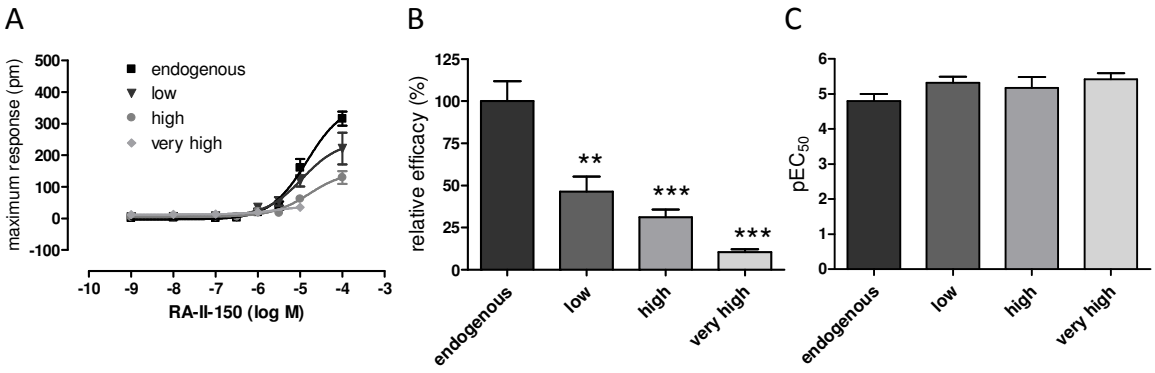

Figure 66 Influence of β-arrestin2 coexpression on RA-II-150-induced concentration-dependent dynamic mass redistribution in the presence of Gαi/o inhibitor PTX

Concentration-effect curves transformed from DMR assays of HEK-293 cells stably expressing GPR17-RLuc (endogenous) and HEK293 cells stably cotransfected with GPR17-RLuc and increasing β-arrestin2-GFP2 amounts (low, high and very high) challenged with indicated concentrations of GPR17 agonist RA-II-150. Cells were preincubated with Gαi/o inhibitor PTX (50 ng/ml, 18 h) A, Data are presented as maximum response of wavelength shift [pm] and all data points represent mean (+/- s.e.m.) of three to six independent experiments performed in triplicates. B-C, Bar charts derived from concentration-response curves (A) presenting E_{max} (B) and pEC_{50} values (C), respectively. C, E_{max} values were normalized and expressed as percent of E_{max} determined with *endogenous* cells. For statistical analyses unpaired t-tests with two-tailed p values and 95% confidence interval were applied (**p < 0.01; ***p < 0.001).

Table 42 Parameters of averaged RA-II-150 concentration-effect curves determined by DMR assays, as depicted in Figure 66, A (± s.e.m.)

β-arrestin level	pEC_{50}	basal value (pm)	E_{max} (%)	n_H	n
endogenous	4.84 ± 0.09	-3.7 ± 6.5	363.6 ± 20.6	1.0 *(fixed)*	5-6
low	4.96 ± 0.13	5.7 ± 6.5	244.4 ± 23.3	1.0 *(fixed)*	3-6
high	4.79 ± 0.12	5.2 ± 3.2	149.7 ± 13.6	1.0 *(fixed)*	3-6
very high	5.52 ± 0.52	12.1 ± 2.4	41.4 ± 10.5	1.0 *(fixed)*	3

4.2.3.2.1 Coexpression of β-arrestin2 reveals different impacts on GPR17-mediated signaling depending on available Gα-proteins

In order to gain a better insight into the effects of β-arrestin2 coexpression on GPR17-initiated optical signatures, pharmacological parameters (pEC_{50}, relative efficacy) determined by DMR assays (4.2.3.1, 4.2.3.2) were summarized, so that differences monitored between unmodified and PTX pretreated cells are clearly highlighted.

Obviously, as presented in Figure 67 (A), the significantly enhanced potencies, caused by increasing amounts of β-arrestin2 concentrations, determined with unmodified cells (w/o), were completely abolished when preincubated with PTX, resulting in lowered potencies with increasing significance between calculated pEC_{50} values of one cell line. Consequently, these investigations indicated that differences of determined potencies caused by increasing β-arrestin2 concentrations were mainly due to Gαi/o-protein-mediated signaling events, establishing an essential role for Gαi/o proteins concerning this phenomenon.

Furthermore, as depicted Figure 67 (B), the relative repression of GPR17-induced DMR was even stronger after elimination of Gαi/o-mediated signaling. Especially regarding the *high* cells, where relative efficacy was more than half (55.4 +/- 4.0%) without pretreatment, but by preincubation with PTX the repression was even stronger (31.1 +/- 4.8%). Thus, indicating a relatively higher PTX sensitivity of GPR17-mediated signaling when coexpressed with increasing β-arrestin2-concentrations.

These observations suggested that the preference of G protein-coupling seems to be shifted to the most preferred one, which was previously determined to be the Gαi/o-protein for GPR17.

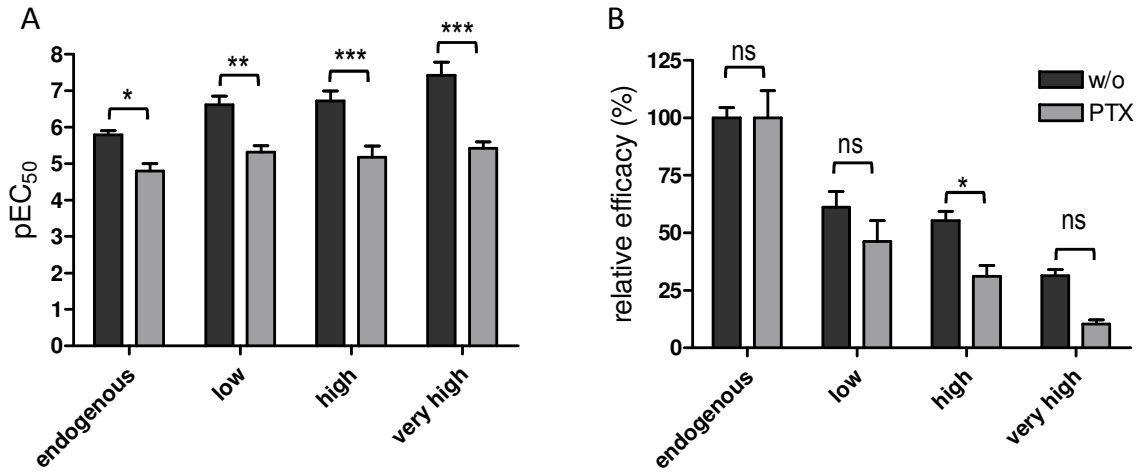

Figure 67 Summary and comparison of pharmacological parameters pEC_{50} and E_{max} determined by DMR assays in HEK293 cells stably expressing GPR17-RLuc and varying amounts of β-arrestin2

Bar charts derived from concentration-response curves (Figure 64, Figure 66) comparing pEC_{50} (A) and E_{max} values (B), respectively, determined in the absence (w/o) or presence of PTX pretreatment (PTX, 50 ng/ml, 18 h) by RA-II-150 stimulation of HEK293 cells stably expressing GPR17-RLuc and increasing amounts of β-arrestin2 (*endogenous, low, high and very high*). B, E_{max} values were normalized and expressed as percent of E_{max} determined with *endogenous* cells. For statistical analyses two-way ANOVA with Bonferroni's correction for multiple comparisons was applied (ns $p > 0.05$, *$p < 0.05$, **$p < 0.01$, ***$p < 0.001$). A-C, All data are means (+/- s.e.m.) of three to nine experiments performed in triplicates.

4.2.4 Coexpression of β-arrestin2 induces enhanced potency but decreased efficacy of GPR17-induced inhibition of cAMP accumulation

Since DMR assays revealed that coexpression of increasing β-arrestin2 amounts causes changes in GPR17-mediated signaling, especially highlighting the essential role of Gαi/o-mediated events, it was the next aim to determine whether this hypothesis can be further confirmed by means of cAMP inhibition assays.

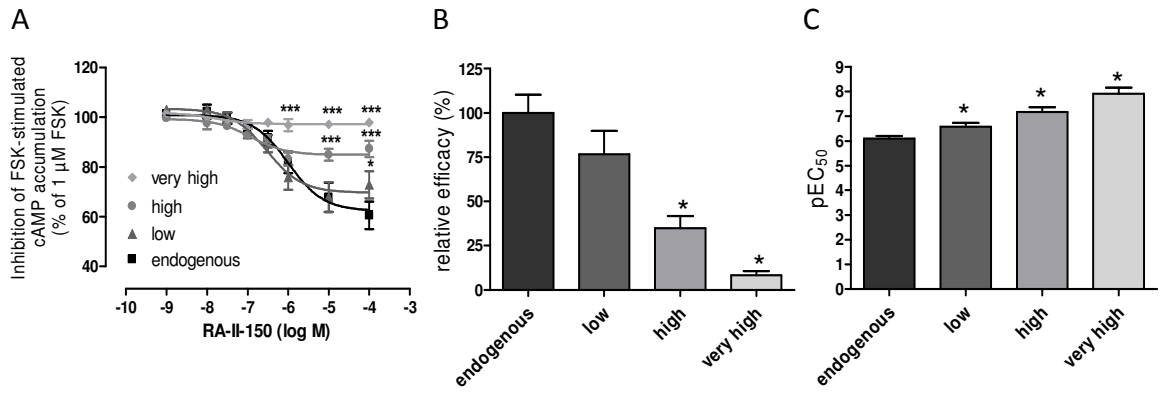

Figure 68 Influence of increasing β-arrestin2 coexpression levels on GPR17-mediated inhibition of cAMP accumulation

A, HEK293 cells stably expressing GPR17 C-terminally fused to Renilla luciferase in the absence (endogenous) or presence of varying amounts of β-arrestin2 coexpression N-terminally fused to GFP2 (*low, high* and *very high*) were stimulated with increasing concentrations of RA-II-150 in the presence of 1 µM forskolin (FSK). GPR17-mediated decrease of intracellular cAMP was calculated as percent inhibition of adenylate cyclase stimulated with FSK (1 µM). For statistical analyses, individual concentrations were compared by two-way ANOVA with Bonferroni's correction for multiple comparisons (*$p < 0.05$, ***$p < 0.001$). B-C, Bar charts derived from concentration-response curves (A) presenting E_{max} (B) and pEC_{50} values (C), respectively. B, E_{max} values were normalized and expressed as percent of E_{max} determined with *endogenous* cells. B-C, For statistical analyses paired t-tests with two-tailed p values and 95% confidence interval were applied (*$p < 0.05$).A-C, All data are means (+/- s.e.m.) of three to four experiments performed in triplicates.

Table 43 Parameters of averaged RA-II-150 concentration-effect curves determined by cAMP assays, as depicted in Figure 68 (± s.e.m.)

β-arrestin2 level	pEC_{50}	top value (%)	bottom value E_{max} (%)	n_H	n
endogenous	6.00 ± 0.16	100.9 ± 1.8	62.4 ± 3.0	1.0 *(fixed)*	3-4
low	6.53 ± 0.19	103.4 ± 2.3	69.7 ± 2.5	1.0 *(fixed)*	3-4
high	6.92 ± 0.25	99.3 ± 1.6	84.9 ± 1.4	1.0 *(fixed)*	3-4
very high	7.82 ± 0.53	101.9 ± 1.5	97.2 ± 0.6	1.0 *(fixed)*	3-4

Therefore concentration-dependent effects of RA-II-150 on forskolin-induced cAMP accumulation were analyzed in parallel in all four cell lines, stably coexpressing GPR17-RLuc and increasing β-arrestin2 amounts (*endogenous, low, high and very high*). In agreement with the previously stated hypothesis, elevated amounts of β-arrestin2 exhibited a strong impact on GPR17-initiated Gαi/o-signaling (Figure 68). Concentration-effect curves (A) were clearly distinguishable amongst each other, in relation to maximum effects as well as potencies. Similar to the data obtained from DMR assays, the relative efficacy (B) was depressed along *endogenous* to *very high* cells. *Low* cells gave rise to 76.6 +/- 13.2% and *high* cells induced 35.0 +/- 6.7%, presented as percent of E_{max} determined with endogenous cells (100.1 +/- 10.3%). The lack of response from very high cells (8.1 +/- 2.5%) needs to be regarded again with care, due to low GPR17 surface expression (Figure 61). Additionally, pEC_{50} values were significantly increased with rising β-arrestin2 amounts (Figure 68, C), yielding comparable potencies as determined with the Epic® system.

Thus, investigations of Gαi/o-mediated signaling by cAMP analyses provided further evidence, that coexpression of increasing β-arrestin2 amounts exhibits alterations of GPR17-initiated signaling, since maximum effects were depressed while potencies were increased.

4.2.5 Increased β-arrestin2 quantities diminish GPR17 mediated IP-One accumulation

In order to further prove the previously observed findings, the impact of β-arrestin2 on GPR17-induced IP1 accumulation was investigated. Therefore, all four stably generated HEK-GPR17 cell lines (*endogenous, low, high and very high*) were challenged with increasing concentrations of RA-II-150. Elevated IP1 concentrations were expressed as arbitrary units and corrected by respective basal values to facilitate comparison of CRCs.

Interestingly, the presence of augmented β arrestin2 amounts exhibited a strong impairment on GPR17-initiated IP1 accumulation, as depicted in Figure 69 (A). Whereas in *endogenous* cells stimulation with RA-II-150 yielded a concentration-dependent IP1 elevation, the challenge of β-arrestin2-coexpressing cells (*low, high and very high*) almost completely impaired IP1 detection. In fact, only the highest applied RA-II-150 concentration (100 µM) induced an increase of IP1 level above basal, making it impossible to compute appropriate CRCs. These results may reflect insufficient Gαq protein-coupling due to an increased desensitization rate caused by the elevated β-arrestin2 amounts. Consequently, to possibly increase or sensitize the Gαq-coupled signaling events, the simultaneously occurring and potentially competing Gαi/o-mediated signaling and subsequent desensitization was interrupted by preincubation with the Gαi/o-inhibitor pertussis toxin (PTX, 50 ng/ml, 18 h). Interestingly, the preincubation with PTX enhanced RA-II-150-promoted IP1-accumulation in cells over-expressing GPR17 and distinct β-arrestin2 amounts (*low, high and very high*), whereas CRC determined in HEK-GPR17 cells with *endogenous* β-arrestin levels did not reveal significant changes (Figure 69, B), neither in potency (pEC_{50}) nor in efficacy (E_{max}) (summarized in Table 44). These findings additionally highlighted that IP1-accumulation occurred independently of Gαi/o proteins. Furthermore, CRCs determined in PTX-pretreated cells (*endogenous, low and high*) did not differ significantly from each other, which was in agreement with data observed with the Epic® system (Figure 66). Additionally it should be noted, that almost no response was observable with *very high* cells (Figure 69), even preincubation with PTX only slightly increased GPR17-induced IP1-accumulation, but due to high variations no significant and reliable CRCs could be computed. The lack of response might correlate with *very high* amounts of β-arrestin2 inducing an amplified desensitization rate, but likewise be due to very low GPR17-expression levels observed in this cell line (Figure 61). The latter would be in agreement with findings observed using the Epic® system (Figure 65, D), as pretreatment with PTX fully obliterated RA-II-150-induced DMR in *very high* cells, thus establishing an essential if not exclusive role for Gαi/o proteins in GPR17 response examined in this cell line.

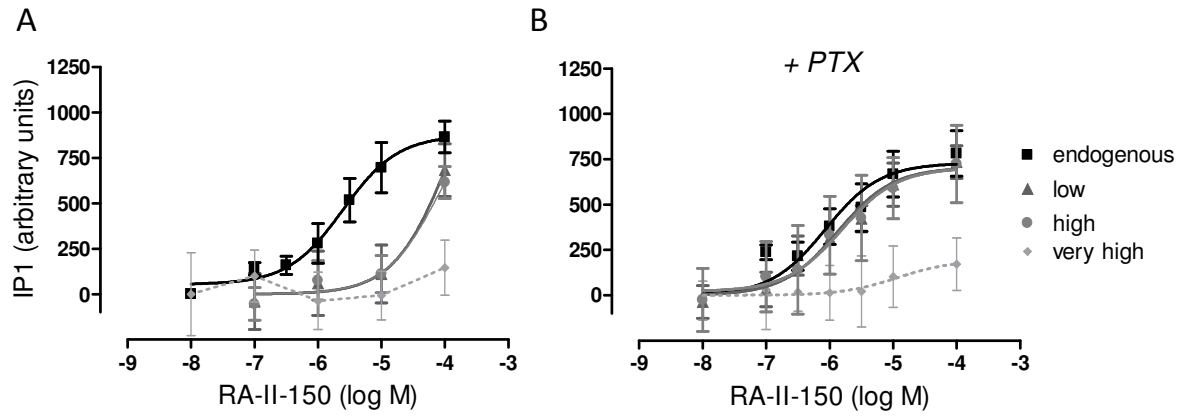

Figure 69 Increased amounts of β-arrestin impair GPR17-induced IP1 accumulation

A-B, HEK293 cells stably expressing GPR17 C-terminally fused to Renilla luciferase in the absence (endogenous) or presence of increasing amounts of β-arrestin2 N-terminally fused to GFP2 (*low, high* and *very high*) were challenged with increasing concentrations of RA-II-150, in the absence (A) or presence (B) of PTX (50 ng/ml, 18 h). GPR17-mediated increase of intracellular IP1 was expressed as arbitrary units and corrected for baseline values obtained with buffer. All data are means (+/- s.e.m.) of three to ten experiments performed in duplicates and triplicates, respectively.

Table 44 Parameters of averaged RA-II-150 concentration-effect curves determined by IP1 assays, as depicted in Figure 69 (± s.e.m.)

β-arrestin2 level	pEC_{50}	bottom value (arbitrary units)	top value (arbitrary units)	n_H	n
endogenous	5.61 ± 0.20	53.7 ± 57.6	875.2 ± 82.6	1.0 *(fixed)*	3-7
endogenous + PTX	6.07 ± 0.30	0.51 ± 95.4	729.4 ± 89.5	1.0 *(fixed)*	3
low	3.93 ± 1.92	0.1 ± 118.9	-	1.0 *(fixed)*	4-10
low + PTX	6.53 ± 0.19	0.1 ± 66.2	705.2 ± 74.8	1.0 *(fixed)*	4
high	4.06 ± 1.04	0.1 ± 74.0	-	1.0 *(fixed)*	3-4
high + PTX	6.92 ± 0.25	0.1 ± 144.4	695.5 ± 163.3	1.0 *(fixed)*	3
very high	-	11.5 ± 95.5	-	-	3-4
very high + PTX	4.94 ± 1.68	0.5 ± 79.8	194.1 ± 202.2	1.0 *(fixed)*	3

Taken together, presence of increasing β-arrestin2 amounts diminishes GPR17-mediated IP1-accumulation, probably caused by an elevated desensitization rate initiated by the simultaneously occurring and possibly preferred Gαi/o-mediated signaling, as elimination of this pathway reversed the observed phenomenon resulting in comparable CRC.

4.3 Analyses of potential GPR17 antagonists

Due to the claimed physiological role of GPR17 (see 1.5.3.2), the development of specific antagonists would have a therapeutic value to prevent cell death in stroke/ischemia as well as to restore deficits in myelination. GPR17 activation has been shown to be counteracted by treatment with already marketed 'specific' CysLT1 receptor antagonists pranlukast and montelukast (Ciana et al. 2006, Fumagalli et al. 2011, Lecca et al. 2008, Pugliese et al. 2009).

Since the inhibition properties of the published CysLT1 receptor antagonists have been analyzed based on LTD4-activated GPR17 signaling, mainly in recombinant 1321N1 cells (Ciana et al. 2006, Lecca et al. 2008, Pugliese et al. 2009) as well as in native OPCs (Fumagalli et al. 2011), it was the aim to examine the antagonistic properties with regard to GPR17 activation by our small molecule agonist RA-II-150. Therefore a set of various functional assays were performed by application of recombinant CHO cells engineered to stably express GPR17. Additionally, HEK293 cells stably coexpressing GPR17 C-terminally fused to Renilla luciferase (GPR17-RLuc) and β-arrestin2 N-terminally labeled with green fluorescent protein 2 (GFP2) were utilized for analyses of β-arrestin2 recruitment.

4.3.1 Preliminary screening of cysteinyl leukotriene receptor antagonists as inhibitors for GPR17-initiated signaling

Initially, the two published antagonists (montelukast, pranlukast) and two additional potent CysLT1 receptor inhibitors (zafirlukast, MK571) were investigated to determine the compound with the most promising antagonistic potencies on RA-II-150-activated GPR17 signaling.

4.3.1.1 Investigation of antagonistic properties by Epic® DMR technology

As a first attempt, the inhibiting properties of pranlukast, montelukast and zafirlukast on GPR17 functionality were studied by the holistic dynamic mass redistribution technology.

GPR17-expressing CHO cells were preincubated with the indicated antagonist for 60 min prior to stimulation with RA-II-150 (3 µM). As depicted in Figure 70, all three tested antagonists (pranlukast (A), montelukast (B) and zafirlukast (C)) diminished the agonist-induced optical signatures in a more or less concentration-dependent manner. Especially pranlukast counteracted GPR17-triggered DMR in a highly significant way; resulting in an almost complete inhibition with the highest applied concentration (30 µM). Results from four to twelve independent DMR experiments were summarized as bar charts (Figure 70, D) that clearly highlight pranlukast as the most promising GPR17 antagonist, whereas data obtained with montelukast were not consistent with previous published data (Ciana et al. 2006), as almost no constant inhibition was detectable. Zafirlukast, whose antagonistic potencies regarding GPR17 have not been investigated before, as well revealed significant and concentration-dependent repression of the optical signatures, but not as strong as pranlukast and furthermore with higher variations. Consequently, the following rank order based on maximum percent inhibition of

GPR17-induced DMR was determined: pranlukast (86.5 +/- 5.5%) > zafirlukast (43.1 +/- 18.3%) > montelukast (30.3 +/- 16.1%).

Taken together, DMR technology uncovered pranlukast as the most potent GPR17-antagonist amongst the three analyzed CysLT1 receptor antagonists.

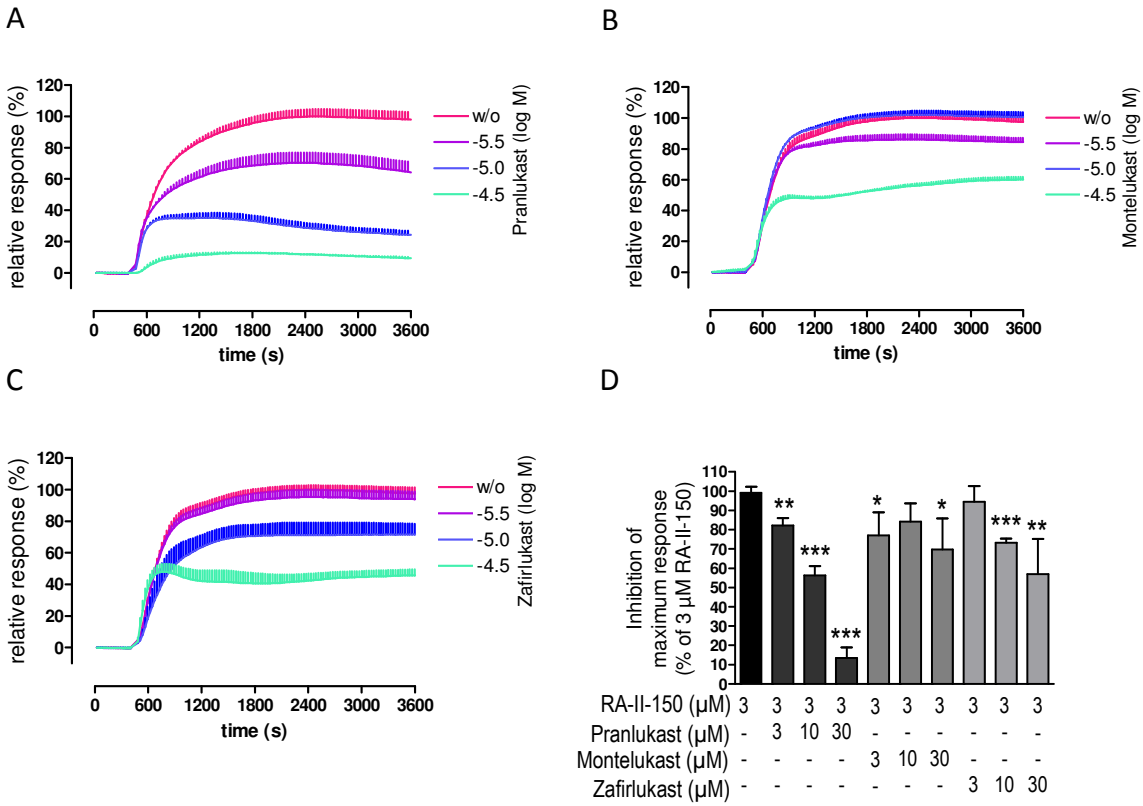

Figure 70 Inhibition effects of cysteinyl leukotriene receptor antagonists on GPR17-induced dynamic mass redistribution upon stimulation with 3 µM RA-II-150

A-C, CHO cells stably expressing GPR17 were challenged with 3 µM RA-II-150 in absence (w/o) and presence of the indicated cysteinyl leukotriene receptor antagonist (pranlukast (A), montelukast (B) and zafirlukast (C)). Cells were preincubated with antagonists for 60 min at 28°C. Agonist-induced relative wavelength shift [%] over time [s] was monitored as a measure of functional activity. Responses were normalized and expressed as percent of wavelength shift induced by 3 µM RA-II-150 determined in the absence of antagonist (w/o). Signatures were baseline-corrected by subtraction of buffer traces from the DMR response after receptor activation. Representative optical trace experiment (mean + s.e.m.) of at least four independent experiments performed in triplicates. D, Bar chart representing summarized DMR analyses normalized and expressed as percent of wavelength shift induced by 3 µM RA-II-150 determined in the absence of antagonist. For statistical analyses unpaired t-tests with two-tailed p values and 95% confidence interval were applied (*$p < 0.05$, **$p < 0.01$, ***$p < 0.001$). A-C, All data are means (+/- s.e.m.) of four to twelve independent experiments performed in triplicates.

4.3.1.2 Evaluation of inhibition effects on IP-One accumulation

In order to further confirm the results obtained by DMR analyses, a classical second messenger assay was chosen to evaluate the antagonistic impact on GPR17-induced elevation of intracellular IP1 accumulation. Additionally, the effect of MK571 as a fourth CysLT1 receptor antagonist was examined.

First of all, the four antagonists, pranlukast, montelukast, zafirlukast and MK571 were tested for their agonistic effects in GPR17-expressing CHO cells (Figure 71, A). Whereas pranlukast and montelukast were devoid of any significant agonist effect, zafirlukast and MK571 revealed some increase of the basal intracellular IP1 concentration, although it was shown to be non significant ($p > 0.05$, unpaired t-tests with two-tailed p values and 95% confidence interval). Functionality of GPR17 was proven by application of RA-II-150, which significantly increased the basal IP1 level.

Preincubation (30 min, 37°C) of GPR17-expressing CHO cells with the four potential GPR17 antagonists, followed by a subsequent stimulation with RA-II-150 (0.3 µM), uncovered pranlukast once more as the most potent antagonist. As depicted in Figure 71 (B), pranlukast caused a complete inhibition of GPR17-induced IP1 accumulation, whereas MK571, zafirlukast and montelukast exhibited only partial effects, resulting in the following potency rank order, based on maximum percent inhibition of GPR17-induced IP1 synthesis: pranlukast (105.0 +/- 3.9%) > MK571 (57.8 +/- 11.2%) > zafirlukast (51.3 +/- 18.4%) > montelukast (16.5 +/- 6.3%). Thus again, montelukast, which has been published several times as a potent GPR17 antagonist with an IC_{50} value in the nanomolar range counteracting LTD4-induced responses (Ciana et al. 2006, Fumagalli et al. 2011, Lecca et al. 2008), surprisingly showed the worst inhibition properties amongst the four analyzed antagonists.

In agreement with previous observations, pranlukast was uncovered as the most potent and most promising GPR17-antagonist and was therefore chosen for further examinations.

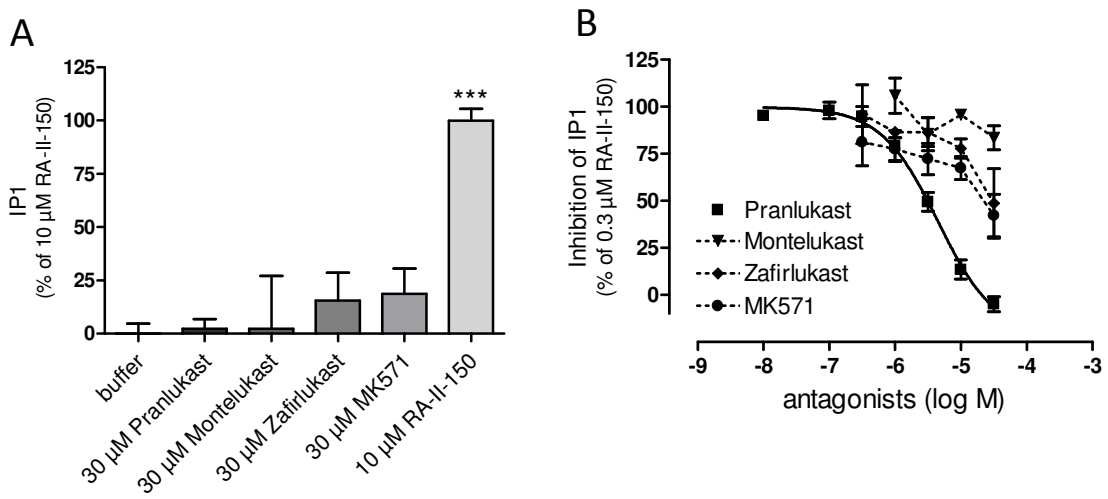

Figure 71 Agonistic and antagonistic effects of cysteinyl leukotriene receptor antagonists analyzed by IP1 assays using GPR17-expressing CHO cells

A, CHO cells stably expressing GPR17 were stimulated with cysteinyl leukotriene receptor antagonists and GPR17 agonist RA-II-150. Increase of intracellular IP1 was normalized and expressed as percent of maximum activation induced by RA-II-150 (10 µM). For statistical analyses unpaired t-tests with two-tailed p values and 95% confidence interval were applied (***$p < 0.001$). B, Concentration-dependent inhibition by cysteinyl leukotriene receptor antagonists of the IP1 accumulation in CHO cells stably expressing GPR17 stimulated by 0.3 µM RA-II-150. Cells were preincubated with antagonists for 30 min at 37°C. Data were expressed as percent of IP1 levels induced by 0.3 µM in the absence of an antagonist. A-B, All data are means (+/- s.e.m.) of three to six independent experiments performed in duplicates.

4.3.2 Pranlukast exhibits biased partial agonistic properties at GPR17

Subsequent to preliminary screening analyses of cysteinyl leukotriene receptor antagonists, which uncovered pranlukast as the most suitable compound to diminish RA-II-150-induced GPR17 signaling, it was the next aim to examine the agonistic properties of pranlukast in order to determine whether pranlukast acts as a pure neutral antagonist, as an inverse agonist or even as a partial agonist. Therefore the effects of pranlukast on cells (CHO and HEK293 cells) stably expressing GPR17 were investigated by means of distinct functional assays.

4.3.2.1 Detection of the agonistic nature via DMR technology

As a first attempt the effect of pranlukast at GPR17 was examined in real time by use of the Epic® system, in order to directly measure the complete cell response. Stimulation of CHO cells stably expressing GPR17 with increasing pranlukast concentrations (3, 10 and 30 µM) elicited dynamic mass redistribution (Figure 72, A) in a concentration-dependent manner, highlighting an agonistic effect of pranlukast at GPR17. Interestingly, preincubation with the Gαi/o inhibitor PTX (50 ng/ml, 18 h) partially diminished pranlukast-induced optical signatures, indicating the involvement of Gαi/o-protein-mediated signaling cascades. To further illustrate this phenomenon, a theoretical DMR signature plot was calculated by subtraction of the data obtained in the presence of PTX from the data determined in the absence of PTX. Since the signatures elicited in the presence of PTX represent every DMR event except for Gαi/o-protein-mediated signaling, subtraction of the overall response represents DMR triggered by Gαi/o-proteins. The theoretical optical signatures, as presented in Figure 72 (B), clearly reveal concentration-dependent DMR induced by pranlukast via Gαi/o-protein.

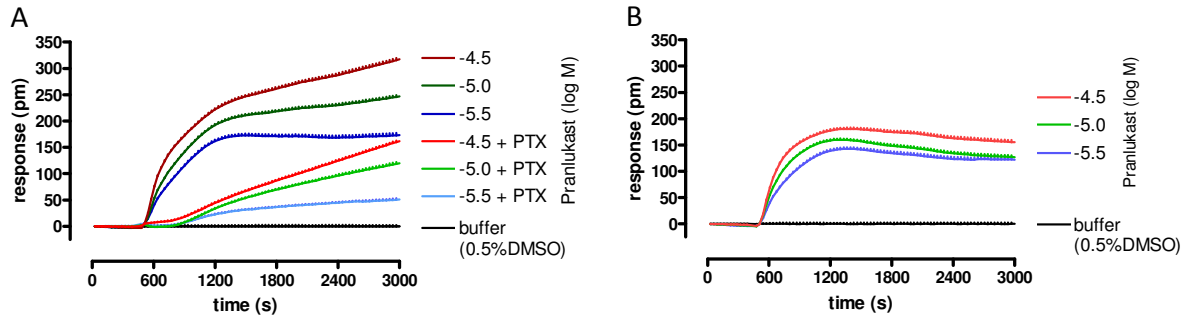

Figure 72 Pranlukast-induced optical DMR signatures on CHO cells stably expressing GPR17 reveal PTX sensitivity

A, CHO cells stably expressing GPR17 were challenged with the indicated concentrations of pranlukast in the absence and presence of Gαi/o inhibitor PTX (50 ng/ml, 18 h). Wavelength shift [pm] over time [s] was monitored as a measure of functional activity. Signatures were baseline-corrected by subtraction of buffer traces from the DMR response after receptor activation. Representative optical trace experiment (mean + s.e.m.) of at least three independent experiments performed in triplicates. B, Theoretical DMR optical signatures determined by subtraction of data obtained in the presence of PTX from data obtained without pretreatment, thus representing the theoretical signature elicited by Gαi/o protein.

In order to ensure that DMR elicited by pranlukast in GPR17-expressing CHO cells was specific due to activation of GPR17, untransfected CHO-K1 cells were stimulated with pranlukast (3 µM (A), 10 µM (B) and 30 µM (C)) and monitored by DMR technology. CHO-GPR17 cells were analyzed in parallel, both in the absence and presence of PTX. Unfortunately, pranlukast additionally induced DMR in

untransfected CHO-K1 cells, but obviously with a smaller extent than in GPR17-expressing cells, thus confirming at least a partial GPR17-mediated effect (Figure 73). In contrary to GPR17-expressing cells, optical signatures monitored in CHO-K1 cells were not influenced by preincubation with PTX, indicating an independence of Gαi/o-mediated signaling. Interestingly, the shapes of the optical signatures elicited by pranlukast in CHO-K1 cells resembled the ones obtained in CHO-GPR17 cells in the presence of PTX (Figure 73, A-C).

These investigations demonstrate that DMR induced by pranlukast in CHO-GPR17 cells is partly due to activation of Gαi/o-protein-mediated signaling through stimulation of GPR17, whereas the remaining part of the overall DMR response is caused by some unspecific, PTX-resistant events, which similarly appear in untransfected CHO-K1 cells. This conclusion further suggests that stimulation of GPR17 with pranlukast only activates the Gαi/o-mediated pathway, although the receptor has been shown to mediate promiscuous G protein-coupling, including Gαi/o, Gαs and Gαq proteins (see 4.1.1), thus pranlukast seems to act as a biased ligand at GPR17.

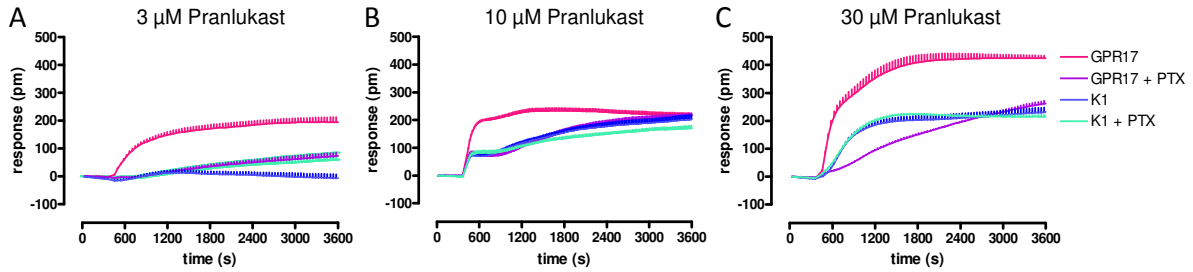

Figure 73 Comparison of optical DMR signatures elicited by pranlukast in untransfected CHO-K1 and CHO cells stably expressing GPR17

Untransfected CHO-K1 (K1) and CHO cells stably expressing GPR17 were challenged with increasing pranlukast concentrations (3 µM (A), 10 µM (B), 30 µM (C) in the absence and presence of Gαi/o inhibitor PTX (50 ng/ml, 18 h). Wavelength shift [pm] over time [s] was monitored by use of the Epic® system as a measure of functional activity. Signatures were baseline-corrected by subtraction of buffer traces from the DMR response after receptor activation. Representative optical trace experiment (mean + s.e.m.) of at least three independent experiments performed in triplicates

4.3.2.2 Pranlukast partially inhibits forskolin-induced cAMP synthesis

To further probe the assumption that pranlukast acts as a biased agonist at GPR17 via Gαi/o-coupling, its inhibition effect on forskolin-stimulated cAMP accumulation was investigated using a traditional cAMP assay. Therefore GPR17-expressing CHO cells as well as HEK-BRET-GPR17 cells *(= HEK293 cells stably cotransfected with GPR17 C-terminally fused to Renilla luciferase and β-arrestin2 N-terminally labeled with GFP2*) were challenged with increasing pranlukast concentrations in the presence of 10 µM forskolin. In agreement with previous hypothesis, pranlukast induced a concentration-dependent inhibition of forskolin-stimulated adenylate cyclase (Figure 74), even though not with the same extent as the full agonist RA-II-150. Inhibition of cAMP accumulation was expressed as percentage inhibition of adenylate cyclase stimulated with forskolin (10 µM). E_{max} and potency values are summarized in Table 45. In CHO cells (A) efficacy of pranlukast yielded approximately one third (35.2 +/- 3.8%), whereas in HEK293 cells efficacy was reduced by half (9.3 +/- 1.2%) relative to RA-II-150 (28.3 +/- 1.0%). Furthermore, indicated by rightward shifts of

CRCs, potency of pranlukast was reduced in both cell lines, 185-fold less potent in CHOs (absolute EC_{50} values 3.72 µM ↔ 0.02 µM) and 40-fold less potent in HEKs (absolute EC_{50} values 2.40 µM ↔ 0.06 µM). Whereas pranlukast exhibited slightly higher potency in HEK-BRET-GPR17 cells, RA-II-150 was more potent in CHO-GPR17 cells.

Taken together, these observations uncovered pranlukast as a partial agonist with decreased potency in comparison to our GPR17 agonist RA-II-150. The intrinsic activity and potency of pranlukast for the GPR17-mediated inhibition of cAMP accumulation was cell line-dependent, since the compound showed weak partial agonist activity in the CHO-GPR17 cell line, but enhanced partial agonist activity in HEK-BRET-GPR17 cells.

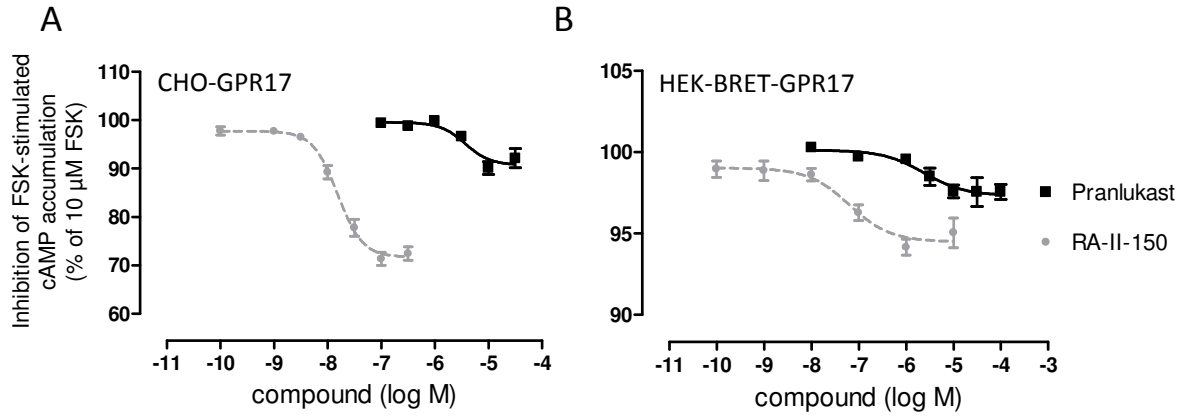

Figure 74 cAMP assays reveal concentration-dependent partial agonistic effects of pranlukast analyzed in cells stably expressing GPR17

CHO cells stably expressing GPR17 (A) and HEK293 cells stably cotransfected with GPR17-RLuc and β-arrestin2-GFP2 (B, HEK-BRET-GPR17 *low*) were stimulated with increasing concentrations of pranlukast and RA-II-150, respectively, in the presence of 10 µM forskolin. GPR17-mediated decrease of intracellular cAMP was calculated as percent inhibition of adenylate cyclase stimulated with FSK (10 µM). All data are means (+/- s.e.m.) of at least three experiments performed in duplicates.

Table 45 Parameters of averaged pranlukast and RA-II-150 concentration-effect curves determined by Gαi/o-cAMP assays, as depicted in Figure 74 (± s.e.m.)

cell line	pEC_{50}	bottom value / E_{max} (%)	top value (%)	n_H	n
CHO-GPR17 *Pranlukast*	5.43 ± 0.18	90.7 ± 1.2	99.6 ± 0.8	-1.9 ± 0.3	4-6
CHO-GPR17 *RA-II-150*	7.81 ± 0.05	71.7 ± 1.0	97.8 ± 0.8	-1.9 ± 0.3	5
HEK-BRET-GPR17 *Pranlukast*	5.62 ± 0.26	97.3 ± 0.3	100.1 ± 0.3	1.0 *(fixed)*	3-4
HEK-BRET-GPR17 *RA-II-150*	7.20 ± 0.27	94.5 ± 0.5	99.0 ± 0.4	1.0 *(fixed)*	4

4.3.2.3 Stimulation of GPR17 with pranlukast does neither elevate intracellular cAMP nor IP-One concentrations

Based on the analyses performed with the Epic® system, it was concluded that pranlukast stimulation of GPR17 only results in coupling with Gαi/o. To further prove this functional selectivity, the ability of pranlukast to elevate intracellular cAMP and IP1 levels, respectively, was examined. As presented in Figure 75, stimulation of cells stably expressing GPR17 (CHO-GPR17, HEK-BRET-GPR17) with pranlukast did not cause an elevation of intracellular second messengers, neither cAMP (A) nor IP1 (B). The cAMP levels in CHO-GPR17 cells were rather decreased, possibly due to partial Gαi/o-agonism. To verify viability of the cells and functionality of the methods, RA-II-150 and forskolin were applied as positive controls for cAMP accumulation assays, and RA-II-150 and carbachol as controls for elevation of IP1. All control compounds did significantly increase the respective intracellular second messengers, thus confirming appropriate conditions. It should be noted that RA-II-150 was not applied on HEK-BRET-GPR17 cells, neither in cAMP nor in IP1 assays, because previously obtained data revealed lack of Gαs-mediated responses (Figure 50) and weak Gαq-initiated effects in HEK293 cells stably coexpressing β-arrestin (Figure 69). Nevertheless, this cell line was additionally applied to examine effects of pranlukast, as these in formations were essential for subsequent analyses by means of BRET2 (Figure 77).

Taken together, pranlukast behaved as a partial agonist for inhibition of cAMP accumulation, yet failed to stimulate cAMP and IP1 production, consequently these investigations further prove the conclusion that pranlukast acts as a functionally selective partial agonist.

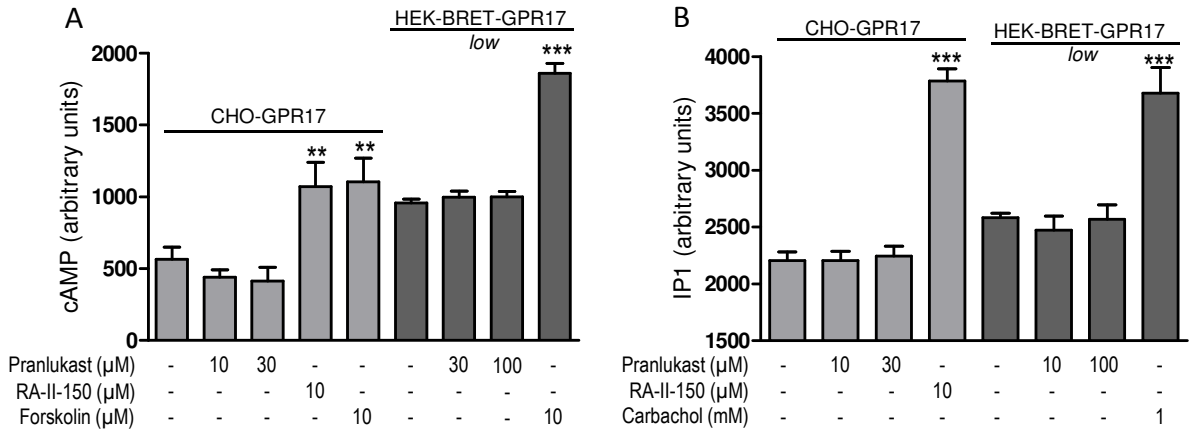

Figure 75 Stimulation of GPR17 with pranlukast does neither raise intracellular cAMP nor IP1 concentrations

CHO cells stably expressing GPR17 (CHO-GPR17) and HEK293 cells stably coexpressing GPR17-RLuc and β-arrestin2-GFP2 (HEK-BRET-GPR17) were challenged with indicated concentrations of RA-II-150 and pranlukast, respectively. Changes of intracellular cAMP (A) and IP1 (B) were determined, whereas forskolin (A) and carbachol (B) were used as positive controls. Data are expressed as arbitrary units. All data are means (+/- s.e.m.) of three to four independent experiments performed in duplicates. For statistical analyses unpaired t-tests with two-tailed p values and 95% confidence interval were applied and revealed no significant differences of pranlukast induced values compared to unstimulated ones, whereas positive controls were significant (**$p < 0.01$, ***$p < 0.001$).

4.3.2.4 Pranlukast shows no activity on untransfected CHO-K1 and HEK293 cells neither in cAMP nor in IP1 assays

As analyses of pranlukast by means of the Epic® system revealed some unspecific DMR events in untransfected CHO-K1 cells, the impact of stimulation with pranlukast was additionally analyzed using second messenger assays (cAMP and IP1) to further characterize unspecific influences in untransfected cells (CHO-K1 and HEK293 cells).

The data presented in Figure 76 obviously demonstrate, that pranlukast caused no significant changes of basal second messenger levels, neither cAMP (A) nor IP1 (B). Furthermore, the elevation of cAMP by forskolin was not inhibited by pranlukast preincubation (A). Carbachol and ATP were applied as positive controls, and they significantly elevated intracellular IP1 levels via stimulation of endogenous Gαq-coupled muscarinic acetylcholine receptors (Mundell & Benovic 2000) and purinergic P2Y1 / P2Y2 receptors (Iredale & Hill 1993, Marcet et al. 2004), respectively (B).

The lack of response clearly demonstrates that on the one hand inhibition of cAMP accumulation in GPR17-expressing cells via Gαi/o coupling can be regarded as a specific response due to stimulation of GPR17, and on the other hand the remaining unspecific effects monitored by use of the Epic® system in untransfected as well as in PTX-pretreated CHO-GPR17 cells were neither elicited by Gαs nor Gαq/11 protein-coupling events, and remain elusive so far.

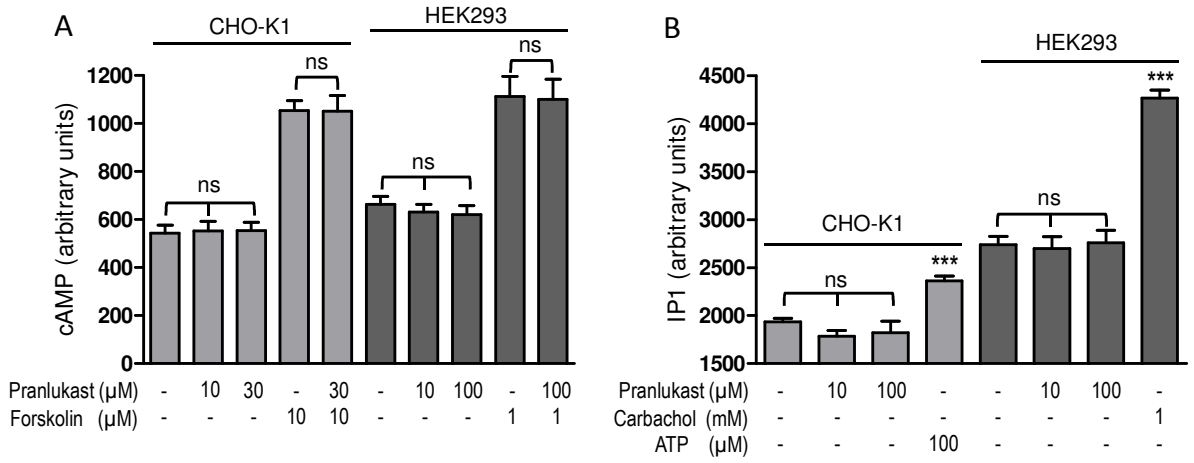

Figure 76 Pranlukast shows no activity on untransfected CHO-K1 or HEK293 neither in cAMP nor in IP1 assays

A-B, Untransfected cell lines (CHO-K1, and HEK293 cells) were challenged with indicated pranlukast concentrations and analyzed by cAMP (A) and IP1 (B) assays, respectively. Forskolin (A), carbachol (B) and ATP (B), respectively, were used as positive controls. All data are means (+/- s.e.m.) of three to six experiments performed in duplicates. For statistical analyses, unpaired t-tests with two-tailed p values and 95% confidence interval were applied and revealed no significant differences of pranlukast induced values compared to unstimulated ones, whereas positive controls were highly significant (***$p < 0.001$).

4.3.2.5 Stimulation of GPR17 by pranlukast elicits translocation of β-arrestin2 in a PTX-sensitive manner

Since at least for some receptors it is known that β-arrestin recruitment occurs independent of G protein-coupling (reviewed by Defea 2008, DeWire et al. 2007, Violin & Lefkowitz 2007) and the GPR17 agonist RA-II-150 was shown to promote both G protein-dependent and -independent β-

arrestin2 translocation, it was the next intention to investigate whether pranlukast is able to trigger β-arrestin2 recruitment to the activated GPR17 and whether this protein-protein-interaction is Gαi/o protein-dependent.

Therefore the established bioluminescence resonance energy transfer method (BRET2) was applied using HEK293 cells stably coexpressing GPR17 C-terminally fused to Renilla luciferase (RLuc) and β-arrestin2 N-terminally labeled with green fluorescent protein 2 (GFP2). These HEK-BRET-GPR17 cells were challenged with increasing pranlukast concentrations in the presence and absence of Gαi/o-inhibitor PTX (50 ng/ml, 18 h).

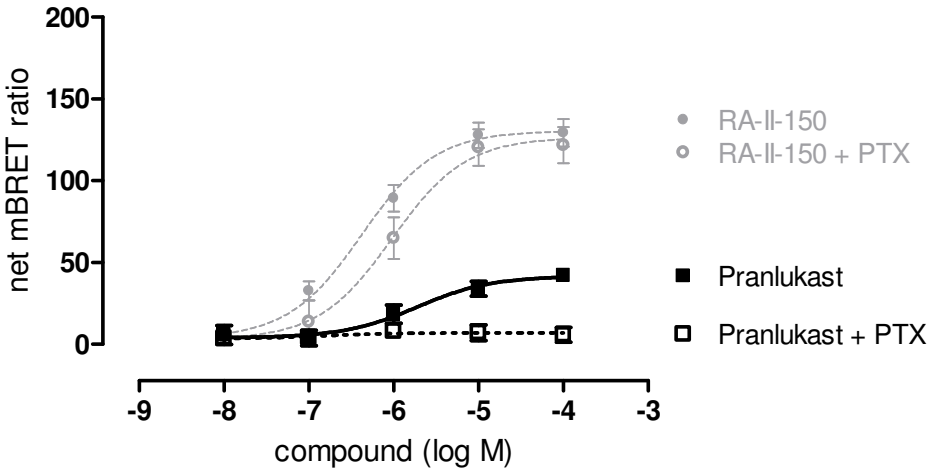

Figure 77 Pranlukast partially recruits β-arrestin2 in a PTX-sensitive manner
HEK293 cells stably transfected with β-arrestin2-GFP2 and GPR17-RLuc (HEK-BRET-GPR17) were exposed to indicated concentrations of pranlukast, and agonist-induced increases in BRET ratio were monitored. Pretreatment with Gαi/o inhibitor PTX (50 ng/ml, 18 h) completely abolished partial recruitment. Data of full agonist RA-II-150 were included for clear comparison. Each data point represents mean (+/- s.e.m.) of three to six independent experiments performed in triplicates.

Table 46 Parameters of averaged RA-II-150 concentration-effect curves determined by DMR assays, as depicted in Figure 77 (± s.e.m.)

agonist	pEC_{50}	bottom value (net BRET ratio)	E_{max} (net BRET ratio)	n_H	n
Pranlukast	5.72 ± 0.30	4.0 ± 3.8	41.7 ± 4.6	1.0 *(fixed)*	6
Pranlukast *+ PTX*	-	3.3 ± 4.6	7.0 ± 2.3	-	3
RA-II-150	*6.38 ± 0.12*	*3.0 ± 4.0*	*130.3 ± 5.2*	*1.0 (fixed)*	*6*
RA-II-150 +PTX	*6.02 ± 0.18*	*2.9 ± 8.6*	*126.6 ± 8.5*	*1.0 (fixed)*	*3*

Stimulation with pranlukast resulted in a concentration-dependent β-arrestin2 recruitment to the activated GPR17 (Figure 77), measured as an increase of BRET ratio. To help clarify the agonist efficacy, the data obtained with RA-II-150 were included in the figure. In agreement with previous results (see 4.3.2.2), pranlukast behaved as a partial agonist with decreased potency relative to RA-II-150. The efficacy was reduced by approximately 32% (E_{max} values: 41.7 +/- 4.6 mBRET ↔ 130.3 +/- 5.2 mBRET), and the potency was ~4.5-fold lower (absolute EC_{50} values:

1.91 µM ↔ 0.42 µM). Interestingly, inhibition of Gαi/o protein-mediated signaling by preincubation with PTX completely abolished pranlukast-induced translocation of β-arrestin2 to the stimulated receptor, whereas, as previously reported, β-arrestin2 recruitment initiated by stimulation of GPR17 with RA-II-150 was only partially diminished by blocking of G protein-dependent signaling (Figure 59).

These observation further confirmed the assumption that pranlukast acts as a partial agonist at GPR17 with functional selectivity relative to RA-II-150. Furthermore, it was shown that translocation of β-arrestin2 to the stimulated receptor proceeds in a Gαi/o protein-dependent manner, whereas RA-II-150-induced recruitment furthermore occurs without the need of G protein activation (Figure 59).

4.3.2.6 GPR17 internalizes upon pranlukast activation

In addition to functional analyses, the influence of pranlukast on GPR17 cell surface expression was studied, since the loss of cell surface receptor density might as well cause an inhibition of receptor mediated signaling. In order to examine endocytosis of GPR17 initiated by pranlukast application, HEK293 cells stably expressing 3xHA-tagged GPR17 were investigated by immunofluorescence microscopy and by indirect cell surface ELISA, which enabled evaluation of the quantitative changes of surface expressed GPR17 upon agonist activation for indicated time periods. The examination of HA-immunoreactivity using fluorescence microscopy gives information about the subcellular localization.

Pranlukast treatment induced endocytosis within 15 min, and GPR17 continued to internalize, leading to ~11.2% (+/- 1.5%) loss of cell surface expression (Figure 78, A). In agreement with the previously described partial agonism, the extent of GPR17 endocytosis was decreased by the factor 2.3 relative to RA-II-150 induced internalization rate (~26.2 +/- 2.3%).

Immunofluorescence analyses of DMSO-treated HEK-3HA-GPR17 cells revealed that, under control conditions GPR17 was predominantly located on the cell surface (B). Stimulation with pranlukast (30 µM, 60 min) induced endocytosis of GPR17 from the cell surface into the cytoplasm with a punctate distribution into intracellular vesicles (Figure 78, C), again with a lower extent relative to RA-II-150 (Figure 44).

Thus, the data obtained from immunofluorescence microscopy and surface ELISA exhibit equivalent patterns, explicitly that pranlukast stimulation of GPR17 induces partial internalization of the receptor from the cell membrane into the intracellular membrane compartments of the cell in a time-dependent manner upon stimulation with pranlukast.

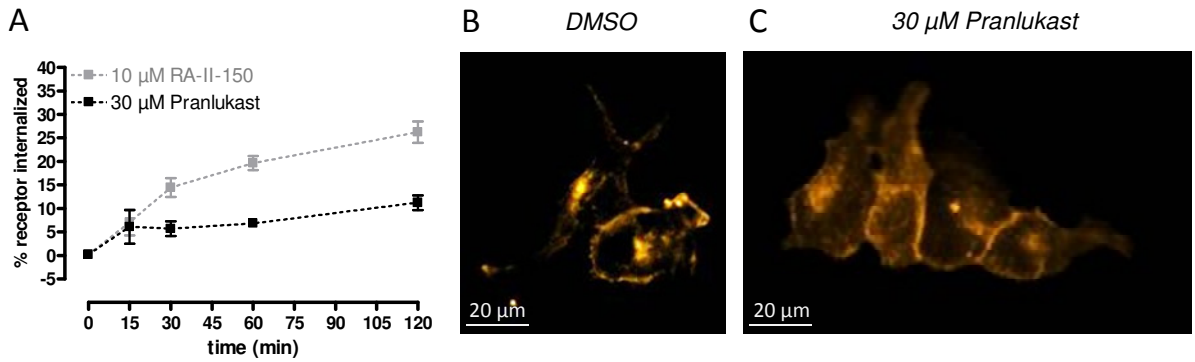

Figure 78 Pranlukast induces partial endocytosis of GPR17
GPR17 internalization behavior was quantitated by indirect cellular ELISA (A) and imaged by immunofluorescence microscopy (B) using HEK293 cells stably expressing GPR17 fused to an N-terminal 3xHA tag. A, Colorimetric ELISA measurements of pranlukast (30 µM) induced GPR17 sequestration for the indicated time period. The amount of internalized receptor was calculated from the decrease in the level of surface-expressed receptor after agonist treatment compared with untreated, control cells (HEK293). Each data point represents mean (+/- s.e.m.) of four to five independent experiments performed in triplicates. B-C, Fluorescence images of cell surface and intracellular 3xHA-GPR17 immunoreactivity. Cells were treated for 1 h at 37°C with 0.1% DMSO (B, C11) or 30 µM pranlukast (C). B, Control cells primarily showed plasma membrane localization of GPR17 and less internalized receptor. B, Cells were pre-labeled with anti-HA antibody (Table 22, A1), and after agonist-induced stimulation, cells were permeabilized with triton X-100 (C52) and immunostained with fluorescence antibody (Alexa Fluor 546 goat anti-mouse IgG, Table 22, A3). The following settings were used for Alexa Fluor 546 recordings: 400 fold magnification, 100 ms exposure time, 0.99 γ and 2-22 histogram. Representative cells from at least three independent experiments are shown. After indirect immunofluorescence staining, no specific fluorescence was observed in untransfected HEK293 cells. Scale bars = 20 µM.

4.3.3 Functional analyses uncover pranlukast as a GPR17-antagonist with a versatile antagonistic profile

To further characterize pranlukast as a GPR17 antagonist, functional consequences of preincubation with pranlukast on RA-II-150-induced responses were evaluated in a set of different functional assays.

4.3.3.1 Determination of antagonistic potencies in various functional assays

Since GPR17 revealed promiscuous G protein-coupling upon activation with RA-II-150, inhibition potencies of pranlukast were investigated by use of two second messenger assays (cAMP for Gαi/o and Gαs and IP1 for Gαq) as well as BRET2 technology to analyze repression of β-arrestin2 recruitment. Due to the functionally selective partial agonistic effects that have been shown to be completely dependent on Gαi/o-mediated signaling, in certain assays (Gαs cAMP, BRET2) cells were pretreated with PTX (50 ng/ml, 18 h) to circumvent influences caused by this partial agonism. Hence, results obtained in Gαs cAMP, IP1 and BRET2 (+PTX) assays can be regarded as pure antagonistic properties.

As presented in Figure 79, pranlukast concentration-dependently inhibited the RA-II-150-induced responses in all performed functional assays (cAMP (A-B), IP1 (C) and β-arrestin-recruitment (D)). Inhibition potencies (pIC_{50} values) and percentage efficacies (bottom values) are summarized in Table

47. At 30 µM, pranlukast completely blocked the RA-II-150-induced cAMP (B) as well as IP1 (C) accumulation, whereas both Gαi/o-mediated inhibition of forskolin-induced cAMP synthesis upon RA-II-150 stimulation (A) and β-arrestin2 recruitment to the activated GPR17 (D) were only partially inhibited. The partial inhibition of Gαi/o-mediated signaling observed by cAMP inhibition assays (56.6 +/- 4.7%) was probably due to a counteracting partial agonistic effect of pranlukast. Conversely, the incomplete repression of β-arrestin2-recruitment was not due to the partial agonistic property as its inhibition by PTX-pretreatment did not significantly change the maximum effect (E_{max} 82.2 +/- 2.9% ↔ E_{max} PTX 85.5 +/- 2.9%). Apparently, RA-II-150-induced translocation of β-arrestin2 cannot be completely blocked by pranlukast pretreatment.

The determined absolute IC_{50} values were all in a micromolar range from 11.2 µM to 1.1 µM with the following rank order: Gαi/o-cAMP (11.2 µM) > IP1 (4.0 µM) > Gαs-cAMP (3.2 µM) > BRET2 (1.5 µM) > BRET2+PTX (1.1 µM).

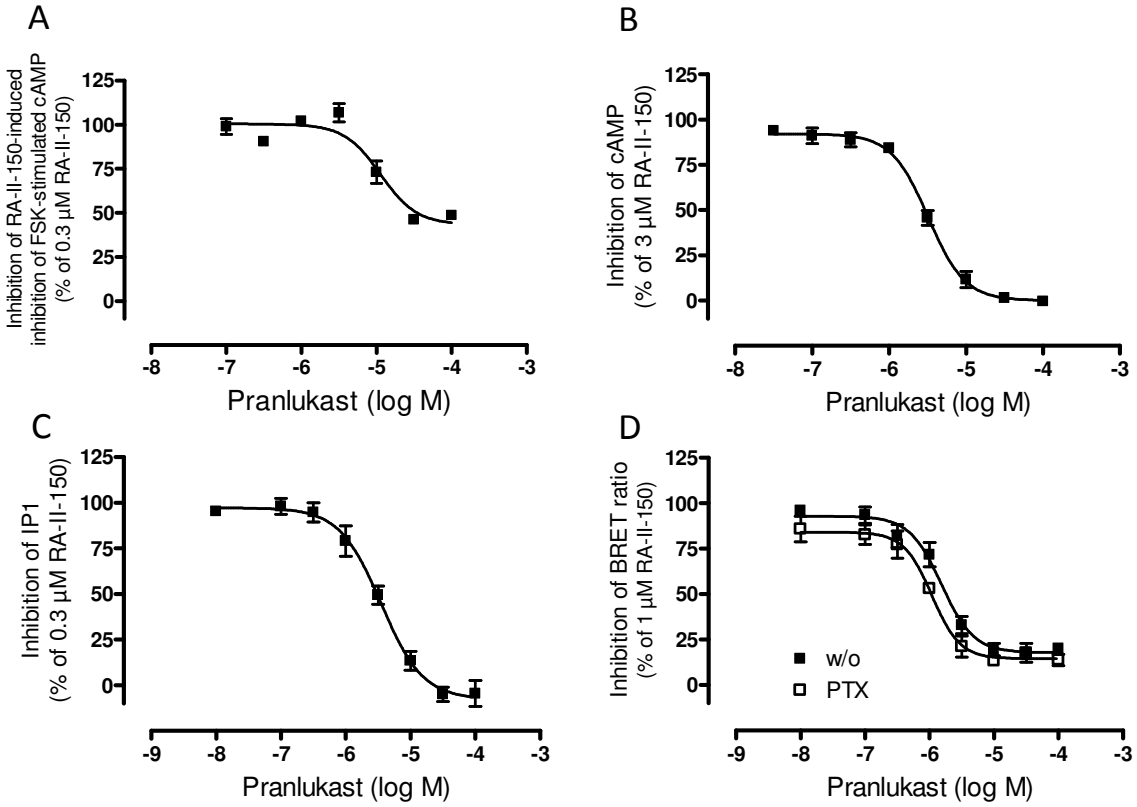

Figure 79 Concentration-dependence of inhibition by pranlukast of RA-II-150-induced functional responses in GPR17-expressing CHO cells

CHO cells stably expressing GPR17 were challenged with RA-II-150 in the presence of increasing pranlukast concentrations (30 min preincubation, 37°C). A, Inhibition of RA-II-150 (0.3 µM) induced inhibition of forskolin-stimulated cAMP accumulation. Data are expressed as percent of maximum inhibition induced by RA-II-150 (0.3 µM) in the absence of pranlukast. All data are means (+/- s.e.m.) of at least three experiments.

Table 47 Parameters of averaged pranlukast inhibition-concentration-effect curves determined various assay methods, as depicted in Figure 79 (± s.e.m.)

assay	pIC_{50}	top value (%)	bottom (%)	n_H	n
Gαi/o cAMP	4.95 ± 0.10	100.4 ± 2.8	43.4 ± 4.7	-1.8 *(fixed)*	3
Gαs cAMP *+ PTX*	5.49 ± 0.04	92.1 ± 2.0	0.1 ± 2.4	-1.8 ± 0.3	3
IP1	5.45 ± 0.07	97.3 ± 3.4	-7.6 ± 4.8	-1.3 ± 0.3	3
BRET2	5.81 ± 0.06	92.6 ± 3.0	17.8 ± 2.9	-1.7 ± 0.4	6
BRET2 *+PTX*	5.96 ± 0.07	84.1 ± 3.4	14.5 ± 2.9	-2.0 ± 0.6	3

4.3.3.2 Schild regression analyses using traditional second messenger assays and DMR technology reveals diverse antagonistic behavior

To further characterize the mode of action, Schild analyses on the effects of pranlukast on GPR17-initiated signaling events were performed. First, pranlukast was tested for its ability to antagonize GPR17-triggered dynamic mass redistribution. The activity of pranlukast was tested in the concentration range of 3 – 30 µM and cells were preincubated for 60 min at 28°C with the antagonist prior to stimulation with increasing concentrations of GPR17-agonist RA-II-150.

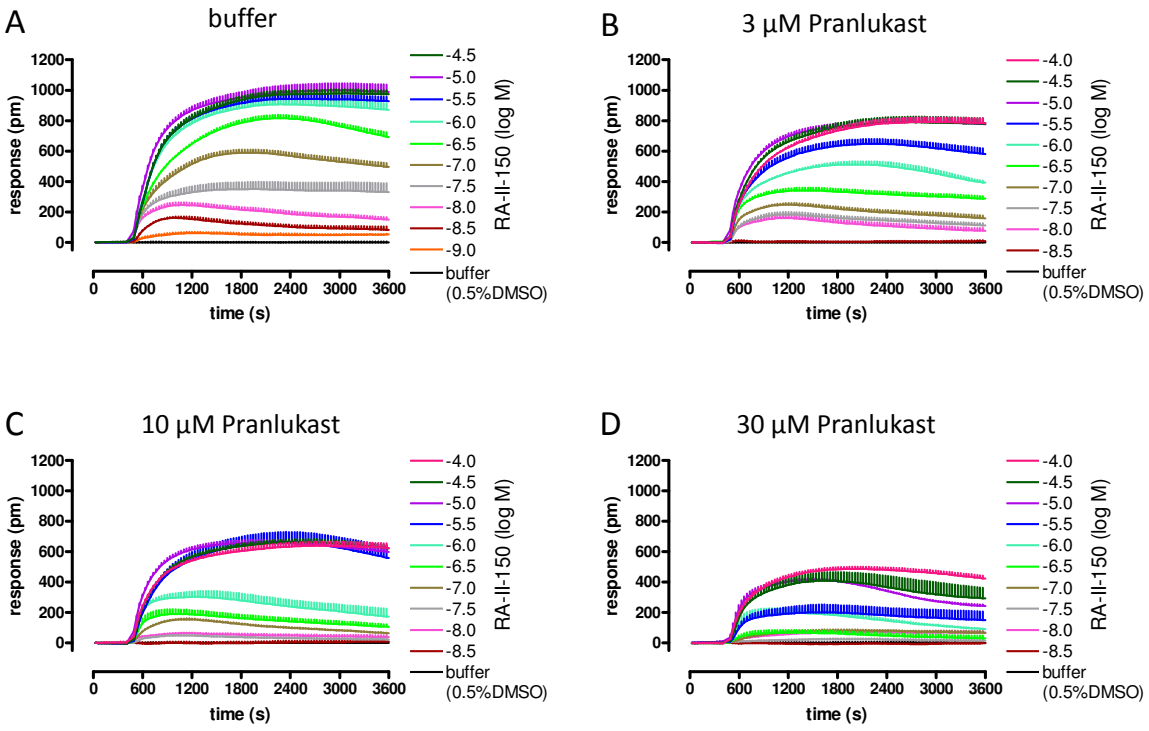

Figure 80 Influence of pranlukast on RA-II-150-induced optical signatures monitored by means of the Epic® system

CHO cells stably expressing GPR17 were challenged with the indicated concentrations of RA-II-150 in the absence (A) and presence of pranlukast (3 µM (B), 10 µM (C) and 30 µM (D)). Cells were preincubated with pranlukast for 60 min at 28°C prior to addition of RA-II-150. Wavelength shift [pm] over time [s] was monitored as a measure of functional activity. Signatures were baseline-corrected by subtraction of buffer traces from the DMR response after receptor activation. Representative optical trace experiment (mean + s.e.m.) of at least three independent experiments performed in triplicates.

Representative optical signatures are presented in Figure 80 (A-D), and clearly highlight a depression of overall response dependent on the applied pranlukast concentration (0 µM (A), 3 µM (B), 10 µM (C) and 30 µM (D)). Interestingly, besides the clear inhibition of the RA-II-150-induced overall responses, the shape of the optical signatures remained unchanged. These observations suggest that all monitored signaling events were inhibited equally, which is in agreement with the findings previously observed by examination of pranlukast potencies in distinct functional assays, which revealed comparable IC_{50} values for all performed analyses (Figure 79).

Furthermore, in accord with data obtained in BRET2 assays as well as in Gαi/o cAMP assays (Figure 79, A, D), preincubation with 30 µM pranlukast did not result in a complete inhibition of RA-II-150 induced response.

In addition to DMR technology, Schild analyses were performed by cAMP and IP1 assays. Figure 81 presents the curves of RA-II-150 concentration-dependent functional responses in the presence of increasing pranlukast concentrations. Concentration-response curves (CRCs) transformed from optical signatures obtained by DMR analyses were shifted to the right and simultaneously revealed a decrease of the maximal RA-II-150 response, indicating insurmountable antagonism (A). In contrary CRCs determined by use of IP1 assays were parallel shifted to the right without affecting the maximum response, indicating surmountable antagonism (B). Additionally, in cAMP accumulation analyses pranlukast induced clear rightward shifts of RA-II-150 CRCs in concentrations up to 10 µM; at a concentration of 30 µM, however, E_{max} of RA-II-150 seemed to be depressed, indicating insurmountable antagonism at the highest applied concentration (C). Examination of pranlukast in Gαi/o cAMP assays revealed a pattern of RA-II-150 curves with decreased baseline (due to partial agonism) shifted to the right of the control curve (due to antagonistic properties of the partial agonist) in concentrations up to 10 µM, and similar to results from Gαs cAMP assays, 30 µM depressed the maximum response of RA-II-150, indicating a mixed surmountable/insurmountable antagonism also in this assay (D).

The decrease of the maximal level, observed in DMR and cAMP assays, was inconsistent with the possibility that pranlukast was a competitive antagonist of GPR17, as suggested from IP1 assays. In conclusion, functional data revealed that pranlukast concentration-dependently counteracted GPR17-mediated responses, but it seemed to exhibit surmountable and insurmountable antagonism, dependent on the respective functional assay, suggesting that the nature of antagonism is dependent on the cellular signaling pathway used by GPR17. Furthermore, it should be taken into account, that pranlukast slightly reduced the available number of GPR17 on the cell surface (Figure 78), which may correlate to insurmountable inhibition of agonist responses in functional assays.

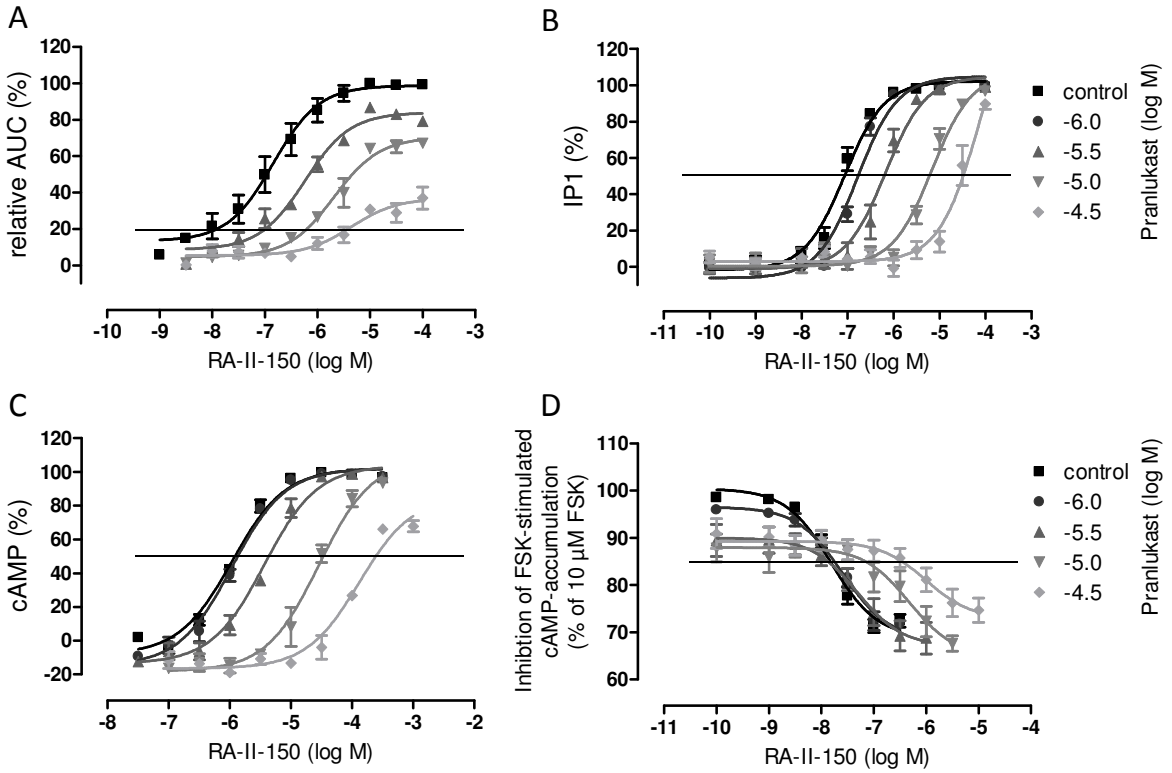

Figure 81 Effects of pranlukast on the concentration-response curve induced by GPR17-agonist RA-II-150 evaluated in a set of different functional assays

CHO cells stably expressing GPR17 were challenged with increasing concentrations of RA-II-150 in the absence (w/o) and presence of the indicated concentrations of pranlukast. A, Concentration-response curves (CRCs) transformed from optical traces monitored using DMR assays (Figure 80). Data are normalized and presented as percent of maximum area under curve (AUC, 0-3600 s) induced by a saturating concentration of RA-II-150 (10 µM) in the absence of pranlukast. B, CRCs analyzed by IP1 assays. Intracellular IP1 levels were expressed as percent of maximum IP1 amounts induced by RA-II-150 (10 µM) in the absence of pranlukast. C, Concentration-dependent stimulation of cAMP synthesis by RA-II-150 was normalized and expressed as percent of maximum activation induced by a saturating concentration of RA-II-150 (100 µM) in the absence of pranlukast. D, Cells were stimulated with increasing concentrations of RA-II-150 in the presence of 10 µM forskolin, besides indicated concentrations of pranlukast GPR17-mediated decrease of intracellular cAMP was calculated as percent inhibition of adenylate cyclase stimulated with forskolin (10 µM). A-D, All data are means (+/- s.e.m.) of at least three independent experiments performed in triplicates (A) and duplicates (B-C), respectively. Black lines highlight response levels that were used to calculate dose ratios (DRs) for subsequent Schild regression analyses.

The pA_2 values for pranlukast analyzed by IP1, Gαs- and Gαi/o-cAMP assays were computed by linear regression of dose ratios (DR), determined from EC_{50} values of the parallel shifted concentration-response curves, whereas for Epic® analyses dose ratios at 20% maximal response were used to calculate pA_2 values, as described by Kenakin et al. (Kenakin, Jenkinson & Watson 2006). By this means estimated pA_2 values for pranlukast of the Schild regression amounted to 5.81 (5.56 to 6.17) for DMR, 5.92 (5.71 to 6.16) for IP1, 5.66 (5.55 to 5.79) for Gαs-cAMP and 5.82 (5.53 to 6.15) for Gαi/o-cAMP. Thus, calculated pA_2 values were comparable in all performed assays, yielding a predicted functional antagonism in the micromolar range (1.2 to 2.2 µM), which agrees very well with previously observed IC_{50} values (Table 47).

In addition, Schild plot analyses revealed steep slopes of 2.04 (+/- 0.23) for DMR, 2.21 (+/- 0.17) for IP1, 1.89 (+/- 0.10) for Gαs-cAMP and 1.55 (+/- 0.15) for Gαi/o-cAMP. In Schild regression analyses, if

pranlukast were a competitive antagonist, a perfect linear line with a slope of 1.0 would be expected. However, as the confidence intervals for the slopes did not include 1.0, in none of the performed functional assays, pranlukast is probably not a simple competitive antagonist, but rather acting in a non-competitive way. Whether this non-competitive antagonism is due to allosteric interactions or based on hemi-equilibrium assay conditions remains elusive so far.

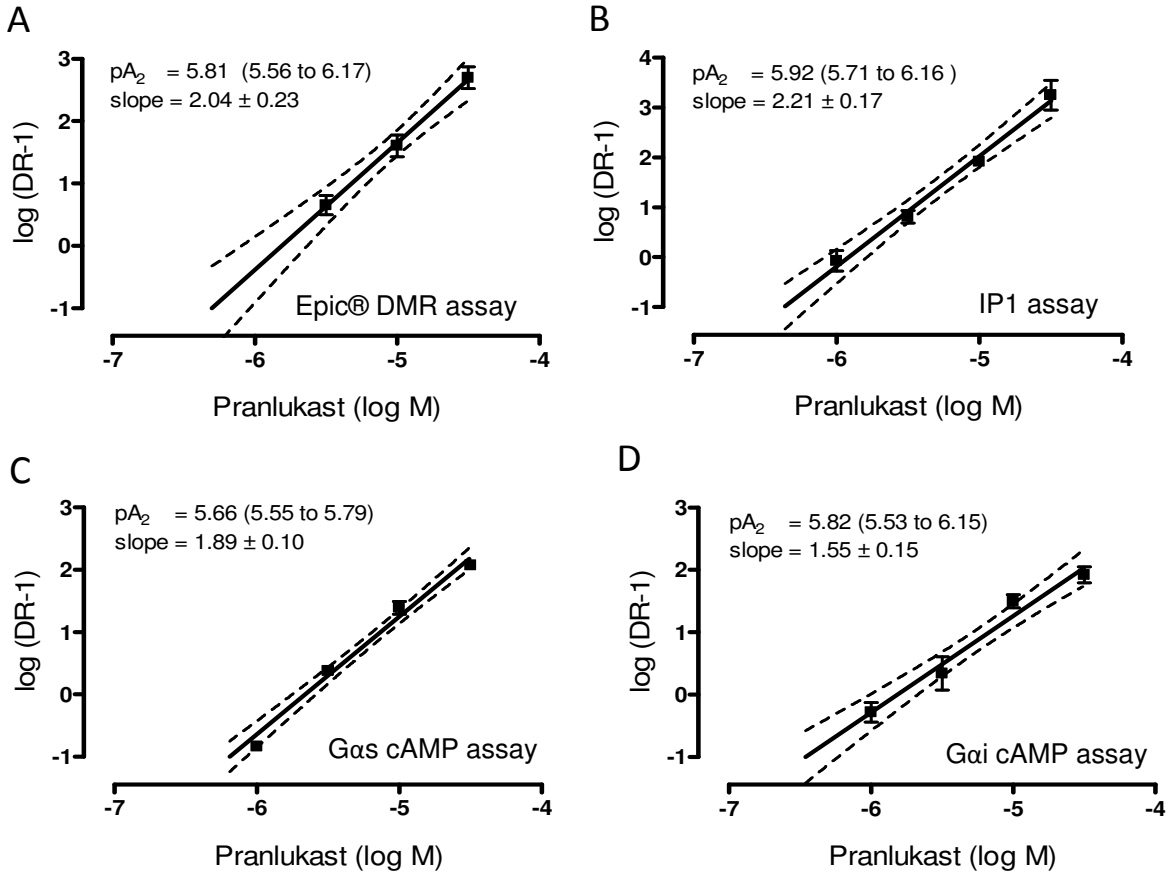

Figure 82 Schild plots corresponding to analyses presented in Figure 81

Response levels applied to determine dose-ratios (DRs) are depicted in Figure 81. The pA2 values were determined as X-intercept when Y = 0.0. Statistical estimations of 95% confidence limits of the slope are presented as dotted lines. Further determined parameters are presented in the respective plot (pA_2 values (95% confidence interval) and slope (+/- s.e.m.)).

In conclusion, pranlukast concentration-dependently counteracted RA-II-150-induced GPR17-mediated functional responses in a mixed competitive/non-competitive manner. Hence, in contrast to the observed differing effects of pranlukast on the RA-II-150-induced CRC (Figure 81) in distinct functional assays, comparable results were noted in corresponding Schild plot analyses.

4.3.4 Pranlukast shows no unspecific inhibiting effects on carbachol-induced cAMP production in CHO cells stably expressing muscarinic receptor M2

Control experiments using carbachol to stimulate cAMP accumulation via the M2 muscarinic acetylcholine receptor stably transfected in CHO cells demonstrated a lack of inhibition by pranlukast. Additionally the effect of atropine on carbachol-induced cAMP accumulation was investigated in parallel as positive control, and preincubation with 1 µM resulted in a clear rightward shift of carbachol CRC, indicating appropriate assay conditions.

Thus, these data demonstrate that pranlukast functionally interacts with GPR17, independent of another adenylate cyclase-coupled receptor.

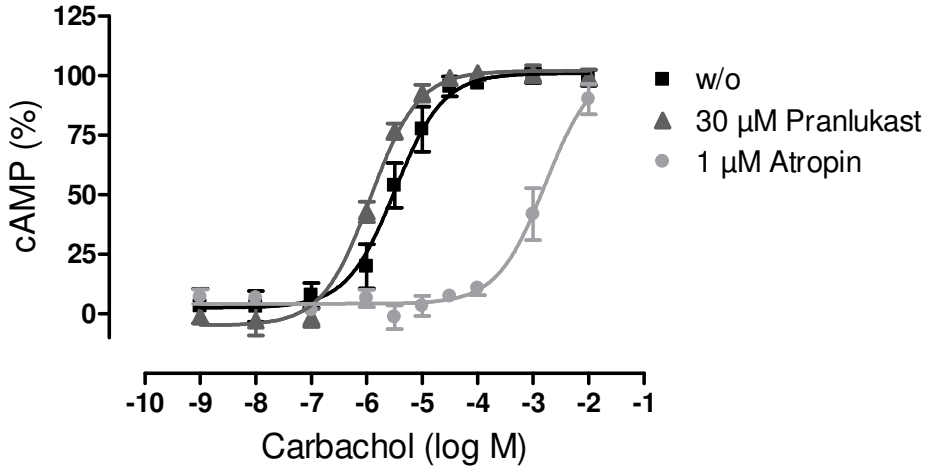

Figure 83 Pranlukast shows no unspecific inhibition on carbachol induced cAMP accumulation
CHO cells stably expressing the muscarinic M2 receptor were challenged with the indicated carbachol concentrations in the absence (w/o) and presence of atropine (1 µM) or pranlukast (30 µM), respectively. M2-mediated increase of intracellular cAMP was normalized and expressed as percent of maximum activation induced by a saturating concentration of carbachol (1 mM). All data are means (+/- s.e.m.) of three independent experiments performed in duplicates.

Table 48 Parameters of averaged carbachol concentration-effect curves determined by Gαs-cAMP assays, depicted in Figure 83 (± s.e.m.)

antagonist	pEC_{50}	bottom value (%)	E_{max} (%)	n_H	n
none (w/o)	5.49 ± 0.09	2.7 ± 3.4	101.0 ± 3.2	1.0 *fixed*	3
pranlukast	5.94 ± 0.05	-4.8 ± 2.2	102 ± 1.8	1.0 *fixed*	3
atropine	2.79 ± 0.12	4.2 ± 1.7	104.2 ± 7.7	1.0 *fixed*	3

5 Discussion

5.1 GPR17 shows common features of GPCR signaling

Deorphanization efforts revealed GPR17 as a dual nucleotide/lipid receptor with two distinct classes of signaling molecules: uracil nucleotides and cysteinyl-leukotrienes (Ciana et al. 2006). However, these postulated endogenous agonists and likewise the previously uncovered signaling properties remain disputable, as verification by independent laboratories has not yet been made. Furthermore, GPR17 was published as a ligand-independent negative regulator of CysLT1 receptor via GPCR-GPCR interaction (Maekawa et al. 2009). The identification of a synthetic small molecule GPR17 agonist (here referred to as RA-II-150) by means of a high throughput pharmacogenomic approach enabled *in vitro* pharmacological characterization of human GPR17. The observed experimental findings using RA-II-150 clearly demonstrate that GPR17 does not lack the common features of GPCR signaling.

5.1.1 Stimulation of human GPR17 with the synthetic small molecule RA-II-150 promotes promiscuous G protein-coupling

As the endogenous G protein-coupling profile of GPR17 has not yet been elucidated, a set of various functional assays was established using two different cellular backgrounds (CHO and HEK293 cells), self-engineered to stably express the short isoform of human GPR17. Traditional assays based on HTRF® technology enable examination of two major second messengers (cyclic adenosine monophosphate (cAMP) and inositol-monophosphate (IP1)), and thus facilitates exploration of signaling outcomes triggered by the three main G proteins (Gαi/o, Gαs and Gαq). These investigations uncovered that GPR17-initiated signaling upon activation with RA-II-150 is mediated via promiscuous G protein-coupling. In both analyzed cell lines, stimulation of cAMP- and IP1-accumulation, as well as inhibition of forskolin-stimulated adenylate cyclase was observed upon activation with RA-II-150, whereas stimulation of untransfected cell lines was shown to lack a response. In the presence of forskolin, stimulation of GPR17 with low concentrations of RA-II-150 induced significant concentration-dependent decrease of cAMP, indicative of GPR17 coupling to Gαi/o, whereas at higher concentrations RA-II-150 yielded a concentration-dependent elevation of cAMP highlighting coupling to stimulatory Gαs, resulting in a reverse bell-shaped concentration-response curve.

Pertussis toxin (PTX) is a bacterial toxin produced by certain Bordetella pertussis strains. PTX catalyzes an irreversible ADP-ribosylation of Gαi and Gαo subunits, leading to functional uncoupling of these proteins from GPCRs (Casey & Gilman 1988, Katada & Ui 1982). Thus, sensitivity to PTX can serve as an indication of the involvement of Gαi/o protein in a signal transduction pathway. Since application of PTX completely abrogated GPR17-mediated inhibition of forskolin-stimulated cAMP accumulation, a substantial need of the Gαi/o subunit for RA-II-150-induced inhibition of adenylate

cyclase has been proven. Conversely, the stimulatory effects on adenylate cyclase were neither diminished nor enhanced by preincubation with Gαi/o inhibitor PTX, which suggests that members of the Gαi/o family of G proteins were not involved in GPR17-mediated elevation of intracellular cAMP. Accordingly, a cross-talk between both G protein subunits in the signal transduction can be neglected and the determined reverse bell-shaped behavior observed in the presence of forskolin is promoted by a promiscuous interaction by agonist-activated GPR17 with both proteins, Gαi/o and Gαs, in an independent manner. Such U-shaped concentration-response curves were initially described by Fraser et al. while analyzing stimulation of human α2-adrenergic receptors with epinephrine (Fraser et al. 1989).

To further verify the role of Gαs proteins, cholera toxin (CTX) has been shown to be an appropriate tool (Schröder et al. 2010). CTX, a secretory product of *Vibrio cholerae*, is commonly used as a modulator of Gαs protein activity. The subunit A of CTX catalyzes ADP-ribosylation of the α-subunit belonging to stimulatory Gαs protein that is associated with activation of adenylate cyclase and generation of cAMP. CTX-catalyzed ADP-ribosylation inhibits the intrinsic GTPase activity of Gαs, thereby prolonging its active state. This, in turn, leads to an extended activation of adenylate cyclase by Gαs (Casey & Gilman 1988, Gill & Meren 1978). Thus, CTX may be used for analysis of Gαs transduction, inducing a full activation of this Gα protein, which cannot be further increased by receptor stimulation. Since HTRF® technology is based on a competitive immunoassay between endogenously accumulated second messengers and added d2-labeled second messengers (see 3.3.2), the elevation of endogenous cAMP through CTX preincubation hampers the subsequent measurement window of GPR17-induced increase of cAMP, independent of Gαs participation. Therefore, CTX could not be applied to further prove activation of Gαs subunit by agonist-activated GPR17.

It should be further noted, that stimulation of IP1 formation through activation of GPR17 has been verified to be insensitive to PTX pretreatment, indicating that Gαi/o subunits, especially the dissociated βγ-subunit that is known to activate phospholipase C (Marinissen & Gutkind 2001, Woehler & Ponimaskin 2009) were not necessary for this signal transduction. The selective Gαq/11 inhibitor YM-254890, isolated from the culture broth of *Chromobacterium sp.* (Takasaki et al. 2004), blocks the exchange of GDP for GTP in Gαq/11 activation, hence keeping the G protein in an inactive state. Due to limited access and thus very low available quantities, YM-254890 could not be applied in this part of the thesis to investigate the involvement of Gαq/11 protein. Nevertheless, subsequent investigations of the G protein-dependence of β-arrestin recruitment to the activated GPR17 revealed that YM-254890 completely abrogated the RA-II-150-induced IP1 accumulation, indicating Gαq/11 protein as the responsible signal transducer.

Taken together, the analyses by traditional second messenger assays demonstrated that GPR17 can couple to both Gαs and to PTX-sensitive Gαi/o to mediate activation and inhibition of adenylate cyclase, respectively, in a concentration-dependent manner. Furthermore, stimulation of GPR17 with RA-II-150 induced accumulation of IP1, resistant to PTX and sensitive to YM-254890, indicating involvement of Gαq/11. Consequently, activation of GPR17 with our small agonist RA-II-150

promotes promiscuous coupling with at least three distinct G protein subunits, namely Gαi/o, Gαs and Gαq/11.

To further analyze GPR17-mediated signaling patterns, a very recently introduced technology was applied. The Epic® system is based on resonant waveguide grating (RWG) that makes use of subtle ligand-induced cellular rearrangements, thus enabling non-invasive, real-time and label-free investigations. Activation of GPCRs is known to cause translocation of multiple signaling molecules upon receptor stimulation, and this process of dynamic redistribution of cellular content, also referred to as dynamic mass redistribution (DMR), is captured as an optical signature. The term 'signature' is used to describe the dynamic response profile displayed over time following ligand stimulation. The holistic nature of DMR measurements allows monitoring GPCR functionality along all four G protein signaling pathways: Gαi/o, Gαs, Gαq and Gα12/13 (Schröder et al. 2010). It unifies and quantifies whole cell effects or outcomes upon stimulation rather than resolving individual components contributing to the overall responses. Furthermore, ligand-induced signatures were reported to be indicative of signaling routes and accordingly can be applied to facilitate the evaluation of respective coupling preferences (Fang, Li & Ferrie, Schröder et al. 2009, Schröder et al. 2010). As demonstrated in this thesis, stimulation of GPR17 with RA-II-150 triggers distinct DMR events. The optical signatures monitored in both cellular backgrounds (CHO and HEK293 cells) were comparable, as both cell lines responded with a positive DMR event, but not identical, which is in agreement with previously reported information that DMR responses can be cell type dependent. Whereas DMR responses induced by Gαi-linked receptors (e.g. CRTH2 or M2) were shown to be similar in HEK293 and CHO cells, respectively, Gαs-linked receptors (e.g. EP2 and β2AR) revealed diverse responses dependent on cellular background, namely downward reflected signatures in CHO cells and positive DMR signals in HEK293 cells (Schröder et al. 2010). Since optical signatures elicited by RA-II-150-activated GPR17 are initiated by at least three independent signaling cascades, including Gαi/o, Gαs and Gαq, it appears correct that signatures differ amongst both analyzed cell lines.

Additional differentiations of signatures with selective pathway modulators turned out to be a challenging task, and so far no detailed elucidation of optical DMR signatures of any GPCR coupling to more than two independent G proteins has been reported. Inhibition of Gαi/o protein with PTX clearly induced shape changes of monitored optical signatures and diminished DMR responses elicited by low RA-II-150 concentrations (< 0.3 µM). Thus supporting the preference of Gαi/o-mediated signaling when challenged with low agonist concentrations. Whereas cholera toxin (CTX) has been proven to be a suitable tool to investigate GPCR coupling simply via Gαs proteins by means of the Epic® system (Schröder et al. 2010), it was found out to be inappropriate to analyze signaling patterns of GPR17, which are composed of promiscuous G protein transduction pathways. As already described above, CTX preincubation promotes an extended activation of adenylate cyclase via Gαs protein, which cannot be further increased by receptor stimulation. The simultaneous activation of additional signaling pathways, in particular those that elevate cAMP, may possess a regulatory control over Ca^{2+} signaling pathways (DeBernardi & Brooker 1996, Hajnóczky et al. 1993, Volpe & Alderson-Lang 1990). Furthermore, Ca^{2+} can also modulate components of the cAMP signaling machinery by either activating or inhibiting different subtypes of adenylate cyclase (Cooper, Mons &

Karpen 1995, Mons et al. 1998). Consequently, changes in Ca^{2+} and cAMP cannot be simply separated into two isolated linear signaling pathways, but they actually interact at multiple levels to effectively form a signaling network (reviewed by Bruce, Straub & Yule 2003). Since CTX does not inhibit Gαs mediated cAMP synthesis, the involving cross-communication between separate signaling units (Gαs↔Gαq) prohibited appropriate interpretation of data obtained with CTX preincubation. Accordingly, that is the reason why this pharmacological tool was not applied in this thesis to unravel optical signatures elicited by GPR17.

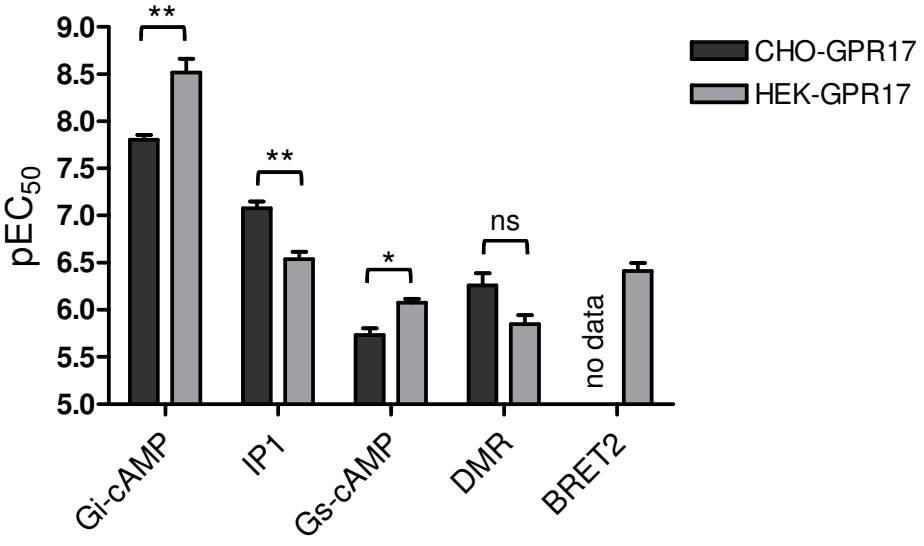

Figure 84 Comparison of pEC_{50} values determined in distinct functional assays in CHO-GPR17 and HEK-GPR17 cells, respectively.

pEC_{50} values were determined by stimulation of CHO (dark grey) and HEK293 (light grey) cells, respectively, stably expressing GPR17, with increasing concentration of RA-II-150 by use of various functional assays (cAMP and IP1 to analyze traditional second messengers, Epic® system to monitor dynamic mass redistribution and BRET2 technology to investigate β-arrestin2 recruitment). For statistical analyses, unpaired t-tests with two-tailed p values and 95% confidence interval were applied (ns $p > 0.05$, *$p < 0.05$, **$p < 0.01$).

When comparing pEC_{50} values determined by varying functional assays, it is obvious that potencies of our GPR17 agonist differ in both analyzed cellular backgrounds (Figure 84). The potencies concerning the adenylate cyclase activity, determined as changes of cAMP levels, exceed in HEK293 cells, whereas the activation of phospholipase C, monitored as increase of intracellular IP1, was more efficient in CHO cells. The potencies determined with the Epic® system do not differ significantly, thus indicating an indistinguishable overall potency of RA-II-150 in both analyzed cell lines. While the pEC_{50} value assessed in CHO cells using DMR analyses represents a mean value of all three independent second messenger assays, this is not the case for HEK293 cells, where DMR analyses revealed the lowest potency. This underlines that the precise nature of how signals appear, and how individual signaling steps relate to monitored DMR signatures is not yet fully understood, and constitutes key areas of further investigation. The difference between CHO and HEK293 cells with respect to absolute potencies after GPR17 stimulation can most probably be attributed to different concentrations of the transduction partners involved in the response to RA-II-150. In general, the nature of the observed response not only depends on the nature of G protein preferentially recognized by the receptor, but may also depend on differential expression of signal transduction

components (e.g. receptors, G proteins, effectors and modulatory proteins such as receptor kinases) by different cells (Nasman et al. 2001, Schulte & Levy 2007), and might thus explain cell-dependent signaling differences.

Disregarding the fact that RA-II-150 exhibits distinct potencies in both analyzed cell lines, it was clearly demonstrated that, independent of the cell line, potency of the GPR17 agonist varies considerably for individual G protein subtypes, as clearly illustrated by determined pEC_{50} values (Figure 84). Agonist potency for stimulation of both Gαq and Gαs is less than for Gαi/o, indicating that the latter is preferentially engaged by GPR17 upon stimulation with RA-II-150. Whereas stimulation of Gαq was ~5 and ~100 (CHO and HEK293 cells, respectively) fold less, the potency for Gαs-mediated responses was even stronger reduced by the factors ~115 and ~280 (CHO and HEK293 cells, respectively), thus GPR17 is relatively weakly coupled to Gαs proteins. These observations are in agreement with previously reported findings, which demonstrated that potencies observed for a ligand could be different considering the different signaling pathways regulated by a unique receptor (Ashkenazi et al. 1987, Berg et al. 1998, Brink, Wade & Neubig 2000, Hall et al. 1999, Krueger et al. 2005, Offermanns et al. 1994, Shoemaker et al. 2005). Multiple signaling and a shift between two response curves may be explained by a difference in the affinity of the ligand-receptor complex for each G protein, or by a difference in the relative concentrations of the G proteins (Kenakin 2003).

Besides the described signaling properties of GPR17, the trafficking upon stimulation by RA-II-150 has been characterized, since agonist-promoted internalization represents a regulatory phenomenon common to most GPCRs to limit receptor activation (Ferguson 2001). An expression vector was constructed containing GPR17 fused with haemagglutinin (HA) to the amino-terminus to enable visualization of GPR17 localization and trafficking by use of immuno-labeling techniques, such as ELISA and immunofluorescence microscopy, in self-engineered stably transfected HEK293 cells. The epitope tag haemagglutinin has been widely used to label GPCRs in order to monitor expression and localization (e.g. Hall et al. 1999, Holliday et al. 2005, Oakley et al. 2001, Reiner et al. 2009, Vrecl et al. 1998) and Epic® analyses revealed proper functionality of HA-tagged GPR17 (Figure 43). Immunofluorescence analyses demonstrate that, under control conditions, GPR17 is predominantly located at the cell membrane, but upon activation with RA-II-150, the receptor internalizes from the cell surface into the cytoplasm with a punctate distribution into intracellular vesicles. This phenomenon has been further confirmed by quantitative surface ELISA measurements, which uncover a rapid reduction of GPR17 surface expression in a time-dependent manner upon RA-II-150 challenge. The fate of internalized GPR17 and the underlying molecular mechanisms of the trafficking have not been of current interest for this thesis, but represent an interesting task for future investigations.

Taken together, these findings provide direct evidence that stimulation of human GPR17 recombinantly expressed in two different cell lines (rodent CHO and human HEK293 cells) with our small molecule agonist RA-II-150 leads to activation of multiple G protein subtypes including Gαi/o, Gαs and Gαq, with subsequent stimulation of at least two intracellular signaling cascades and agonist-induced endocytosis. Furthermore, these investigations demonstrate that GPR17 couples to

multiple signaling pathways with the activation of a specific pathway being dependent on the agonist concentration. Receptor coupling to multiple G proteins may provide regulation of different activities within the cell and may play an important role in adjusting the effectiveness of the signals in different tissues. Promiscuity of GPR17 might represent an important means of differentially regulating multiple physiological events by a single molecule interacting with a single receptor.

5.1.2 Characterization of GPR17-BRET2-fusion protein

Prior to examination of β-arrestin recruitment to the agonist-activated GPR17, the generated fusion receptors had to be investigated regarding their pharmacological properties, in order to ensure subsequent BRET2 data to be interpreted as precisely reflecting cellular function (Pfleger & Eidne 2006). Labeling of the N-terminus with 3xHA-tag comprising 27 amino acids did not impair functionality of GPR17 as determined by use of DMR assays (Figure 43).To obtain detailed information of the pharmacological characteristics further functional validations were performed with stable engineered cell lines (HEK293 cells stably transfected with dual labeled human GPR17: 3xHA and RLuc). The cellular localization of the receptor fusion protein was visualized by immunofluorescence microscopy and quantitated by indirect ELISA analyses. Furthermore, signaling properties and internalization behavior upon agonist-stimulation were evaluated and compared to results obtained with unmodified receptor. The investigations demonstrated that GPR17-RLuc retains its capability to couple with Gαi/o and Gαq proteins, promoting inhibition of adenylate cyclase and elevation of intracellular IP1 concentrations, respectively, but cell surface expression is diminished and even more surprisingly, fusion of the receptor to RLuc impairs its stimulatory character on intracellular cAMP levels mediated through Gαs proteins.

Both, quantitative ELISA analyses as well as immunofluorescence microscopy, demonstrated that 3xHA-GPR17-RLuc is expressed at the cell surface, but with a significantly diminished cell surface expression in comparison to wild type GPR17. The decrease in cell surface expression was not due to deficient cellular expression, as indistinguishable total cellular levels of wild type and RLuc-fusion receptor were detected using ELISA assays on permeabilized cells. The internalization rate determined by ELISA was slightly increased for RLuc-fusion GPR17, which could be related to the lowered cell surface expression levels, as it has been demonstrated for B2 bradykinin receptor (Faussner et al. 2003).

In contrast to the data obtained with unmodified GPR17, the preferential activation of Gαi/o versus Gαq by RA-II-150 was diminished in the presence of GPR17-RLuc, as potencies of RA-II-150 did not differ amongst the distinct analysis methods (Figure 85). Although agonist potencies to activate Gαi/o- and Gαq-mediated signaling are significantly lowered when GPR17 is fused to RLuc, the potency to elicit the overall functional response, as determined with the Epic® system, does not differ significantly. This might be owing to the deficit of the least preferred Gαs-promoted signaling pathway, since no stimulating effect on cAMP synthesis was detectable upon challenge with RA-II-150. Another interesting observation is the extreme increase of the relative efficacy in inhibition of cAMP accumulation (Gαi/o-cAMP), despite significantly lower cell surface expression.

This phenomenon is further reflected in DMR analyses, as the optical signatures exceeded those of the unmodified receptor. These findings are probably related to the loss of the counteracting stimulatory Gαs-mediated pathway.

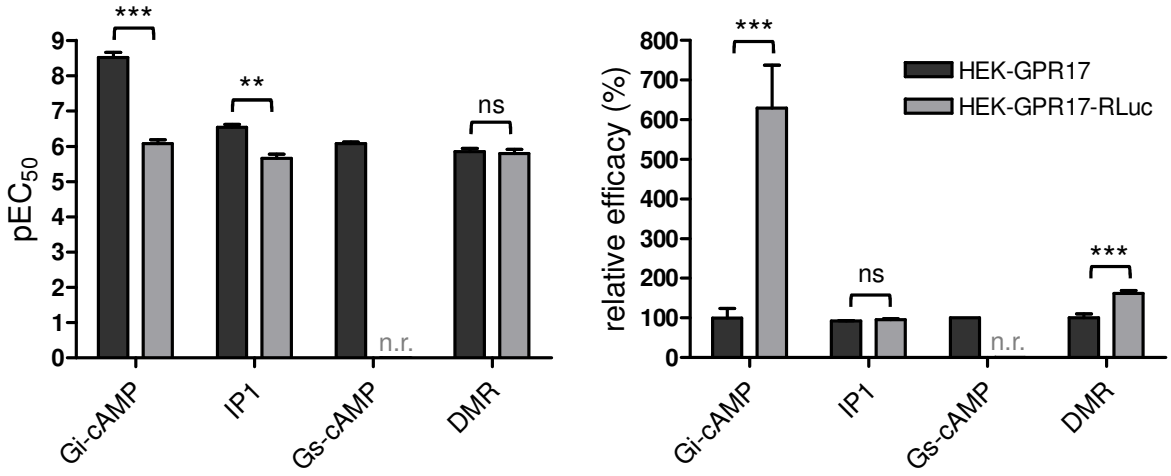

Figure 85 Comparison of pEC_{50} values and relative efficacies of wild type GPR17 and GPR17 C-terminally fused to Renilla luciferase (RLuc) stably transfected in HEK293 cells as determined in a set of distinct functional assays

pEC_{50} values were determined by stimulation of HEK293 cells stably expressing wild type GPR17 (dark grey) and fusion receptor GPR17 C-terminally fused to Renilla luciferase (RLuc) (light grey) cells, respectively, with increasing concentration of RA-II-150 by various functional assays (cAMP and IP1 to analyze traditional second messengers and Epic® technology to monitor dynamic mass redistribution). No response (n.r.) was obtained for HEK-GPR17-RLuc cells in Gs-cAMP assay. For statistical analyses, unpaired t-tests with two-tailed p values and 95% confidence interval were applied (ns $p > 0.05$, **$p < 0.01$), ***$p < 0.001$).

Substantial body of evidence indicates that the C-terminus of GPCRs represents a critical region determining various aspects of receptor functionality, such as expression and trafficking (Delhaye et al. 2007, Pankevych et al. 2003), but as well G protein-dependent and -independent signaling (Hoare et al. 1999, Kang & Leeb-Lundberg 2002, Labasque et al. 2008, Pankevych et al. 2003, Schröder et al. 2009). Consequently, the observed changes of GPR17 fusion protein in comparison to unmodified receptor properties might be induced through elongation of the GPR17 C-terminus. A change in the conformation of cytoplasmic receptor domain may have impaired receptor-G protein-coupling in general, most intensely uncoupling Gαs protein that interacts less efficiently with receptor, resulting in complete abrogation of only one signaling pathway (Gudermann, Schöneberg & Schultz 1997). Interestingly, to the best of my knowledge, so far no BRET fusion receptor has been reported to reveal different pharmacological properties in such an extent as presented here for GPR17. Usually appropriate functionalities of fusion receptors are examined by confocal microscopy, binding studies, internalization assays and second messenger analyses such as cAMP and IP1, and none of the reported fusion receptors (representative for 13 class A GPCRs) was significantly affected regarding its functionality (Angers et al. 2000, Ayoub et al. 2002, Hanyaloglu et al. 2002, Issafras et al. 2002, Kroeger et al. 2001, Ramsay et al. 2002, Terrillon et al. 2003, Vrecl et al. 2004).

Another important aspect that should be noted concerning the remarkable change of signaling properties, is the fact that multiplicity in G protein-coupling was found to depend on the receptor expression level (Brink, Wade & Neubig 2000, Cordeaux et al. 2000, George et al. 1988, Thibonnier et

al. 1997, Zhu et al. 1994). For example Brink et al. reported that the full agonist UK-14,304 inhibits cAMP production in CHO cells expressing α2-adrenergic receptors at high as well as low densities. When the Gαi/o-mediated process is inhibited by preincubation with PTX, UK-14,304 stimulates cAMP accumulation, but this response is very low in CHO cells expressing low receptor densities and much higher in cells with high receptor abundance (Brink, Wade & Neubig 2000). Regarding the fact that cell lines stably expressing GPR17-RLuc were shown to display lower cell surface expression levels compared to wild type, it is tempting to hypothesize that after high abundance of GPR17, coupling of activated receptors to G proteins becomes less specific, leading to the recruitment of additional transducers that are not engaged at lower receptor densities. Accordingly, it could be concluded that the human GPR17 activates several signaling pathways via different G proteins, depending on the level of receptor expression. Under these conditions, the receptor level can control not only the quantity of observed response but also the quality of response. Additional studies would be necessary to further prove this phenomenon, such as gene dosing experiments with the wild type receptor to see whether increasing GPR17 densities are really responsible for pleiotropically G protein-coupling. Answering this question was beyond the scope of this work, as it was only important to characterize pharmacological properties of the fusion receptor to achieve precise interpretations of subsequent BRET2 analyses data.

5.1.3 Classification of GPR17 as a class B receptor recruiting β-arrestin2 in a very rapid and partially G protein-independent manner

As described in the introduction of this thesis, β-arrestins uncouple GPCRs from their cognate G proteins and promote their internalization, leading to desensitization and down-regulation, thus serving as negative regulators of G protein-dependent GPCR signaling. Additionally, β-arrestins function as scaffold proteins, interacting with several cytoplasmic proteins and linking GPCRs to intracellular signaling pathways such as the mitogen-activated protein kinase (MAPK) cascade, hence promoting agonist-induced signaling in their own right.

The natural phenomenon of bioluminescence resonance energy transfer (BRET) is a powerful and increasingly popular tool for studying dynamic protein-protein interactions in intact living cells and real time (for review, see Pfleger & Eidne 2006, Pfleger et al. 2007). Using this technique, an assay was established, based on the observation that translocation of β-arrestin to GPCRs upon ligand-stimulation is a hallmark of receptor activation, as the majority of GPCRs recruit β-arrestin independently of their signaling pathway (Angers et al. 2000, Hamdan et al. 2005, Vrecl et al. 2004, for review see Pierce & Lefkowitz 2001, Perry & Lefkowitz 2002). Using a GFP2-tagged β-arrestin2, it was possible to measure changes in the amount of β-arrestin2 that was in close proximity to the RLuc-tagged-GPR17. The analyses of β-arrestin recruitment upon receptor stimulation by means of BRET2 technology revealed that β-arrestin2 interacted with RA-II-150-activated GPR17 in a concentration-dependent manner, and the obtained pEC_{50} value corresponds well to previously determined values using other functional assays (Figure 85). Moreover the observed sustained signal disclosed stable and persistent association between both proteins. GPCRs can be classified into two distinct classes (class A and B) according to their stability of receptor/β-arrestin interactions (Oakley

et al. 2000, Freedman & Lefkowitz 1996). The members of class A possess higher affinity for β-arrestin2 than β-arrestin1, and only interact in a transient manner, whereas the members of class B bind both β-arrestin1 and 2 with equivalent affinity and their interactions are more stable. Members of class A do not co-internalize with β-arrestin and are rapidly dephosphorylated and recycled back to the plasma membrane, whereas members of class B internalize together with β-arrestin into endosomes and are weakly dephosphorylated and recovered to the cell surface. The stability of the GPR17/β-arrestin2 association determined by BRET2 assays is in agreement with a class B phenotype where the receptor internalizes with β-arrestin in endosomes and slowly recycles back to the plasma membrane (Oakley et al. 1999, Oakley et al. 2000, Oakley et al. 2001, Tohgo et al. 2003). Accordingly, GPR17 would be classified as a class B receptor when stimulated with the small synthetic agonist RA-II-150. These findings are further proven, as the amplitude of the RA-II-150-induced BRET2 signal (~130 mBRET) is considerably high in comparison to other published findings (e.g. Hamdan et al. 2005), an effect that could also be explained by the observation that the association of β-arrestin2 with agonist-stimulated GPR17 is very stable. Another possibility is that the interaction of β-arrestin2 with GPR17 favors optimal distance and relative orientation, respectively, between the energy acceptor and the donor, leading to larger BRET2 signals than seen for other receptors, which previously has been postulated for class B receptors (Hamdan et al. 2005).

In addition to the described long-term receptor-arrestin interaction, real time readings over short time periods to investigate kinetic of RA-II-150-induced recruitment of β-arrestin2 to the activated GPR17 have been performed. Since the applied Renilla luciferase substrate coelenterazine 400A is not stable over time (t½ ~1 min, Hamdan et al. 2005), the assay time span was restricted to 140 seconds, taking measurements every 2.4 seconds. The temporal setting of the measurement can exceed the half-life of the substrate since the assay is ratiometric, thus a decrease in luminescence does not necessarily influence the BRET signal as long the luminescence signal does not decline below the sensitivity of the detector used. Interestingly, RA-II-150-induced BRET increase occurs considerably rapid without any lag time and maximum β-arrestin2-association is already reached after ~60 s. In contrast to these findings, several reports indicate that the interaction between agonist-activated GPCR and β-arrestin occurs in a much slower rate. Neuropeptide Y receptors (NPY1, NPY2, NPY4 and NPY5 receptors) have been shown to reach maximal β-arrestin association not until 20 to 60 min after agonist activation as determined by BRET2 analyses (Berglund et al. 2003). Similar to these observations, Ayoub et al. demonstrated by use of BRET1 technology that association of β-arrestin with the activated protease-activated receptor 1 reaches its maximum not until ~30 min after ligand stimulation (Ayoub et al. 2007). Further real time BRET1 examinations of agonist-promoted β-arrestin recruitment to GPCRs are given by Hamdan et al., who reported that V1a and V2 vasopressin receptor, β2-adrenergic receptor, chemokine receptor CCR5 and platelet-activating factor receptor require at least 5 minutes to reach maximum of respective β-arrestin association (Hamdan et al. 2005).

Kinetics of G protein-coupled receptor signaling and desensitization have been reviewed by Krasel et al, and they propose GRK phosphorylation as the time-limiting step in receptor–arrestin interaction. Receptor phosphorylation has been shown to be the slowest of all analyzed processes, including

receptor activation measured as conformational changes within the receptor, G protein activation measured as G protein subunit rearrangement, receptor phosphorylation by GRK, and β-arrestin-recruitment. Subsequent binding of β-arrestin to the activated receptor is fairly rapid and may occur within a few seconds (reviewed by Krasel et al. 2004). Further BRET studies investigating the interaction between oxytocin receptor and GRK2 revealed that the time course for the interaction with β-arrestin lagged behind the interaction of GRK, with the GRK2 interaction occurring within 4 s, and the β-arrestin interaction occurring after a 10 s delay, which is consistent with the requirement, that GRK-catalyzed phosphorylation must precede arrestin binding (Hasbi et al. 2004). Moreover, FRET based analyses between β2-adrenoceptor and βarrestin2 revealed a rapid phosphorylation-independent association followed by a slower phosphorylation-dependent phase (Violin, Ren & Lefkowitz 2006). Regarding the observed rapid β-arrestin recruitment kinetic to agonist-activated GPR17, one could conclude that receptor phosphorylation seems to play no essential part in β-arrestin translocation. Although the majority of GPCRs has been reported to be phosphorylated to enhance β-arrestin affinity, it is also clear that for some receptors, phosphorylation is not an absolute requirement for arrestin binding. Leukotriene B4 receptors (Jala, Shao & Haribabu 2005), protease-activated receptor-1 (Chen, Paing & Trejo 2004), lutropin receptor (Mukherjee et al. 2002) and substance P receptor (Richardson et al. 2003) are examples of receptors whereby β-arrestin binding occurs independently of receptor phosphorylation. Additionally, β-arrestin binding is maintained in mutants of the orexin-1 (Milasta et al. 2005), dopamine D2 (Cho et al. 2010) and protease-activated receptor-2 receptors (Stalheim et al. 2005) despite the removal of the putative phosphorylation sites. However, where phosphorylation seems to be not obligatory for arrestin translocation, it seems that the interaction of the active conformation of the receptor with the β-arrestin itself is sufficient to provide a functional receptor–arrestin complex. Since these conclusions are only hypotheses based on real time β-arrestin2 recruitment kinetics, additional studies are absolutely essential to decipher the necessity of prior receptor phosphorylation. For example, analyses could be performed to see whether over-expression of GRKs and their dominant-negative mutants, respectively, or deactivation by small interfering RNA exhibit effects on β-arrestin recruitment (Hasbi et al. 2004, Violin, Ren & Lefkowitz 2006). The use of transgenic and knock-out mouse models represents another important tool to determine *in vivo* specifity of GRKs and β-arrestins (Kohout & Lefkowitz 2003).

In addition to this phosphorylation-independent association, GPCRs have been demonstrated to interact with β-arrestins independent of heterotrimeric G protein-coupling. Furthermore, increasing evidence is emerging that this interaction is capable to elicit signals in its own right, as extensively reviewed by many authors, e.g. (Defea 2008), (DeWire et al. 2007), (Ferguson 2001), (Lefkowitz & Shenoy 2005), (Luttrell & Lefkowitz 2002), (Luttrell & Gesty-Palmer 2010), (Reiter & Lefkowitz). Thus, it was another aim to get more insight into the underlying mechanism of β-arrestin2 recruitment to the agonist-activated BRET2-fusion receptor GPR17-RLuc, and interestingly complete abolishment of present G protein-dependent signaling by pharmacological inhibitors reveals only partial inhibition of the GPR17-promoted β-arrestin2 translocation. At first the pharmacological tools have been tested for their property to inhibit GPR17-mediated G protein-dependent signaling, and investigations by traditional second messenger assays clearly demonstrate that preincubation with either PTX to

diminish Gαi/o-mediated cAMP inhibition or YM-254890 to abolish Gαq-triggered IP1 accumulation, completely abrogates RA-II-150-induced second messenger alterations. Additional Epic® analyses further support these conclusions, as application of individual inhibitors (PTX or YM-254890) partly diminishes GPR17-triggered DMR response, whereas simultaneous usage completely abrogates the monitored optical signatures elicited by RA-II-150. Subsequent BRET2 analyses clearly demonstrate that inhibition of G protein-dependent signaling, obtained by simultaneous preincubation with both PTX and YM-254890, does not completely impair translocation of β-arrestin2, since almost the half (45.2 +/- 6.6%) is still recruited to the RA-II-150-activated receptor. Consequently, GPR17 can be described as a 'balanced' receptor that features the capability to recruit the scaffolding protein β-arrestin2 in a G protein-dependent as well as –independent manner. To demonstrate whether the latter behavior exhibits signaling properties in its own right, such as activation of mitogen-activated protein kinase (MAPK) cascade, further investigations are necessary, but not part of the present thesis and thus, up to now, remain so far elusive.

Nevertheless, the Epic® analyses revealed further interesting conclusions: one, regarding signaling properties of GPR17 and the other one, revealing information about detection sensitivity provided by DMR analyses. Whereas second messenger assays are suitable to uncover activation of Gαi/o, Gαq and Gαs sensitive receptors, such assays do not exist to detect Gα12/Gα13 signaling, but DMR technology has been reported to identify signaling along the Gα12/Gα13 pathway (Schröder et al. 2010). Since simultaneous preincubation with PTX and YM-254890 completely abrogated optical signatures elicited by RA-II-150 stimulation, it is clearly demonstrated that the Gα12/Gα13 pathway does not play a role in GPR17 signaling, at least for the BRET2-fusion receptor, which is investigated here. Another important aspect, based on the complete abolishment of GPR17-triggered DMR response through pharmacological inhibition of both involved G protein-dependent pathways (Gαi/o and Gαq), is the fact that although GPR17-mediated DMR is entirely prevented, BRET2 assays still reveal recruitment of β-arrestin2. Consequently, the Epic® technology is not able to detect the G protein-independent β-arrestin2 recruitment to the RA-II-150-activated GPR17, which is an important information that has not been reported before, especially regarding the existence of arrestin-biased ligands (e.g. Gao & Jacobson 2008, Wei et al. 2003, for review see Violin & Lefkowitz 2007) that could be missed while screening with the Epic® system.

Another important general aspect for future analyses is that the generated double stable BRET2 cell line represents a suitable tool to monitor and quantify GPR17 activation in a pathway unbiased manner, for G protein-dependent and -independent events, in real time and in living cells. Consequently, this cell line will be helpful for further universally applicable functional cell-based screening analyses to characterize ligand-GPR17 interactions, since the inclusion of G protein-independent pathways represents a helpful tool for future deorphanization studies.

5.1.3.1 Uncovering the postulated small molecule pan-G protein inhibitor BIM-46187 to act in a cell type-dependent manner

While analyzing G protein-dependence of β-arrestin2 recruitment to the agonist-activated GPR17, the small molecule pan-inhibitor of GPCR signaling BIM-46187, published to inhibit all isoforms of Gα

proteins (Ayoub et al. 2009), has been shown to exhibit cell type-dependent inhibition properties. Recently, BIM-46187 was demonstrated to prevent the accurate interaction of receptors with the G protein heterotrimer through a direct binding to the Gα subunit, consequently promoting inhibition of the agonist-induced GDP/GTP exchange (Ayoub et al. 2009). Based on the reported information, BIM-46187 has been applied as a promising tool to simultaneously abrogate both GPR17-RLuc-activated signaling pathways (Gαi/o and Gαq), but surprisingly traditional second messenger analyses disprove the postulated characteristics. Preincubation of HEK293 cells stably expressing GPR17-RLuc with BIM-46187 does neither alter RA-II-150-induced decrease of adenylate cyclase activity nor significantly inhibit prostaglandin E1 mediated increase of intracellular cAMP via endogenously expressed Gαs-linked prostanoid receptors (EP2R and EP4R, Willoughby et al. 2007). However, IP1 analyses revealed that BIM-46187 significantly and almost completely diminishes the GPR17-mediated IP1 production in a concentration-dependent manner. This apparent pathway-specific inhibition property has been further proven, as carbachol-induced IP1 production through activation of endogenously expressed muscarinic receptors (M1 and M3, Estacion et al. 2004, Mundell & Benovic 2000) is likewise inhibited by preincubation with BIM-46187, whereas the small molecule inhibitor exhibits no significant impact on basal IP1 levels of HEK293 cells. Further evidence of Gαq-selective inhibition has been provided by BRET2 analyses of β-arrestin recruitment, since both inhibitors YM-254890 (known as selective Gαq/11-inhibitor) and BIM-46187 reveal comparable results. Consequently, since BIM-46187 inhibits neither Gαi/o- nor Gαs- mediated modifications of intracellular cAMP accumulation, but rather exclusively prevents Gαq-promoted increase of IP1 concentrations, the small molecule can be regarded as a pathway-selective inhibitor in HEK293 cells, despite the previously reported pan-inhibition properties. In contrary, subsequent analyses in COS-7 cells, which have also been applied in the original report, support the results presented by Ayoub et al., since prostaglandin E1-stimulated cAMP accumulation via endogenously expressed Gαs-linked prostanoid receptors is significantly impaired by preincubation with BIM-46187, whereas forskolin-stimulated cAMP accumulation is not sensitive to the pretreatment, indicating G protein-dependent modifications. This led to the conclusion, that BIM-46187 does not only exhibit pathway-selective inhibition properties, as demonstrated in HEK293 cells, but furthermore cell-type dependent action.

A very recent report demonstrated that HEK293 cells express an almost full complement of mRNA encoding for G protein isoforms for each subunit, whereas Gαq was shown to be the least abundant subunit compared to Gαi/o and Gαs, as determined by means of microarray technology (Atwood et al. 2011). This lower expression could be a reason for the selective inhibition of Gαq-mediated signaling by BIM-46187 observed in HEK293 cells, since less substance would inherently be necessary to fully abrogate activity of this G protein subunit. If this would be the case, application of higher BIM-46187 amounts should diminish the remaining G protein-dependent signaling pathways, but due to poor solubility of the inhibitor no concentration higher than the applied (100 µM) could be added, thus it remains elusive whether the expression levels of G protein subunits are the reason for the selective inhibition. Furthermore, this consideration can be translated to differential inhibition behavior observed between both analyzed cell lines, HEK293 and COS-7. Similar to discrepancies of signaling properties that do not only depend on which G protein is preferentially recognized by the

receptor, but also based on differential expression of signal transduction components (e.g. G proteins) by different cells (Nasman et al. 2001, Schulte & Levy 2007), the observed cell type-dependent inhibition potencies of BIM-46187 can be explained, assuming that COS-7 cells possess lower amounts of G protein subunits.

As so far only one selective inhibitor for Gαq/11 has been reported (Taniguchi et al. 2003), which is not commercially available, BIM-46187 as a novel Gαq/11 inhibitor represents a valuable tool for signaling analyses of GPCRs, although to date restricted to HEK293 cells.

5.1.4 In search of an appropriate cellular system to investigate natural occurring signaling pathways

Several GPCRs are known to activate multiple signaling systems, such as corticotropin-releasing hormone receptor, metabotrophic glutamate receptor or the prostacyclin receptor to name but a few (Grammatopoulos et al. 2001, Hermans et al. 2000, Lawler, Miggin & Kinsella 2001, summarized in Table 1). The involvement of multiple G proteins may arise from differences in the expression levels of the participating G proteins (Nasman et al. 2001). Furthermore, it is known that the use of recombinant systems might produce results that depend on cell type, transducer or effector availability, especially when dealing with GPCRs (Kenakin 1997). Multiplicity is frequently observed in recombinant over-expression systems where elevated densities of receptors are present, suggesting that over-expression of the receptor might favor additional coupling with the most abundant G protein (Gudermann, Schöneberg & Schultz 1997). Controversially, sufficient studies have confirmed the pleiotropic nature of GPCRs in native tissues. One such example is given by the thyrotropin (TSH) receptor, which was found to simultaneously activate members of all four classes of G proteins (Gαs, Gαi/o, Gαq/11 and Gα12) in human thyroid membranes (Laugwitz et al. 1996). Another example is given by the CB1 cannabinoid receptor that has been demonstrated to couple both Gαs (Glass & Felder 1997, Bash et al.) and Gαq/11 (McIntosh et al. 2007) in models where cannabinoid receptors are endogenously expressed.

To further verify demonstrated multiplicity of GPR17 observed in recombinant cell systems and elucidate naturally occurring signaling pathways of GPR17, an experimental approach was chosen to identify an appropriate cell system by means of the Epic® system, which enables whole-cell and label-free analyses of endogenously expressed GPCRs with high sensitivity (Fang, Li & Ferrie, Fang & Ferrie 2007, Schröder et al. 2010). Since none of the analyzed immortalized and primary cell lines responds to the stimulation with the GPR17-agonist RA-II-150, the natural occurrence of promiscuous coupling of GPR17 upon activation with RA-II-150 remains elusive at present. However, establishment and validation of primary cultures endogenously expressing GPR17 will be a task of the near future, especially oligodendrocyte precursor cells (OPCs), which have been reported to express GPR17 (Lecca et al. 2008, Chen et al. 2009, Fumagalli et al. 2011, Ceruti et al. 2011), represent an interesting cellular system to analyze influence of our synthetic agonist RA-II-150 on oligodendrogliogenesis.

The modification of murine embryonic stem cells by gene targeting to obtain pluripotent cells with heterozygous knocked-out GPR17 was successfully performed. Although a second modification is necessary to completely knock-out the GPR17 gene, these cells already represent a promising cellular tool lacking the desired receptor, and featuring the capability to be differentiated into a desired cell system, especially of neural cell type such as cortical neurons (Gaspard et al. 2009) or spinal cord motor neurons (Wichterle et al. 2002). Thus, pharmacological comparison of wild type and knock-out neural cells will provide further information about the physiological role of GPR17 without the need of animal experiments, as generation of transgenic knock-out mice can be circumvented.

5.1.5 Fascinating dualistic role of GPR17

Increasing evidence is emerging that heterodimerization between orphan and non-orphan GPCRs opens an interesting possibility that orphan receptors regulate the ligand binding, signaling and/or trafficking of GPCRs with known ligands. The first and best characterized heterodimer that is composed of an orphan and a non-orphan GPCR is the metabotrophic γ-aminobutyric acid B ($GABA_B$) receptor heterodimer. The functional $GABA_B$ receptor is composed of two homologous subunits called $GABA_{B1}$ and $GABA_{B2}$ (Jones et al. 1998, Kaupmann et al. 1998, White et al. 1998). While the non-orphan $GABA_{B1}$ provides ligand binding, the orphan $GABA_{B2}$ subunit is obligatory for efficient transport of $GABA_{B1}$ to the cell surface and promotes G protein-coupling (Pin et al. 2005). Further support for the role of orphan GPCRs in ligand-independent modulation of receptor signaling and internalization comes from the Mas-related gene (Mrg) family members that consist of orphan and non-orphan GPCRs. MrgD subtype, known to be activated by β-alanine and MrgE, which has not been matched with any known ligand, have been shown to form heterodimers when transfected in HEK293 cells (Milasta et al. 2006). Binding of β-alanine to MrgD, when expressed alone, activates the extracellular-signal-regulated kinase (ERK1 and 2) pathway and receptor internalization. Coexpression of MrgD with the orphan MrgE potentiates ß-alanine induced MrgD signaling and impairs ligand-promoted MrgD internalization in the MrgD/MrgE heterodimer (Milasta et al. 2006). Another example of the association between orphan 7TM proteins with non-orphan GPCRs shows that orphans can also negatively modify the signaling of their interacting partners. Engagement of the orphan GPR50 into heterodimers with melatonin receptor (MT1), known to bind the circadian neurohormone melatonin, drastically impairs ligand-induced MT1 functionality, namely inhibition of high-affinity agonist binding, heterotrimeric G protein-coupling and β-arrestin binding in cells expressing both proteins heterologously (HEK293 cells) and endogenously (human endothelial cerebral CMEC/D3 cells) (Levoye et al. 2006). Consequently, GPR50 can be considered as a natural negative modulator of MT1.

One could consider that GPR17 provides similar characteristics as described for GPR50, since GPR17 has been reported to act as ligand-independent negative regulator of CysLT1 receptor (Maekawa et al. 2009). Furthermore GPR17 has been demonstrated to be constitutively active through Gαi (Benned-Jensen & Rosenkilde 2010), thus proclaiming that GPR17 acts ligand-independent, but nonetheless exhibits functional activity. Whereas the ligand-independent functional activity of GPR17 could not be verified, neither in stably (as presented in this work) nor in transiently (data not shown,

Lucas Peters, AK Kostenis) transfected HEK293 cells, the dominant negative ligand-independent inhibition of CysLT1 receptor has been further proven in our laboratory. Upon transient coexpression of both receptors in HEK293 cells, GPR17 silenced CysLT1 functionality as monitored by means of the Epic® system (data not shown, Lucas Peters, AK Kostenis). Conversely, CysLT1 did not impair signaling properties of GPR17, thus indicating that no reciprocal inhibition by CysLT1 of GPR17 took place. Having characterized GPR17 as a receptor featuring common properties like the majority of known GPCRs upon agonist-stimulation, such as G protein-dependent signaling events (Gαi/o, Gαs and Gαq), recruitment of β-arrestin2 to the activated receptor in G protein-dependent and -independent behavior, and internalization in a ligand- and time-dependent manner (Figure 86), leads to the conclusion that this receptor, in contrast to the above mentioned orphan GPCRs, exhibits a dualistic role, that to the best of my knowledge has not been described before. On the one hand a ligand-independent function as negative-regulator of CysLT1 receptor, and on the other hand GPR17 features signaling in its own right upon agonist stimulation.

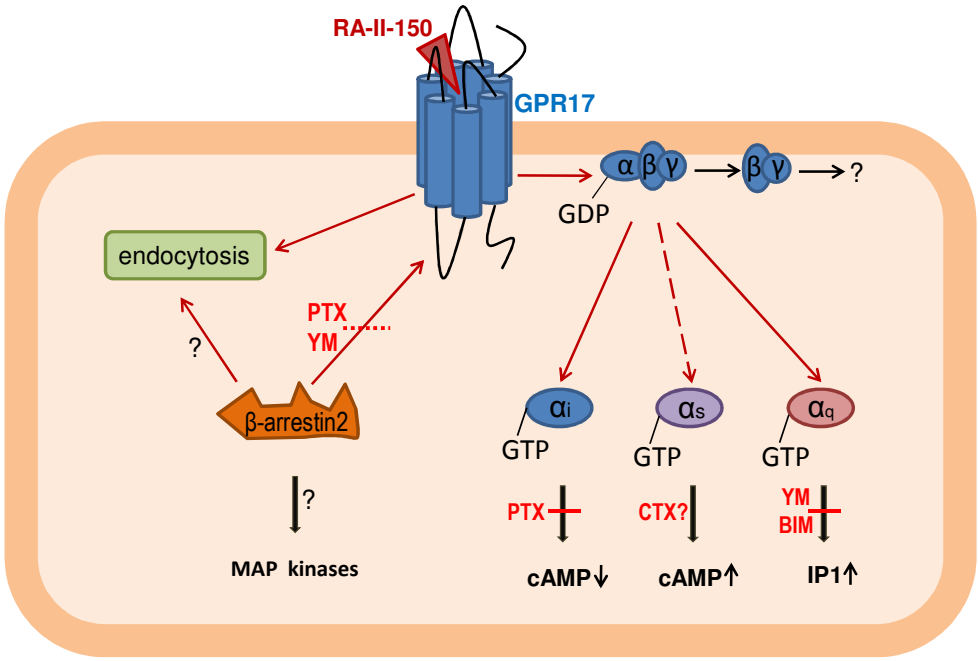

Figure 86 Multiple cellular events initiated by GPR17 upon stimulation with RA-II-150
Activation of GPR17 with RA-II-150 causes endocytosis of the activated receptor and recruitment of β-arrestin2, the latter shown to be only partially G protein-dependent. The dependence of β-arrestin2 for GPR17 endocytosis, the cellular response mediated by the βγ-subunit, as well as β-arrestin-mediated activation of mitogen-activated protein kinase (MAPK) remains elusive so far (indicated with a ?). RA-II-150-activated GPR17 preferentially couples to pertussis toxin (PTX)-sensitive Gαi/o protein, which was demonstrated in the inhibition of adenylate cyclase leading to decrease of cyclic adenosine monophosphate (cAMP) synthesis. Furthermore, GPR17-induced activation of phospholipase C and the consequent synthesis of inositol monophosphate (IP1) was shown to be sensitive to YM-254890 and BIM-46187, indicating an involvement of Gαq/11. High concentrations of GPR17 receptor agonist RA-II-150 were also capable to mediate adenylate cyclase activation, indicating a possible coupling with Gαs proteins. This stimulatory effect was lost (broken arrow) in analyzed HEK-BRET-GPR17 cell lines (for detailed information see main text).

It is conceivable that this phenomenon of dual activity may represent a currently underappreciated strategy of a wide range of liganded GPCRs to fine-tune cellular signaling with great implication for development of GPCR targeted drugs.

It should be further mentioned that high-level expression of GPCRs may induce artificial interactions that might not be present in a physiological environment. Therefore, the application of cells with endogenous receptor expression is of interest. Both GPR17 and CysLT1 have been demonstrated to be expressed in bone-marrow derived CD11c-positive dendritic cells (DC) by RT-PCR analyses (Itagaki et al. 2009). Dendritic cells are potent antigen-presenting cells (APCs), and are known to promote and modulate the immune response through a variety of mechanisms, whereby one major function is stimulation of quiescent, naïve and memory B and T lymphocytes (Banchereau & Steinman 1998). Furthermore, CysLTs (LTD4 and LTC4) were found to regulate DC migration (Robbiani et al. 2000), and Machida et al. reported that *in vitro* treatment with LTD4 modifies the cytokine profile (IL-10) of DCs pulsed with house dust mite allergens (*Dermatophagoides farina*) and enhance these DCs to induce a Th2 response *in vivo* (Machida et al. 2004). Additionally, CysLTs were reported to potentiate DC functions such as Ag-presenting capacity and cytokine production (Okunishi et al. 2004). Consequently, primary bone marrow-derived DCs or an immortal DC line termed JAWSII (ATCC® CRL-11904™), that exhibits similar immunobiological characteristics and functions (Jiang et al. 2008), could represent an appropriate cellular system for further investigations of the regulatory role of GPR17 on CysLT1 receptor and its physiological relevance, especially consequences of GPR17 activation with our small molecule agonist on immunobiological responses represent an interesting task for future analyses.

5.2 Emerging role for β-arrestin as a modifier of GPR17-triggered G protein-dependent signaling

In the present thesis four HEK293 cell lines were engineered to stably coexpress GPR17 and differing amounts of β-arrestin2 to uncover the impact of the scaffolding protein as a regulator for the agonist-activated GPR17. HEK293 cells stably transfected with β-arrestin2 were kindly provided by J. M. Mathiesen, and the amino-terminal fusion of β-arrestin2 with the autofluorescent epitope tag green fluorescent protein 2 (GFP2) allows determination of respective expression levels and was assessed by fluorescence activated cell sorting (FACS) analyses, as conducted by J. M. Mathiesen (Department of Medicinal Chemistry, University of Copenhagen). Imaging of the cells by use of a fluorescence microscope revealed an even distribution of β-arrestin2 within the cell cytosol (Annex Figure 2).

5.2.1 Increase of β-arrestin2 levels reveal no obvious impact on RA-II-150-induced GPR17 endocytosis in HEK293 cells

Numerous studies to date have employed over-expression of either wild type or dominant negative arrestins with heterologously expressed GPCRs to elucidate the role of these scaffolding proteins for GPCR trafficking (e.g., Anborgh et al. 2000, Aramori et al. 1997, Ferguson et al. 1996, Kim et al. 2001, Ménard et al. 1997, Vrecl et al. 1998, Zhang et al. 1996). Further techniques to reduce endogenous arrestin levels, such as RNA interference (e.g., Ahn et al. 2003, Li et al. 2010), antisense strategies (e.g., Mundell, Loudon & Benovic 1999, Mundell & Benovic 2000) and generation of β-arrestin-

deficient mice (e.g., Kohout et al. 2001, Vines et al. 2003) were employed to determine the impact of β-arrestins on internalization, desensitization and resensitization of GPCRs.

In the present thesis the effect of increased β-arrestin2 amounts on GPR17 internalization was evaluated, and despite a suspected augmented endocytosis due to the previously determined long lasting association between GPR17 and β-arrestin, all three analyzed cell lines reveal undistinguishable internalization rates upon stimulation with RA-II-150, which might suggest a β-arrestin-independent internalization mechanism. Although it is known that β-arrestin serves as trafficking molecule participating in agonist-promoted receptor internalization, it has been reported that GPCRs might react differently on arrestin-over-expression, amongst others depending on the respective cellular differences. The angiotensin AT1a receptor, for example, has been shown to significantly increase internalization upon agonist-stimulation due to elevated expression of β-arrestin1 amounts both in HEK293 and COS-7 cells (Zhang et al. 1996), and thyrotropin-releasing hormone (TRH) receptor was reported to show a significant higher sequestration rate in COS-7 cells when coexpressed with increased β-arrestin concentrations (Vrecl et al. 1998). In contrary, agonist-induced endocytosis of gonadotropin-releasing hormone (GnRH) receptor was unchanged despite increased β-arrestin concentrations in COS-7 cells (Vrecl et al. 1998), whereas the β2 adrenergic receptor (β2AR) revealed cell dependent characteristics, as β-arrestin over-expression induced significantly increased sequestration in COS-7 cells (Zhang et al. 1996), but not in HEK293 cells (Ferguson et al. 1996, Ménard et al. 1997, Zhang et al. 1996). Cellular differences were claimed to be due to known higher endogenous β-arrestin expression levels in HEK293 cells compared to COS-7 cells, which express about 70% less total β-arrestins/mg protein (Ménard et al. 1997). Consequently, under conditions chosen for the present thesis, β-arrestins probably do not represent the limiting factor necessary for the endocytotic machinery. Since influence of β-arrestin2 on RA-II-150-promoted GPR17 endocytosis was only examined in HEK293 cells, further investigations are necessary to determine whether agonist-induced internalization occurs independently of β-arrestin2-recruitment or whether sequestration rate already reaches its maximum in the presence of endogenous β-arrestin amounts present in HEK293 cells and other, recently unknown participants, represent the rate limiting factors.

5.2.2 A novel role for β-arrestin as a fine-tuner of promiscuous G protein-dependent signaling

For many GPCRs it has been shown that besides the mentioned effect on internalization, the presence of β-arrestins is required to quench receptor signal and to enhance the desensitization process (Wilden, Hall & Kühn 1986, Benovic et al. 1987, Schlador & Nathanson 1997, for review, see Ferguson et al. 1998, Ferguson 2001). Nevertheless, only little and partly controversial information is given about the direct effect of β-arrestin on G protein-triggered signaling events, especially regarding the formation of downstream signaling, such as modification of second messengers. However, over-expression of β-arrestins, which are known to accelerate the uncoupling of GPCRs from their cognate G proteins, would be expected to attenuate receptor-mediated signaling events. In agreement with this hypothesis, inhibition of endogenously expressed β-arrestin2 by means of

RNA interference (Ahn et al. 2003) and transgenic knock-out of β-arrestin1 and 2 (Kohout et al. 2001), respectively, were shown to enhance cAMP elevation induced by agonist activation (isoproterenol) of Gαs-linked β2 adrenergic receptor (β2AR), whereas Mundell et al. reported that repression of both β-arrestins using an antisense strategy did not significantly alter β2AR-mediated cAMP accumulation (Mundell, Loudon & Benovic 1999). Application of the same antisense strategy further revealed that inhibition of β-arrestins enhanced neither somatostatin receptor- nor AT1a angiotensin receptor-mediated inhibition of forskolin-stimulated adenylate cyclase activity (Mundell & Benovic 2000). Furthermore, the calcium responses for Gαq-linked muscarinic M1 mACh, and purinergic P2Y1 and P2Y2 receptors were shown to be unchanged in antisense-expressing cells compared with vector transfected controls, whereas solely the IP1 accumulation mediated by M1 mACh receptor, neither by P2Y1 nor by P2Y2 receptor, was enhanced via repression of endogenous β-arrestins (Mundell & Benovic 2000). Further contradictory examples demonstrate the positive effect of reduced β-arrestin levels on GPCR triggered calcium release, e.g. silencing of β-arrestin by means of RNA interference increased carbachol-induced calcium release via M3 mACh receptor (Luo, Busillo & Benovic 2008), and calcium mobilization promoted by the chemokine receptor CXCR2 was elevated in neutrophils obtained from transgenic β-arrestin2-deficient mice (Su et al. 2005). All the mentioned examples have only evaluated the effect of reduced β-arrestin levels on GPCR-mediated second messenger modifications, and just one possible signaling pathway has been considered, although the receptor might reveal dual coupling, as shown for the angiotensin AT1a receptor. Whereas Mundell et al. only investigated the Gαi/o-linked inhibition of adenylate cyclase (Mundell & Benovic 2000), Kohout et al. examined the Gαq-mediated IP1 accumulation (Kohout et al. 2001), and Tohgo et al. analyzed the effect of elevated β-arrestin levels on intracellular IP1 concentrations, all three investigating the effect of AT1a receptor upon stimulation with angiotensin II, but none of them evaluated reciprocal or overall influences of distinct β-arrestin amounts on the dual G protein-dependent signaling pathways.

In the present thesis the use of the Epic® technology enabled to analyze the effect of increased β-arrestin levels on the overall DMR response that has been shown to be based on Gαi/o-and Gαq-promoted signaling pathways. In agreement with the studies mentioned before, the overall relative efficacies determined by stimulation with RA-II-150 are diminished in the presence of increasing amounts of β-arrestin, whereas, surprisingly, the obtained data further demonstrate that the presence of elevated β-arrestin2 amounts boosts the potency of our small molecule agonist RA-II-150, as depicted by pEC_{50} values in Figure 87. Moreover, this enhanced potency is clearly diminished in the presence of PTX, highlighting an important role for Gαi/o protein-triggered signaling, which is further confirmed by an enhanced PTX-sensitivity of GPR17-induced DMR responses in the presence of elevated β-arrestin2 amounts, as illustrated by impaired relative efficacies (Figure 87). Consequently, these findings indicate that besides the expected inhibition of the overall response due to an accelerated uncoupling from the cognate G proteins, the preference of the promiscuous G protein-coupling mediated by agonist-activated GPR17 seems to be shifted to the most preferred one (here Gαi/o-protein), as manifested by elevated potencies.

This phenomenon was further investigated by traditional second messenger assays, namely by examination of intracellular cAMP and IP1 modifications. Interestingly, the results obtained by cAMP analyses clearly resemble the data determined by use of the DMR technology in the absence of PTX, as illustrated by similar ascending pEC_{50} values in the presence of increasing β-arrestin2 amounts. Thus, the Gαi/o protein-mediated signaling events can be regarded as major if not even sole initiator for GPR17-elicited DMR responses in the presence of elevated β-arrestin2 amounts. This conclusion is further supported by the fact that investigations of intracellular IP1 changes revealed, in all cell lines coexpressing β-arrestin2, an almost complete inhibition of GPR17-mediated increase of inositol-1-phosphate (IP1), whereby only the highest applied RA-II-150 concentration (100 µM) triggered a measurable hydrolysis of inositol phospholipids. This lack of response agrees very well with the conclusions drawn from DMR analyses, namely that in the presence of augmented β-arrestin2 levels the optical signatures elicited by challenge of GPR17 are almost exclusively caused by downstream events of Gαi/o proteins. Further inhibition of the simultaneously occurring and probably competing Gαi/o-mediated signaling by use of PTX preincubation, prior to IP1 analyses, triggers a reversal of the observed phenomenon and sensitizes the Gαq-coupled signaling, resulting in similar magnitudes and potencies of determined concentration-response curves amongst all analyzed cell lines. Accordingly, the observed insufficient coupling with Gαq proteins is probably caused by an elevated desensitization rate due to increased β-arrestin2 amounts, and initiated by the concurrently occurring and preferred Gαi/o-mediated signaling.

Another interesting aspect that should be noted is the fact that relative efficacies determined by DMR and cAMP assays are clearly impaired by coexpression of augmented β-arrestin2 levels, as it would be expected due to enhanced uncoupling mechanisms, but the relative efficacies observed by use of IP1 analyses, in the presence of PTX, were almost indistinguishable, with the exception of the *very high* cells revealing very low GPR17 expression levels. Thus, these findings somehow mirror the beforehand mentioned controversial effects of β-arrestin on GPCR-triggered signaling, since e.g. Tohgo et al. postulated a reduction of AT1a receptor-mediated IP1 accumulation by over-expression of β-arrestin2 (Tohgo et al. 2002), and Kohout et al. demonstrated that both single and double knock-out of both β-arrestins increases AT1a receptor-triggered hydrolysis of phosphatidylinositol hydrolysis (Kohout et al. 2001), whereas Mundell et al. reported an increase of M1 mACh receptor-induced IP1 response but neither of P2Y1- nor of P2Y2-mediated IP1 production via antisense strategy to silence β-arrestin1 and 2 (Mundell & Benovic 2000).

Taken together, the observed findings demonstrate that over-expression of β-arrestin2 with heterologously expressed GPR17 not only exhibits the expected capability to impair the agonist-induced response efficacies, but rather enhances the potency of the overall responses upon stimulation with RA-II-150, as confirmed by increased pEC_{50} values using the DMR technology. This potency boost has been shown to emerge from a preference shift of the promiscuous G protein-coupling to the most preferred one, which has been previously determined to be the Gαi/o protein. Consequently, the Gαi/o protein-mediated signaling consequences gain more overall weight for GPR17-triggered responses.

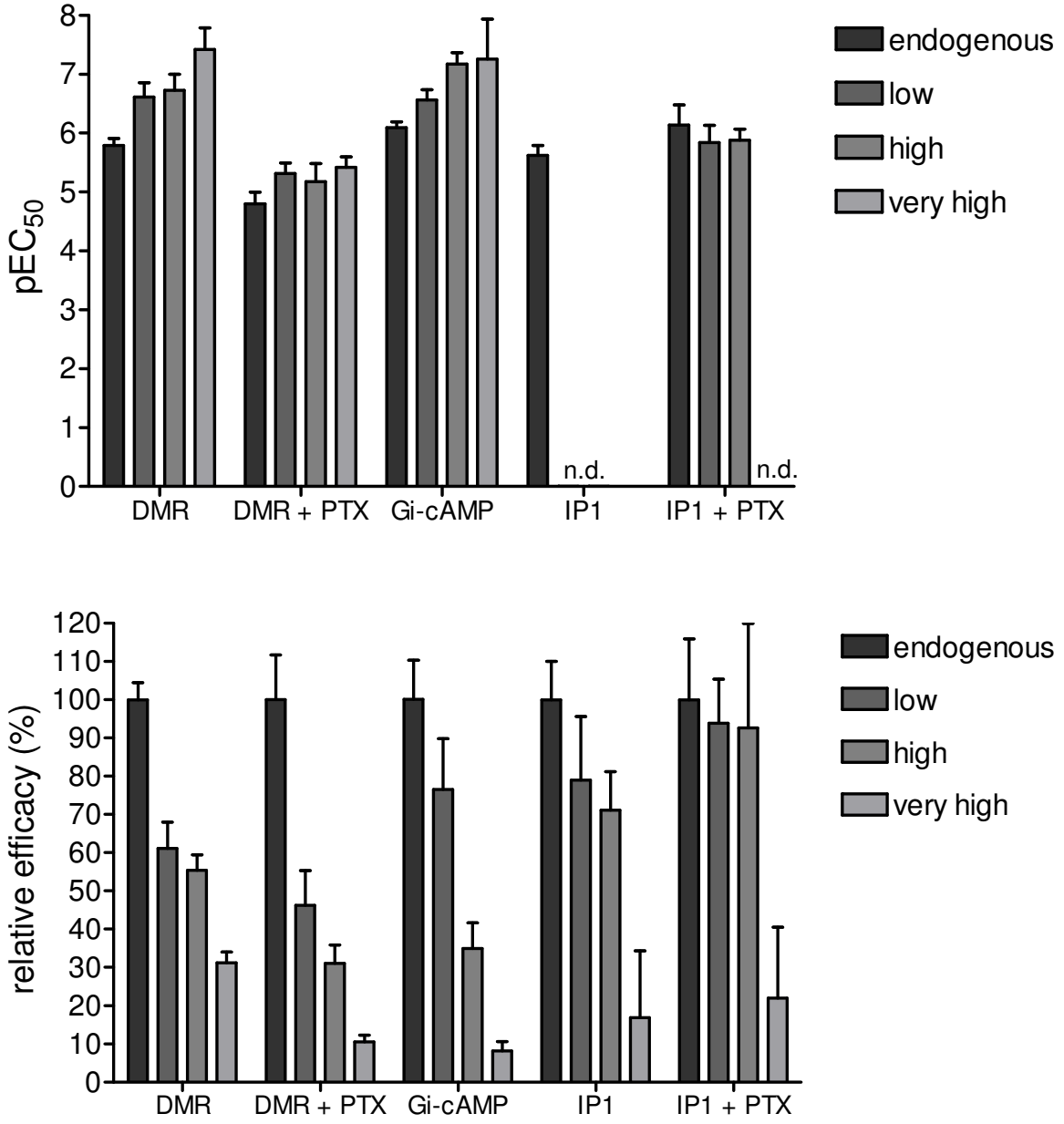

Figure 87 Comparison of pEC_{50} values and relative efficacies determined in HEK293 cells stably coexpressing GPR17 and distinct amounts of β-arrestin2 upon stimulation with RA-II-150

pEC_{50} values were determined by RA-II-150 challenge of HEK293 cells stably coexpressing fusion receptor GPR17 C-terminally fused to Renilla luciferase and increasing amounts of β-arrestin2 N-terminally labeled with GFP2 (endogenous, low, high and very high). Data were achieved by various functional assays (cAMP and IP1 to analyze traditional second messengers and Epic® technology to monitor dynamic mass redistribution (DMR)), in absence and presence of pertussis toxin (PTX, 50 ng/ml, 18 h). No data (n.d.) were obtained by IP1 assays in the presence of elevated β-arrestin levels, as no appropriate CRC could be computed.

These observed functional response differences depending on the amount of β-arrestin2 expression levels, represent a new example of fine-tuning in G protein-dependent receptor signaling. These findings become even more important regarding the information that different cell types have been shown to express distinct amounts of β-arrestins, such as the immortalized cell lines A431 (human epithelial carcinoma cell line*)*, CHO, CHW (chinese hamster fibroblast cell line), COS-7 and HEK293 as detected by use of western blot analyses (Ménard et al. 1997), or for AtT20 (murine pituitary

epithelial-like tumor cell line*)*, BV2 (mouse microglial cell line), N18 (murine neuroblastoma cell line) and HEK293 cells as identified by means of microarray analyses (Atwood et al. 2011). Even more interesting, pertaining to a physiological relevance of this phenomenon, is the fact that although studies of arrestin expression levels in native tissues are still limited, there is evidence of changes in the expression amounts of this protein during neuronal development (Gurevich, Benovic & Gurevich 2004). Moreover, alterations of β-arrestin expression levels have been correlated with neuropathological incidents, as shown for MPTP-treated (1-Methyl-4-phenyl-1,2,3,6-tetrahydropyridin, a neurotoxin to induce dopaminergic degeneration) Macaque monkeys (Bezard et al. 2005), and for patients with Parkinson's disease with dementia at postmortem using western blotting (Bychkov et al. 2008). Furthermore, immunopathological reactions were demonstrated to influence β-arrestin-expression levels, since during inflammation, an increased expression of β-arrestins was observed in spleens and in inflamed peripheral tissue (Lattin et al. 2007), and decreased amounts of β-arrestin2 were detected on intravascular renal graft leukocytes during acute rejection of kidney allografts, where the decrease in β-arrestin2 protein levels was only observed in monocytes but not in T lymphocytes, further suggesting cell specific expression patterns (Zakrzewicz et al. 2010).

Consequently, the reported tissue-dependent, developmental- and disease-regulated alterations of β-arrestin expression levels cannot only influence the trafficking and desensitization of GPCRs as postulated several times (e.g. Li et al. 2010, Vrecl et al. 1998, Ahn et al. 2003, Mundell & Benovic 2000, reviewed by Luttrell & Lefkowitz 2002, Reiter & Lefkowitz, Shenoy & Lefkowitz 2003), but additionally might influence the coupling preference of GPCRs interacting with promiscuous G proteins, leading to a potency boost of the respective agonist for the most preferred signaling pathway, and a possible abrogation of a usually simultaneously occurring but less preferred signaling pathway. Accordingly, in addition to the known roles of β-arrestins for GPCR desensitization, trafficking and signaling in their own right, an additional function can be postulated, namely the fine-tuning of promiscuous G protein-dependent signaling.

5.3 Uncovering Pranlukast as a mixed agonist/antagonist for GPR17

The already marketed 'specific' CysLT1 receptor antagonists pranlukast and montelukast (Brink et al. 2003) were reported to abrogate functional responses of LTD4-activated GPR17, as determined by [^{35}S]GTPγS binding, electrophysiological studies, kinase (ERK1/2) and cAMP assays using 1321N1 cells transiently transfected with short and long isoform of GPR17, PC-12 cells and primary OPCs endogenously expressing GPR17 (Ciana et al. 2006, Fumagalli et al. 2011, Lecca et al. 2008, Pugliese et al. 2009). Anyhow, it should be noted that inhibition properties of pranlukast to counteract GPR17-mediated functional responses were only demonstrated by use of [^{35}S]GTPγS binding in 1321N1 cells transiently overexpressing the short GPR17 splice variant (Ciana et al. 2006), whereas the other observations were obtained solely with montelukast. Since activation of GPR17 with LTD4 so far could not be verified by independent laboratories (Benned-Jensen & Rosenkilde 2010, Maekawa et al. 2009, Wunder et al. 2010), the inhibition efficiency of the postulated antagonists

remains as well disputable. Furthermore, Benned-Jensen et al. published that montelukast was not able to counteract their observed constitutive activity of GPR17 (Benned-Jensen & Rosenkilde 2010). Consequently, it was the goal to examine the antagonistic properties regarding GPR17 activation with our small molecule agonist RA-II-150. Additionally, two more specific CysLT1 receptor antagonists, zafirlukast (Aharony 1998) and MK571 (Jones et al. 1989), which have not been tested yet on GPR17, were included in the investigations.

Preliminary screening analyses by use of the Epic® system and IP1 assays clearly demonstrate that the previously reported observations of montelukast and pranlukast could not be confirmed. Although all four tested antagonists functionally inhibit GPR17 to some extent, pranlukast represents the most promising compound to interfere with RA-II-150-induced GPR17 signaling. On the contrary, montelukast, which has been published several times as a potent GPR17 antagonist with an IC_{50} value in the nanomolar range (Ciana et al. 2006, Fumagalli et al. 2011, Lecca et al. 2008), surprisingly revealed the worst inhibition properties amongst the analyzed antagonists. Therefore pranlukast was chosen to be further characterized regarding its pharmacological properties.

5.3.1 Pranlukast reveals ligand-biased agonism at GPR17

First of all the agonistic effects of pranlukast at GPR17 were evaluated to determine whether the compound acts as a pure neutral antagonist, as an inverse agonist or even as a partial agonist. Surprisingly, the use of the Epic® system uncovered dynamic mass redistribution elicited by GPR17 upon stimulation with pranlukast in a concentration-dependent and PTX-sensitive manner, establishing an essential role for Gαi/o-mediated signaling. Indeed, these findings were further confirmed by traditional second messenger analyses that revealed pranlukast-induced inhibition of forskolin-stimulated adenylate cyclase, sensitive to PTX preincubation in CHO and HEK293 cells stably expressing GPR17, whereas a lack of response was monitored in untransfected cells, thus clearly indicating a GPR17-mediated coupling with Gαi/o proteins. Further evidence was supplied by use of BRET2 technology, since stimulation of HEK293 cells stably expressing BRET2 fusion proteins (GPR17-RLuc and β-arrestin2-GFP2) with pranlukast yielded in a significant increase of the BRET ratio, indicating a recruitment of β-arrestin2 to GPR17, which is known to be a convergent step of GPCR signaling (Barak et al. 1997). Similar to results obtained by use of cAMP assays, the translocation of β-arrestin2 upon pranlukast-stimulation is completely abrogated in the presence of PTX, in contrast to the BRET2 results obtained with RA-II-150, highlighting a functional selectivity of GPR17 activation by pranlukast. This supposed ligand-biased agonism was further verified by second messenger analyses that revealed a lack of functionality in Gαs-cAMP and IP1 assays, although GPR17 has previously been shown to couple with promiscuous G proteins upon RA-II-150 challenge, including Gαi/o, Gαs and Gαq. The observed functional response of GPR17 upon stimulation with pranlukast is not only selective for Gαi/o-pathway but furthermore exhibits only partial agonism with lowered potencies in comparison to RA-II-150 as depicted by pEC_{50} values and relative efficacies in Figure 88. Thus, pranlukast represents a weak GPR17 agonist only stimulating the most sensitive pathway. Interestingly neither pEC_{50} values nor relative efficacies exhibited by pranlukast differ significantly amongst the evaluated cell lines (CHO and HEK293 cells) and the applied functional assays (cAMP and

BRET2), respectively, even analyses of internalization rate confirmed the partial agonism with a relative efficacy of ~40% compared to RA-II-150 (Figure 88, B).

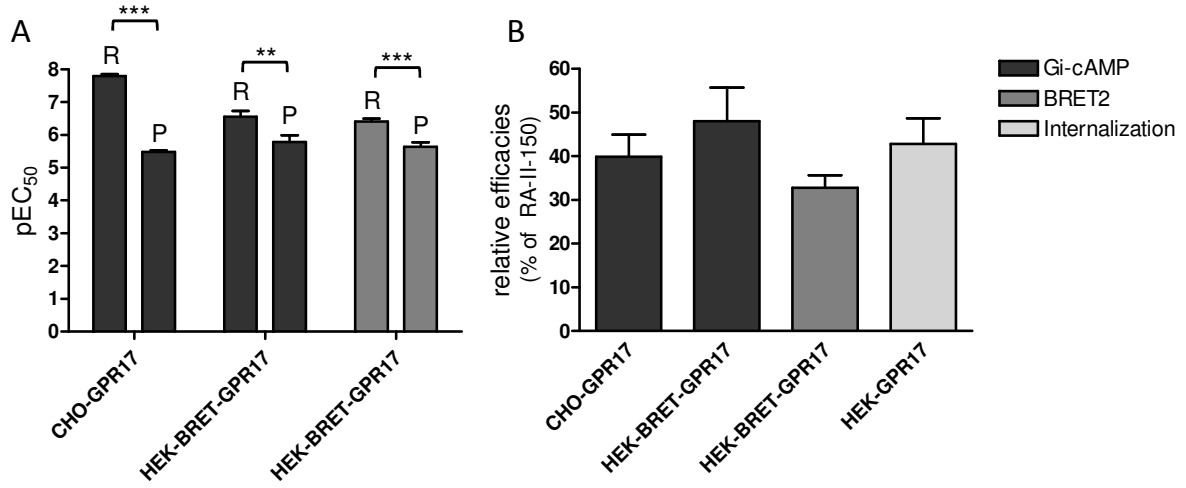

Figure 88 Comparison of pEC_{50} values and relative efficacies of the partial GPR17 agonist pranlukast
A-B, pEC_{50} values and relative efficacies were determined by pranlukast challenge of CHO and HEK293 cells stably expressing GPR17, and HEK293 cells stably coexpressing fusion receptor GPR17 C-terminally fused to Renilla luciferase and β-arrestin2 N-terminally labeled with GFP2 (HEK-BRET-GPR17). Data were achieved by various functional assays (cAMP to analyze Gαi/o-mediated decrease of cAMP accumulation, BRET2 assays to investigate β-arrestin recruitment, and ELISA to determine GPR17 internalization upon agonist stimulation). For statistical analyses, unpaired t-tests with two-tailed p values and 95% confidence interval were applied and revealed no significant differences for pranlukast between cell lines and assays, respectively, but between pranlukast and RA-II-150 as presented in the plot ($p > 0.05$, $^{**}p < 0.01$, $^{***}p < 0.001$). A, pEC_{50} values of full agonist RA-II-150 were included for better comparisons with partial agonist pranlukast (P). B, Relative efficacies were normalized to maximum effect achieved with RA-II-150.

Taken together, pranlukast not only counteracts GPR17-mediated functional responses as postulated by Ciana et al. (Ciana et al. 2006) and demonstrated in the present thesis, but rather induces signaling in its own right by activation of only one G protein-dependent signaling pathway (Gαi/o) of the versatile repertoire of possible modification as shown for activation by RA-II-150. This phenomenon was not controlled by the cell system, since it was observed in two different cellular backgrounds (CHO and HEK293 cells) with comparable extent, indicating dependence on the ligand-related receptor conformation. Consequently, it could be referred to as a "true receptor active state based selectivity" (Kenakin 2007), revealing both partial agonist and pure antagonist actions at different functions mediated via a single receptor. Although this is the first time describing pranlukast as an agonist at GPR17, Pugliese et al. were not able to examine antagonistic properties of pranlukast on LTD4-stimulated GPR17 in electrophysiological studies due to a significant increase "per se" in outward currents (Pugliese et al. 2009). Consequently, even if not postulated as such by the authors and not knowing the underlying mechanism, this described 'unspecific' activity could be the regarded as a first hint for stimulating effects of pranlukast at GPR17 as demonstrated in the present thesis.

5.3.2 Non-competitive antagonism of pranlukast at GPR17

Due to promiscuous G protein-coupling of GPR17 observed upon stimulation with RA-II-150, inhibition potencies of pranlukast were examined by use of two traditional second messenger assays

to monitor the impact on G protein-dependent signaling (cAMP for Gαi/o and Gαs, IP1 for Gαq) as well as by means of BRET2 technology to evaluate repression of β-arrestin2 translocation. Whereas pranlukast exhibits functional selectivity for Gαi/o-coupled signaling in GPR17-activation, all observed RA-II-150-induced functional responses are concentration-dependently counteracted by prestimulation with pranlukast, even though inhibition potencies and relative efficacies differ according to the respective experimental approach (Figure 89). However, the observed findings did not agree with the previously published inhibition properties of pranlukast at GPR17, since IC_{50} values were reported to be in nanomolar range as examined by means of [^{35}S]GTPγS binding assays in 1321N1 cells expressing GPR17 (human and rat) (Ciana et al. 2006). Nevertheless, these controversial findings might be due to application of distinct GPR17 agonists, as Ciana et al. investigated inhibition potencies on LTD4-activated GPR17. Interestingly, their determined antagonistic properties resemble the ones obtained by inhibition of the LTD4-induced (33 nM) Ca^{2+} mobilization in HEK293 cells stably expressing CysLT receptor, with an IC_{50} value of 0.1 nM (Sarau et al. 1999). The effect of pranlukast on nucleotide-induced (UDP and UTP) increase of Ca^{2+} via nucleotide receptors in dU937 cells were similar to the data mentioned here, with IC_{50} values in micromolar range (Mamedova et al. 2005). Thus, although the antagonistic behavior of pranlukast has been demonstrated to be not as selective as originally assumed (Obata et al. 1992), the concentrations required to functionally counteract the effects of RA-II-150 in the present thesis are not comparable to the nanomolar amounts needed to inhibit the CysLT1 receptor.

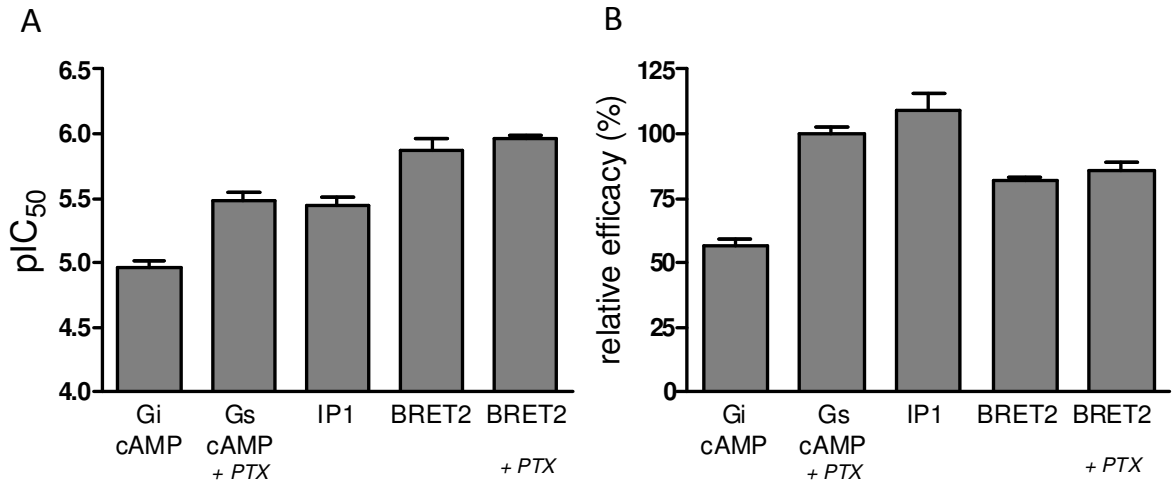

Figure 89 Comparison of pIC_{50} values and relative efficacies determined by preincubation with pranlukast prior to stimulation with RA-II-150

Inhibition properties of pranlukast to impair RA-II-150-triggered (EC_{80}) functional responses of CHO cells stably expressing GPR17 (cAMP and IP1 assays) and HEK293 cells stably transfected with GPR17-RLuc and β-arrestin2 –GFP2 (= HEK-BRET-GR17 cells, *low, for BRET2 analyses*), expressed as pIC_{50} values and relative efficacies (%). Data were obtained by means of various functional assays (cAMP and IP1 to analyze traditional second messengers, BRET2 technology to monitor β-arrestin recruitment), in absence and presence of pertussis toxin (PTX, 50 ng/ml, 18 h).

In agreement with the postulated partial Gαi/o-agonism of pranlukast at GPR17, the RA-II-150-elicited inhibition of forskolin-stimulated cAMP accumulation is only partially diminished (~50%) by pranlukast prestimulation, whereas GPR17-mediated increase of intracellular IP1 and cAMP concentrations is completely abolished by the neutral antagonistic properties of pranlukast, provided

by preincubation with PTX to circumvent influences caused by the partial Gαi/o-mediated agonism (Figure 89, B). Interestingly, the recruitment of β-arrestin2 to the agonist-activated GPR17 as well was only partially inhibited, but this time not due to the partial agonistic property, since it's blocking by PTX-pretreatment does not significantly change the maximum inhibition effect (~75%), indicating a RA-II-150-induced translocation of β-arrestin2 that cannot be completely abolished by pranlukast pretreatment. The fact that previous data have revealed that approximately the half of RA-II-150-induced β-arrestin2 recruitment occurs independently of activated G proteins, indicates that pranlukast partially inhibits G protein-independent-induced β-arrestin2 recruitment besides the demonstrated inhibition of G protein-dependent events.

Control data clearly demonstrated that the observed inhibition properties of pranlukast are not due to any unspecific heterologous desensitization events and independent of another receptor stimulating the adenylate cyclase, since 30 µM pranlukast have no effect on the carbachol-mediated increase of intracellular cAMP in CHO cells stably expressing M2 muscarinic receptor.

Having established antagonistic properties of pranlukast at GPR17, it was another goal to get some information about the underlying nature of antagonism. The performed Schild analyses revealed at first controversial results besides the common concentration-dependent parallel rightward shift of RA-II-150-induced concentration-response curves. Pranlukast was found to inhibit RA-II-150-induced IP1 accumulation in a surmountable manner, whereas GPR17-triggered DMR as monitored by the Epic® system was shown to be counteracted in an insurmountable nature, and both inhibition and stimulation of adenylate cyclase reveals a mixed mechanism as only application of the highest pranlukast concentration (30 µM) additionally suppresses the maximal responses. However, the plots of these Schild analyses revealed consistent steep slopes for all applied approaches (1.55-2.21), thus indicating not a simple competitive antagonism, but rather a non-competitive mechanism of action.

Consequently, these data obtained by Schild analyses suggest that pranlukast most likely acts non-competitively to inhibit receptor function and binds to an allosteric site, inducing a conformational change in GPR17 that compromises its interaction with RA-II-150 and/or its ability to elicit a response. Since besides these antagonistic effects on RA-II-150-activated GPR17, biased agonistic effects are demonstrated, pranlukast could be referred to as an "ago-allosteric modulator that is a ligand that functions both as an agonist on its own and as an allosteric modulator of the efficacy and/or potency of the orthosteric ligand" as described by Schwartz et al. (Schwartz & Holst 2007). Recent reports have postulated bitopic or dualsteric ligands, which simultaneously target both orthosteric and allosteric sites at the same time. Valant et al. demonstrated, using several different binding and functional assays, that McN-A-343, originally described as a selective M2 mAChR partial agonist, actually is a bitopic ligand binding to both allosteric and orthosteric binding sites on M2 muscarinic receptors (Valant et al. 2008). Another recent report, as well using the mACh receptor as a template, presented a *de novo* design of dualsteric ligands by synthesis of hybrids fusing a highly potent orthosteric activator with M2-selective allosteric fragments. Radioligand binding analyses in wild type and mutant receptors supplemented by docking simulations studies revealed an M2-selective and true allosteric/orthosteric binding. Furthermore, G protein activation was shown to be

mediated by the orthosteric site, and dualsteric hybrid compounds showed ligand-biased signaling properties activating only the most preferred Gαi/o pathways (Antony et al. 2009). Further evidence indicating that one bivalent ligand can simultaneously occupy both orthosteric and allosteric site is provided by Narlawar et al., who synthesized a series of bitopic hybrid ligands linking both the orthosteric and allosteric pharmacophores of the adenosine receptor A1 (A1AR) to locate the allosteric site on the A1AR (Narlawar et al. 2010). However, as the orthosteric binding site is defined as the site where the endogenous ligand binds and as the endogenous ligand of GPR17 has not been identified yet, no information is given about the "true" orthosteric binding site of GPR17. Thus, it is elusive and just speculation to describe our small molecule agonist RA-II-150 as an orthosteric activator and pranlukast as a potential bitopic ligand.

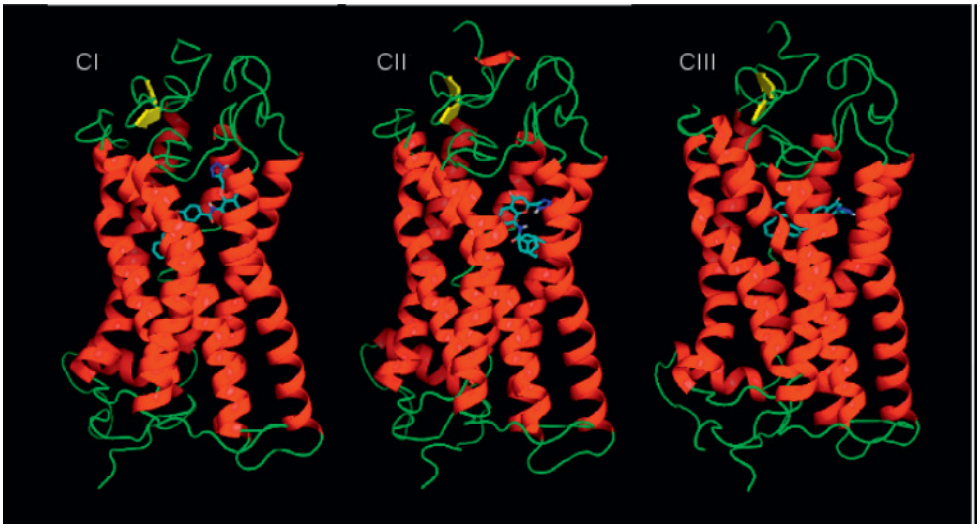

Figure 90 Macroscopic view of three best configurations of pranlukast docked to GPR17 (adapted from Parravicini et al. 2010)

The picture illustrates three potential binding poses (CI, CII and CIII) obtained for the antagonist pranlukast (stick representation) on GPR17 (cartoon representation), determined by means of docking studies and molecular dynamic simulations. The chance of pranlukast to assume different and energetically comparable configurations, as for CI, CII and CIII, probably is due to the high flexibility of the molecule yielding its high conformational freedom (Parravicini et al. 2010).

Docking studies combined with molecular dynamic simulations unveiled three distinct potential binding sites for pranlukast, stabilizing three energetically favored conformations of GPR17 (Figure 90, Parravicini et al. 2010), due to the high flexibility of the molecule, which already might be a hint for the observed multifaceted functional behavior in the present thesis. Thus, it can be hypothesized that the receptor conformations stabilized by pranlukast produce different changes in the various regions interacting with signaling proteins such as G protein and β-arrestins resulting in different modifications of one signaling pathway versus another, and potentially make GPR17 inaccessible to our small molecule agonist RA-II-150. Furthermore it can be hypothesized that the active receptor conformation state induced by RA-II-150 capable of interacting with multiple cellular components differs from the ones induced by pranlukast.

Furthermore, it was suggested by Parravicini et al. that two different binding subsites are present on GPR17, and that intermolecular interactions with the ligands are different between UDP and

pranlukast (Parravicini et al. 2008, Parravicini et al. 2010). Hence, these observations could be another indication for allosteric interactions of pranlukast with GPR17, disregarding the fact that the postulated ligand UDP could not yet be verified as a GPR17-agonist, and thus the published results need to be regarded with care and further considerations about the nature of antagonism are only speculations at the moment, but represent an interesting task that will be addressed in future studies. To verify an allosteric interaction of pranlukast with GPR17, binding studies would be necessary to prove a displacement of our full agonist RA-II-150. Since no radiolabeled GPR17 agonist is readily available, the interaction remains elusive and can only be hypothesized.

Additionally, it should be noted that the monitored insurmountability might be partially related to the disappearance of GPR17 cell surface receptors upon stimulation with pranlukast, since such phenomena of antagonists have been described previously (Perry et al. 2005, Roettger et al. 1997).

An alternative explanation for the observed insurmountability could be the kinetic of pranlukast-GPR17 interactions. Reversible but slow-dissociating competitive antagonists might also depress the maximal functional response if the chosen assay time window is insufficient to liberate the entire receptor site before agonist is added. Consequently, the insurmountable nature might be due to limited duration of the agonist challenge and insufficient readjustment of the receptor. This phenomenon is known as “hemi-equilibrium” conditions (Kenakin, Jenkinson & Watson 2006), and based on the demonstrated observations in the present thesis it cannot be excluded that this is the reason for insurmountability, although chosen time windows were quite long (30-60 min preincubation with pranlukast followed by a 60 min of agonist stimulation), but as no information is given about the dissociation kinetic of pranlukast for GPR17 it can just be speculated at the moment.

5.3.3 Hypotheses of physiological relevance

5.3.3.1 Does the clinical efficacy of pranlukast for the treatment of allergic respiratory diseases depend on GPR17 expression levels?

Pranlukast was the first marketed leukotriene receptor antagonist, and actually is an orally administered, selective, competitive inhibitor of the cysteinyl leukotrienes (LTC4, LTD4 and LTE4), currently on the market only in Japan (Onon®, since 1995) and Latin America (Azlaire®, since 2002) launched by Ono Pharmaceutical Co., Ltd. (Osaka, Japan). The antagonist is applied in the treatment of inflammatory conditions of the respiratory system, such as asthma and allergic rhinitis (reviewed by Drazen, Israel & O'Byrne 1999, Lipworth 1999, Mastalerz & Kumik 2010, Riccioni et al. 2004). Many clinical studies have demonstrated that pranlukast acts as an anti-inflammatory and bronchodilator drug effective in reducing bronchial hyperresponsiveness and allergen-induced bronchoconstriction, and furthermore exhibits an adverse event profile similar to that of the placebo, indicating a good tolerance (Barnes & Pujet 1997, O'Shaughnessy et al. 1997 , reviewed by Hay 1997). Since other selective CysLT1 receptor antagonists, such as montelukast or zafirlukast, exhibit similar *in vitro* and *in vivo* profiles, and only differ in terms of relative potency (Aharony 1998, Hay 1997), the

above mentioned physiological effects induced by pranlukast are probably independent of its property to modify signaling of GPR17.

Another interesting consideration regarding the relevance of pranlukast for the treatment of asthma and allergic rhinitis arises from the postulation that GPR17 acts as a negative regulator of the CysLT1 receptor, which is known to trigger a range of proinflammatory effects (Maekawa et al. 2009, Maekawa et al. 2010). Unfortunately, no detailed information is available about GPR17 expression levels in peripheral blood leukocytes (e.g. monocytes, eosinophils, neutrophils, B lymphocytes), spleen or smooth muscle cells (lung, intestine), which are known to express high levels of CysLT1 (Rovati & Capra 2007). Anyhow, it would be interesting to know whether asthmatic or allergic patients reveal distinct expression levels of GPR17 and whether these differences exert influence on the efficacy of the pranlukast treatment maybe in comparison to montelukast application. When GPR17 would be present and thus acting as down-regulator of the CysLT1-triggered inflammatory responses, the treatment with pranlukast could possibly counteract this repressive effect, consequently the actual inhibition effect on CysLT1 receptor could be compensated resulting in a lowered overall clinical efficacy. Maybe this could even be a reason for the restricted commercialization of pranlukast in comparison to montelukast for example. As already mentioned above, both receptors have been shown to be present in bone-marrow derived CD11c-positive dendritic cells (DC) by RT-PCR analyses (Itagaki et al. 2009), and therefore could represent an interesting cellular system to analyze not just the reciprocal effects of both receptors, but also the influence of pranlukast on both triggered immunobiological responses.

Another consideration based on the postulated heterodimerization of GPR17 and CysLT1 receptor (Maekawa et al. 2009) could be that the observed effects of pranlukast at GPR17 are due to an allosteric regulation between these two proteins, since pranlukast originally was identified as a selective CysLT1R antagonist, and thus inhibition of CysLT1R-mediated responses could possibly modify signaling of GPR17. However, such considerations can be neglected as the CysLT1R is not present in the examined cellular systems (HEK293 and CHO cells). Recently published microarray analyses of HEK293 cells clearly demonstrate that neither CysLT1 nor CysLT2 mRNA is present in this cell line (Atwood et al. 2011). Although, to the best of my knowledge, no expression data of the CysLT1R in CHO cells is reported, several publications demonstrate that CHO cells do not respond to a challenge with cysteinyl leukotrienes (LTD4, LTC4), indicating the lack of their corresponding receptors in this cell line (Maekawa et al. 2009, Mellor et al. 2001, Sarau et al. 1999). Furthermore, as already mentioned above, cotransfection of both receptor proteins in HEK293 cells does not result in a reciprocal influence of CysLT1R on GPR17-mediated functional responses, as monitored by the Epic® system (data not shown, AK Kostenis), consequently it would be unlikely that inhibition of CysLT1R modifies GPR17-mediated signaling. Nevertheless, further investigations are necessary to elucidate the precise reciprocal interactions of both GPCRs.

5.3.3.2 Mixed agonist-antagonist properties at the same receptor

A mixed agonist-antagonist is a ligand that exhibits pharmacological characteristics alike to both agonists and antagonists at a particular receptor, thus representing an extension of the traditional

classification as full agonists, partial agonists, neutral antagonists or inverse agonists based on the extended ternary complex model (Samama et al. 1993). Already known examples provide evidence that the observed results demonstrating pranlukast acting as a biased partial agonist and pure antagonist at the same receptor depending on the end point under investigation (as summarized in Figure 91) is not an artifact.

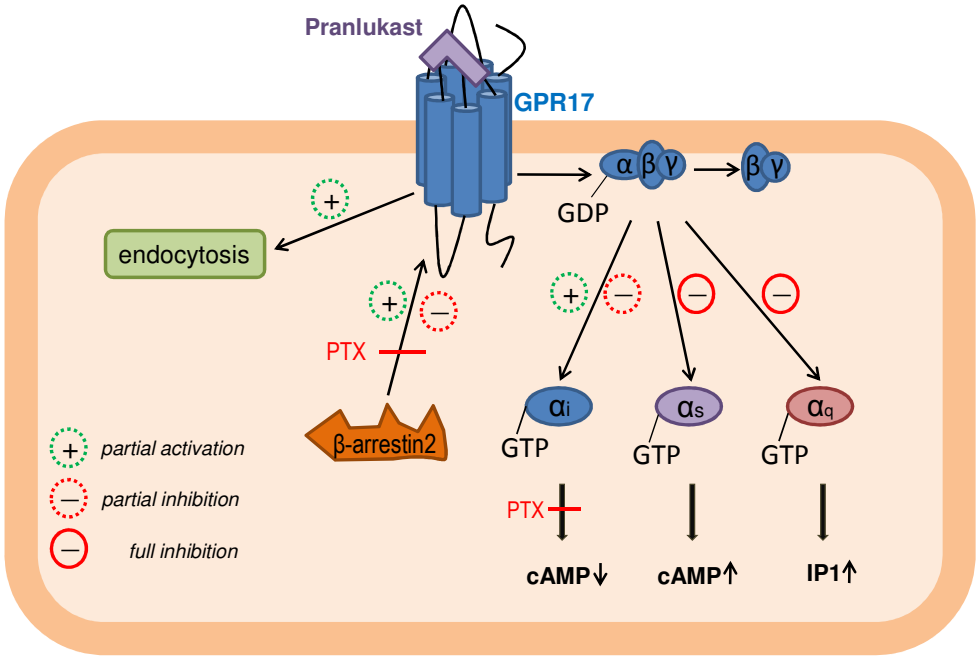

Figure 91 Multifaceted functions of pranlukast as a mixed agonist/antagonist at GPR17
Activation of GPR17 with pranlukast causes endocytosis of the activated receptor and recruitment of β-arrestin2, whereby the latter was shown to be completely blocked by pertussis toxin (PTX) preincubation, indicating Gαi/o protein-dependence. Challenge of GPR17 with pranlukast triggers a partial coupling to PTX-sensitive Gαi/o protein, which was demonstrated by the inhibition of adenylate cyclase leading to decrease of cyclic adenosine monophosphate (cAMP) synthesis. Furthermore, RA-II-150-induced activation of GPR17 is partially (β-arrestin-recruitment and Gαi/o-coupling) or completely (Gαs- and Gαq-coupling) inhibited by preincubation with pranlukast. (for detailed information see main text).

The therapeutic and clinical relevance of functionally selective compounds has been exemplified in the medication of schizophrenia; especially the mode of action of the third generation antipsychotic prototype aripiprazole has been extensively described and controversially discussed (reviewed by Mailman 2007, Mailman & Murthy 2010). Aripiprazole (Abilify, Aripiprex) is an atypical antipsychotic and antidepressant drug developed by Otsuka in Japan, and applied for the treatment of schizophrenia, bipolar disorder and clinical depression. Originally, the clinical benefit is described to be based on a partial dopamine D2 receptor agonistic activity, demonstrated by D2 receptor-mediated inhibition of cAMP accumulation (Lawler et al. 1999, Shapiro et al. 2003), “stabilizing” the dopamine system by normalization of both dopamine hypoactivity and hyperactivity in pathologically affected dopaminergic events (Stahl 2001, Tamminga 2002). But furthermore, aripiprazole has been demonstrated to act as a pure antagonist at both D2 agonist-mediated GTPγS binding and GIRK channel activity (Shapiro et al. 2003). Taken together, the available data support the hypothesis that aripiprazol acts as a functionally selective D2 agonist and antagonist depending on the evaluated outcome, thus the observed beneficial “dopamine stabilization” results from mixed direct effects on the receptor and not just from a simple partial agonism. Consequently, this example provides

evidence that the extreme ligand-induced differential signaling exhibiting agonistic and antagonistic properties at the same receptor constitutes a promising mode of action. Whether this is likewise the case for pranlukast modifying GPR17-mediated physiological effects still remains elusive, but represents an interesting task for the future.

Postulating that the observed functionally selective signaling is linked to the structure of pranlukast, a structure-activity relationship analysis, using distinct pranlukast analogs, could be useful to identify the responsible moieties, thus helping to design more specific and as well more potent ligands, which would further help elucidating the physiological and pathophysiological role of GPR17 as well as represent a valuable tool for drug development, since GPR17 has been proposed to be a potential drug target for developing new therapeutic approaches to demyelinating diseases such as multiple sclerosis (Chen et al. 2009, Fumagalli et al. 2011, Ceruti et al. 2011) or ischemic and traumatic injury of CNS such as stroke and spinal cord injury (Ciana et al. 2006, Lecca et al. 2008, Ceruti et al. 2009).

5.3.3.3 Importance of functional selectivity of pranlukast

When GPR17 receptor density is upregulated, which has been demonstrated for specific pathophysiological conditions, such as early stages of ischemic and traumatic damage (Ceruti et al. 2009, Lecca et al. 2008), demyelinating diseases (Chen et al. 2009) or chronic lymphocytic leukemia (Aalto et al. 2001), it could be hypothesized, based on the *in vitro* results of the present thesis, that the Gαs-linked signaling pathway gains in importance, and thus might play a central role during the acute phase of pathophysiological incidents. Furthermore, it is known that inflammatory mediators (such as nucleotides and leukotrienes) are upregulated during cell damage and CNS trauma, and although the endogenous ligand for GPR17 has not yet been identified, it is conceivable that the extracellular concentration of the so far unknown ligand is as well increased, which would be consistent with the gain of importance for Gαs-mediated events, since *in vitro* results of the present work clearly demonstrate the prevalence of the stimulating pathway by a challenge with high ligand concentrations, at least with our small molecule agonist RA-II-150. Now bearing these considerations in mind, pranlukast, exhibiting partial agonist properties for Gαi/o-mediated signaling and neutral "pure" antagonist qualities for Gαq- and Gαs-triggered functional responses, would represent a valuable tool to modify the postulated dual role of GPR17 during CNS dysfunctions. In the presence of high ligand concentrations, during an early and acute time-window, pranlukast would completely block Gαs- and Gαq-elicited functional responses, suggesting that it may afford neuroprotection and prevent cell death initiated by GPR17. Conversely, in situations where extracellular concentrations of the endogenous ligand are low and Gαi/o-linked signaling prevails, pranlukast can occupy GPR17 and induce partial Gαi/o-mediated functional responses, preserving and stabilizing 'normal' conditions. Since these postulations are based on our own *in vitro* studies, assuming differential physiological relevance of GPR17-mediated promiscuous coupling with distinct Gα protein subunits, further *in vivo* analyses are absolutely essential to prove the beneficial influence of the biased mixed agonist/antagonist pranlukast, and implication of these findings for the clinical relevance of pranlukast is yet to be explored.

Furthermore, it should be noted that several *in vivo* studies demonstrated that pranlukast exhibits neuroprotective effects on cerebral ischemia induced by middle cerebral artery occlusion (MCAO) in rats and mice (Zhang et al. 2002, Yu et al. 2005). However, since pranlukast originally has been identified as a selective CysLT1 receptor antagonist, exhibiting higher antagonistic potencies at this leukotriene receptor in comparison to GPR17, and further has been shown to inhibit the effects of nucleotides acting at P2Y receptors (Mamedova et al. 2005), it is difficult to distinguish between GPR17-, CysLT1- or even P2Y-mediated events, especially when receptor expression levels are not considered in the examinations. Furthermore, the demonstrated neuroprotective effects were also shown for montelukast that is, similar to pranlukast, known to inhibit CysLT1 as well as P2Y receptors, but in contrast lacking significant inhibition at ligand-activated GPR17, as demonstrated in the present thesis. Hence, physiologically relevant events monitored with both compounds in a comparable extent, obviously cannot be mediated by modification of GPR17-triggered responses. Interestingly, the dose-effect of pranlukast-induced neuroprotection was a bell-shaped relationship, and application of higher pranlukast doses was demonstrated to be ineffective, which has not been sufficiently explained by the authors (Zhang et al. 2002). Now, having the knowledge that pranlukast exhibits a higher potency to counteract CysLT1- than GPR17-mediated events, one could conclude that the controversial effects observed with high doses could be caused by modulation of GPR17, especially as this bell-shaped phenomenon was not observed with montelukast (Yu et al. 2005), and regarding the fact that GPR17 has been postulated to be related to ischemic brain damage (Ciana et al. 2006, Lecca et al. 2008). However, if these considerations are true, the previously mentioned treatment with pranlukast to modify GPR17 in the acute phase of ischemic damage would not represent a suitable approach. Accordingly, it is necessary to further investigate whether pranlukast exhibits beneficial *in vivo* effects on the implicated CNS dysfunctions or not, so far only speculations are possible.

6 Summary

Uncertain deorphanization attempts uncovered the seven-transmembrane receptor GPR17 as a dual nucleotide/lipid receptor activated by two distinct classes of signaling molecules: uracil nucleotides and cysteinyl-leukotrienes (Ciana et al. 2006). However, there are a number of inconsistencies, since the activity of postulated endogenous ligands and likewise the associated previously uncovered signaling properties could not be verified yet by independent laboratories, and thus remain a controversial matter. The identification of our synthetic small molecule GPR17 agonist (here referred to as RA-II-150), by means of a high throughput pharmacogenomic approach raised the possibility to carry out *in vitro* investigations on the molecular signaling events elicited by agonist-activated human GPR17.

The present work increases our understanding of GPR17 pharmacology, since the observed experimental findings using RA-II-150 clearly demonstrate that GPR17 is a functionally active receptor that does not lack the common features of GPCR signaling, as shown by data in a set of diverse functional assays using two distinct recombinant cellular systems (CHO and HEK293 cells), engineered to stably express the short splice variant of human GPR17. These investigations reveal that the signaling pathway of ligand-activated GPR17 involves reduction of intracellular cyclic adenosine monophosphate (cAMP) as well as the generation of inositol monophosphate (IP1) and cAMP as determined by means of traditional second messenger assays based on the HTRF® technology, establishing GPR17 as a GPCR that promiscuously couples with three classes of G proteins, namely Gαi/o, Gαq/11 and Gαs. This signaling multiplicity is further confirmed by combination of pharmacological tools (PTX and YM) to counteract respective G protein subunits signaling in a recently developed label-free assay that involves optical measurement of dynamic mass redistribution (DMR) following receptor activation. Additionally, for the first time evidence is provided, that the putative G protein pan-inhibitor BIM-46178, postulated to abrogate signaling mediated by all G protein subunits (Ayoub et al. 2009), acts in a cell-type-dependent manner likely regulated by the particular expression levels of G protein subunits.

The results of the present thesis indicate that despite some observed differences in potencies and efficacies, the coupling preferences are comparable between both analyzed cell systems. GPR17 is mainly coupled to Gαi/o proteins and, to a minor extent, to the Gαq/11 protein subtype and, to an even smaller degree, to the Gαs proteins. G protein subtype activation by our GPR17-agonist RA-II-150 is shown to depend on ligand-concentration and the presented data further provide new hints that receptor-density plays another important role for coupling specifity. This demonstrates how signaling can be channeled into specific routes in particular cells, depending on receptor expression levels and availability of activating ligand. Accordingly, such aspects must be taken into consideration to have a complete understanding of a given receptor's signaling properties and cellular function.

Moreover, ELISA analyses and immunofluorescence investigations for the first time revealed that GPR17 internalizes upon ligand-stimulation, which represents a regulatory phenomenon common to most GPCRs to limit receptor activation.

The experiments described in the present thesis further provide the first detailed information about β-arrestin recruitment to the agonist-activated GPR17, which is another hallmark of receptor activation, as the majority of GPCRs recruit β-arrestin independent of their signaling capacity. Bioluminescence resonance energy transfer (BRET2)-based approaches shed light on both kinetics and mechanistic procedure of β-arrestin2 translocation upon stimulation with RA-II-150. The findings indicate a ligand concentration- and time-dependent manner of β-arrestin2 recruitment to the activated receptor, establishing GPR17 as a class B receptor that interacts very rapidly with the scaffolding protein and forms stable and long lasting associations. Furthermore, β-arrestin2 recruitment is shown to be promoted by G protein-dependent and -independent mechanisms. Whether this observed G protein-independent translocation to the activated GPR17 gives rise to β-arrestin2-mediated signaling, such as activation of mitogen-activated protein kinases (MAPK), remains to be elucidated. Nevertheless, another interesting so far unknown technical phenomenon has emerged during these investigations, in particular that the Epic® optical biosensor technique fails to monitor the G protein-independent β-arrestin2 translocation, at least in the case of GPR17.

Furthermore, the scaffolding protein β-arrestin is shown to exhibit a so far uncharacterized function for GPCR-mediated signaling, besides the already known and frequently described roles for desensitization and trafficking of GPCRs as well as the recently emerged function as signal transducer in its own right. The findings indicate that coexpression of β-arrestin2 can regulate specific signaling outcomes triggered by GPR17 through shifting the promiscuous G protein-coupling to the most preferred one (here Gαi/o) and preventing signaling via less favored G protein subunits (here Gαq/11). Consequently, it is possible that this mechanism is employed by a cell to tailor GPCR signaling to suit a specific physiological role, especially as it is known that expression levels of β-arrestins vary amongst distinct cell types and may change during development or pathological conditions.

Taken together, these findings help to resolve some of the issues surrounding the pharmacology of GPR17, and highlight differences in the effector coupling associated with distinct ligand-concentration, receptor-density and the intracellular levels of β-arrestin2, which seem to have sufficient diversity and dynamic range to accommodate the physiological demands placed on GPR17.

Whereas the cysteinyl leukotriene receptor (CysLTR) antagonists montelukast, zafirlukast and MK571 are shown to lack significant antagonistic properties to counteract GPR17-elicited functional responses, pranlukast for the first time has been identified and characterized as a biased mixed agonist/antagonist at GPR17. Detailed analyses uncovered a functionally selective partial agonism mediated via Gαi/o protein upon stimulation of GPR17. The promiscuous G protein-coupling as well as β-arrestin2 recruitment elicited by RA-II-150 is shown to be diminished with IC_{50} values in micromolar range and very likely in a non-competitive manner. Thus, this already marketed drug could represent a valuable tool for further understanding the physiological and pathophysiological

roles of GPR17, and provide a chemical starting point that may lead to the development of more specific and more potent modifiers of GPR17 functionality.

In the end it should be noted, that the presented data are all based on studies of recombinant human GPR17 in two distinct heterologous expression models. Therefore, further analyses of the signaling mechanisms by the natively occurring receptor are inevitable to unveil the accurate physiological relevance of the observed findings. Regarding recently published data (Chen et al. 2009, Fumagalli et al. 2011) oligodendrocyte precursor cells would represent a suitable primary cell line to examine the natively occurring functional responses elicited by GPR17 upon stimulation with RA-II-150. Furthermore, application of our specific GPR17 agonist would enable to unequivocally establish a link between GPR17 modulation and progression of preoligodendrocytes towards mature myelinating cells.

7 List of abbreviations

AC	adenylate cyclase
ad	Latin word for up to
ADP	adenosine 5'-diphosphate
ATP	adenosine 5'-triphosphate
AUC	area under the curve
bp	base pairs
BRET	bioluminescence resonance energy transfer
cAMP	cyclic adenosine monophosphate
cDNA	complementary DNA
CNS	central nervous system
CRC	concentration-response curve
CysLT	cysteinyl-leukotriene
CysLT1R	type 1 cysteinyl-leukotriene receptor
CysLT2R	type 2 cysteinyl-leukotriene receptor
DAG	diacylglycerol
DC	Dendritic cell
dH_2O	demineralized water
DMR	dynamic mass redistribution
DNA	deoxyribonucleic acid
dNTP	deoxynucleotide phosphate
DR	dose ratio
DRC	dose-response curve
EAE	experimental autoimmune encephalomyelitis *(animal model of multiple sclerosis)*
E.coli	*Escherichia coli*
EC_{50}	concentration of half maximum effect
e.g.	exempli gratia *(for example)*
ELISA	enzyme linked immunosorbent assay
endo 1-3	intracellular loops of 7TMR
ERK	extracellular-signal regulated kinase
ES cell	embryonic stem cell
et al.	et alia, Latin word for and others
exo 1-3	extracellular loops of 7TMR

f.c.	final concentration
FITR	Flp-In™ T-Rex™
FRET	fluorescence resonance energy transfer
FSK	forskolin
g	acceleration by gravity
g	gram
GDP	guanosine 5′-diphosphate
GEF	guanine nucleotide exchange factor
GFP	green fluorescent protein
GIRK channel	G protein-coupled inwardly-rectifying potassium channel
GPCR	G protein-coupled receptor
G protein	guanine nucleotide-binding protein
GRK	G protein-coupled receptor kinases
GTP	guanosine 5′-triphosphate
h	human
h	hour(s)
HA	haemagglutinin
HSV-TK	herpes simplex virus thymidine kinase
HTRF®	homogeneous time resolved fluorescence
IC_{50}	concentration of half maximum inhibition
IP1	inositol 4-phosphate
IP3	inositol 1,3,4-triphosphate
JNK	c-Jun N-terminal kinase
kb	kilo base(s)
LTC4 / D4	leukotriene C4 / D4
LTRA	leukotriene receptor antagonist
log M	logarithm of molar concentration to base 10
M	molar concentration (mol/liter)
m	murine / mouse
Mab	monoclonal antibody
MAPK	mitogen-activated protein kinase
mBRET	milliBRET
MCAO	middle cerebral artery occlusion (focal ischemia model)
min	minute(s)
ml	milliliter
mRNA	messenger RNA

MS	multiple sclerosis
ms	millisecond
µl	microliter
µM	micromolar
n	number
n.d.	no data
neo	neomycin
n_H	Hill slope
nm	nanometer
nM	nanomolar
n.r.	no response
ns	non-significant
N-terminus	amino-terminus
OD	optical density
ORF	open reading frame
OPC	oligodendrocyte precursor cell
P	phosphate group
pA_2	negative logarithm of the antagonist concentration that produces a 2-fold shift in the CRC for an agonist
PAR	protease-activated receptor
PCR	polymerase chain reaction
pEC_{50}	negative logarithm of EC_{50}
PI	phosphatidylinositol
PI3	phosphatidylinositol 3-kinase
pIC50	negative logarithm of IC_{50}
PIP_2	phosphatidylinositol 4,5-bisphosphate
PKA	protein kinase A
PKC	protein kinase C
PLC	phospholipase C
pm	picometer
PP	polypropylene
PScr	screening primer
PTX	Pertussis toxin
q.s.	quantum satis (as much as needed)
RhoA	Ras homolog gene family, member A
RLuc	Renilla luciferase

rpm	rounds per minute
RT	room temperature
RT-PCR	reverse transcription polymerase chain reaction
RWG	resonant waveguide grating
s	second(s)
SCI	spinal cord injury
s.e.m.	standard error of mean
7 TMR	seven transmembrane receptor
TC	tissue culture
TM	transmembrane
U	unit
UDP	uridine diphosphate
UTR	untranslated region
UV	ultraviolet
V	volt
w/o	without
zeo	zeomycin

8 References

Aalto, Y, El-Rifa, W, Vilpo, L, Ollila, J, Nagy, B, Vihinen, M, Vilpo, J & Knuutila, S 2001, 'Distinct gene expression profiling in chronic lymphocytic leukemia with 11q23 deletion', *Leukemia : official journal of the Leukemia Society of America, Leukemia Research Fund, U.K*, vol. 15, no. 11, pp. 1721–1728.

Aharony, D 1998, 'Pharmacology of leukotriene receptor antagonists', *American journal of respiratory and critical care medicine*, vol. 157, 6 Pt 2, pp. S214-8.

Ahn, S, Nelson, CD, Garrison, TR, Miller, WE & Lefkowitz, RJ 2003, 'Desensitization, internalization, and signaling functions of beta-arrestins demonstrated by RNA interference', *Proceedings of the National Academy of Sciences of the United States of America*, vol. 100, no. 4, pp. 1740–1744.

Anborgh, PH, Seachrist, JL, Dale, LB & Ferguson, SS 2000, 'Receptor/beta-arrestin complex formation and the differential trafficking and resensitization of beta2-adrenergic and angiotensin II type 1A receptors', *Molecular endocrinology (Baltimore, Md.)*, vol. 14, no. 12, pp. 2040–2053.

Angers, S, Salahpour, A, Joly, E, Hilairet, S, Chelsky, D, Dennis, M & Bouvier, M 2000, 'Detection of beta 2-adrenergic receptor dimerization in living cells using bioluminescence resonance energy transfer (BRET)', *Proceedings of the National Academy of Sciences of the United States of America*, vol. 97, no. 7, pp. 3684–3689.

Antony, J, Kellershohn, K, Mohr-Andrä, M, Kebig, A, Prilla, S, Muth, M, Heller, E, Disingrini, T, Dallanoce, C, Bertoni, S, Schrobang, J, Tränkle, C, Kostenis, E, Christopoulos, A, Höltje, H, Barocelli, E, Amici, M de, Holzgrabe, U & Mohr, K 2009, 'Dualsteric GPCR targeting: a novel route to binding and signaling pathway selectivity', *The FASEB journal : official publication of the Federation of American Societies for Experimental Biology*, vol. 23, no. 2, pp. 442–450.

Aramori, I, Ferguson, SS, Bieniasz, PD, Zhang, J, Cullen, B & Cullen, MG 1997, 'Molecular mechanism of desensitization of the chemokine receptor CCR-5: receptor signaling and internalization are dissociable from its role as an HIV-1 co-receptor', *The EMBO journal*, vol. 16, no. 15, pp. 4606–4616.

ARUNLAKSHANA, O & SCHILD, HO 1959, 'Some quantitative uses of drug antagonists', *British journal of pharmacology and chemotherapy*, vol. 14, no. 1, pp. 48–58.

Ashkenazi, A, Winslow, JW, Peralta, EG, Peterson, GL, Schimerlik, MI, Capon, DJ & Ramachandran, J 1987, 'An M2 muscarinic receptor subtype coupled to both adenylyl cyclase and phosphoinositide turnover', *Science (New York, N.Y.)*, vol. 238, no. 4827, pp. 672–675.

Attramadal, H, Arriza, JL, Aoki, C, Dawson, TM, Codina, J, Kwatra, MM, Snyder, SH, Caron, MG & Lefkowitz, RJ 1992, 'Beta-arrestin2, a novel member of the arrestin/beta-arrestin gene family', *The Journal of biological chemistry*, vol. 267, no. 25, pp. 17882–17890.

Atwood, BK, Lopez, J, Wager-Miller, J, Mackie, K & Straiker, A 2011, 'Expression of G protein-coupled receptors and related proteins in HEK293, AtT20, BV2, and N18 cell lines as revealed by microarray analysis', *BMC genomics*, vol. 12, no. 1, p. 14.

Ayoub, MA, Couturier, C, Lucas-Meunier, E, Angers, S, Fossier, P, Bouvier, M & Jockers, R 2002, 'Monitoring of ligand-independent dimerization and ligand-induced conformational changes of melatonin receptors in living cells by bioluminescence resonance energy transfer', *The Journal of biological chemistry*, vol. 277, no. 24, pp.

Ayoub, MA, Maurel, D, Binet, V, Fink, M, Prézeau, L, Ansanay, H & Pin, J 2007, 'Real-time analysis of agonist-induced activation of protease-activated receptor 1/Galphai1 protein complex measured by bioluminescence resonance energy transfer in living cells', *Molecular pharmacology*, vol. 71, no. 5, pp. 1329–1340.

Ayoub, MA, Damian, M, Gespach, C, Ferrandis, E, Lavergne, O, Wever, O de, Banères, J, Pin, J & Prévost, GP 2009, 'Inhibition of heterotrimeric G protein signaling by a small molecule acting on Galpha subunit', *The Journal of biological chemistry*, vol. 284, no. 42, pp. 29136–29145.

Azzi, M, Charest, PG, Angers, S, Rousseau, G, Kohout, T, Bouvier, M & Piñeyro, G 2003, 'Beta-arrestin-mediated activation of MAPK by inverse agonists reveals distinct active conformations for G protein-coupled receptors', *Proceedings of the National Academy of Sciences of the United States of America*, vol. 100, no. 20, pp. 11406–11411.

Baldwin, JM 1994, 'Structure and function of receptors coupled to G proteins', *Current opinion in cell biology*, vol. 6, no. 2, pp. 180–190.

Banchereau, J & Steinman, RM 1998, 'Dendritic cells and the control of immunity', *Nature*, vol. 392, no. 6673, pp. 245–252.

Banfi, C, Ferrario, S, Vincenti, O de, Ceruti, S, Fumagalli, M, Mazzola, A, Ambrosi, N d', Volontè, C, Fratto, P, Vitali, E, Burnstock, G, Beltrami, E, Parolari, A, Polvani, G, Biglioli, P, Tremoli, E & Abbracchio, MP 2005, 'P2 receptors in human heart: upregulation of P2X6 in patients undergoing heart transplantation, interaction with TNFalpha and potential role in myocardial cell death', *Journal of molecular and cellular cardiology*, vol. 39, no. 6, pp. 929–939.

Barak, LS, Ferguson, SS, Zhang, J & Caron, MG 1997, 'A beta-arrestin/green fluorescent protein biosensor for detecting G protein-coupled receptor activation', *The Journal of biological chemistry*, vol. 272, no. 44, pp. 27497–27500.

Barnes, NC & Pujet, JC 1997, 'Pranlukast, a novel leukotriene receptor antagonist: results of the first European, placebo controlled, multicentre clinical study in asthma', *Thorax*, vol. 52, no. 6, pp. 523–527.

Bash, R, Rubovitch, V, Gafni, M & Sarne, Y, 'The stimulatory effect of cannabinoids on calcium uptake is mediated by Gs GTP-binding proteins and cAMP formation', *Neuro-Signals*, vol. 12, no. 1, pp. 39–44.

Benned-Jensen, T & Rosenkilde, MM 2010, 'Distinct expression and ligand-binding profiles of two constitutively active GPR17 splice variants', *British journal of pharmacology*, vol. 159, no. 5, pp. 1092–1105.

Benovic, JL, Kühn, H, Weyand, I, Codina, J, Caron, MG & Lefkowitz, RJ 1987, 'Functional desensitization of the isolated beta-adrenergic receptor by the beta-adrenergic receptor kinase: potential role of an analog of the retinal protein arrestin (48-kDa protein)', *Proceedings of the National Academy of Sciences of the United States of America*, vol. 84, no. 24, pp. 8879–8882.

Berg, KA, Maayani, S, Goldfarb, J, Scaramellini, C, Leff, P & Clarke, WP 1998, 'Effector pathway-dependent relative efficacy at serotonin type 2A and 2C receptors: evidence for agonist-directed trafficking of receptor stimulus', *Molecular pharmacology*, vol. 54, no. 1, pp. 94–104.

Berglund, MM, Schober, DA, Statnick, MA, McDonald, PH & Gehlert, DR 2003, 'The use of bioluminescence resonance energy transfer 2 to study neuropeptide Y receptor agonist-induced beta-arrestin 2 interaction', *The Journal of pharmacology and experimental therapeutics*, vol. 306, no. 1, pp. 147–156.

Bertrand, L, Parent, S, Caron, M, Legault, M, Joly, E, Angers, S, Bouvier, M, Brown, M, Houle, B & Ménard, L, 'The BRET2/arrestin assay in stable recombinant cells: a platform to screen for compounds that interact with G protein-coupled receptors (GPCRS)', *Journal of receptor and signal transduction research*, vol. 22, 1-4, pp. 533–541.

Bezard, E, Gross, CE, Qin, L, Gurevich, VV, Benovic, JL & Gurevich, EV 2005, 'L-DOPA reverses the MPTP-induced elevation of the arrestin2 and GRK6 expression and enhanced ERK activation in monkey brain', *Neurobiology of disease*, vol. 18, no. 2, pp. 323–335.

Birnboim, HC & Doly, J 1979, 'A rapid alkaline extraction procedure for screening recombinant plasmid DNA', *Nucleic acids research*, vol. 7, no. 6, pp. 1513–1523.

Bläsius, R, Weber, RG, Lichter, P & Ogilvie, A 1998, 'A novel orphan G protein-coupled receptor primarily expressed in the brain is localized on human chromosomal band 2q21', *Journal of neurochemistry*, vol. 70, no. 4, pp. 1357–1365.

Bokoch, GM, Katada, T, Northup, JK, Ui, M & Gilman, AG 1984, 'Purification and properties of the inhibitory guanine nucleotide-binding regulatory component of adenylate cyclase', *The Journal of biological chemistry*, vol. 259, no. 6, pp. 3560–3567.

Bond, RA, Leff, P, Johnson, TD, Milano, CA, Rockman, HA, McMinn, TR, Apparsundaram, S, Hyek, MF, Kenakin, TP & Allen, LF 1995, 'Physiological effects of inverse agonists in transgenic mice with myocardial overexpression of the beta 2-adrenoceptor', *Nature*, vol. 374, no. 6519, pp. 272–276.

Bosier, B & Hermans, E 2007, 'Versatility of GPCR recognition by drugs: from biological implications to therapeutic relevance', *Trends in pharmacological sciences*, vol. 28, no. 8, pp. 438–446.

Brink, CB, Wade, SM & Neubig, RR 2000, 'Agonist-directed trafficking of porcine alpha(2A)-adrenergic receptor signaling in Chinese hamster ovary cells: l-isoproterenol selectively activates G(s)', *The Journal of pharmacology and experimental therapeutics*, vol. 294, no. 2, pp. 539–547.

Brink, C, Dahlén, S, Drazen, J, Evans, JF, Hay, DWP, Nicosia, S, Serhan, CN, Shimizu, T & Yokomizo, T 2003, 'International Union of Pharmacology XXXVII. Nomenclature for leukotriene and lipoxin receptors', *Pharmacological reviews*, vol. 55, no. 1, pp. 195–227.

Bruce, JIE, Straub, SV & Yule, DI 2003, 'Crosstalk between cAMP and Ca2+ signaling in non-excitable cells', *Cell calcium*, vol. 34, no. 6, pp. 431–444.

Bünemann, M, Frank, M & Lohse, MJ 2003, 'Gi protein activation in intact cells involves subunit rearrangement rather than dissociation', *Proceedings of the National Academy of Sciences of the United States of America*, vol. 100, no. 26, pp. 16077–16082.

Bychkov, ER, Gurevich, VV, Joyce, JN, Benovic, JL & Gurevich, EV 2008, 'Arrestins and two receptor kinases are upregulated in Parkinson's disease with dementia', *Neurobiology of aging*, vol. 29, no. 3, pp. 379–396.

Calleri, E, Ceruti, S, Cristalli, G, Martini, C, Temporini, C, Parravicini, C, Volpini, R, Daniele, S, Caccialanza, G, Lecca, D, Lambertucci, C, Trincavelli, ML, Marucci, G, Wainer, IW, Ranghino, G, Fantucci, P, Abbracchio, MP & Massolini, G 2010, 'Frontal affinity chromatography-mass spectrometry useful for characterization of new ligands for GPR17 receptor', *Journal of medicinal chemistry*, vol. 53, no. 9, pp. 3489–3501.

Capra, V, Thompson, MD, Sala, A, Cole, DE, Folco, G & Rovati, GE 2007, 'Cysteinyl-leukotrienes and their receptors in asthma and other inflammatory diseases: critical update and emerging trends', *Medicinal research reviews*, vol. 27, no. 4, pp. 469–527.

Casey, PJ & Gilman, AG 1988, 'G protein involvement in receptor-effector coupling', *The Journal of biological chemistry*, vol. 263, no. 6, pp. 2577–2580.

Ceruti, S, Viganò, F, Boda, E, Ferrario, S, Magni, G, Boccazzi, M, Rosa, P, Buffo, A & Abbracchio, MP 2011, 'Expression of the new P2Y-like receptor GPR17 during oligodendrocyte precursor cell maturation regulates sensitivity to ATP-induced death', *Glia*, vol. 59, no. 3, pp. 363–378.

Ceruti, S, Villa, G, Genovese, T, Mazzon, E, Longhi, R, Rosa, P, Bramanti, P, Cuzzocrea, S & Abbracchio, MP 2009, 'The P2Y-like receptor GPR17 as a sensor of damage and a new potential target in spinal cord injury', *Brain : a journal of neurology*, vol. 132, Pt 8, pp. 2206–2218.

Chen, CA & Okayama, H, 'Calcium phosphate-mediated gene transfer: a highly efficient transfection system for stably transforming cells with plasmid DNA', *BioTechniques*, vol. 6, no. 7, pp. 632–638.

Chen, C, Paing, MM & Trejo, J 2004, 'Termination of protease-activated receptor-1 signaling by beta-arrestins is independent of receptor phosphorylation', *The Journal of biological chemistry*, vol. 279, no. 11, pp. 10020–10031.

Chen, Y, Wu, H, Wang, S, Koito, H, Li, J, Ye, F, Hoang, J, Escobar, SS, Gow, A, Arnett, HA, Trapp, BD, Karandikar, NJ, Hsieh, J & Lu, QR 2009, 'The oligodendrocyte-specific G protein-coupled receptor GPR17 is a cell-intrinsic timer of myelination', *Nature neuroscience*, vol. 12, no. 11, pp. 1398–1406.

Cho, D, Zheng, M, Min, C, Ma, L, Kurose, H, Park, JH & Kim, K 2010, 'Agonist-induced endocytosis and receptor phosphorylation mediate resensitization of dopamine D(2) receptors', *Molecular endocrinology (Baltimore, Md.)*, vol. 24, no. 3, pp. 574–586.

Chuang, TT, Iacovelli, L, Sallese, M & Blasi, A de 1996, 'G protein-coupled receptors: heterologous regulation of homologous desensitization and its implications', *Trends in pharmacological sciences*, vol. 17, no. 11, pp. 416–421.

Ciana, P, Fumagalli, M, Trincavelli, ML, Verderio, C, Rosa, P, Lecca, D, Ferrario, S, Parravicini, C, Capra, V, Gelosa, P, Guerrini, U, Belcredito, S, Cimino, M, Sironi, L, Tremoli, E, Rovati, GE, Martini, C & Abbracchio, MP 2006, 'The orphan receptor GPR17 identified as a new dual uracil nucleotides/cysteinyl-leukotrienes receptor', *The EMBO journal*, vol. 25, no. 19, pp. 4615–4627.

Civelli, O, Nothacker, HP, Saito, Y, Wang, Z, Lin, SH & Reinscheid, RK 2001, 'Novel neurotransmitters as natural ligands of orphan G-protein-coupled receptors', *Trends in neurosciences*, vol. 24, no. 4, pp. 230–237.

Civelli, O 2005, 'GPCR deorphanizations: the novel, the known and the unexpected transmitters', *Trends in pharmacological sciences*, vol. 26, no. 1, pp. 15–19.

Civelli, O, Saito, Y, Wang, Z, Nothacker, H & Reinscheid, RK 2006, 'Orphan GPCRs and their ligands', *Pharmacology & therapeutics*, vol. 110, no. 3, pp. 525–532.

Claing, A, Laporte, SA, Caron, MG & Lefkowitz, RJ 2002, 'Endocytosis of G protein-coupled receptors: roles of G protein-coupled receptor kinases and beta-arrestin proteins', *Progress in neurobiology*, vol. 66, no. 2, pp. 61–79.

Cockcroft, S & Gomperts, BD, 'Role of guanine nucleotide binding protein in the activation of polyphosphoinositide phosphodiesterase', *Nature*, vol. 314, no. 6011, pp. 534–536.

Cooper, DM, Mons, N & Karpen, JW 1995, 'Adenylyl cyclases and the interaction between calcium and cAMP signalling', *Nature*, vol. 374, no. 6521, pp. 421–424.

Cordeaux, Y, Briddon, SJ, Megson, AE, McDonnell, J, Dickenson, JM & Hill, SJ 2000, 'Influence of receptor number on functional responses elicited by agonists acting at the human adenosine A(1) receptor: evidence for signaling pathway-dependent changes in agonist potency and relative intrinsic activity', *Molecular pharmacology*, vol. 58, no. 5, pp. 1075–1084.

Costa, T & Cotecchia, S 2005, 'Historical review: Negative efficacy and the constitutive activity of G-protein-coupled receptors', *Trends in pharmacological sciences*, vol. 26, no. 12, pp. 618–624.

Daniele, S, Lecca, D, Trincavelli, ML, Ciampi, O, Abbracchio, MP & Martini, C 2010, 'Regulation of PC12 cell survival and differentiation by the new P2Y-like receptor GPR17', *Cellular signalling*, vol. 22, no. 4, pp. 697–706

Davis, S, Aldrich, TH, Stahl, N, Pan, L, Taga, T, Kishimoto, T, Ip, NY & Yancopoulos, GD 1993, 'LIFR beta and gp130 as heterodimerizing signal transducers of the tripartite CNTF receptor', *Science (New York, N.Y.)*, vol. 260, no. 5115, pp. 1805–1808.

DeBernardi, MA & Brooker, G 1996, 'Single cell Ca2+/cAMP cross-talk monitored by simultaneous Ca2+/cAMP fluorescence ratio imaging', *Proceedings of the National Academy of Sciences of the United States of America*, vol. 93, no. 10, pp. 4577–4582.

Defea, K 2008, 'Beta-arrestins and heterotrimeric G-proteins: collaborators and competitors in signal transduction', *British journal of pharmacology*, 153 Suppl 1, pp. S298-309.

Degorce, F, Card, A, Soh, S, Trinquet, E, Knapik, GP & Xie, B 2009, 'HTRF: A technology tailored for drug discovery - a review of theoretical aspects and recent applications', *Current chemical genomics*, vol. 3, pp. 22–32.

Delhaye, M, Gravot, A, Ayinde, D, Niedergang, F, Alizon, M & Brelot, A 2007, 'Identification of a postendocytic sorting sequence in CCR5', *Molecular pharmacology*, vol. 72, no. 6, pp. 1497–1507.

DeWire, SM, Ahn, S, Lefkowitz, RJ & Shenoy, SK 2007, 'Beta-arrestins and cell signaling', *Annual review of physiology*, vol. 69, pp. 483–510.

Downes, GB & Gautam, N 1999, 'The G protein subunit gene families', *Genomics*, vol. 62, no. 3, pp. 544–552.

Drake, MT, Violin, JD, Whalen, EJ, Wisler, JW, Shenoy, SK & Lefkowitz, RJ 2008, 'beta-arrestin-biased agonism at the beta2-adrenergic receptor', *The Journal of biological chemistry*, vol. 283, no. 9, pp. 5669–5676.

Drazen, JM, Israel, E & O'Byrne, PM 1999, 'Treatment of asthma with drugs modifying the leukotriene pathway', *The New England journal of medicine*, vol. 340, no. 3, pp. 197–206.

Drews, J 2000, 'Drug discovery: a historical perspective', *Science (New York, N.Y.)*, vol. 287, no. 5460, pp. 1960–1964.

Drews, J 2006, 'What's in a number?', *Nature reviews. Drug discovery*, vol. 5, no. 12, p. 975.

Eglen, RM 2005, 'Emerging concepts in GPCR function--the influence of cell phenotype on GPCR pharmacology', *Proceedings of the Western Pharmacology Society*, vol. 48, pp. 31–34.

Estacion, M, Li, S, Sinkins, WG, Gosling, M, Bahra, P, Poll, C, Westwick, J & Schilling, WP 2004, 'Activation of human TRPC6 channels by receptor stimulation', *The Journal of biological chemistry*, vol. 279, no. 21, pp. 22047–22056.

Evans, BA, Sato, M, Sarwar, M, Hutchinson, DS & Summers, RJ 2010, 'Ligand-directed signalling at beta-adrenoceptors', *British journal of pharmacology*, vol. 159, no. 5, pp. 1022–1038.

Evans, MJ & Kaufman, MH 1981, 'Establishment in culture of pluripotential cells from mouse embryos', *Nature*, vol. 292, no. 5819, pp. 154–156.

Fang, Y & Ferrie, AM 2007, 'Optical biosensor differentiates signaling of endogenous PAR1 and PAR2 in A431 cells', *BMC cell biology*, vol. 8, p. 24.

Fang, Y, Ferrie, AM, Fontaine, NH, Mauro, J & Balakrishnan, J 2006, 'Resonant waveguide grating biosensor for living cell sensing', *Biophysical journal*, vol. 91, no. 5, pp. 1925–1940.

Fang, Y, Ferrie, AM, Fontaine, NH & Yuen, PK 2005, 'Characteristics of dynamic mass redistribution of epidermal growth factor receptor signaling in living cells measured with label-free optical biosensors', *Analytical chemistry*, vol. 77, no. 17, pp. 5720–5725.

Fang, Y, Ferrie, AM & Tran, E 2009, 'Resonant waveguide grating biosensor for whole-cell GPCR assays', *Methods in molecular biology (Clifton, N.J.)*, vol. 552, pp. 239–252.

Fang, Y, Frutos, AG & Verklereen, R 2008, 'Label-free cell-based assays for GPCR screening', *Combinatorial chemistry & high throughput screening*, vol. 11, no. 5, pp. 357–369.

Fang, Y, Li, G & Ferrie, AM, 'Non-invasive optical biosensor for assaying endogenous G protein-coupled receptors in adherent cells', *Journal of pharmacological and toxicological methods*, vol. 55, no. 3, pp. 314–322.

Faussner, A, Bauer, A, Kalatskaya, I, Jochum, M & Fritz, H 2003, 'Expression levels strongly affect ligand-induced sequestration of B2 bradykinin receptors in transfected cells', *American journal of physiology. Heart and circulatory physiology*, vol. 284, no. 6, pp. H1892-8.

Ferguson, SS 2001, 'Evolving concepts in G protein-coupled receptor endocytosis: the role in receptor desensitization and signaling', *Pharmacological reviews*, vol. 53, no. 1, pp. 1–24.

Ferguson, SS & Caron, MG 1998, 'G protein-coupled receptor adaptation mechanisms', *Seminars in cell & developmental biology*, vol. 9, no. 2, pp. 119–127.

Ferguson, SS, Downey, WE, Colapietro, AM, Barak, LS, Ménard, L & Caron, MG 1996, 'Role of beta-arrestin in mediating agonist-promoted G protein-coupled receptor internalization', *Science (New York, N.Y.)*, vol. 271, no. 5247, pp. 363–366.

Ferguson, SS, Zhang, J, Barak, LS & Caron, MG 1998, 'Molecular mechanisms of G protein-coupled receptor desensitization and resensitization', *Life sciences*, vol. 62, 17-18, pp. 1561–1565.

Flower, DR 1999, 'Modelling G-protein-coupled receptors for drug design', *Biochimica et biophysica acta*, vol. 1422, no. 3, pp. 207–234.

Frank, M, Thümer, L, Lohse, MJ & Bünemann, M 2005, 'G Protein activation without subunit dissociation depends on a G{alpha}(i)-specific region', *The Journal of biological chemistry*, vol. 280, no. 26, pp. 24584–24590.

Fraser, CM, Arakawa, S, McCombie, WR & Venter, JC 1989, 'Cloning, sequence analysis, and permanent expression of a human alpha 2-adrenergic receptor in Chinese hamster ovary cells. Evidence for independent pathways of receptor coupling to adenylate cyclase attenuation and activation', *The Journal of biological chemistry*, vol. 264, no. 20, pp. 11754–11761.

Fredriksson, R, Lagerström, MC, Lundin, L & Schiöth, HB 2003, 'The G-protein-coupled receptors in the human genome form five main families. Phylogenetic analysis, paralogon groups, and fingerprints', *Molecular pharmacology*, vol. 63, no. 6, pp. 1256–1272.

Freedman, NJ & Lefkowitz, RJ 1996, 'Desensitization of G protein-coupled receptors', *Recent progress in hormone research*, vol. 51, pp. 319-51; discussion 352-3.

Fumagalli, M, Daniele, S, Lecca, D, Lee, PR, Parravicini, C, Fields, RD, Rosa, P, Antonucci, F, Verderio, C, Trincavelli, ML, Bramanti, P, Martini, C & Abbracchio, MP 2011, 'Phenotypic changes, signaling pathway and functional correlates of GPR17-expressing neural precursor cells during oligodendrocyte differentiation', *The Journal of biological chemistry*.

Gabriel, D, Vernier, M, Pfeifer, MJ, Dasen, B, Tenaillon, L & Bouhelal, R 2003, 'High throughput screening technologies for direct cyclic AMP measurement', *Assay and drug development technologies*, vol. 1, no. 2, pp. 291–303.

Gao, Z & Jacobson, KA 2008, 'Translocation of arrestin induced by human A(3) adenosine receptor ligands in an engineered cell line: comparison with G protein-dependent pathways', *Pharmacological research : the official journal of the Italian Pharmacological Society*, vol. 57, no. 4, pp. 303–311.

Gaspard, N, Bouschet, T, Herpoel, A, Naeije, G, van den Ameele, J & Vanderhaeghen, P 2009, 'Generation of cortical neurons from mouse embryonic stem cells', *Nature protocols*, vol. 4, no. 10, pp. 1454–1463.

Gearing, DP, Thut, CJ, VandeBos, T, Gimpel, SD, Delaney, PB, King, J, Price, V, Cosman, D & Beckmann, MP 1991, 'Leukemia inhibitory factor receptor is structurally related to the IL-6 signal transducer, gp130', *The EMBO journal*, vol. 10, no. 10, pp. 2839–2848.

George, ST, Berrios, M, Hadcock, JR, Wang, HY & Malbon, CC 1988, 'Receptor density and cAMP accumulation: analysis in CHO cells exhibiting stable expression of a cDNA that encodes the beta 2-adrenergic receptor', *Biochemical and biophysical research communications*, vol. 150, no. 2, pp. 665–672.

Gether, U 2000, 'Uncovering molecular mechanisms involved in activation of G protein-coupled receptors', *Endocrine reviews*, vol. 21, no. 1, pp. 90–113.

Gill, DM & Meren, R 1978, 'ADP-ribosylation of membrane proteins catalyzed by cholera toxin: basis of the activation of adenylate cyclase', *Proceedings of the National Academy of Sciences of the United States of America*, vol. 75, no. 7, pp. 3050–3054.

Gilman, AG 1987, 'G proteins: transducers of receptor-generated signals', *Annual review of biochemistry*, vol. 56, pp. 615–649

Gilman, AG 1995, 'Nobel Lecture. G proteins and regulation of adenylyl cyclase', *Bioscience reports*, vol. 15, no. 2, pp. 65–97.

Glass, M & Felder, CC 1997, 'Concurrent stimulation of cannabinoid CB1 and dopamine D2 receptors augments cAMP accumulation in striatal neurons: evidence for a Gs linkage to the CB1 receptor', *The Journal of neuroscience : the official journal of the Society for Neuroscience*, vol. 17, no. 14, pp. 5327–5333.

Goodman, OB, Krupnick, JG, Santini, F, Gurevich, VV, Penn, RB, Gagnon, AW, Keen, JH & Benovic, JL 1996, 'Beta-arrestin acts as a clathrin adaptor in endocytosis of the beta2-adrenergic receptor', *Nature*, vol. 383, no. 6599, pp. 447–450.

Grammatopoulos, DK, Randeva, HS, Levine, MA, Kanellopoulou, KA & Hillhouse, EW 2001, 'Rat cerebral cortex corticotropin-releasing hormone receptors: evidence for receptor coupling to multiple G-proteins', *Journal of neurochemistry*, vol. 76, no. 2, pp. 509–519.

Gudermann, T, Schöneberg, T & Schultz, G 1997, 'Functional and structural complexity of signal transduction via G-protein-coupled receptors', *Annual review of neuroscience*, vol. 20, pp. 399–427.

Gurevich, EV, Benovic, JL & Gurevich, VV 2004, 'Arrestin2 expression selectively increases during neural differentiation', *Journal of neurochemistry*, vol. 91, no. 6, pp. 1404–1416.

Hajnóczky, G, Gao, E, Nomura, T, Hoek, JB & Thomas, AP 1993, 'Multiple mechanisms by which protein kinase A potentiates inositol 1,4,5-trisphosphate-induced Ca2+ mobilization in permeabilized hepatocytes', *The Biochemical journal*, 293 (Pt 2), pp. 413–422.

Hall, DA, Beresford, IJ, Browning, C & Giles, H 1999, 'Signalling by CXC-chemokine receptors 1 and 2 expressed in CHO cells: a comparison of calcium mobilization, inhibition of adenylyl cyclase and stimulation of GTPgammaS binding induced by IL-8 and GROalpha', *British journal of pharmacology*, vol. 126, no. 3, pp. 810–818.

Hamdan, FF, Audet, M, Garneau, P, Pelletier, J & Bouvier, M 2005, 'High-throughput screening of G protein-coupled receptor antagonists using a bioluminescence resonance energy transfer 1-based beta-arrestin2 recruitment assay', *Journal of biomolecular screening : the official journal of the Society for Biomolecular Screening*, vol. 10, no. 5, pp. 463–475.

Hanyaloglu, AC, Seeber, RM, Kohout, TA, Lefkowitz, RJ & Eidne, KA 2002, 'Homo- and hetero-oligomerization of thyrotropin-releasing hormone (TRH) receptor subtypes. Differential regulation of beta-arrestins 1 and 2', *The Journal of biological chemistry*, vol. 277, no. 52, pp. 50422–50430.

Hasbi, A, Devost, D, Laporte, SA & Zingg, HH 2004, 'Real-time detection of interactions between the human oxytocin receptor and G protein-coupled receptor kinase-2', *Molecular endocrinology (Baltimore, Md.)*, vol. 18, no. 5, pp. 1277–1286.

Hasty, P, Rivera-Pérez, J & Bradley, A 1991, 'The length of homology required for gene targeting in embryonic stem cells', *Molecular and cellular biology*, vol. 11, no. 11, pp. 5586–5591.

Hay, DW 1997, 'Pharmacology of leukotriene receptor antagonists. More than inhibitors of bronchoconstriction', *Chest*, vol. 111, 2 Suppl, pp. 35S-45S.

Hepler, JR & Gilman, AG 1992, 'G proteins', *Trends in biochemical sciences*, vol. 17, no. 10, pp. 383–387.

Hermans, E, Saunders, R, Selkirk, JV, Mistry, R, Nahorski, SR & Challiss, RA 2000, 'Complex involvement of pertussis toxin-sensitive G proteins in the regulation of type 1alpha metabotropic glutamate receptor signaling in baby hamster kidney cells', *Molecular pharmacology*, vol. 58, no. 2, pp. 352–360.

Hermans, E 2003, 'Biochemical and pharmacological control of the multiplicity of coupling at G-protein-coupled receptors', *Pharmacology & therapeutics*, vol. 99, no. 1, pp. 25–44.

Hoare, S, Copland, JA, Strakova, Z, Ives, K, Jeng, YJ, Hellmich, MR & Soloff, MS 1999, 'The proximal portion of the COOH terminus of the oxytocin receptor is required for coupling to g(q), but not g(i). Independent mechanisms for elevating intracellular calcium concentrations from intracellular stores', *The Journal of biological chemistry*, vol. 274, no. 40, pp. 28682–28689.

Holliday, ND, Lam, C, Tough, IR & Cox, HM 2005, 'Role of the C terminus in neuropeptide Y Y1 receptor desensitization and internalization', *Molecular pharmacology*, vol. 67, no. 3, pp. 655–664.

Holloway, AC, Qian, H, Pipolo, L, Ziogas, J, Miura, S, Karnik, S, Southwell, BR, Lew, MJ & Thomas, WG 2002, 'Side-chain substitutions within angiotensin II reveal different requirements for signaling, internalization, and phosphorylation of type 1A angiotensin receptors', *Molecular pharmacology*, vol. 61, no. 4, pp. 768–777.

Hulme, EC, Lu, ZL, Ward, SD, Allman, K & Curtis, CA 1999, 'The conformational switch in 7-transmembrane receptors: the muscarinic receptor paradigm', *European journal of pharmacology*, vol. 375, 1-3, pp. 247–260.

Iñiguez-Lluhi, JA, Simon, MI, Robishaw, JD & Gilman, AG 1992, 'G protein beta gamma subunits synthesized in Sf9 cells. Functional characterization and the significance of prenylation of gamma', *The Journal of biological chemistry*, vol. 267, no. 32, pp. 23409–23417.

Iredale, PA & Hill, SJ 1993, 'Increases in intracellular calcium via activation of an endogenous P2-purinoceptor in cultured CHO-K1 cells', *British journal of pharmacology*, vol. 110, no. 4, pp. 1305–1310.

Issafras, H, Angers, S, Bulenger, S, Blanpain, C, Parmentier, M, Labbé-Jullié, C, Bouvier, M & Marullo, S 2002, 'Constitutive agonist-independent CCR5 oligomerization and antibody-mediated clustering occurring at physiological levels of receptors', *The Journal of biological chemistry*, vol. 277, no. 38, pp. 34666–34673.

Itagaki, K, Barton, BE, Murphy, TF, Taheri, S, Shu, P, Huang, H & Jordan, ML 2009, 'Eicosanoid-Induced Store-Operated Calcium Entry in Dendritic Cells', *The Journal of surgical research*.

Jala, VR, Shao, W & Haribabu, B 2005, 'Phosphorylation-independent beta-arrestin translocation and internalization of leukotriene B4 receptors', *The Journal of biological chemistry*, vol. 280, no. 6, pp. 4880–4887.

Ji, TH, Grossmann, M & Ji, I 1998, 'G protein-coupled receptors. I. Diversity of receptor-ligand interactions', *The Journal of biological chemistry*, vol. 273, no. 28, pp. 17299–17302.

Jiang, X, Shen, C, Rey-Ladino, J, Yu, H & Brunham, RC 2008, 'Characterization of murine dendritic cell line JAWS II and primary bone marrow-derived dendritic cells in Chlamydia muridarum antigen presentation and induction of protective immunity', *Infection and immunity*, vol. 76, no. 6, pp. 2392–2401.

Jin, R, Yang, G & Li, G 2010, 'Inflammatory mechanisms in ischemic stroke: role of inflammatory cells', *Journal of leukocyte biology*, vol. 87, no. 5, pp. 779–789.

Jones, KA, Borowsky, B, Tamm, JA, Craig, DA, Durkin, MM, Dai, M, Yao, WJ, Johnson, M, Gunwaldsen, C, Huang, LY, Tang, C, Shen, Q, Salon, JA, Morse, K, Laz, T, Smith, KE, Nagarathnam, D, Noble, SA, Branchek, TA & Gerald,

C 1998, 'GABA(B) receptors function as a heteromeric assembly of the subunits GABA(B)R1 and GABA(B)R2', *Nature*, vol. 396, no. 6712, pp. 674–679.

Jones, TR, Labelle, M, Belley, M, Champion, E, Charette, L, Evans, J, Ford-Hutchinson, AW, Gauthier, JY, Lord, A & Masson, P 1995, 'Pharmacology of montelukast sodium (Singulair), a potent and selective leukotriene D4 receptor antagonist', *Canadian journal of physiology and pharmacology*, vol. 73, no. 2, pp. 191–201.

Jones, TR, Zamboni, R, Belley, M, Champion, E, Charette, L, Ford-Hutchinson, AW, Frenette, R, Gauthier, JY, Leger, S & Masson, P 1989, 'Pharmacology of L-660,711 (MK-571): a novel potent and selective leukotriene D4 receptor antagonist', *Canadian journal of physiology and pharmacology*, vol. 67, no. 1, pp. 17–28.

Kang, DS & Leeb-Lundberg, LMF 2002, 'Negative and positive regulatory epitopes in the C-terminal domains of the human B1 and B2 bradykinin receptor subtypes determine receptor coupling efficacy to G(q/11)-mediated [correction of G(9/11)-mediated] phospholipase Cbeta activity', *Molecular pharmacology*, vol. 62, no. 2, pp. 281–288.

Katada, T, Bokoch, GM, Northup, JK, Ui, M & Gilman, AG 1984, 'The inhibitory guanine nucleotide-binding regulatory component of adenylate cyclase. Properties and function of the purified protein', *The Journal of biological chemistry*, vol. 259, no. 6, pp. 3568–3577.

Katada, T & Ui, M 1982, 'Direct modification of the membrane adenylate cyclase system by islet-activating protein due to ADP-ribosylation of a membrane protein', *Proceedings of the National Academy of Sciences of the United States of America*, vol. 79, no. 10, pp. 3129–3133.

Kaupmann, K, Malitschek, B, Schuler, V, Heid, J, Froestl, W, Beck, P, Mosbacher, J, Bischoff, S, Kulik, A, Shigemoto, R, Karschin, A & Bettler, B 1998, 'GABA(B)-receptor subtypes assemble into functional heteromeric complexes', *Nature*, vol. 396, no. 6712, pp. 683–687.

Kebig, A, Kostenis, E, Mohr, K & Mohr-Andrä, M 2009, 'An optical dynamic mass redistribution assay reveals biased signaling of dualsteric GPCR activators', *Journal of receptor and signal transduction research*, vol. 29, 3-4, pp. 140–145.

Kenakin, T 1997, 'Differences between natural and recombinant G protein-coupled receptor systems with varying receptor/G protein stoichiometry', *Trends in pharmacological sciences*, vol. 18, no. 12, pp. 456–464.

Kenakin, T 2002, 'Drug efficacy at G protein-coupled receptors', *Annual review of pharmacology and toxicology*, vol. 42, pp. 349–379.

Kenakin, T 2003, 'Ligand-selective receptor conformations revisited: the promise and the problem', *Trends in pharmacological sciences*, vol. 24, no. 7, pp. 346–354.

Kenakin, T 2005, 'New concepts in drug discovery: collateral efficacy and permissive antagonism', *Nature reviews. Drug discovery*, vol. 4, no. 11, pp. 919–927.

Kenakin, T 2007, 'Functional selectivity through protean and biased agonism: who steers the ship?', *Molecular pharmacology*, vol. 72, no. 6, pp. 1393–1401.

Kenakin, T 2011, 'Functional selectivity and biased receptor signaling', *The Journal of pharmacology and experimental therapeutics*, vol. 336, no. 2, pp. 296–302.

Kenakin, T, Jenkinson, S & Watson, C 2006, 'Determining the potency and molecular mechanism of action of insurmountable antagonists', *The Journal of pharmacology and experimental therapeutics*, vol. 319, no. 2, pp. 710–723.

Kenakin, T & Miller, LJ 2010, 'Seven transmembrane receptors as shapeshifting proteins: the impact of allosteric modulation and functional selectivity on new drug discovery', *Pharmacological reviews*, vol. 62, no. 2, pp. 265–304.

Kholodenko, BN 2006, 'Cell-signalling dynamics in time and space', *Nature reviews. Molecular cell biology*, vol. 7, no. 3, pp. 165–176.

Kim, KM, Valenzano, KJ, Robinson, SR, Yao, WD, Barak, LS & Caron, MG 2001, 'Differential regulation of the dopamine D2 and D3 receptors by G protein-coupled receptor kinases and beta-arrestins', *The Journal of biological chemistry*, vol. 276, no. 40, pp. 37409–37414.

Kobilka, B 1992, 'Adrenergic receptors as models for G protein-coupled receptors', *Annual review of neuroscience*, vol. 15, pp. 87–114.

Kohout, TA, Lin, FS, Perry, SJ, Conner, DA & Lefkowitz, RJ 2001, 'beta-Arrestin 1 and 2 differentially regulate heptahelical receptor signaling and trafficking', *Proceedings of the National Academy of Sciences of the United States of America*, vol. 98, no. 4, pp. 1601–1606.

Kohout, TA & Lefkowitz, RJ 2003, 'Regulation of G protein-coupled receptor kinases and arrestins during receptor desensitization', *Molecular pharmacology*, vol. 63, no. 1, pp. 9–18.

Kolodziej, PA & Young, RA 1991, 'Epitope tagging and protein surveillance', *Methods in enzymology*, vol. 194, pp. 508–519.

Krasel, C, Vilardaga, J, Bünemann, M & Lohse, MJ 2004, 'Kinetics of G-protein-coupled receptor signalling and desensitization', *Biochemical Society transactions*, vol. 32, Pt 6, pp. 1029–1031.

Krell, RD, Aharony, D, Buckner, CK, Keith, RA, Kusner, EJ, Snyder, DW, Bernstein, PR, Matassa, VG, Yee, YK & Brown, FJ 1990, 'The preclinical pharmacology of ICI 204,219. A peptide leukotriene antagonist', *The American review of respiratory disease*, vol. 141, 4 Pt 1, pp. 978–987.

Kroeger, KM, Hanyaloglu, AC, Seeber, RM, Miles, LE & Eidne, KA 2001, 'Constitutive and agonist-dependent homo-oligomerization of the thyrotropin-releasing hormone receptor. Detection in living cells using bioluminescence resonance energy transfer', *The Journal of biological chemistry*, vol. 276, no. 16, pp. 12736–12743.

Krueger, KM, Witte, DG, Ireland-Denny, L, Miller, TR, Baranowski, JL, Buckner, S, Milicic, I, Esbenshade, TA & Hancock, AA 2005, 'G protein-dependent pharmacology of histamine H3 receptor ligands: evidence for heterogeneous active state receptor conformations', *The Journal of pharmacology and experimental therapeutics*, vol. 314, no. 1, pp. 271–281.

Kühn, H & Wilden, U 1987, 'Deactivation of photoactivated rhodopsin by rhodopsin-kinase and arrestin', *Journal of receptor research*, vol. 7, 1-4, pp. 283–298.

Labasque, M, Reiter, E, Becamel, C, Bockaert, J & Marin, P 2008, 'Physical interaction of calmodulin with the 5-hydroxytryptamine2C receptor C-terminus is essential for G protein-independent, arrestin-dependent receptor signaling', *Molecular biology of the cell*, vol. 19, no. 11, pp. 4640–4650.

Lagerström, MC & Schiöth, HB 2008, 'Structural diversity of G protein-coupled receptors and significance for drug discovery', *Nature reviews. Drug discovery*, vol. 7, no. 4, pp. 339–357.

Lander, ES, Linton, LM, Birren, B, Nusbaum, C, Zody, MC, Baldwin, J, Devon, K, Dewar, K, Doyle, M, FitzHugh, W, Funke, R, Gage, D, Harris, K, Heaford, A, Howland, J, Kann, L, Lehoczky, J, LeVine, R, et al. 2001, 'Initial sequencing and analysis of the human genome', *Nature*, vol. 409, no. 6822, pp. 860–921.

Laporte, SA, Oakley, RH, Zhang, J, Holt, JA, Ferguson, SS, Caron, MG & Barak, LS 1999, 'The beta2-adrenergic receptor/betaarrestin complex recruits the clathrin adaptor AP-2 during endocytosis', *Proceedings of the National Academy of Sciences of the United States of America*, vol. 96, no. 7, pp. 3712–3717.

Lattin, J, Zidar, DA, Schroder, K, Kellie, S, Hume, DA & Sweet, MJ 2007, 'G-protein-coupled receptor expression, function, and signaling in macrophages', *Journal of leukocyte biology*, vol. 82, no. 1, pp. 16–32.

Laugwitz, KL, Allgeier, A, Offermanns, S, Spicher, K, van Sande, J, Dumont, JE & Schultz, G 1996, 'The human thyrotropin receptor: a heptahelical receptor capable of stimulating members of all four G protein families', *Proceedings of the National Academy of Sciences of the United States of America*, vol. 93, no. 1, pp. 116–120.

Lawler, CP, Prioleau, C, Lewis, MM, Mak, C, Jiang, D, Schetz, JA, Gonzalez, AM, Sibley, DR & Mailman, RB 1999, 'Interactions of the novel antipsychotic aripiprazole (OPC-14597) with dopamine and serotonin receptor subtypes', *Neuropsychopharmacology : official publication of the American College of Neuropsychopharmacology*, vol. 20, no. 6, pp. 612–627.

Lawler, OA, Miggin, SM & Kinsella, BT 2001, 'Protein kinase A-mediated phosphorylation of serine 357 of the mouse prostacyclin receptor regulates its coupling to G(s)-, to G(i)-, and to G(q)-coupled effector signaling', *The Journal of biological chemistry*, vol. 276, no. 36, pp. 33596–33607.

Lecca, D, Trincavelli, ML, Gelosa, P, Sironi, L, Ciana, P, Fumagalli, M, Villa, G, Verderio, C, Grumelli, C, Guerrini, U, Tremoli, E, Rosa, P, Cuboni, S, Martini, C, Buffo, A, Cimino, M & Abbracchio, MP 2008, 'The recently identified P2Y-like receptor GPR17 is a sensor of brain damage and a new target for brain repair', *PloS one*, vol. 3, no. 10, pp. e3579.

Lee, PH, Gao, A, van Staden, C, Ly, J, Salon, J, Xu, A, Fang, Y & Verkleeren, R 2008, 'Evaluation of dynamic mass redistribution technology for pharmacological studies of recombinant and endogenously expressed g protein-coupled receptors', *Assay and drug development technologies*, vol. 6, no. 1, pp. 83–94.

Lefkowitz, RJ 1993, 'G protein-coupled receptor kinases', *Cell*, vol. 74, no. 3, pp. 409–412.

Lefkowitz, RJ 1998, 'G protein-coupled receptors. III. New roles for receptor kinases and beta-arrestins in receptor signaling and desensitization', *The Journal of biological chemistry*, vol. 273, no. 30, pp. 18677–18680.

Lefkowitz, RJ & Shenoy, SK 2005, 'Transduction of receptor signals by beta-arrestins', *Science (New York, N.Y.)*, vol. 308, no. 5721, pp. 512–517.

Levoye, A, Dam, J, Ayoub, MA, Guillaume, J, Couturier, C, Delagrange, P & Jockers, R 2006, 'The orphan GPR50 receptor specifically inhibits MT1 melatonin receptor function through heterodimerization', *The EMBO journal*, vol. 25, no. 13, pp. 3012–3023.

Li, G, Shi, Y, Huang, H, Zhang, Y, Wu, K, Luo, J, Sun, Y, Lu, J, Benovic, JL & Zhou, N 2010, 'Internalization of the human nicotinic acid receptor GPR109A is regulated by G(i), GRK2, and arrestin3', *The Journal of biological chemistry*, vol. 285, no. 29, pp. 22605–22618.

Lipworth, BJ 1999, 'Leukotriene-receptor antagonists', *Lancet*, vol. 353, no. 9146, pp. 57–62.

Lohse, MJ, Benovic, JL, Codina, J, Caron, MG & Lefkowitz, RJ 1990, 'beta-Arrestin: a protein that regulates beta-adrenergic receptor function', *Science (New York, N.Y.)*, vol. 248, no. 4962, pp. 1547–1550.

Luo, J, Busillo, JM & Benovic, JL 2008, 'M3 muscarinic acetylcholine receptor-mediated signaling is regulated by distinct mechanisms', *Molecular pharmacology*, vol. 74, no. 2, pp. 338–347.

Luttrell, LM & Gesty-Palmer, D 2010, 'Beyond desensitization: physiological relevance of arrestin-dependent signaling', *Pharmacological reviews*, vol. 62, no. 2, pp. 305–330.

Luttrell, LM & Lefkowitz, RJ 2002, 'The role of beta-arrestins in the termination and transduction of G-protein-coupled receptor signals', *Journal of cell science*, vol. 115, Pt 3, pp. 455–465.

Machida, I, Matsuse, H, Kondo, Y, Kawano, T, Saeki, S, Tomari, S, Obase, Y, Fukushima, C & Kohno, S 2004, 'Cysteinyl leukotrienes regulate dendritic cell functions in a murine model of asthma', *Journal of immunology (Baltimore, Md. : 1950)*, vol. 172, no. 3, pp. 1833–1838.

Maekawa, A, Balestrieri, B, Austen, KF & Kanaoka, Y 2009, 'GPR17 is a negative regulator of the cysteinyl leukotriene 1 receptor response to leukotriene D4', *Proceedings of the National Academy of Sciences of the United States of America*, vol. 106, no. 28, pp. 11685–11690.

Maekawa, A, Xing, W, Austen, KF & Kanaoka, Y 2010, 'GPR17 regulates immune pulmonary inflammation induced by house dust mites', *Journal of immunology (Baltimore, Md. : 1950)*, vol. 185, no. 3, pp. 1846–1854.

Mailman, RB 2007, 'GPCR functional selectivity has therapeutic impact', *Trends in pharmacological sciences*, vol. 28, no. 8, pp. 390–396.

Mailman, RB & Murthy, V 2010, 'Third generation antipsychotic drugs: partial agonism or receptor functional selectivity?', *Current pharmaceutical design*, vol. 16, no. 5, pp. 488–501.

Maisel, M, Herr, A, Milosevic, J, Hermann, A, Habisch, H, Schwarz, S, Kirsch, M, Antoniadis, G, Brenner, R, Hallmeyer-Elgner, S, Lerche, H, Schwarz, J & Storch, A 2007, 'Transcription profiling of adult and fetal human neuroprogenitors identifies divergent paths to maintain the neuroprogenitor cell state', *Stem cells (Dayton, Ohio)*, vol. 25, no. 5, pp. 1231–1240.

Mamedova, L, Capra, V, Accomazzo, MR, Gao, Z, Ferrario, S, Fumagalli, M, Abbracchio, MP, Rovati, GE & Jacobson, KA 2005, 'CysLT1 leukotriene receptor antagonists inhibit the effects of nucleotides acting at P2Y receptors', *Biochemical pharmacology*, vol. 71, 1-2, pp. 115–125.

Mansour, SL, Thomas, KR & Capecchi, MR 1988, 'Disruption of the proto-oncogene int-2 in mouse embryo-derived stem cells: a general strategy for targeting mutations to non-selectable genes', *Nature*, vol. 336, no. 6197, pp. 348–352.

Marcet, B, Chappe, V, Delmas, P & Verrier, B 2004, 'Pharmacological and signaling properties of endogenous P2Y1 receptors in cystic fibrosis transmembrane conductance regulator-expressing Chinese hamster ovary cells', *The Journal of pharmacology and experimental therapeutics*, vol. 309, no. 2, pp. 533–539.

Marinissen, MJ & Gutkind, JS 2001, 'G-protein-coupled receptors and signaling networks: emerging paradigms', *Trends in pharmacological sciences*, vol. 22, no. 7, pp. 368–376.

Martin, GR 1981, 'Isolation of a pluripotent cell line from early mouse embryos cultured in medium conditioned by teratocarcinoma stem cells', *Proceedings of the National Academy of Sciences of the United States of America*, vol. 78, no. 12, pp. 7634–7638.

Mastalerz, L & Kumik, J 2010, 'Antileukotriene drugs in the treatment of asthma', *Polskie Archiwum Medycyny Wewnętrznej*, vol. 120, no. 3, pp. 103–108.

Mathiesen, JM, Ulven, T, Martini, L, Gerlach, LO, Heinemann, A & Kostenis, E 2005, 'Identification of indole derivatives exclusively interfering with a G protein-independent signaling pathway of the prostaglandin D2 receptor CRTH2', *Molecular pharmacology*, vol. 68, no. 2, pp. 393–402.

Matsumoto, M, Straub, RE, Marenco, S, Nicodemus, KK, Matsumoto, S, Fujikawa, A, Miyoshi, S, Shobo, M, Takahashi, S, Yarimizu, J, Yuri, M, Hiramoto, M, Morita, S, Yokota, H, Sasayama, T, Terai, K, Yoshino, M, Miyake, A, Callicott, JH, Egan, MF, Meyer-Lindenberg, A, Kempf, L, Honea, R, Vakkalanka, RK, Takasaki, J, Kamohara, M, Soga, T, Hiyama, H, Ishii, H, Matsuo, A, Nishimura, S, Matsuoka, N, Kobori, M, Matsushime, H, Katoh, M, Furuichi, K & Weinberger, DR 2008, 'The evolutionarily conserved G protein-coupled receptor SREB2/GPR85 influences brain size, behavior, and vulnerability to schizophrenia', *Proceedings of the National Academy of Sciences of the United States of America*, vol. 105, no. 16, pp. 6133–6138.

McIntosh, BT, Hudson, B, Yegorova, S, Jollimore, CAB & Kelly, MEM 2007, 'Agonist-dependent cannabinoid receptor signalling in human trabecular meshwork cells', *British journal of pharmacology*, vol. 152, no. 7, pp. 1111–1120.

Mellor, EA, Maekawa, A, Austen, KF & Boyce, JA 2001, 'Cysteinyl leukotriene receptor 1 is also a pyrimidinergic receptor and is expressed by human mast cells', *Proceedings of the National Academy of Sciences of the United States of America*, vol. 98, no. 14, pp. 7964–7969.

Ménard, L, Ferguson, SS, Zhang, J, Lin, FT, Lefkowitz, RJ, Caron, MG & Barak, LS 1997, 'Synergistic regulation of beta2-adrenergic receptor sequestration: intracellular complement of beta-adrenergic receptor kinase and beta-arrestin determine kinetics of internalization', *Molecular pharmacology*, vol. 51, no. 5, pp. 800–808.

Metpally, RPR & Sowdhamini, R 2005, 'Cross genome phylogenetic analysis of human and Drosophila G protein-coupled receptors: application to functional annotation of orphan receptors', *BMC genomics*, vol. 6, p. 106.

Milasta, S, Evans, NA, Ormiston, L, Wilson, S, Lefkowitz, RJ & Milligan, G 2005, 'The sustainability of interactions between the orexin-1 receptor and beta-arrestin-2 is defined by a single C-terminal cluster of hydroxy amino acids and modulates the kinetics of ERK MAPK regulation', *The Biochemical journal*, vol. 387, Pt 3, pp. 573–584.

Milasta, S, Pediani, J, Appelbe, S, Trim, S, Wyatt, M, Cox, P, Fidock, M & Milligan, G 2006, 'Interactions between the Mas-related receptors MrgD and MrgE alter signalling and trafficking of MrgD', *Molecular pharmacology*, vol. 69, no. 2, pp. 479–491.

Milligan, G 1993, 'Mechanisms of multifunctional signalling by G protein-linked receptors', *Trends in pharmacological sciences*, vol. 14, no. 6, pp. 239–244.

Milligan, G, Bond, RA & Lee, M 1995, 'Inverse agonism: pharmacological curiosity or potential therapeutic strategy?', *Trends in pharmacological sciences*, vol. 16, no. 1, pp. 10–13.

Milligan, G 2004, 'Applications of bioluminescence- and fluorescence resonance energy transfer to drug discovery at G protein-coupled receptors', *European journal of pharmaceutical sciences : official journal of the European Federation for Pharmaceutical Sciences*, vol. 21, no. 4, pp. 397–405.

Mons, N, Decorte, L, Jaffard, R & Cooper, DM 1998, 'Ca2+-sensitive adenylyl cyclases, key integrators of cellular signalling', *Life sciences*, vol. 62, 17-18, pp. 1647–1652.

Mukherjee, S, Gurevich, VV, Preninger, A, Hamm, HE, Bader, M, Fazleabas, AT, Birnbaumer, L & Hunzicker-Dunn, M 2002, 'Aspartic acid 564 in the third cytoplasmic loop of the luteinizing hormone/choriogonadotropin receptor is crucial for phosphorylation-independent interaction with arrestin2', *The Journal of biological chemistry*, vol. 277, no. 20, pp. 17916–17927.

Mullis, KB & Faloona, FA 1987, 'Specific synthesis of DNA in vitro via a polymerase-catalyzed chain reaction', *Methods in enzymology*, vol. 155, pp. 335–350.

Mundell, SJ & Benovic, JL 2000, 'Selective regulation of endogenous G protein-coupled receptors by arrestins in HEK293 cells', *The Journal of biological chemistry*, vol. 275, no. 17, pp. 12900–12908.

Mundell, SJ, Loudon, RP & Benovic, JL 1999, 'Characterization of G protein-coupled receptor regulation in antisense mRNA-expressing cells with reduced arrestin levels', *Biochemistry*, vol. 38, no. 27, pp. 8723–8732.

Narlawar, R, Lane, JR, Doddareddy, M, Lin, J, Brussee, J & Ijzerman, AP 2010, 'Hybrid ortho/allosteric ligands for the adenosine A(1) receptor', *Journal of medicinal chemistry*, vol. 53, no. 8, pp. 3028–3037.

Nasman, J, Kukkonen, JP, Ammoun, S & Akerman, KE 2001, 'Role of G-protein availability in differential signaling by alpha 2-adrenoceptors', *Biochemical pharmacology*, vol. 62, no. 7, pp. 913–922.

Neumann, E, Schaefer-Ridder, M, Wang, Y & Hofschneider, PH 1982, 'Gene transfer into mouse lyoma cells by electroporation in high electric fields', *The EMBO journal*, vol. 1, no. 7, pp. 841–845.

Neves, SR, Ram, PT & Iyengar, R 2002, 'G protein pathways', *Science (New York, N.Y.)*, vol. 296, no. 5573, pp. 1636–1639.

Newman-Tancredi, A, Conte, C, Chaput, C, Spedding, M & Millan, MJ 1997, 'Inhibition of the constitutive activity of human 5-HT1A receptors by the inverse agonist, spiperone but not the neutral antagonist, WAY 100,635', *British journal of pharmacology*, vol. 120, no. 5, pp. 737–739.

Nichols, DE 2004, 'Hallucinogens', *Pharmacology & therapeutics*, vol. 101, no. 2, pp. 131–181.

Oakley, RH, Laporte, SA, Holt, JA, Barak, LS & Caron, MG 1999, 'Association of beta-arrestin with G protein-coupled receptors during clathrin-mediated endocytosis dictates the profile of receptor resensitization', *The Journal of biological chemistry*, vol. 274, no. 45, pp. 32248–32257.

Oakley, RH, Laporte, SA, Holt, JA, Barak, LS & Caron, MG 2001, 'Molecular determinants underlying the formation of stable intracellular G protein-coupled receptor-beta-arrestin complexes after receptor endocytosis*', *The Journal of biological chemistry*, vol. 276, no. 22, pp. 19452–19460.

Oakley, RH, Laporte, SA, Holt, JA, Caron, MG & Barak, LS 2000, 'Differential affinities of visual arrestin, beta arrestin1, and beta arrestin2 for G protein-coupled receptors delineate two major classes of receptors', *The Journal of biological chemistry*, vol. 275, no. 22, pp. 17201–17210.

Obata, T, Okada, Y, Motoishi, M, Nakagawa, N, Terawaki, T & Aishita, H 1992, 'In vitro antagonism of ONO-1078, a newly developed anti-asthma agent, against peptide leukotrienes in isolated guinea pig tissues', *Japanese journal of pharmacology*, vol. 60, no. 3, pp. 227–237.

Offermanns, S, Wieland, T, Homann, D, Sandmann, J, Bombien, E, Spicher, K, Schultz, G & Jakobs, KH 1994, 'Transfected muscarinic acetylcholine receptors selectively couple to Gi-type G proteins and Gq/11', *Molecular pharmacology*, vol. 45, no. 5, pp. 890–898.

Okunishi, K, Dohi, M, Nakagome, K, Tanaka, R & Yamamoto, K 2004, 'A novel role of cysteinyl leukotrienes to promote dendritic cell activation in the antigen-induced immune responses in the lung', *Journal of immunology (Baltimore, Md. : 1950)*, vol. 173, no. 10, pp. 6393–6402.

Orrantia, E & Chang, PL 1990, 'Intracellular distribution of DNA internalized through calcium phosphate precipitation', *Experimental cell research*, vol. 190, no. 2, pp. 170–174.

O'Shaughnessy, TC, Georgiou, P, Howland, K, Dennis, M, Compton, CH & Barnes, NC 1997, 'Effect of pranlukast, an oral leukotriene receptor antagonist, on leukotriene D4 (LTD4) challenge in normal volunteers', *Thorax*, vol. 52, no. 6, pp. 519–522.

Overington, JP, Al-Lazikani, B & Hopkins, AL 2006, 'How many drug targets are there?', *Nature reviews. Drug discovery*, vol. 5, no. 12, pp. 993–996.

Palczewski, K, Kumasaka, T, Hori, T, Behnke, CA, Motoshima, H, Fox, BA, Le Trong, I, Teller, DC, Okada, T, Stenkamp, RE, Yamamoto, M & Miyano, M 2000, 'Crystal structure of rhodopsin: A G protein-coupled receptor', *Science (New York, N.Y.)*, vol. 289, no. 5480, pp. 739–745.

Pankevych, H, Korkhov, V, Freissmuth, M & Nanoff, C 2003, 'Truncation of the A1 adenosine receptor reveals distinct roles of the membrane-proximal carboxyl terminus in receptor folding and G protein coupling', *The Journal of biological chemistry*, vol. 278, no. 32, pp. 30283–30293.

Parravicini, C, Abbracchio, MP, Fantucci, P & Ranghino, G 2010, 'Forced unbinding of GPR17 ligands from wild type and R255I mutant receptor models through a computational approach', *BMC structural biology*, vol. 10, p. 8.

Parravicini, C, Ranghino, G, Abbracchio, MP & Fantucci, P 2008, 'GPR17: molecular modeling and dynamics studies of the 3-D structure and purinergic ligand binding features in comparison with P2Y receptors', *BMC bioinformatics*, vol. 9, p. 263.

Pasternack, SM, Kügelgen, I von, Aboud, KA, Lee, Y, Rüschendorf, F, Voss, K, Hillmer, AM, Molderings, GJ, Franz, T, Ramirez, A, Nürnberg, P, Nöthen, MM & Betz, RC 2008, 'G protein-coupled receptor P2Y5 and its ligand LPA are involved in maintenance of human hair growth', *Nature genetics*, vol. 40, no. 3, pp. 329–334.

Perez, DM & Karnik, SS 2005, 'Multiple signaling states of G-protein-coupled receptors', *Pharmacological reviews*, vol. 57, no. 2, pp. 147–161.

Perry, SJ, Junger, S, Kohout, TA, Hoare, SRJ, Struthers, RS, Grigoriadis, DE & Maki, RA 2005, 'Distinct conformations of the corticotropin releasing factor type 1 receptor adopted following agonist and antagonist binding are differentially regulated', *The Journal of biological chemistry*, vol. 280, no. 12, pp. 11560–11568.

Perry, SJ & Lefkowitz, RJ 2002, 'Arresting developments in heptahelical receptor signaling and regulation', *Trends in cell biology*, vol. 12, no. 3, pp. 130–138.

Pfleger, KDG, Dalrymple, MB, Dromey, JR & Eidne, KA 2007, 'Monitoring interactions between G-protein-coupled receptors and beta-arrestins', *Biochemical Society transactions*, vol. 35, Pt 4, pp. 764–766.

Pfleger, KDG & Eidne, KA 2005, 'Monitoring the formation of dynamic G-protein-coupled receptor-protein complexes in living cells', *The Biochemical journal*, vol. 385, Pt 3, pp. 625–637.

Pfleger, KDG & Eidne, KA 2006, 'Illuminating insights into protein-protein interactions using bioluminescence resonance energy transfer (BRET)', *Nature methods*, vol. 3, no. 3, pp. 165–174.

Pierce, KL & Lefkowitz, RJ 2001, 'Classical and new roles of beta-arrestins in the regulation of G-protein-coupled receptors', *Nature reviews. Neuroscience*, vol. 2, no. 10, pp. 727–733.

Pierce, KL, Premont, RT & Lefkowitz, RJ 2002, 'Seven-transmembrane receptors', *Nature reviews. Molecular cell biology*, vol. 3, no. 9, pp. 639–650.

Pin, J, Kniazeff, J, Liu, J, Binet, V, Goudet, C, Rondard, P & Prézeau, L 2005, 'Allosteric functioning of dimeric class C G-protein-coupled receptors', *The FEBS journal*, vol. 272, no. 12, pp. 2947–2955.

Pronin, AN & Gautam, N 1992, 'Interaction between G-protein beta and gamma subunit types is selective', *Proceedings of the National Academy of Sciences of the United States of America*, vol. 89, no. 13, pp. 6220–6224.

Pugliese, AM, Trincavelli, ML, Lecca, D, Coppi, E, Fumagalli, M, Ferrario, S, Failli, P, Daniele, S, Martini, C, Pedata, F & Abbracchio, MP 2009, 'Functional characterization of two isoforms of the P2Y-like receptor GPR17: [35S]GTPgammaS binding and electrophysiological studies in 1321N1 cells', *American journal of physiology. Cell physiology*, vol. 297, no. 4, pp. C1028-40.

Rajagopal, S, Rajagopal, K & Lefkowitz, RJ 2010, 'Teaching old receptors new tricks: biasing seven-transmembrane receptors', *Nature reviews. Drug discovery*, vol. 9, no. 5, pp. 373–386.

Ramsay, D, Kellett, E, McVey, M, Rees, S & Milligan, G 2002, 'Homo- and hetero-oligomeric interactions between G-protein-coupled receptors in living cells monitored by two variants of bioluminescence resonance energy transfer (BRET): hetero-oligomers between receptor subtypes form more efficiently than between less closely related sequences', *The Biochemical journal*, vol. 365, Pt 2, pp. 429–440.

Raport, CJ, Schweickart, VL, Chantry, D, Eddy, RL, Shows, TB, Godiska, R & Gray, PW 1996, 'New members of the chemokine receptor gene family', *Journal of leukocyte biology*, vol. 59, no. 1, pp. 18–23.

Reiner, S, Ziegler, N, Leon, C, Lorenz, K, Hayn, K von, Gachet, C, Lohse, MJ & Hoffmann, C 2009, 'beta-Arrestin-2 interaction and internalization of the human P2Y1 receptor are dependent on C-terminal phosphorylation sites', *Molecular pharmacology*, vol. 76, no. 6, pp. 1162–1171.

Reinscheid, RK, Nothacker, HP, Bourson, A, Ardati, A, Henningsen, RA, Bunzow, JR, Grandy, DK, Langen, H, Monsma, FJ & Civelli, O 1995, 'Orphanin FQ: a neuropeptide that activates an opioidlike G protein-coupled receptor', *Science (New York, N.Y.)*, vol. 270, no. 5237, pp. 792–794.

Reiter, E & Lefkowitz, RJ, 'GRKs and beta-arrestins: roles in receptor silencing, trafficking and signaling', *Trends in endocrinology and metabolism: TEM*, vol. 17, no. 4, pp. 159–165.

Riccioni, G, Di Ilio, C, Conti, P, Theoharides, TC & D'Orazio, N 2004, 'Advances in therapy with antileukotriene drugs', *Annals of clinical and laboratory science*, vol. 34, no. 4, pp. 379–387.

Richardson, MD, Balius, AM, Yamaguchi, K, Freilich, ER, Barak, LS & Kwatra, MM 2003, 'Human substance P receptor lacking the C-terminal domain remains competent to desensitize and internalize', *Journal of neurochemistry*, vol. 84, no. 4, pp. 854–863.

Robbiani, DF, Finch, RA, Jäger, D, Muller, WA, Sartorelli, AC & Randolph, GJ 2000, 'The leukotriene C(4) transporter MRP1 regulates CCL19 (MIP-3beta, ELC)-dependent mobilization of dendritic cells to lymph nodes', *Cell*, vol. 103, no. 5, pp. 757–768.

Roettger, BF, Ghanekar, D, Rao, R, Toledo, C, Yingling, J, Pinon, D & Miller, LJ 1997, 'Antagonist-stimulated internalization of the G protein-coupled cholecystokinin receptor', *Molecular pharmacology*, vol. 51, no. 3, pp. 357–362.

Rosethorne, EM & Charlton, SJ 2010, 'Agonist-biased signalling at the histamine H4 receptor: JNJ7777120 recruits beta-arrestin without activating G proteins', *Molecular pharmacology*.

Ross, EM & Gilman, AG 1980, 'Biochemical properties of hormone-sensitive adenylate cyclase', *Annual review of biochemistry*, vol. 49, pp. 533–564.

Rovati, GE & Capra, V 2007, 'Cysteinyl-leukotriene receptors and cellular signals', *TheScientificWorldJournal*, vol. 7, pp. 1375–1392.

Ryberg, E, Larsson, N, Sjögren, S, Hjorth, S, Hermansson, N, Leonova, J, Elebring, T, Nilsson, K, Drmota, T & Greasley, PJ 2007, 'The orphan receptor GPR55 is a novel cannabinoid receptor', *British journal of pharmacology*, vol. 152, no. 7, pp. 1092–1101.

Saiki, RK, Gelfand, DH, Stoffel, S, Scharf, SJ, Higuchi, R, Horn, GT, Mullis, KB & Erlich, HA 1988, 'Primer-directed enzymatic amplification of DNA with a thermostable DNA polymerase', *Science (New York, N.Y.)*, vol. 239, no. 4839, pp. 487–491.

Samama, P, Cotecchia, S, Costa, T & Lefkowitz, RJ 1993, 'A mutation-induced activated state of the beta 2-adrenergic receptor. Extending the ternary complex model', *The Journal of biological chemistry*, vol. 268, no. 7, pp. 4625–4636.

Sarau, HM, Ames, RS, Chambers, J, Ellis, C, Elshourbagy, N, Foley, JJ, Schmidt, DB, Muccitelli, RM, Jenkins, O, Murdock, PR, Herrity, NC, Halsey, W, Sathe, G, Muir, AI, Nuthulaganti, P, Dytko, GM, Buckley, PT, Wilson, S, Bergsma, DJ & Hay, DW 1999, 'Identification, molecular cloning, expression, and characterization of a cysteinyl leukotriene receptor', *Molecular pharmacology*, vol. 56, no. 3, pp. 657–663.

SCHILD, HO 1997, 'pA, a new scale for the measurement of drug antagonism. 1947', *British journal of pharmacology*, vol. 120, 4 Suppl, pp. 29-46.

Schlador, ML & Nathanson, NM 1997, 'Synergistic regulation of m2 muscarinic acetylcholine receptor desensitization and sequestration by G protein-coupled receptor kinase-2 and beta-arrestin-1', *The Journal of biological chemistry*, vol. 272, no. 30, pp. 18882–18890.

Schröder, R, Janssen, N, Schmidt, J, Kebig, A, Merten, N, Hennen, S, Müller, A, Blättermann, S, Mohr-Andrä, M, Zahn, S, Wenzel, J, Smith, NJ, Gomeza, J, Drewke, C, Milligan, G, Mohr, K & Kostenis, E 2010, 'Deconvolution of complex G protein-coupled receptor signaling in live cells using dynamic mass redistribution measurements', *Nature biotechnology*, vol. 28, no. 9, pp. 943–949.

Schröder, R, Merten, N, Mathiesen, JM, Martini, L, Kruljac-Letunic, A, Krop, F, Blaukat, A, Fang, Y, Tran, E, Ulven, T, Drewke, C, Whistler, J, Pardo, L, Gomeza, J & Kostenis, E 2009, 'The C-terminal tail of CRTH2 is a key molecular determinant that constrains Galphai and downstream signaling cascade activation', *The Journal of biological chemistry*, vol. 284, no. 2, pp. 1324–1336.

Schulte, G & Levy, FO 2007, 'Novel aspects of G-protein-coupled receptor signalling--different ways to achieve specificity', *Acta physiologica (Oxford, England)*, vol. 190, no. 1, pp. 33–38.

Schwartz, TW & Holst, B 2007, 'Allosteric enhancers, allosteric agonists and ago-allosteric modulators: where do they bind and how do they act?', *Trends in pharmacological sciences*, vol. 28, no. 8, pp. 366–373.

Seamon, KB, Padgett, W & Daly, JW 1981, 'Forskolin: unique diterpene activator of adenylate cyclase in membranes and in intact cells', *Proceedings of the National Academy of Sciences of the United States of America*, vol. 78, no. 6, pp. 3363–3367.

Selvin, PR 2000, 'The renaissance of fluorescence resonance energy transfer', *Nature structural biology*, vol. 7, no. 9, pp. 730–734.

Shapiro, DA, Renock, S, Arrington, E, Chiodo, LA, Liu, L, Sibley, DR, Roth, BL & Mailman, R 2003, 'Aripiprazole, a novel atypical antipsychotic drug with a unique and robust pharmacology', *Neuropsychopharmacology : official publication of the American College of Neuropsychopharmacology*, vol. 28, no. 8, pp. 1400–1411.

Shenoy, SK & Lefkowitz, RJ 2003, 'Multifaceted roles of beta-arrestins in the regulation of seven-membrane-spanning receptor trafficking and signalling', *The Biochemical journal*, vol. 375, Pt 3, pp. 503–515.

Shoemaker, JL, Ruckle, MB, Mayeux, PR & Prather, PL 2005, 'Agonist-directed trafficking of response by endocannabinoids acting at CB2 receptors', *The Journal of pharmacology and experimental therapeutics*, vol. 315, no. 2, pp. 828–838.

Simon, MI, Strathmann, MP & Gautam, N 1991, 'Diversity of G proteins in signal transduction', *Science (New York, N.Y.)*, vol. 252, no. 5007, pp. 802–808.

Smith, AG, Heath, JK, Donaldson, DD, Wong, GG, Moreau, J, Stahl, M & Rogers, D 1988, 'Inhibition of pluripotential embryonic stem cell differentiation by purified polypeptides', *Nature*, vol. 336, no. 6200, pp. 688–690.

Stahl, SM 2001, 'Dopamine system stabilizers, aripiprazole, and the next generation of antipsychotics, part 1, "Goldilocks" actions at dopamine receptors', *The Journal of clinical psychiatry*, vol. 62, no. 11, pp. 841–842.

Stalheim, L, Ding, Y, Gullapalli, A, Paing, MM, Wolfe, BL, Morris, DR & Trejo, J 2005, 'Multiple independent functions of arrestins in the regulation of protease-activated receptor-2 signaling and trafficking', *Molecular pharmacology*, vol. 67, no. 1, pp. 78–87.

Sternweis, PC & Robishaw, JD 1984, 'Isolation of two proteins with high affinity for guanine nucleotides from membranes of bovine brain', *The Journal of biological chemistry*, vol. 259, no. 22, pp. 13806–13813.

Strathmann, MP & Simon, MI 1991, 'G alpha 12 and G alpha 13 subunits define a fourth class of G protein alpha subunits', *Proceedings of the National Academy of Sciences of the United States of America*, vol. 88, no. 13, pp. 5582–5586.

Su, Y, Raghuwanshi, SK, Yu, Y, Nanney, LB, Richardson, RM & Richmond, A 2005, 'Altered CXCR2 signaling in beta-arrestin-2-deficient mouse models', *Journal of immunology (Baltimore, Md. : 1950)*, vol. 175, no. 8, pp. 5396–5402.

Sukharev, SI, Klenchin, VA, Serov, SM, Chernomordik, LV & Chizmadzhev YuA 1992, 'Electroporation and electrophoretic DNA transfer into cells. The effect of DNA interaction with electropores', *Biophysical journal*, vol. 63, no. 5, pp. 1320–1327.

Suzuki, N, Nakamura, S, Mano, H & Kozasa, T 2003, 'Galpha 12 activates Rho GTPase through tyrosine-phosphorylated leukemia-associated RhoGEF', *Proceedings of the National Academy of Sciences of the United States of America*, vol. 100, no. 2, pp. 733–738.

Takasaki, J, Saito, T, Taniguchi, M, Kawasaki, T, Moritani, Y, Hayashi, K & Kobori, M 2004, 'A novel Galphaq/11-selective inhibitor', *The Journal of biological chemistry*, vol. 279, no. 46, pp. 47438–47445.

Takei, K & Haucke, V 2001, 'Clathrin-mediated endocytosis: membrane factors pull the trigger', *Trends in cell biology*, vol. 11, no. 9, pp. 385–391.

Tamminga, CA 2002, 'Partial dopamine agonists in the treatment of psychosis', *Journal of neural transmission (Vienna, Austria : 1996)*, vol. 109, no. 3, pp. 411–420.

Taniguchi, M, Nagai, K, Arao, N, Kawasaki, T, Saito, T, Moritani, Y, Takasaki, J, Hayashi, K, Fujita, S, Suzuki, K & Tsukamoto, S 2003, 'YM-254890, a novel platelet aggregation inhibitor produced by Chromobacterium sp. QS3666', *The Journal of antibiotics*, vol. 56, no. 4, pp. 358–363.

Temporini, C, Ceruti, S, Calleri, E, Ferrario, S, Moaddel, R, Abbracchio, MP & Massolini, G 2009, 'Development of an immobilized GPR17 receptor stationary phase for binding determination using frontal affinity chromatography coupled to mass spectrometry', *Analytical biochemistry*, vol. 384, no. 1, pp. 123–129.

Terrillon, S, Durroux, T, Mouillac, B, Breit, A, Ayoub, MA, Taulan, M, Jockers, R, Barberis, C & Bouvier, M 2003, 'Oxytocin and vasopressin V1a and V2 receptors form constitutive homo- and heterodimers during biosynthesis', *Molecular endocrinology (Baltimore, Md.)*, vol. 17, no. 4, pp. 677–691.

Thibonnier, M, Preston, JA, Dulin, N, Wilkins, PL, Berti-Mattera, LN & Mattera, R 1997, 'The human V3 pituitary vasopressin receptor: ligand binding profile and density-dependent signaling pathways', *Endocrinology*, vol. 138, no. 10, pp. 4109–4122.

Thomas, KR & Capecchi, MR 1987, 'Site-directed mutagenesis by gene targeting in mouse embryo-derived stem cells', *Cell*, vol. 51, no. 3, pp. 503–512.

Thomas, KR, Folger, KR & Capecchi, MR 1986, 'High frequency targeting of genes to specific sites in the mammalian genome', *Cell*, vol. 44, no. 3, pp. 419–428.

Tohgo, A, Choy, EW, Gesty-Palmer, D, Pierce, KL, Laporte, S, Oakley, RH, Caron, MG, Lefkowitz, RJ & Luttrell, LM 2003, 'The stability of the G protein-coupled receptor-beta-arrestin interaction determines the mechanism and functional consequence of ERK activation', *The Journal of biological chemistry*, vol. 278, no. 8, pp. 6258–6267.

Tohgo, A, Pierce, KL, Choy, EW, Lefkowitz, RJ & Luttrell, LM 2002, 'beta-Arrestin scaffolding of the ERK cascade enhances cytosolic ERK activity but inhibits ERK-mediated transcription following angiotensin AT1a receptor stimulation', *The Journal of biological chemistry*, vol. 277, no. 11, pp. 9429–9436.

Trinquet, E, Maurin, F, Préaudat, M & Mathis, G 2001, 'Allophycocyanin 1 as a near-infrared fluorescent tracer: isolation, characterization, chemical modification, and use in a homogeneous fluorescence resonance energy transfer system', *Analytical biochemistry*, vol. 296, no. 2, pp. 232–244.

Trinquet, E, Fink, M, Bazin, H, Grillet, F, Maurin, F, Bourrier, E, Ansanay, H, Leroy, C, Michaud, A, Durroux, T, Maurel, D, Malhaire, F, Goudet, C, Pin, J, Naval, M, Hernout, O, Chrétien, F, Chapleur, Y & Mathis, G 2006, 'D-myo-inositol 1-phosphate as a surrogate of D-myo-inositol 1,4,5-tris phosphate to monitor G protein-coupled receptor activation', *Analytical biochemistry*, vol. 358, no. 1, pp. 126–135.

Trinquet, E & Mathis, G 2006, 'Fluorescence technologies for the investigation of chemical libraries', *Molecular bioSystems*, vol. 2, no. 8, pp. 380–387.

Tsien, RY 1998, 'The green fluorescent protein', *Annual review of biochemistry*, vol. 67, pp. 509–544.

Tsien, RY, Bacskai, BJ & Adams, SR 1993, 'FRET for studying intracellular signalling', *Trends in cell biology*, vol. 3, no. 7, pp. 242–245.

Tunaru, S, Kero, J, Schaub, A, Wufka, C, Blaukat, A, Pfeffer, K & Offermanns, S 2003, 'PUMA-G and HM74 are receptors for nicotinic acid and mediate its anti-lipolytic effect', *Nature medicine*, vol. 9, no. 3, pp. 352–355.

Tybulewicz, VL, Crawford, CE, Jackson, PK, Bronson, RT & Mulligan, RC 1991, 'Neonatal lethality and lymphopenia in mice with a homozygous disruption of the c-abl proto-oncogene', *Cell*, vol. 65, no. 7, pp. 1153–1163.

Urban, JD, Vargas, GA, Zastrow, M von & Mailman, RB 2007, 'Aripiprazole has functionally selective actions at dopamine D2 receptor-mediated signaling pathways', *Neuropsychopharmacology : official publication of the American College of Neuropsychopharmacology*, vol. 32, no. 1, pp. 67–77.

Valant, C, Gregory, KJ, Hall, NE, Scammells, PJ, Lew, MJ, Sexton, PM & Christopoulos, A 2008, 'A novel mechanism of G protein-coupled receptor functional selectivity. Muscarinic partial agonist McN-A-343 as a bitopic orthosteric/allosteric ligand', *The Journal of biological chemistry*, vol. 283, no. 43, pp. 29312–29321.

Vassilatis, DK, Hohmann, JG, Zeng, H, Li, F, Ranchalis, JE, Mortrud, MT, Brown, A, Rodriguez, SS, Weller, JR, Wright, AC, Bergmann, JE & Gaitanaris, GA 2003, 'The G protein-coupled receptor repertoires of human and mouse', *Proceedings of the National Academy of Sciences of the United States of America*, vol. 100, no. 8, pp. 4903–4908.

Venter, JC, Adams, MD, Myers, EW, Li, PW, Mural, RJ, Sutton, GG, Smith, HO, Yandell, M, Evans, CA, Holt, RA, Gocayne, JD, Amanatides, P, Ballew, RM, Huson, DH, Wortman, JR, Zhang, Q, Kodira, CD, et al. 2001, 'The sequence of the human genome', *Science (New York, N.Y.)*, vol. 291, no. 5507, pp. 1304–1351.

Vines, CM, Revankar, CM, Maestas, DC, LaRusch, LL, Cimino, DF, Kohout, TA, Lefkowitz, RJ & Prossnitz, ER 2003, 'N-formyl peptide receptors internalize but do not recycle in the absence of arrestins', *The Journal of biological chemistry*, vol. 278, no. 43, pp. 41581–41584.

Violin, JD, DeWire, SM, Yamashita, D, Rominger, DH, Nguyen, L, Schiller, K, Whalen, EJ, Gowen, M & Lark, MW 2010, 'Selectively engaging {beta}-arrestins at the angiotensin II type 1 receptor reduces blood pressure and increases cardiac performance', *The Journal of pharmacology and experimental therapeutics*, vol. 335, no. 3, pp. 572–579.

Violin, JD & Lefkowitz, RJ 2007, 'Beta-arrestin-biased ligands at seven-transmembrane receptors', *Trends in pharmacological sciences*, vol. 28, no. 8, pp. 416–422.

Violin, JD, Ren, X & Lefkowitz, RJ 2006, 'G-protein-coupled receptor kinase specificity for beta-arrestin recruitment to the beta2-adrenergic receptor revealed by fluorescence resonance energy transfer', *The Journal of biological chemistry*, vol. 281, no. 29, pp. 20577–20588.

Vogelstein, B & Gillespie, D 1979, 'Preparative and analytical purification of DNA from agarose', *Proceedings of the National Academy of Sciences of the United States of America*, vol. 76, no. 2, pp. 615–619.

Volpe, P & Alderson-Lang, BH 1990, 'Regulation of inositol 1,4,5-trisphosphate-induced Ca2+ release. II. Effect of cAMP-dependent protein kinase', *The American journal of physiology*, vol. 258, 6 Pt 1, pp. C1086-91.

Voyno-Yasenetskaya, T, Conklin, BR, Gilbert, RL, Hooley, R, Bourne, HR & Barber, DL 1994, 'G alpha 13 stimulates Na-H exchange', *The Journal of biological chemistry*, vol. 269, no. 7, pp. 4721–4724.

Voyno-Yasenetskaya, TA, Faure, MP, Ahn, NG & Bourne, HR 1996, 'Galpha12 and Galpha13 regulate extracellular signal-regulated kinase and c-Jun kinase pathways by different mechanisms in COS-7 cells', *The Journal of biological chemistry*, vol. 271, no. 35, pp. 21081–21087.

Vrecl, M, Anderson, L, Hanyaloglu, A, McGregor, AM, Groarke, AD, Milligan, G, Taylor, PL & Eidne, KA 1998, 'Agonist-induced endocytosis and recycling of the gonadotropin-releasing hormone receptor: effect of beta-arrestin on internalization kinetics', *Molecular endocrinology (Baltimore, Md.)*, vol. 12, no. 12, pp. 1818–1829.

Vrecl, M, Jorgensen, R, Pogacnik, A & Heding, A 2004, 'Development of a BRET2 screening assay using beta-arrestin 2 mutants', *Journal of biomolecular screening : the official journal of the Society for Biomolecular Screening*, vol. 9, no. 4, pp. 322–333.

Vrecl, M, Nørregaard, PK, Almholt, DLC, Elster, L, Pogacnik, A & Heding, A 2009, 'Beta-arrestin-based Bret2 screening assay for the "non"-beta-arrestin binding CB1 receptor', *Journal of biomolecular screening : the official journal of the Society for Biomolecular Screening*, vol. 14, no. 4, pp. 371–380.

Walters, RW, Shukla, AK, Kovacs, JJ, Violin, JD, DeWire, SM, Lam, CM, Chen, JR, Muehlbauer, MJ, Whalen, EJ & Lefkowitz, RJ 2009, 'beta-Arrestin1 mediates nicotinic acid-induced flushing, but not its antilipolytic effect, in mice', *The Journal of clinical investigation*, vol. 119, no. 5, pp. 1312–1321.

Wang, P, Wu, Y, Ge, X, Ma, L & Pei, G 2003, 'Subcellular localization of beta-arrestins is determined by their intact N domain and the nuclear export signal at the C terminus', *The Journal of biological chemistry*, vol. 278, no. 13, pp. 11648–11653.

Ward, WW & Cormier, MJ 1979, 'An energy transfer protein in coelenterate bioluminescence. Characterization of the Renilla green-fluorescent protein', *The Journal of biological chemistry*, vol. 254, no. 3, pp. 781–788.

Wei, H, Ahn, S, Shenoy, SK, Karnik, SS, Hunyady, L, Luttrell, LM & Lefkowitz, RJ 2003, 'Independent beta-arrestin 2 and G protein-mediated pathways for angiotensin II activation of extracellular signal-regulated kinases 1 and 2', *Proceedings of the National Academy of Sciences of the United States of America*, vol. 100, no. 19, pp. 10782–10787.

Wess, J 1997, 'G-protein-coupled receptors: molecular mechanisms involved in receptor activation and selectivity of G-protein recognition', *The FASEB journal : official publication of the Federation of American Societies for Experimental Biology*, vol. 11, no. 5, pp. 346–354.

Wess, J 1998, 'Molecular basis of receptor/G-protein-coupling selectivity', *Pharmacology & therapeutics*, vol. 80, no. 3, pp. 231–264.

Whalen, EJ, Rajagopal, S & Lefkowitz, RJ 2010, 'Therapeutic potential of β-arrestin- and G protein-biased agonists', *Trends in molecular medicine*.

White, JH, Wise, A, Main, MJ, Green, A, Fraser, NJ, Disney, GH, Barnes, AA, Emson, P, Foord, SM & Marshall, FH 1998, 'Heterodimerization is required for the formation of a functional GABA(B) receptor', *Nature*, vol. 396, no. 6712, pp. 679–682

Wichterle, H, Lieberam, I, Porter, JA & Jessell, TM 2002, 'Directed differentiation of embryonic stem cells into motor neurons', *Cell*, vol. 110, no. 3, pp. 385–397.

Wilden, U, Hall, SW & Kühn, H 1986, 'Phosphodiesterase activation by photoexcited rhodopsin is quenched when rhodopsin is phosphorylated and binds the intrinsic 48-kDa protein of rod outer segments', *Proceedings of the National Academy of Sciences of the United States of America*, vol. 83, no. 5, pp. 1174–1178.

Williams, C 2004, 'cAMP detection methods in HTS: selecting the best from the rest', *Nature reviews. Drug discovery*, vol. 3, no. 2, pp. 125–135.

Williams, RL, Hilton, DJ, Pease, S, Willson, TA, Stewart, CL, Gearing, DP, Wagner, EF, Metcalf, D, Nicola, NA & Gough, NM 1988, 'Myeloid leukaemia inhibitory factor maintains the developmental potential of embryonic stem cells', *Nature*, vol. 336, no. 6200, pp. 684–687.

Willoughby, D, Baillie, GS, Lynch, MJ, Ciruela, A, Houslay, MD & Cooper, DMF 2007, 'Dynamic regulation, desensitization, and cross-talk in discrete subcellular microdomains during beta2-adrenoceptor and prostanoid receptor cAMP signaling', *The Journal of biological chemistry*, vol. 282, no. 47, pp. 34235–34249.

Wise, A, Jupe, SC & Rees, S 2004, 'The identification of ligands at orphan G-protein coupled receptors', *Annual review of pharmacology and toxicology*, vol. 44, pp. 43–66.

Wisler, JW, DeWire, SM, Whalen, EJ, Violin, JD, Drake, MT, Ahn, S, Shenoy, SK & Lefkowitz, RJ 2007, 'A unique mechanism of beta-blocker action: carvedilol stimulates beta-arrestin signaling', *Proceedings of the National Academy of Sciences of the United States of America*, vol. 104, no. 42, pp. 16657–16662.

Woehler, A & Ponimaskin, EG 2009, 'G protein--mediated signaling: same receptor, multiple effectors', *Current molecular pharmacology*, vol. 2, no. 3, pp. 237–248.

Wunder, F, Tinel, H, Kast, R, Geerts, A, Becker, EM, Kolkhof, P, Hütter, J, Ergüden, J & Härter, M 2010, 'Pharmacological characterization of the first potent and selective antagonist at the cysteinyl leukotriene 2 (CysLT(2)) receptor', *British journal of pharmacology*, vol. 160, no. 2, pp. 399–409.

Xu, Y, Piston, DW & Johnson, CH 1999, 'A bioluminescence resonance energy transfer (BRET) system: application to interacting circadian clock proteins', *Proceedings of the National Academy of Sciences of the United States of America*, vol. 96, no. 1, pp. 151–156.

Yan, K, Kalyanaraman, V & Gautam, N 1996, 'Differential ability to form the G protein betagamma complex among members of the beta and gamma subunit families', *The Journal of biological chemistry*, vol. 271, no. 12, pp. 7141–7146.

Yu, G, Wei, E, Zhang, S, Xu, H, Chu, L, Zhang, W, Zhang, Q, Chen, Z, Mei, R & Zhao, M 2005, 'Montelukast, a cysteinyl leukotriene receptor-1 antagonist, dose- and time-dependently protects against focal cerebral ischemia in mice', *Pharmacology*, vol. 73, no. 1, pp. 31–40.

Zakrzewicz, A, Krasteva, G, Wilhelm, J, Dietrich, H, Wilker, S, Padberg, W, Wygrecka, M & Grau, V 2010, 'Reduced expression of arrestin beta 2 by graft monocytes during acute rejection of rat kidneys', *Immunobiology*.

Zhang, J, Ferguson, SS, Barak, LS, Ménard, L & Caron, MG 1996, 'Dynamin and beta-arrestin reveal distinct mechanisms for G protein-coupled receptor internalization', *The Journal of biological chemistry*, vol. 271, no. 31, pp. 18302–18305.

Zhang, JY, Kowal, DM, Nawoschik, SP, Dunlop, J, Pausch, MH & Peri, R 2010, 'Development of an improved IP(1) assay for the characterization of 5-HT(2C) receptor ligands', *Assay and drug development technologies*, vol. 8, no. 1, pp. 106–113.

Zhang, W, Wei, E, Mei, R, Zhu, C & Zhao, M 2002, 'Neuroprotective effect of ONO-1078, a leukotriene receptor antagonist, on focal cerebral ischemia in rats', *Acta pharmacologica Sinica*, vol. 23, no. 10, pp. 871–877.

Zhu, X, Gilbert, S, Birnbaumer, M & Birnbaumer, L 1994, 'Dual signaling potential is common among Gs-coupled receptors and dependent on receptor density', *Molecular pharmacology*, vol. 46, no. 3, pp. 460–469.

9 Annex

9.1 Targeting vector maps

The maps of the targeting vector used for homologous recombination of murine GPR17 were designed with the bioinformatic software Vector NTI. As already mentioned in the present thesis, the vector construct exhibits a neomycin resistance cassette (neo) as well as a herpes simplex virus thymidine kinase (HSV-TK) for positive-negative selection of targeted ES cell clones (see 3.4.4). A NotI/XhoI flanked 5' homologous DNA fragment of 4.7kb (long arm) and a 3' homologous DNA fragment of 1.5kb (short arm) flanked with BamHI/EcoRI were subcloned into pPNT vector by standard cloning techniques (see 3.4.1.1).

In order to ensure the correct sequence and especially the absence of point mutations of the generated construct, oligonucleotides were designed to serve as sequencing primers. The sequences of these primers are listed in chapter 2.14.2, and their respective binding sites are depicted in Annex Figure 1Annex Figure 1 (A). The actual sequencing procedure was performed by GATC Biotech AG, Konstanz (see 3.1.6). The correctness of the constructed vector was further proven by restriction enzyme cleavages, as presented in Figure 29 and Figure 30. The endonuclease restriction recognition sites of the applied enzymes are illustrated in Annex Figure 1 (B).

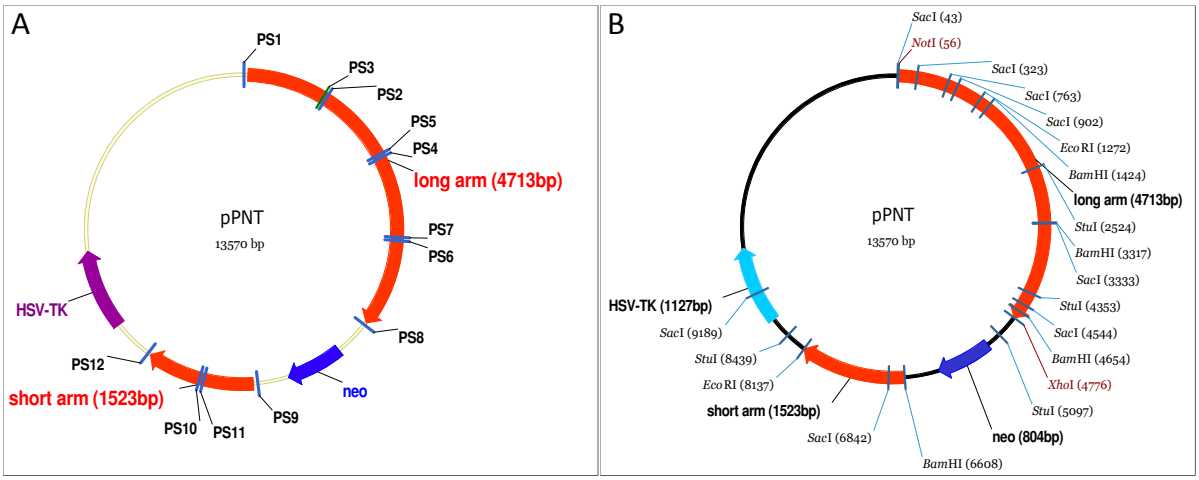

Annex Figure 1 Vector maps of targeting vector including sequencing primer binding and endonuclease restriction recognition sites

These vector maps, designed by use of Vector NTI software, represent the self-constructed targeting vector for homologous recombination of murine GPR17, demonstrating the bindings sites of sequencing primers (PS1-12, A), as well as the endonuclease restriction enzyme recognition sites of the utilized enzymes (B). The applied pPNT vector exhibits a neomycin resistance sequence (neo) as well as a herpes simplex virus thymidine kinase (HSV-TK) that enables positive-negative selection of targeted ES cell clones. The homologous regions of murine GPR17 are denoted as long (5') and short (3') arm. Genes are represented by solid arrows, which indicate the direction of transcription.

9.2 HEK293 cells stably expressing β-arrestin2 fused to GFP2

HEK293 cells stably expressing distinct β-arrestin2 amounts were generously provided by J. M. Mathiesen, Department of Medicinal Chemistry, University of Copenhagen. These cells stably expressing β-arrestin2 N-terminally fused to autofluorescent tag green fluorescent protein 2 (GFP2) were sorted regarding their fluorescence intensity by means of fluorescence activated cell sorting (FACS) analyses, which were conducted by J. M. Mathiesen, Department of Medicinal Chemistry, University of Copenhagen.

9.2.1 Fluorescence microscopy

The investigations by use of immunofluorescence microscopy revealed that β-arrestin2 is mainly localized in the cytoplasm, which is in agreement with previously reported information (Wang et al. 2003).

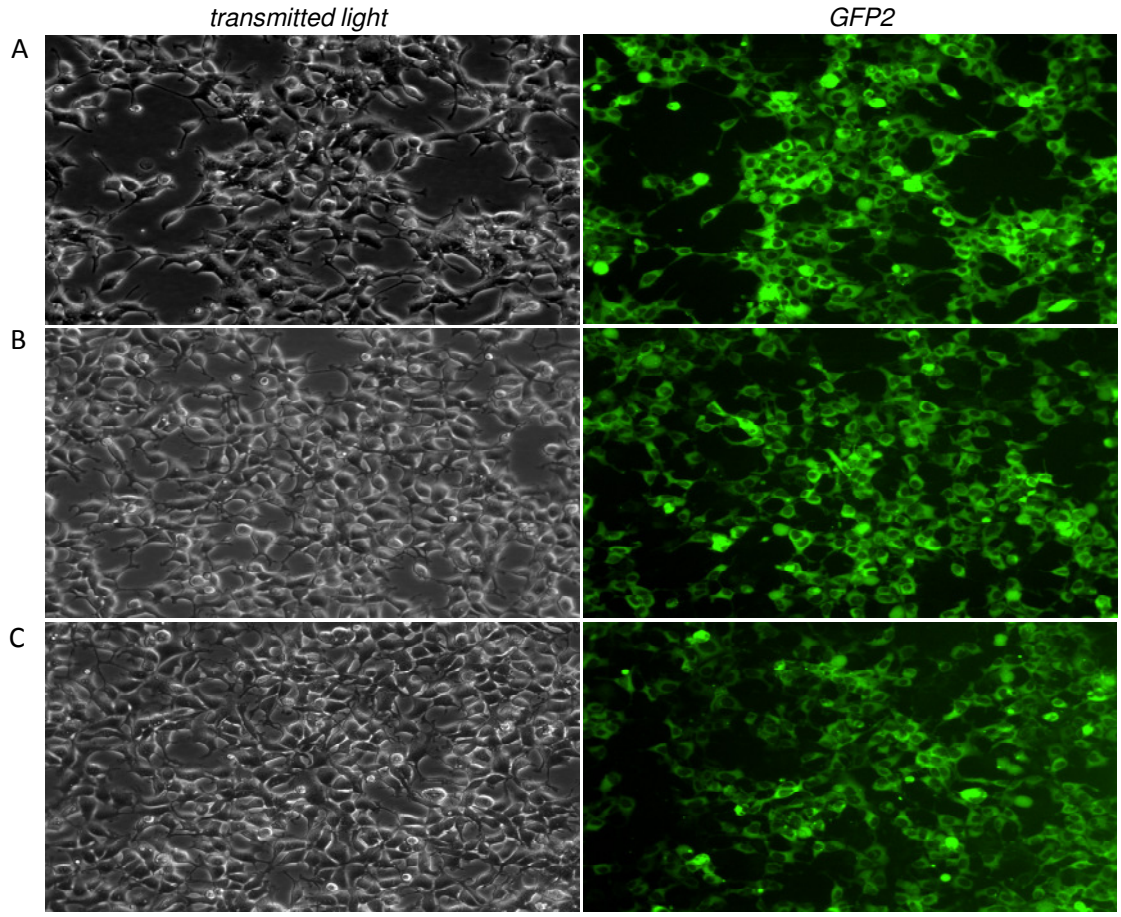

Annex Figure 2 Subcellular localization of β-arrestin2 fused to GFP2 stably expressed HEK293 cells.
A-C, The subcellular localization of GFP2 labeled β-arrestin2 stably transfected in HEK293 cells (A: *very high*, B: *high*, C: *low*) was analyzed by fluorescent microscopy, by application of the following settings for GFP2 recordings (right panels): 200 fold magnification, 500 ms exposure time, 0.99 γ and 1-13 histogram. For transmitted light photos (left panels) exposure time was diminished to 10 ms and histogram was set 8-50.

The three different cell lines stably expressing distinct amounts (referred to as *very high, high and low*) of β-arrestin2 amino-terminally fused with the autofluorescent epitope tag GFP2, are hardly distinguishable from each other, only slight descending intensities are visible using the employed

fluorescence microscope from the top panel (*very high*) down to the bottom panel (*low*). The observation of β-arrestin translocation upon GPR17-activation by use of fluorescence microscopy failed, but as a direct, agonist-dependent interaction of the GPR17-RLuc receptor and β-arrestin2-GFP2 by means of BRET2 assays was possible (see 4.1.6.3), one could conclude that the applied BRET2 technology is a more sensitive method to discover such receptor/β-arrestin interactions.

Register of publications

Publications

Schröder R, Janssen N, Schmidt J, Kebig A, Merten N, **Hennen S**, Müller A, Blättermann S, Mohr-Andrä M, Zahn S, Wenzel J, Smith NJ, Gomeza J, Drewke C, Milligan G, Mohr K, Kostenis E. (2010) Deconvolution of complex G protein-coupled receptor signaling in live cells using dynamic mass redistribution measurements. *Nature Biotechnology, Volume: 28, Pages: 943–949*

Posters

Spinrath, A., **Hennen, S**., Akkari, R., von Kügelgen, I., Müller, C. E., Gomeza, J. & Kostenis, E. (2009) *GPR17: a new dual uracil nucleotide/cysteinyl-leukotriene receptor or still an orphan?* Minisymposium of the Graduate College GRK 677 - Structure and Molecular Interaction as Basis of Drug Action, Bonn, Germany, 1. April 2009.

Spinrath, A., **Hennen, S**., Dallmeyer, M., von Kügelgen, I., Müller, C. E., Gomeza, J. & Kostenis, E. (2009) *Uracil nucleotides do not activate the orphan G protein coupled receptor GPR17* Small Purine Meeting, Stockholm, Sweden, 18.-19. September 2009.

Spinrath, A., **Hennen, S**., Dallmeyer, M., von Kügelgen, I., Müller, C. E., Gomeza, J. & Kostenis, E. (2009) *GPR17: an orphan G protein-coupled receptor on a journey to find its identity*…, International Symposium of the Graduate College GRK 677 - Structure and Molecular Interaction as Basis of Drug Action, Bonn, Germany, 21.-23. September 2009.

Janßen, N., Kebig, A., Müller, A., **Hennen, S**., Kostenis, E. & Mohr, K. (2010) Dynamic mass redistribution identifies the analysis of signaling pathways of Gi, Gq and Gs coupled receptors. 76. Jahrestagung der Deutschen Gesellschaft für Experimentelle und Klinische Pharmakologie und Toxikologie, Frankfurt am Main, Germany, 23.-25. März 2010

Acknowledgement

I would like to thank everyone who has helped and inspired me over the last three years.

Special thanks to my advisor, Prof. Dr. Evi Kostenis, for her great guidance, unconditional support and inspiration. I would like to whole heartedly appreciate her constant encouragement in the progress of my work in a fantastically normal and human way. The joy and enthusiasm she has for her research was always contagious and motivational for me.

I also wish to thank my dissertation committee members Prof. Dr. Klaus Mohr, Prof. Dr. Gerd Bendas and Prof. Dr. Heinz Bönisch.

I am much obliged to Daniel Schulz and Simone Hildenbrand, who revised the language of the present thesis.

I would like to show my graditude to Dr. Jesús Gomeza for helping me with every step of my work involving the molecular biology and gene targeting aspect, since his long standing research experience and in-depth knowledge in the field of gene targeting was crucial for supporting my work. In addition to the help from Dr. Gomeza, I am also grateful to Daniel Schulz who was a great help in all molecular biology aspects in my thesis and assisted in the establishment of gene-modified stem cells.

I am also grateful for the excellent technical help from Mrs. Marianne Vasmer-Ehses and Mrs. Ulrike Rick, on which I could rely throughout my experimental work.

Labmates and colleagues are true companions, without whom a researcher is incomplete, thus I would like to thank all of the people who have accompanied me during this period of my work, which has made the duration of my stay in the lab an educational, memorable, stimulating and pleasurable one. I am especially grateful to Daniel Schulz, Andreas Spinrath, Dr. Nicole Merten, Johannes Schmidt, Stefanie Blättermann, Julia Morschel, Lucas Peters, Ralf Schröder, Anke Müller, Manuel Grundmann, Waltraud Läer, Katrin Bell and Dr. Christel Drewke.

Furthermore I would like to show my gratitude to the members of Mohr group for excellent cooperation. The group has been a source of encouragement as well as friendship, especially Ms. Nicole Janssen and Ms. Annette Stumpf, who were both always frank, warm and open in their advice.

Additionally, I would like to thank to Mrs. Elke Gassen and Mr. Thomas Kögler for assisting me in many different ways.

I am also indebted to Dr. Hilmer Stiftung for the financial support received in the form of a doctoral scholarship.

Of course, my deepest thanks to my family especially my parents Gabriele and Ansgar Hennen for their love, support and understanding. To them I dedicate this thesis.